Supporting Information

Deoxyfluorination tunes the aggregation of cellulose and chitin oligosaccharides and highlights the role of specific hydroxyl groups in the crystallization process

Giulio Fittolani,[1,2] Surusch Djalali,[1,2] Manishkumar A. Chaube,[1] Theodore Tyrikos-Ergas,[1,2,3] Marlene C. S. Dal Colle,[1,2] Andrea Grafmüller,[4] Peter H. Seeberger,[1,2] and Martina Delbianco[1*]

[1]Department of Biomolecular Systems, Max Planck Institute of Colloids and Interfaces, Am Mühlenberg 1, 14476 Potsdam, Germany
[2]Department of Chemistry and Biochemistry, Freie Universität Berlin, Arnimallee 22, 14195 Berlin, Germany
[3]Current affiliation: Department of Chemistry, University of Illinois, 61801 Urbana, Illinois, United States
[4]Department of Theory and Biosystems, Max Planck Institute of Colloids and Interfaces, Am Mühlenberg 1, 14476 Potsdam, Germany

E-mail: martina.delbianco@mpikg.mpg.de

Table of Contents

1 General materials and methods

All chemicals used were reagent grade and used as supplied unless otherwise noted. The automated syntheses were performed on a home-built synthesizer developed at the Max Planck Institute of Colloids and Interfaces.[1] Analytical thin-layer chromatography (TLC) was performed on Merck silica gel 60 F254 plates (0.25 mm). Compounds were visualized by UV irradiation or dipping the plate in a staining solution (sugar stain: 10% H_2SO_4 in EtOH; CAM: 48 g/L ammonium molybdate, 60 g/L ceric ammonium molybdate in 6% H_2SO_4 aqueous solution). Flash column chromatography was carried out by using forced flow of the indicated solvent on Fluka Kieselgel 60 M (0.04 – 0.063 mm). Analysis and purification by normal and reverse phase HPLC was performed by using an Agilent 1200 series. Products were lyophilized using a Christ Alpha 2-4 LD plus freeze dryer. ^{1}H, ^{13}C and HSQC NMR spectra were recorded on a Varian 400-MR (400 MHz), Varian 600-NMR (600 MHz), Bruker Biospin AVANCE700 (700 MHz) Bruker AVANCE III 800 (800 MHz) spectrometer. Spectra were recorded in $CDCl_3$ or MeOD using the solvent residual peak chemical shift as the internal standard in ^{1}H and ^{13}C NMR ($CDCl_3$: 7.26 ppm ^{1}H, 77.0 ppm ^{13}C, MeOD: 3.31 ppm ^{1}H, 49.0 ppm ^{13}C) or in D_2O using the solvent as the internal standard in ^{1}H NMR (D_2O: 4.79 ppm ^{1}H). ^{1}H NMR spectra for all compounds were recorded without ^{13}C decoupling. Weak intensity ^{13}C resonances were derived from the respective HSQC crosspeaks. ^{1}H NMR integrals of the resonances corresponding to residues at the reducing end are reported as non-integer numbers and the sum of the integrals of α and β anomers, H-1 α and H-1 β respectively, is set to 1. High resolution mass spectra were obtained using a 6210 ESI-TOF mass spectrometer (Agilent) and a MALDI-TOF autoflexTM (Bruker). MALDI and ESI mass spectra were run on IonSpec Ultima instruments. IR spectra were recorded on a Perkin-Elmer 1600 FTIR spectrometer. Optical rotations were measured by using a Perkin-Elmer 241 and Unipol L1000 polarimeter. X-ray diffraction experiments were carried out using a D8 Avance diffractometer (Bruker) in reflection mode with monochromatic Cu Kα radiation (λ= 1.5418 Å) generated at 40 kV and 40 mA (Siemens X-ray tube KFL CU 2K). The scans were performed in the scattering angle range between 4°and 40° with a step of 0.02°and an accumulation time of 6 or 10 s. Raw XRD profiles were corrected by subtraction of the sample holder signal, smoothing, and baseline correction. The oligosaccharide samples were lyophilized prior to XRD measurement. The solubility of the oligosaccharides in water was estimated by adding 0.5 mL of water the pure lyophilized powders (0.5 mg for fluorinated cellulose and 1.0 mg for fluorinated chitin analogues). After sonication and mixing, the sample was inspected to look for the presence of a precipitate.

2 Synthesis of building blocks

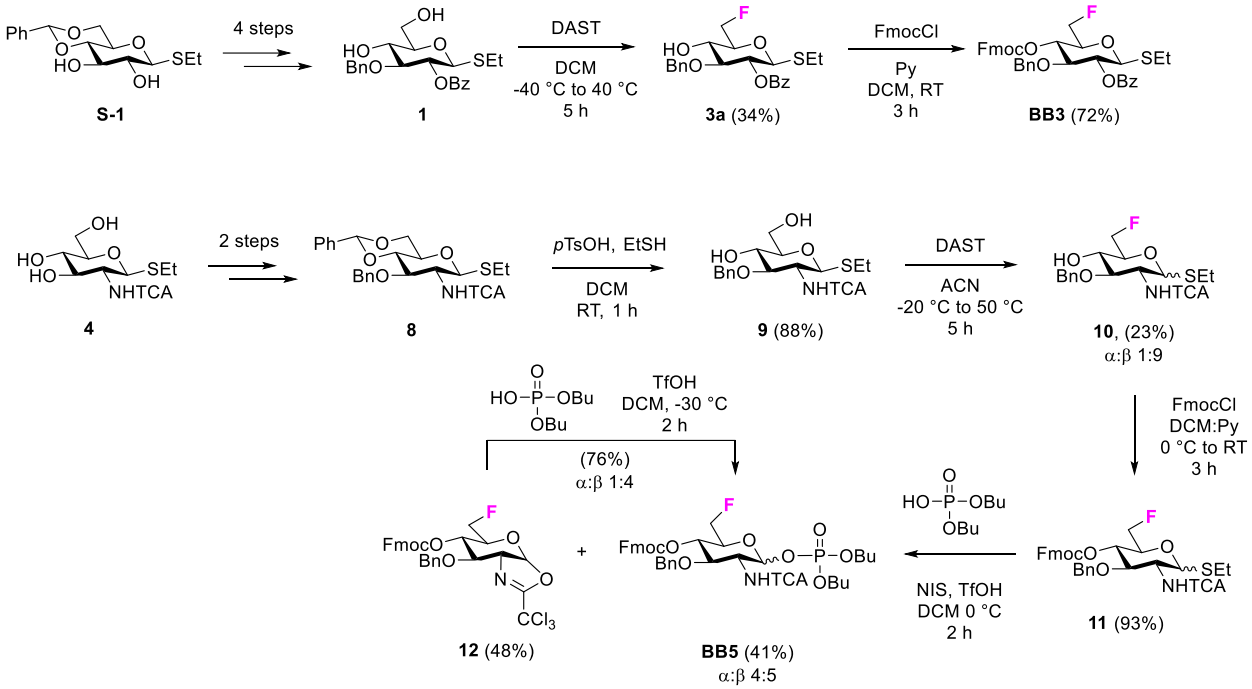

Scheme S1 Synthesis of **BB3** and **BB5**.

Compounds **S-1** and **4** were purchased from GlycoUniverse (Germany). Compound **1** and **8** were synthesized according to previously reported protocols.[2,3]

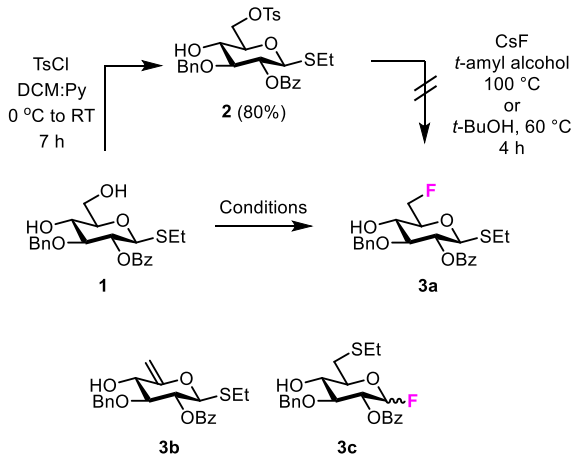

Entry	Reagents	Conditions	Yield for **3**	Notes
1	i) TsCl (1.3 equiv.), Py ii) CsF (3.0 equiv.)	i) DCM, 0 °C to RT, 7 h ii) *t*-amyl alcohol, 100 °C, 1 h	Traces	**3b** major product
2	i) TsCl (1.3 equiv.), Py ii) CsF (3.0 equiv.)	i) DCM, 0 °C to RT, 7 h ii) *t*-BuOH, 60 °C, 1h	Traces	**3b** major product
3	DAST (1.2 equiv.)	Py, -20 °C to 70 °C	-	**1** decomposition
4	DAST (1.2 equiv.), Py (2.0 equiv.)	DCM, -40 °C to 40°C, 5 h	Traces	*
5	DAST (1.2 equiv.)	DCM, -40 °C to RT, 5 h	29%	*
6	DAST (1.2 equiv.)	DCM, -40 °C to 40 °C, 5 h	34%	*
7	DAST (1.2 equiv.)	DCE, -20 °C to 70 °C, 3 h	27%	*

Table S1 Screening of conditions for the selective C-6 deoxyfluorination of **1**. *Several unidentified side products among which **3b** and **3c**. Isolated yields are reported. Side-product **3b** was characterized using ESI-MS m/z 401.1 [M+H]+ and ^{1}H NMR ($CDCl_3$) δ 6.02 ppm (d, J = 4.8 Hz).

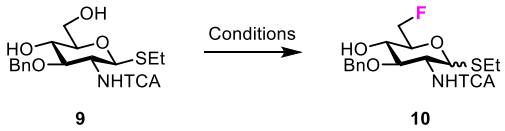

Entry	Reagents	Conditions	Yield for **10**
1	DAST (1.1 equiv.)	DCM:1,4-dioxane (1:1), -20 °C to RT, 5 h	26% (α:β 3:2)*
2	DAST (1.1 equiv.)	ACN, -40 °C to 50 °C, 5 h	23% (α:β 4:96)*

Table S2 Conditions used for the C-6 deoxyfluorination of intermediate **9**. Isolated yields are reported.*The anomeric ratio was measured by integration of the H-1 signals in the ^{1}H NMR.

2.1.1 Synthesis of 1

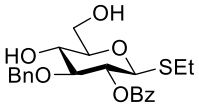

1

1 was prepared according to previously established procedures.[2]

^{1}H NMR (400 MHz, Chloroform-*d*) δ 8.12 – 8.05 (m, 2H), 7.62 (t, *J* = 7.4 Hz, 1H), 7.49 (t, *J* = 7.7 Hz, 2H), 7.27 – 7.19 (m, 5H), 5.34 – 5.25 (m, 1H), 4.77 (d, *J* = 11.4 Hz, 1H), 4.68 – 4.59 (m, 2H), 3.96 (dd, *J* = 12.0, 3.4 Hz, 1H), 3.84 (dd, *J* = 12.0, 5.0 Hz, 1H), 3.75 (p, *J* = 8.9 Hz, 2H), 3.49 (ddd, *J* = 8.8, 4.8, 3.5 Hz, 1H), 2.73 (qd, *J* = 7.4, 3.1 Hz, 2H), 2.39 (s, 2H), 1.25 (t, *J* = 7.5 Hz, 3H).

^{1}H NMR of 1 (400 MHz, $CDCl_3$)

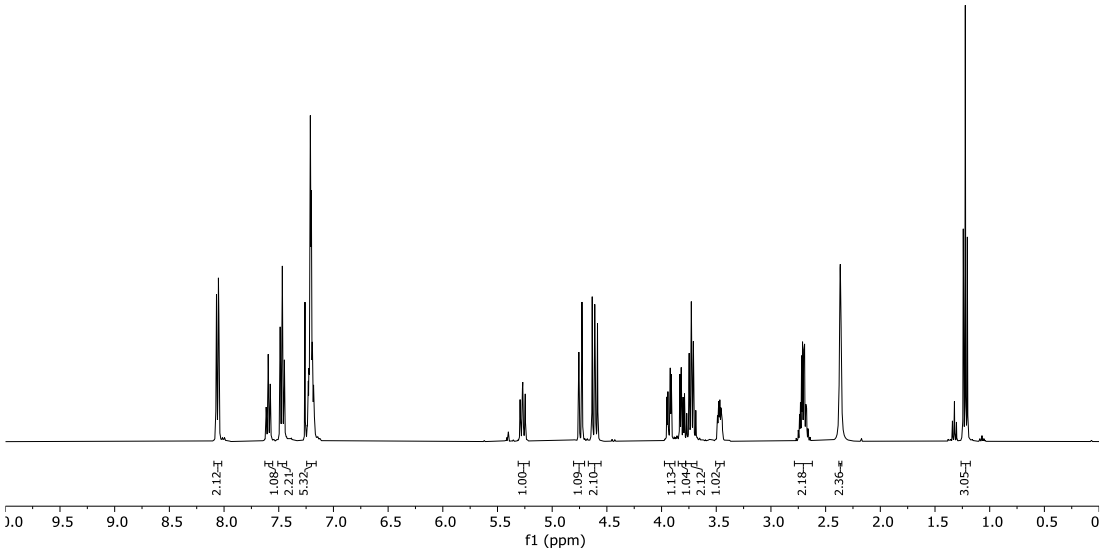

2.1.2 Synthesis of 3a

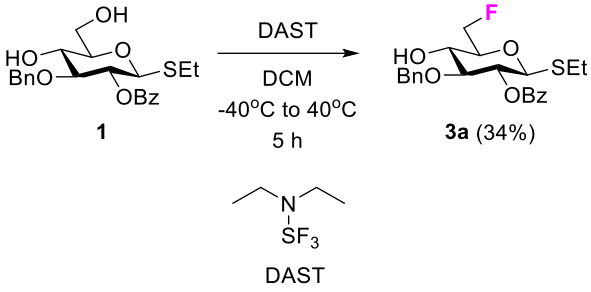

1 (490 mg, 1.17 mmol) was dissolved in anhydrous DCM (10 mL) and cooled to -40 °C (dry ice/ACN bath) under Ar atmosphere. DAST (171 µL, 1.29 mmol) was dissolved in anhydrous DCM (200 µL) and added dropwise to the reaction mixture. After 30 min, the cooling bath was removed and the reaction heated to 40 °C. The solution was stirred for additional 5 h and then quenched with MeOH at 0 °C. The crude reaction mixture was diluted with DCM and washed once with brine. The crude compound was purified by silica gel flash column chromatography (Hexane : EtOAc = 3:1→1:1) to give **3a** as a colorless oil (167 mg, 34%).

^{1}H NMR (400 MHz, Chloroform-*d*) δ 8.11 – 8.02 (m, 2H), 7.64 – 7.56 (m, 1H), 7.47 (tt, *J* = 6.7, 1.2 Hz, 2H), 7.32 – 7.15 (m, 5H), 5.36 – 5.24 (m, 1H, H-2), 4.81 – 4.51 (m, 5H, H-1, H-6, H-6', C*H*$_2$ Bn), 3.78 – 3.67 (m, 2H, H-4, H-3), 3.58 (dddd, *J* = 21.5, 8.3, 5.0, 2.7 Hz, 1H, H-5), 2.82 – 2.63 (m, 2H, C*H*$_2$ SEt), 2.34 (s, 1H, OH-4), 1.24 (t, *J* = 7.5 Hz, 3H, C*H*$_3$ SEt). ^{13}C NMR (101 MHz, Chloroform-*d*) δ 165.34, 137.77, 133.51, 129.99, 129.79, 128.78, 128.66, 128.29, 128.17, 84.14 (C-3), 83.80 (C-1), 82.19 (d, *J* = 173.4 Hz, C-6), 78.55 (d, *J* = 18.6 Hz, C-5), 74.94, 72.25 (C-2), 69.07 (d, *J* = 7.2 Hz, C-4), 24.12, 14.92. ^{19}F NMR (376 MHz, Chloroform-*d*) δ -233.66 (td, *J* = 47.3, 22.8 Hz). $[\alpha]_D^{20}$ -18.12 (c 1.2 g/100 mL, $CHCl_3$). IR *v* = 3482, 2927, 1724, 1268, 1086, 1070, 1027, 710, 700 cm^{-1}. (ESI-HRMS) m/z 443.1291 $[M+Na]^+$ ($C_{22}H_{25}FO_5SNa$ requires 443.1302).

^{1}H NMR of 3a (400 MHz, $CDCl_3$)

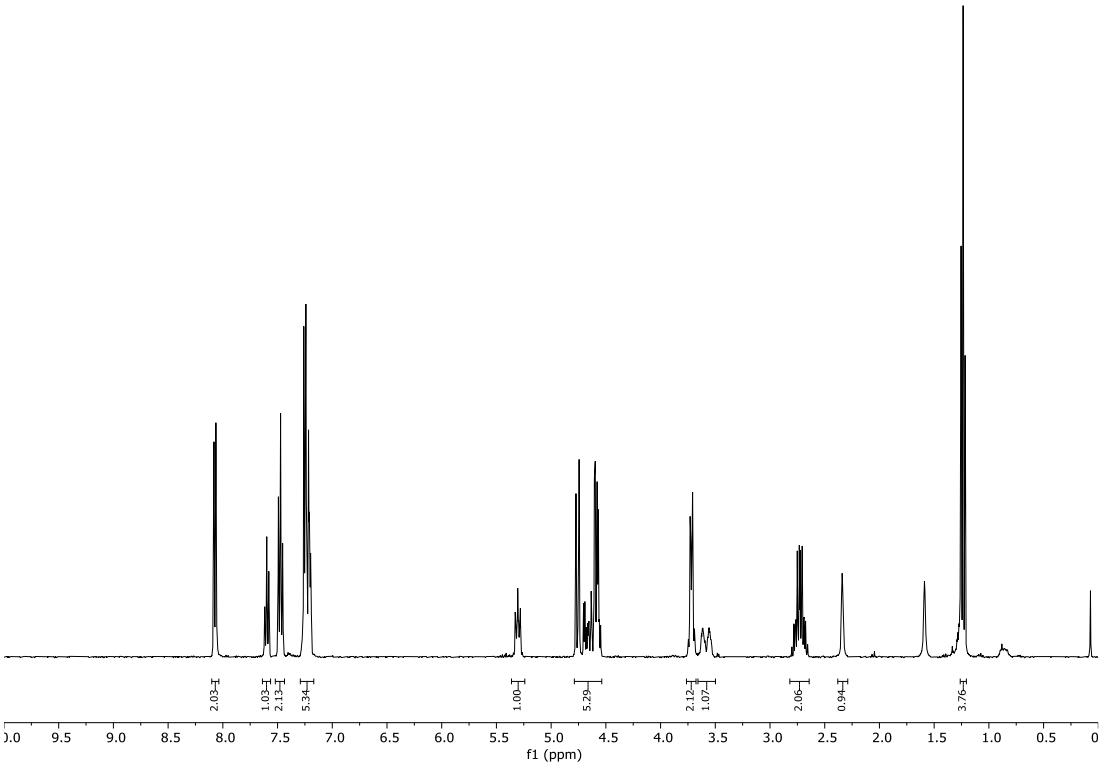

^{13}C NMR of 3a (101 MHz, $CDCl_3$)

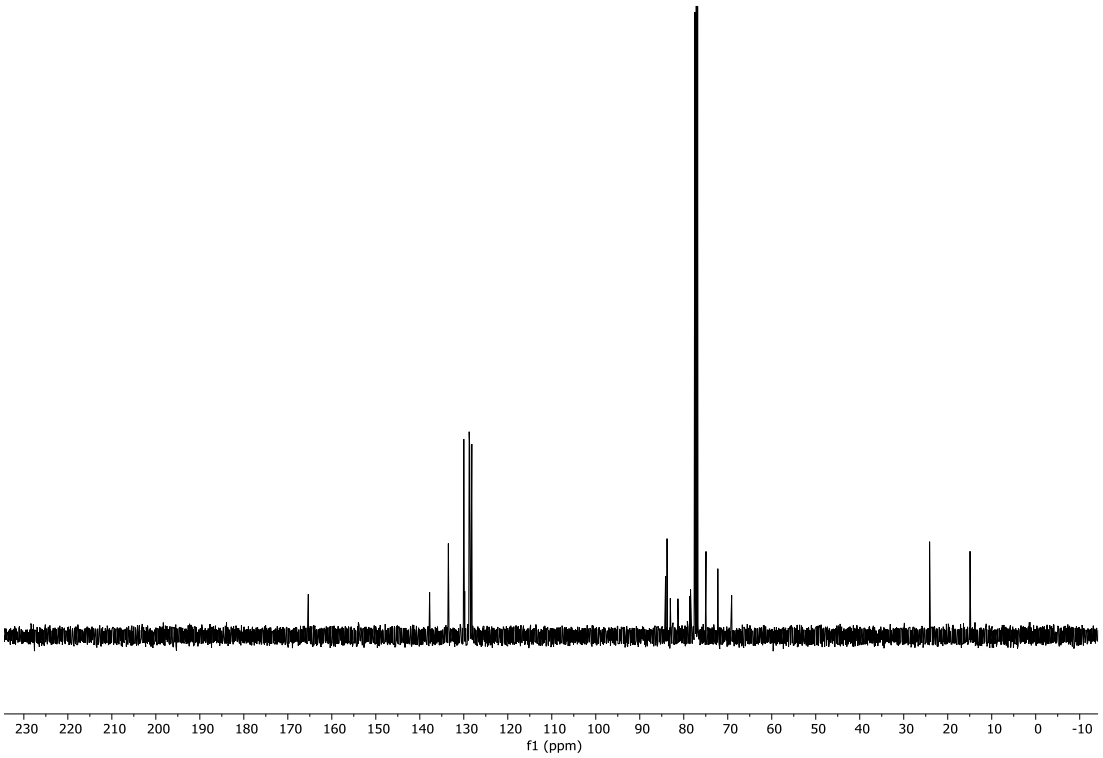

^{19}F NMR of 3a (376 MHz, $CDCl_3$)

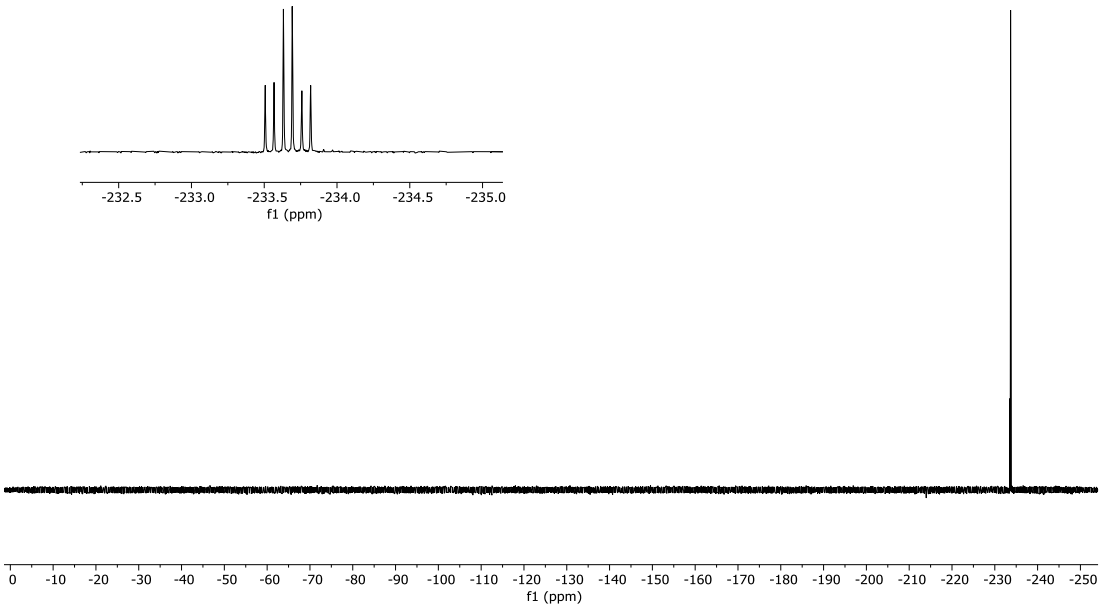

HSQC NMR of 3a ($CDCl_3$)

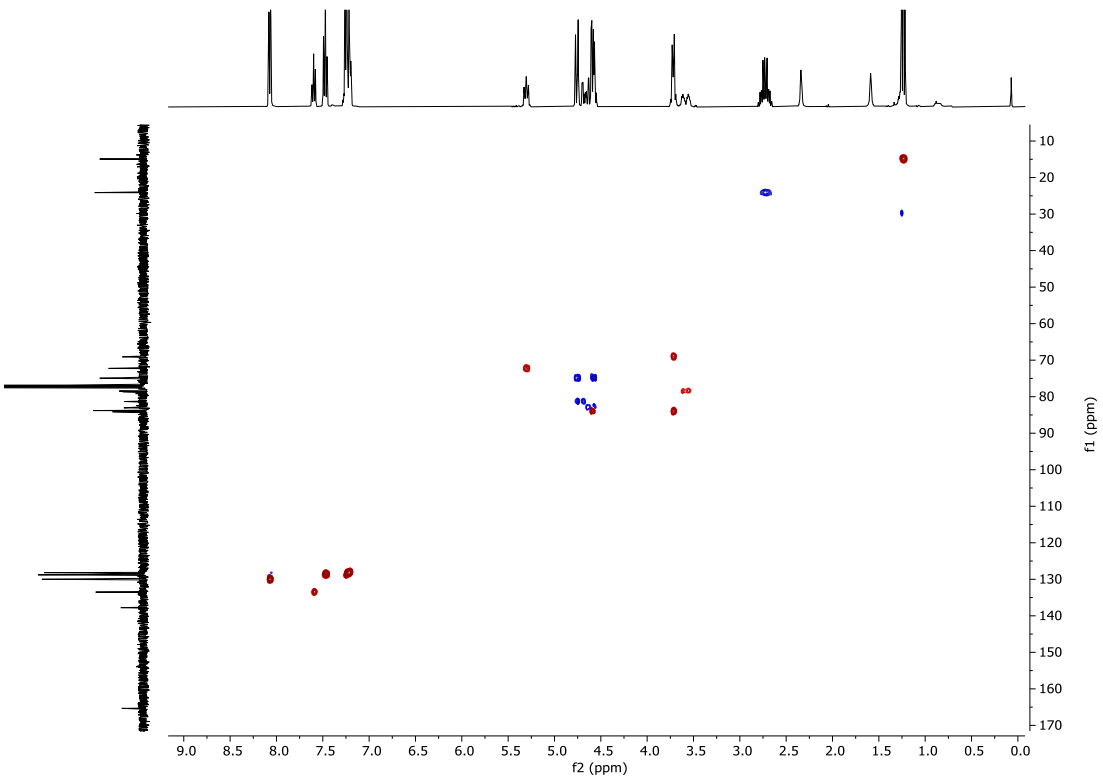

COSY NMR of 3a ($CDCl_3$)

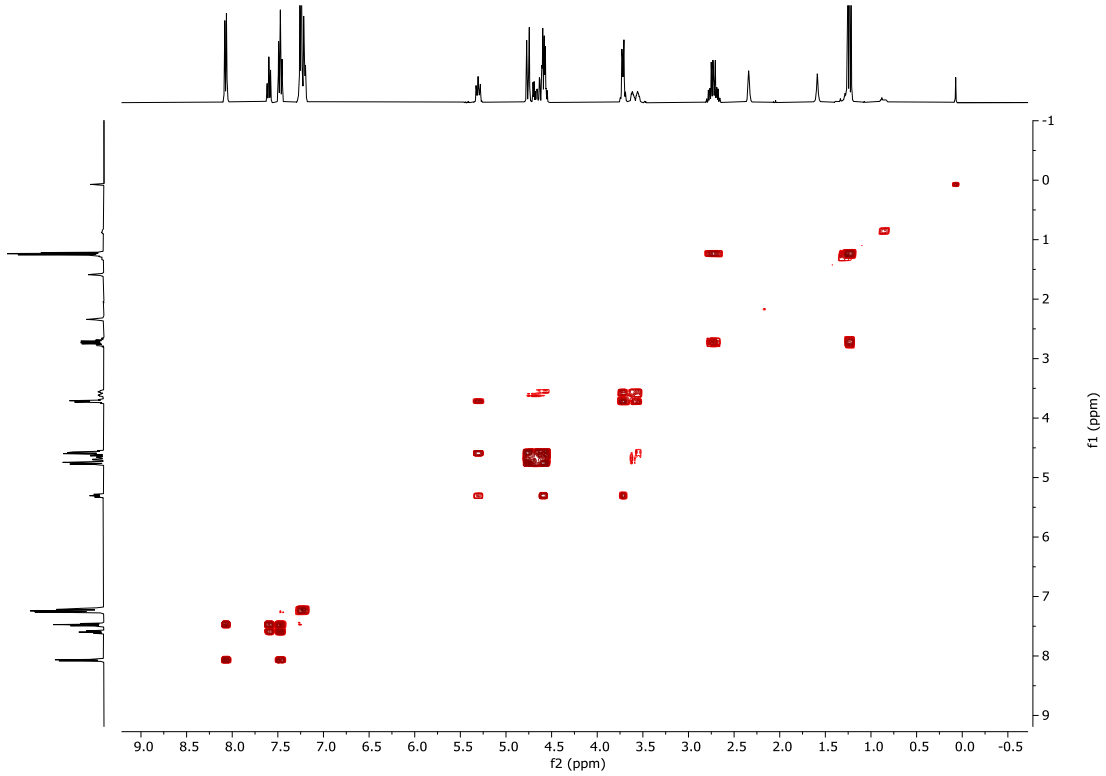

2.1.3 Synthesis of BB3

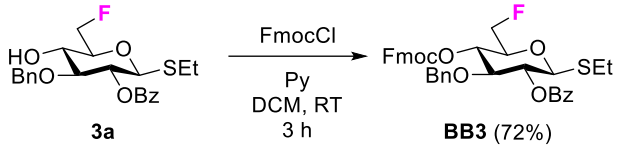

3a (167 mg, 0.40 mmol) was dissolved in DCM (5 mL) and pyridine was added (100 µL, 1.2 mmol). FmocCl (200 mg, 0.77 mmol) was dissolved in DCM (1.5 mL) and added to the reaction mixture at RT under Ar atmosphere. The solution was stirred for 3 h and then quenched with a 1 M solution of HCl. The crude reaction mixture was diluted with DCM, washed once with 1 M HCl, and once with brine. The crude compound was purified by silica gel flash column chromatography (Toluene : DCM = 4:1→3:1 then Toluene : EtOAc = 4:1) and recrystallized from DCM : Hexane to give the **BB3** as a white solid (186 mg, 72%).

^{1}H NMR (400 MHz, Chloroform-*d*) δ 8.05 – 7.96 (m, 2H), 7.81 – 7.72 (m, 2H), 7.66 – 7.53 (m, 3H), 7.50 – 7.36 (m, 4H), 7.30 (tt, J = 7.5, 1.0 Hz, 2H), 7.20 – 7.00 (m, 5H), 5.33 (dd, J = 10.0, 9.1 Hz, 1H, H-2), 4.95 (dd, J = 10.2, 9.2 Hz, 1H, H-4), 4.63 – 4.49 (m, 5H, C*H*$_2$ Bn (1), C*H*$_2$ Fmoc, H-1, H-6), 4.48 – 4.40 (m, 2H, C*H*$_2$ Bn (1), H-6'), 4.20 (t, J = 6.8 Hz, 1H, C*H* Fmoc), 3.91 (t, J = 9.1 Hz, 1H, H-3), 3.82 – 3.69 (m, 1H, H-5), 2.82 – 2.65 (m, 2H, C*H*$_2$ SEt), 1.23 (t, J = 7.5 Hz, 3H, C*H*$_3$ SEt). ^{13}C NMR (101 MHz, Chloroform-*d*) δ 164.99, 154.17, 143.08, 143.04, 141.36, 137.18, 133.38, 129.91, 129.54, 128.48, 128.21, 128.00, 127.88, 127.73, 127.24, 125.04, 124.91, 120.17, 120.15, 83.69 (C-1), 81.56 (d, J = 175.3 Hz, C-6), 80.81 (C-3), 76.73 (C-5), 74.45, 73.92 (d, J = 6.2 Hz, C-4), 71.64 (C-2), 70.14, 46.79, 24.00, 14.80. ^{19}F NMR (376 MHz, Chloroform-*d*) δ -230.76 (td, J = 47.0, 20.0 Hz). $[\alpha]_D^{20}$ 23.35 (c 0.6 g/100 mL, $CHCl_3$). IR ν = 2928, 1754, 1729, 1248, 1028, 742, 710 cm^{-1}. (ESI-HRMS) m/z 665.1992 $[M+Na]^+$ ($C_{37}H_{35}FO_7SNa$ requires 665.1980).

^{1}H NMR of BB3 (400 MHz, $CDCl_3$)

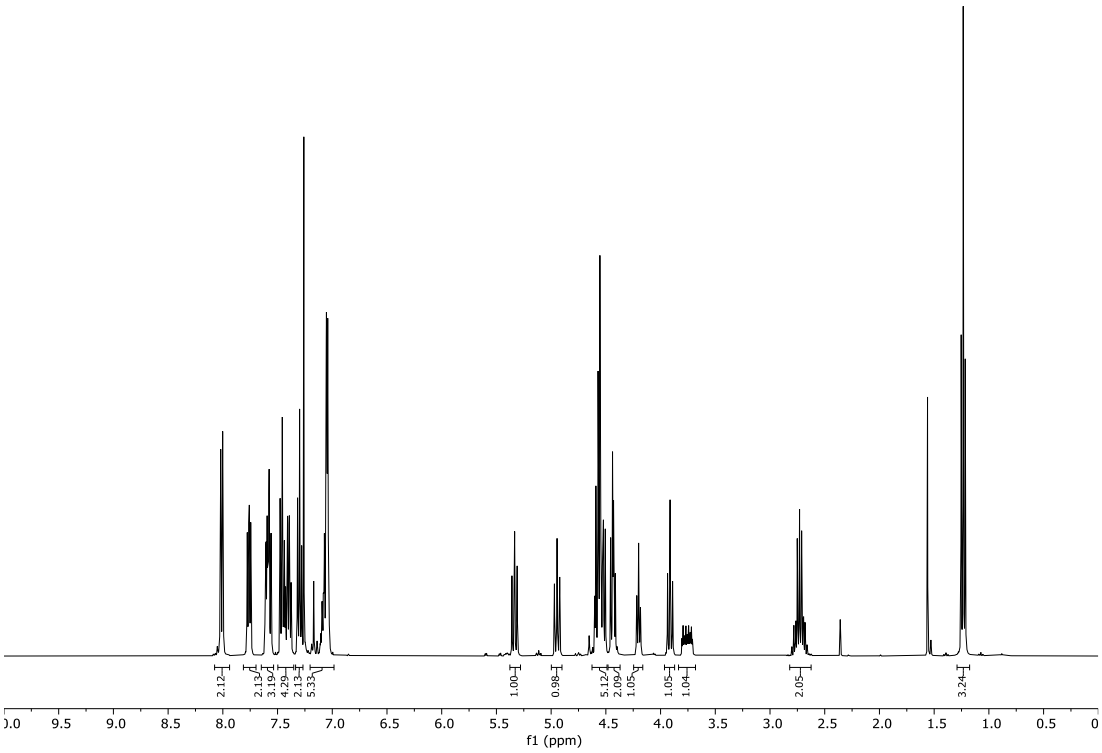

^{13}C NMR of BB3 (101 MHz, $CDCl_3$)

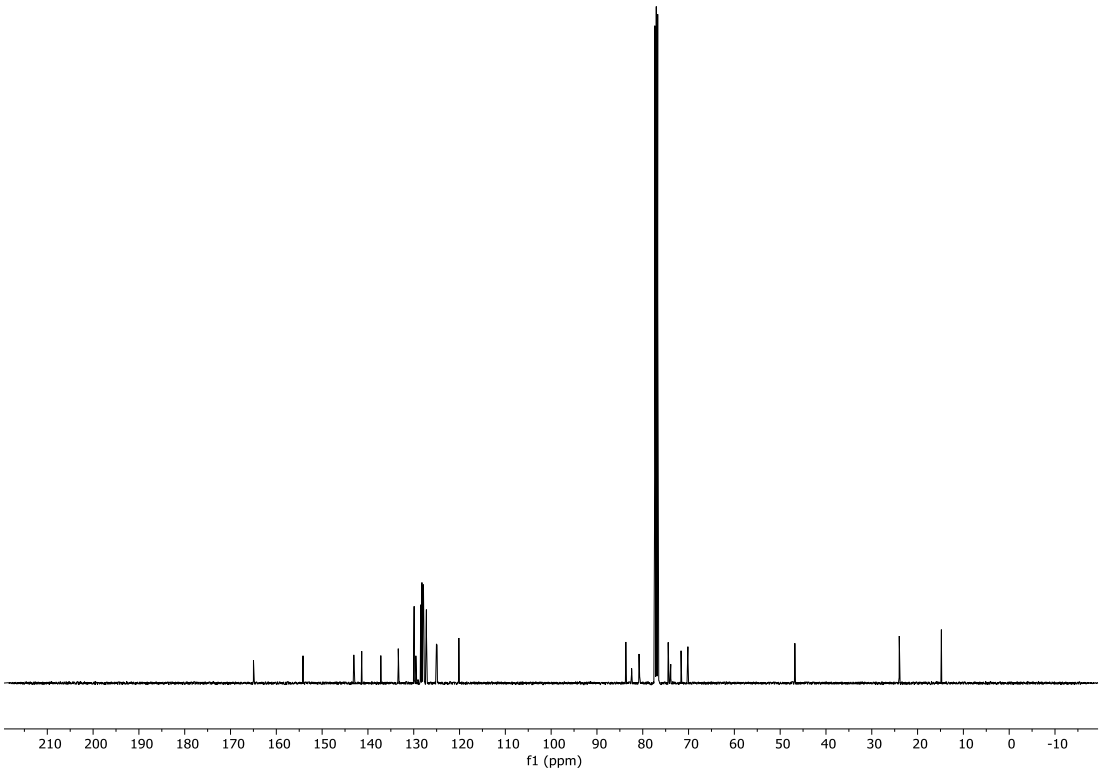

^{19}F NMR of BB3 (376 MHz, $CDCl_3$)

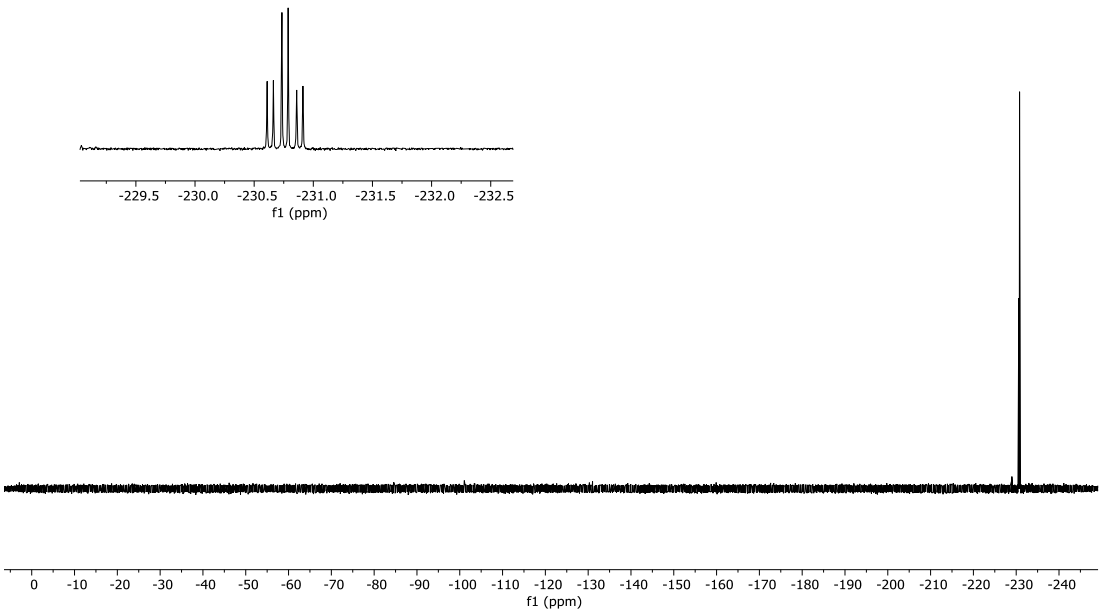

HSQC NMR of BB3 ($CDCl_3$)

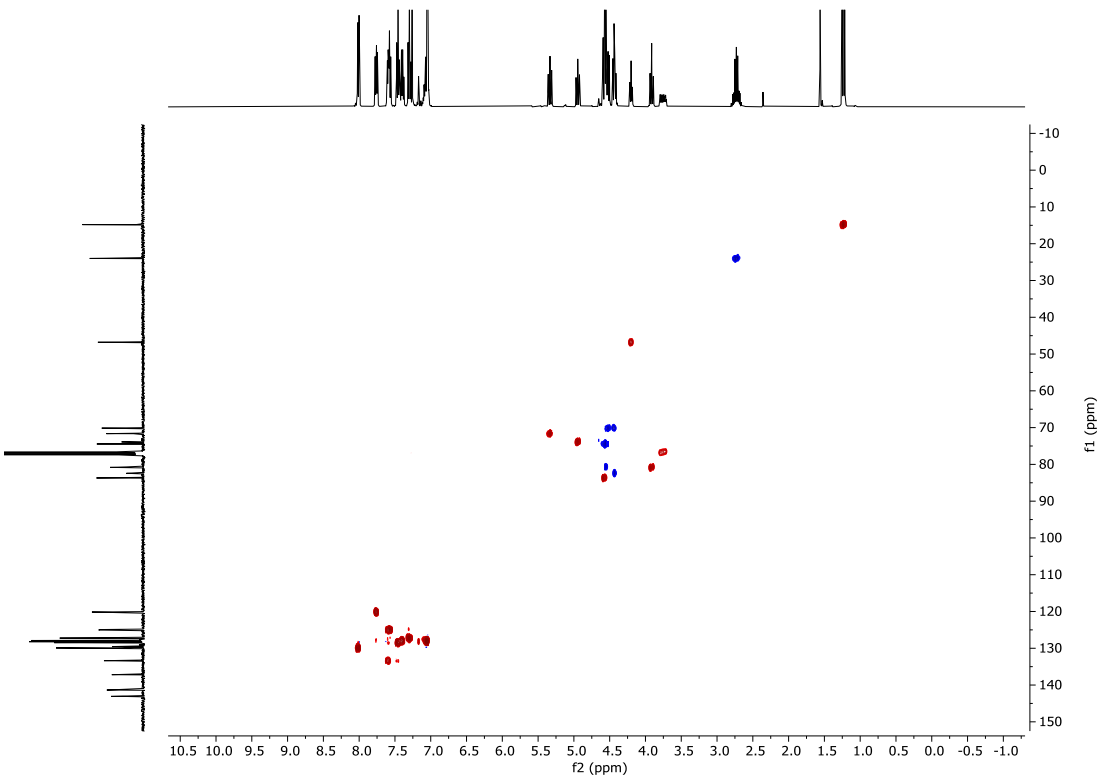

COSY NMR of BB3 ($CDCl_3$)

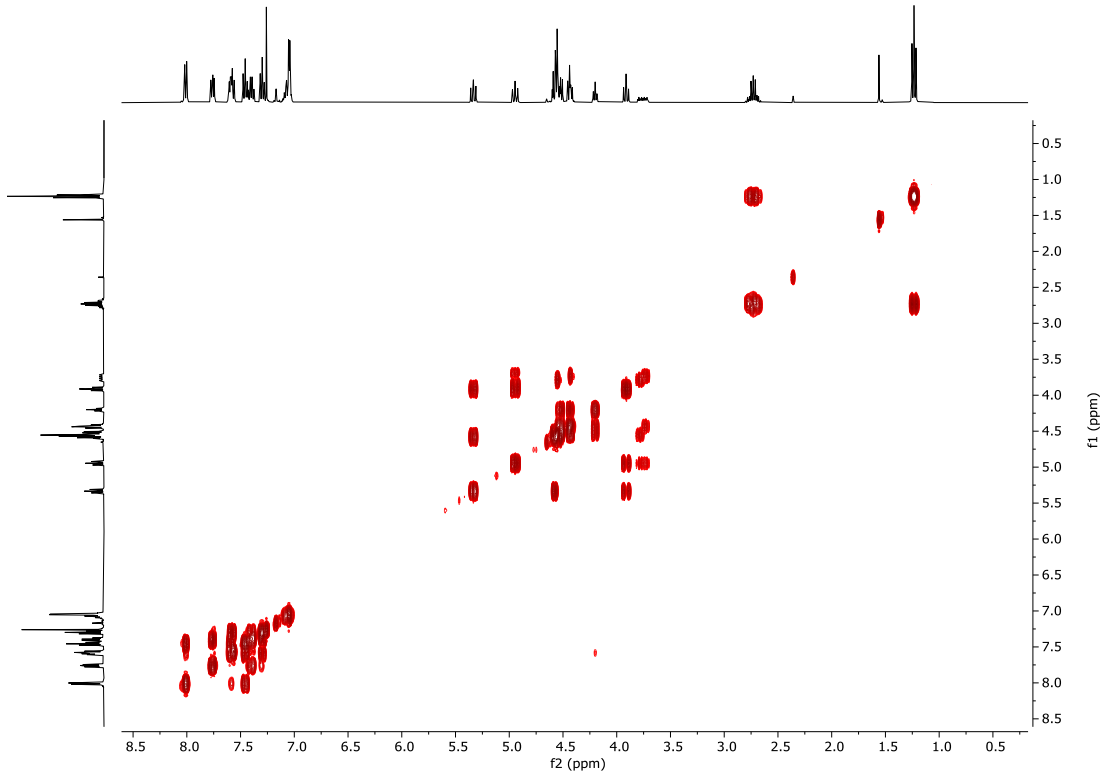

2.1.4 Synthesis of 8

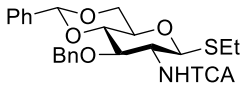

8

Compound **8** was synthesized according to a previously reported procedure.[3]

^{1}H NMR (400 MHz, Chloroform-*d*) δ 7.55 – 7.50 (m, 2H), 7.45 – 7.40 (m, 3H), 7.36 – 7.30 (m, 5H), 6.86 (d, *J* = 8.1 Hz, 1H), 5.63 (s, 1H), 5.05 (d, *J* = 10.5 Hz, 1H), 4.93 (d, *J* = 11.2 Hz, 1H), 4.74 (d, *J* = 11.2 Hz, 1H), 4.41 (dd, *J* = 10.5, 5.0 Hz, 1H), 4.22 – 4.13 (m, 1H), 3.88 – 3.75 (m, 2H), 3.71 (td, *J* = 10.0, 8.2 Hz, 1H), 3.60 (td, *J* = 9.8, 5.0 Hz, 1H), 2.84 – 2.67 (m, 2H), 1.33 – 1.26 (m, 3H).

^{1}H NMR of 8 (400 MHz, $CDCl_3$)

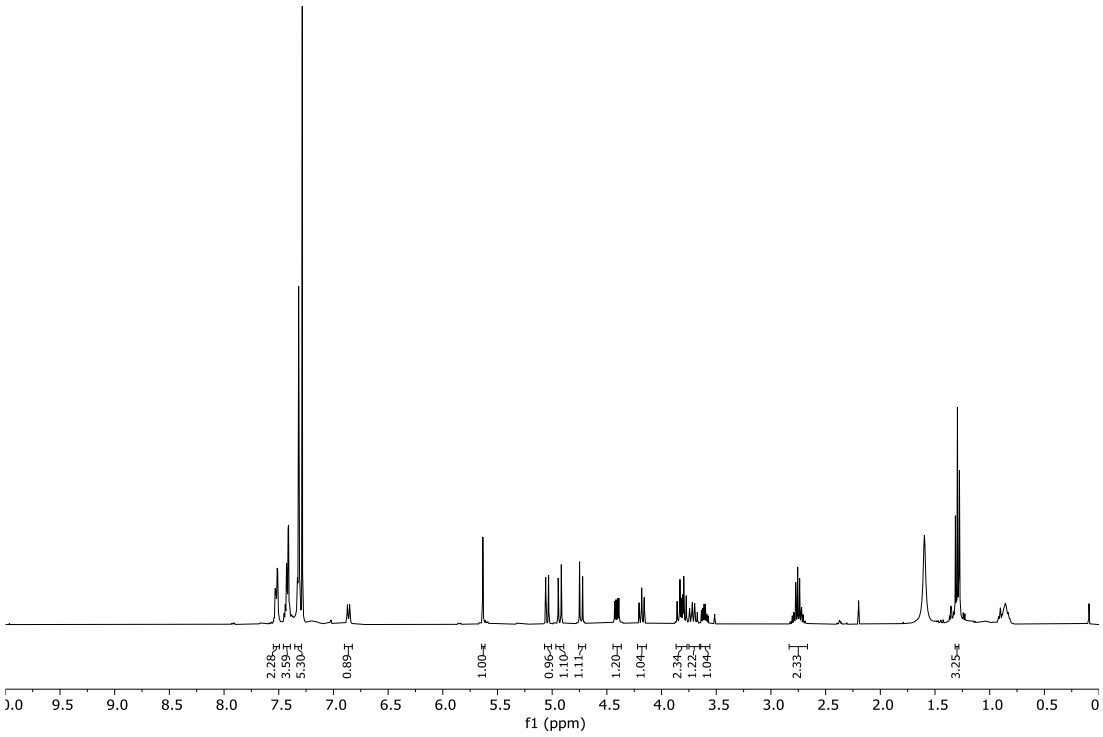

2.1.5 Synthesis of 9

8 **9** (88%)

8 (8.30 g, 15.2 mmol) was dissolved in anhydrous DCM (200 mL). EtSH (2.20 mL, 29.7 mmol) and pTsOH (577 mg, 3.0 mmol) were added to the reaction mixture under Ar atmosphere and stirred at RT. After 10 min, a white precipitate formed. The solution was stirred for 1 h and quenched with NEt_3 (1 mL). The crude reaction mixture was dried under vacuum and purified by flash column chromatography (Hexane : Acetone = 2:1→1:1→1:2) to give **9** as a white solid (6.17 g, 88%).

^{1}H NMR (400 MHz, MeOD) δ 7.44 – 7.16 (m, 6H), 4.89 (d, *J* = 8.5 Hz, 1H, C*H*$_2$ Bn (1)), 4.77 – 4.66 (m, 2H, C*H*$_2$ Bn (1), H-1), 3.95 – 3.81 (m, 2H, H-6, H-2), 3.75 – 3.64 (m, 2H, H-6', H-3), 3.57 – 3.49 (m, 1H, H-4), 3.42 – 3.33 (m, 1H, H-5), 2.84 – 2.65 (m, 2H, C*H*$_2$ Bn), 1.26 (t, *J* = 7.5 Hz, 3H, C*H*$_3$ Bn). ^{13}C NMR (101 MHz, MeOD) δ 163.88, 139.86, 129.17, 128.82, 128.51, 84.72 (C-1), 84.59 (C-6), 82.38 (C-5), 76.13, 72.07 (C-4), 62.79 (C-6), 57.35 (C-2), 24.89, 15.28. $[\alpha]_D^{20}$ -0.87 (c 1.05 g/100 mL, MeOH). IR ν = 3322, 2931, 1691, 1527, 1071, 1043, 822 cm^{-1}. (ESI-HRMS) m/z 480.0172 $[M+Na]^+$ ($C_{17}H_{22}Cl_3NO_5SNa$ requires 480.0176).

^{1}H NMR of 9 (400 MHz, MeOD)

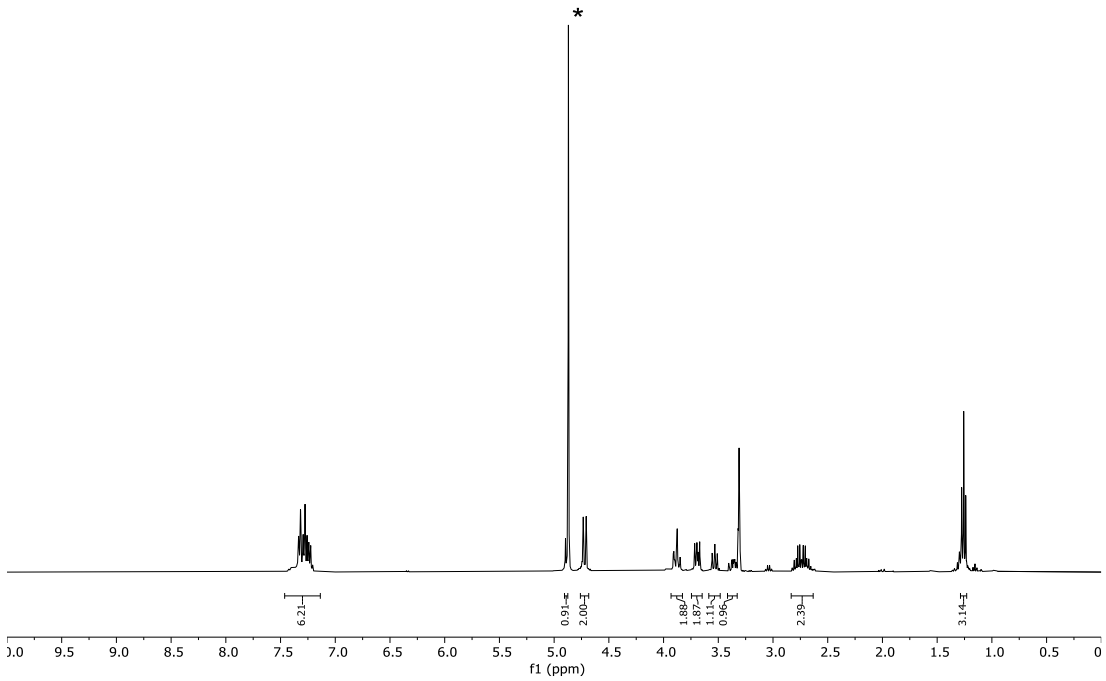

*The peak at 4.87 ppm belongs to residual water.

^{13}C NMR of 9 (101 MHz, MeOD)

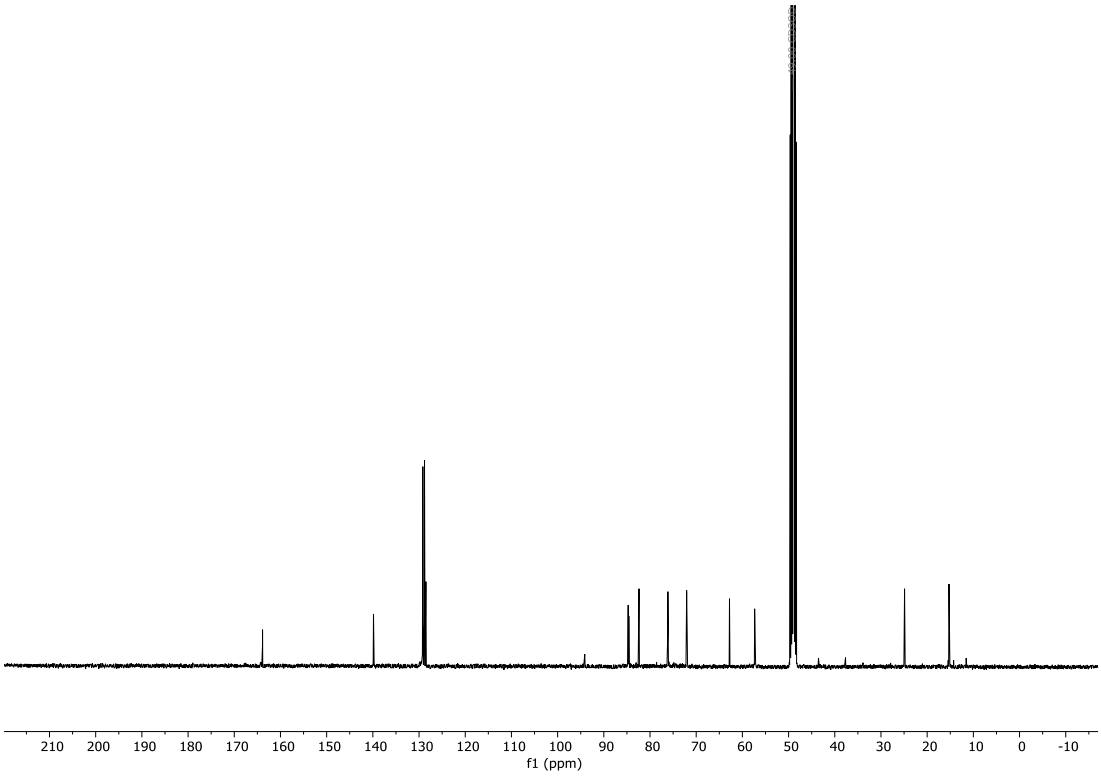

HSQC NMR of 9 (MeOD)

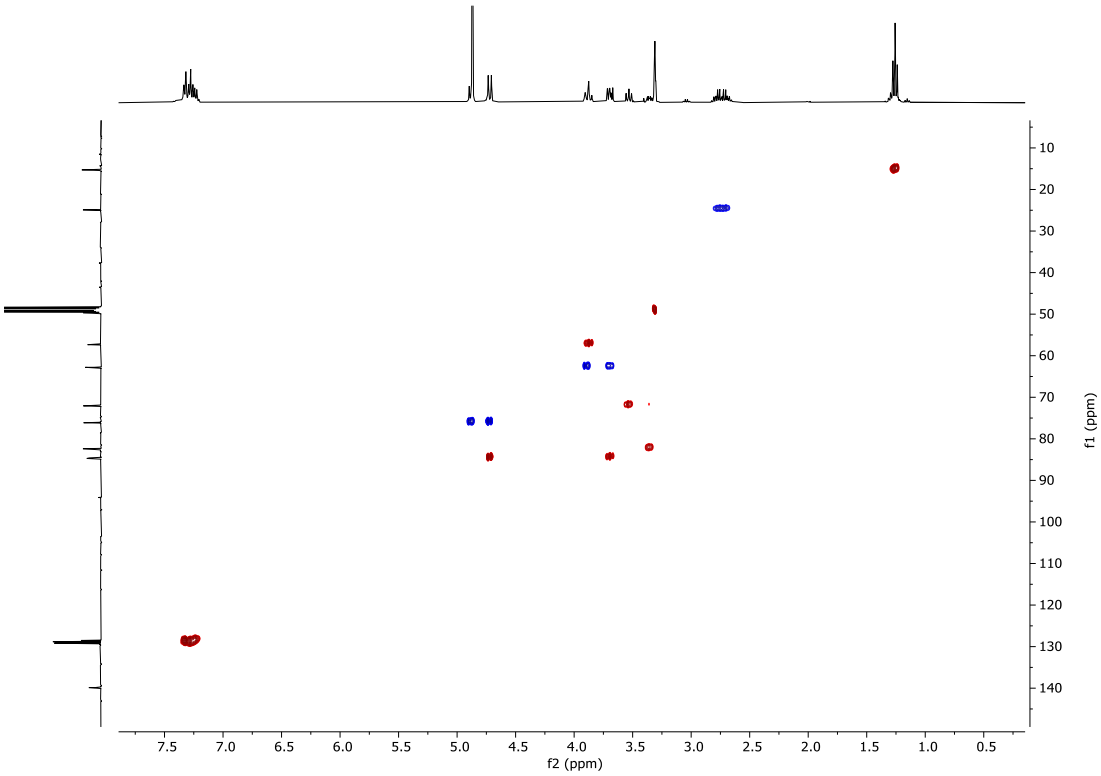

COSY NMR of 9 (MeOD)

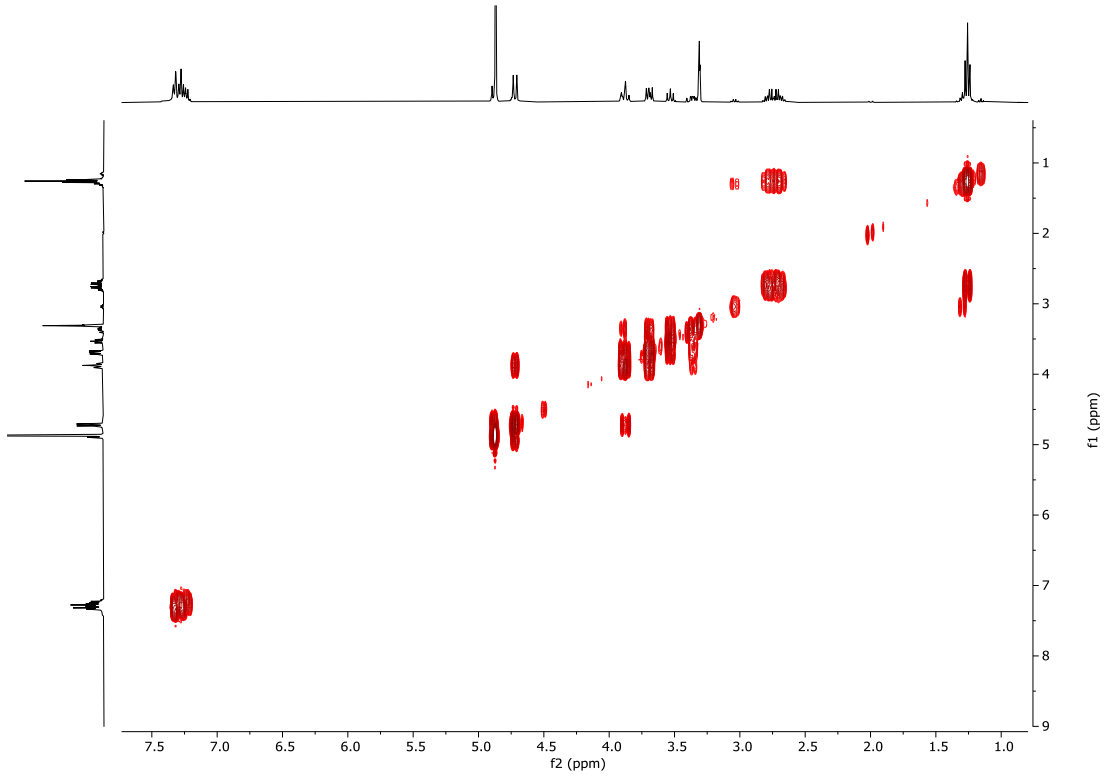

2.1.6 Synthesis of 10

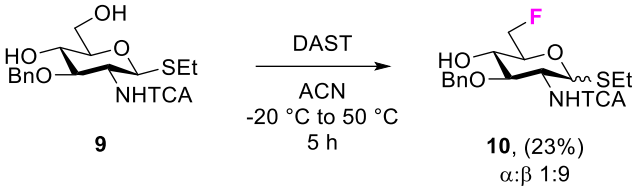

9 **10**, (23%)
α:β 1:9

9 (6.17 g, 13.4 mmol) was dissolved in anhydrous ACN (130 mL) and cooled down to -20 °C. DAST (1.96 mL, 14.8 mmol) was added dropwise to the reaction mixture under Ar atmosphere. After 20 min the cooling bath was removed and the reaction heated to 50 °C. The solution was stirred for additional 3 h and quenched with MeOH at 0 °C. During the reaction, anomerization was observed. The crude reaction mixture was dried under vacuum and purified by flash column chromatography (Hexane : EtOAc = 3:1→2:1→1:1) to give **10** as an inseparable mixture of anomers (1.42 mg, 23%, α:β ratio 7:93).

Analytical data for the β anomer: ^{1}H NMR (400 MHz, Chloroform-*d*) δ 7.45 – 7.27 (m, 5H), 6.94 (d, *J* = 8.1 Hz, 1H, N*H*), 4.98 (d, *J* = 10.3 Hz, 1H, H-1 β), 4.84 (d, *J* = 11.3 Hz, 1H, C*H*$_2$ Bn (1)), 4.76 – 4.51 (m, 3H, C*H*$_2$ Bn (1), H-6, H-6'), 3.98 (dd, *J* = 10.0, 8.4 Hz, 1H, H-3), 3.71 – 3.48 (m, 3H, H-2, H-4, H-5), 2.82 – 2.63 (m, 2H, C*H*$_2$ SEt), 2.23 (s, 1H, OH-4), 1.28 (t, *J* = 7.4 Hz, 3H, C*H*$_3$ SEt). ^{13}C NMR (101 MHz, Chloroform-*d*) δ 161.87, 137.73, 129.00, 128.53, 128.20, 82.69 (C-1), 82.13 (d, *J* = 173.4 Hz, C-6), 81.78 (C-3), 78.49 (d, *J* = 18.4 Hz, C-5), 75.12, 69.91 (d, *J* = 7.2 Hz, C-4), 57.52 (C-2), 24.74, 15.21. ^{19}F NMR (376 MHz, Chloroform-*d*) δ -234.01 (td, *J* = 47.1, 22.9 Hz, F-6 β), -236.12 (td, *J* = 47.4, 26.7 Hz, F-6 α). $[\alpha]_D^{20}$ -23.91 (c 0.7 g/100 mL, $CHCl_3$). IR *ν* = 3302, 2928, 1688, 1539, 1084. 834, 825 cm^{-1}. (ESI-HRMS) m/z 482.0163 $[M+Na]^+$ ($C_{17}H_{21}Cl_3FNO_4SNa$ requires 482.0133).

^{1}H NMR of 10 (400 MHz, $CDCl_3$)

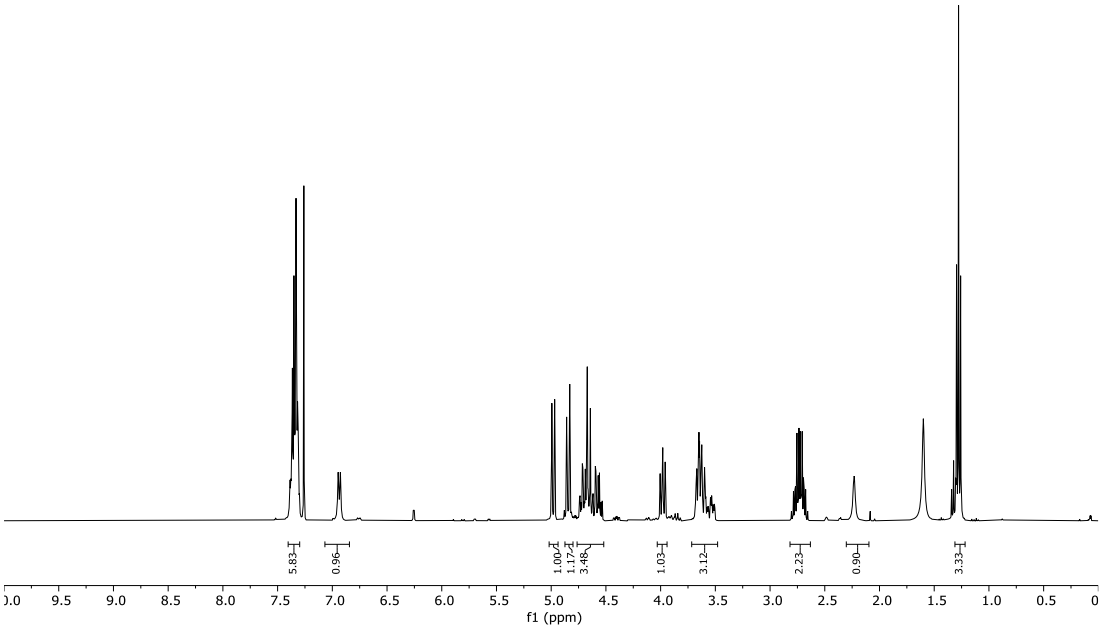

^{13}C NMR of 10 (101 MHz, $CDCl_3$)

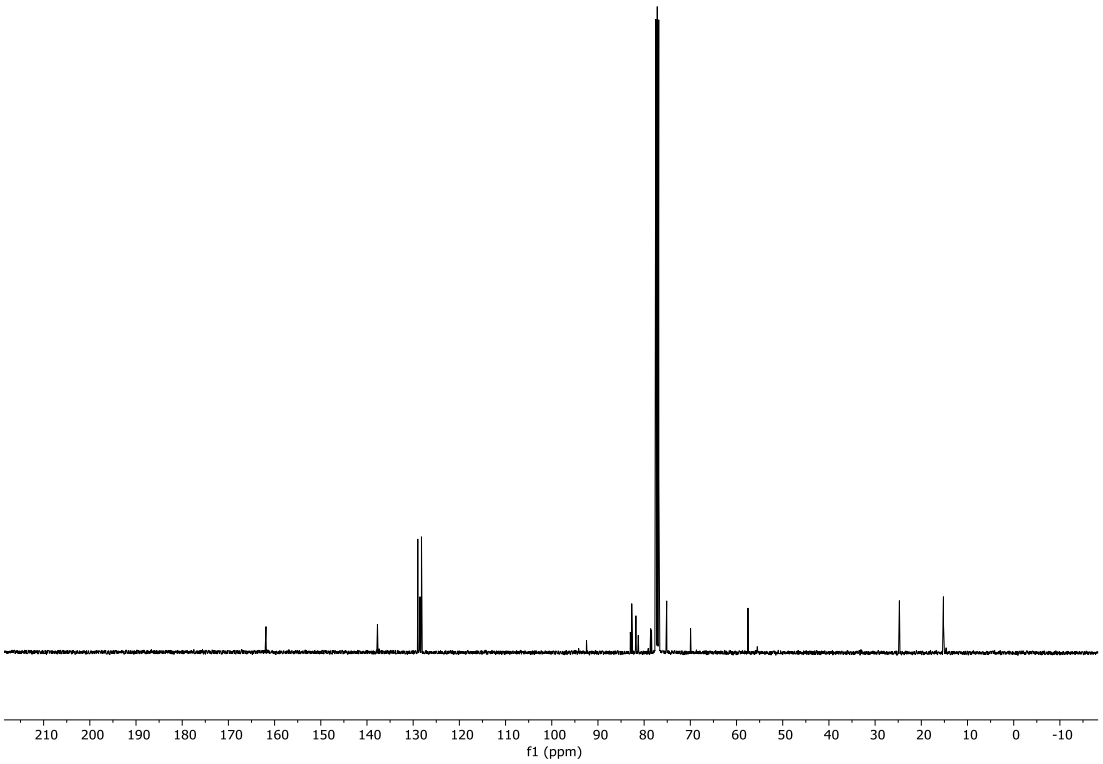

^{19}F NMR of 10 (101 MHz, $CDCl_3$)

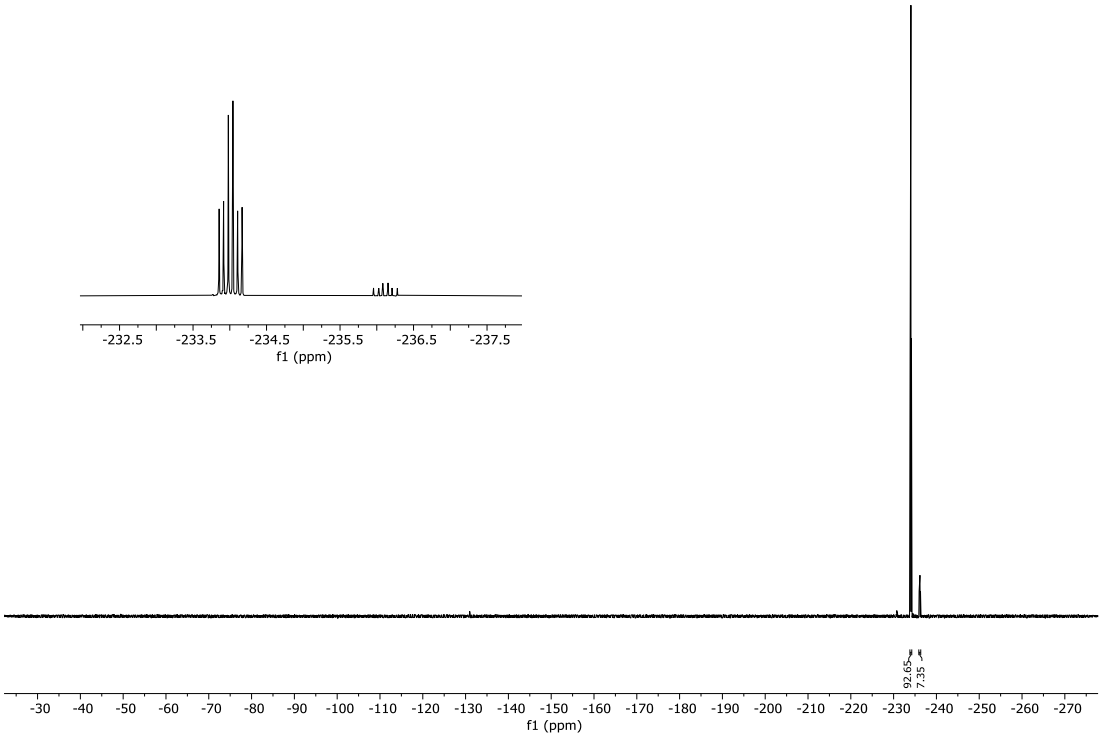

HSQC NMR of 10 ($CDCl_3$)

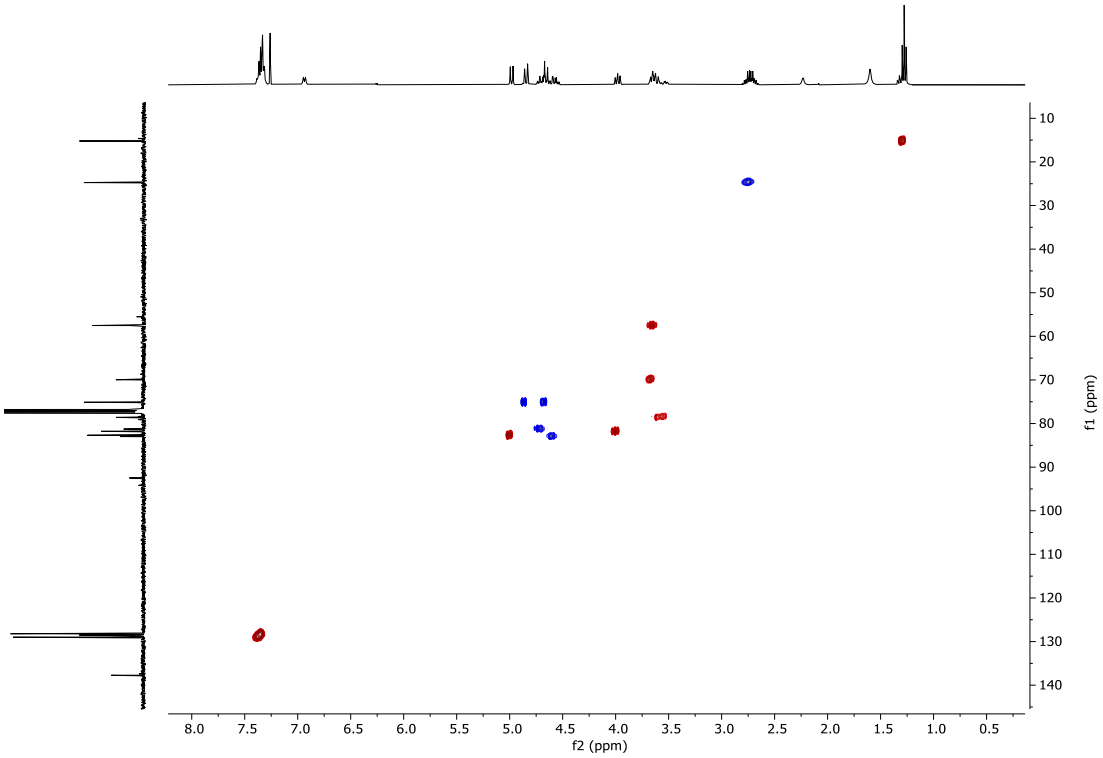

COSY NMR of 10 ($CDCl_3$)

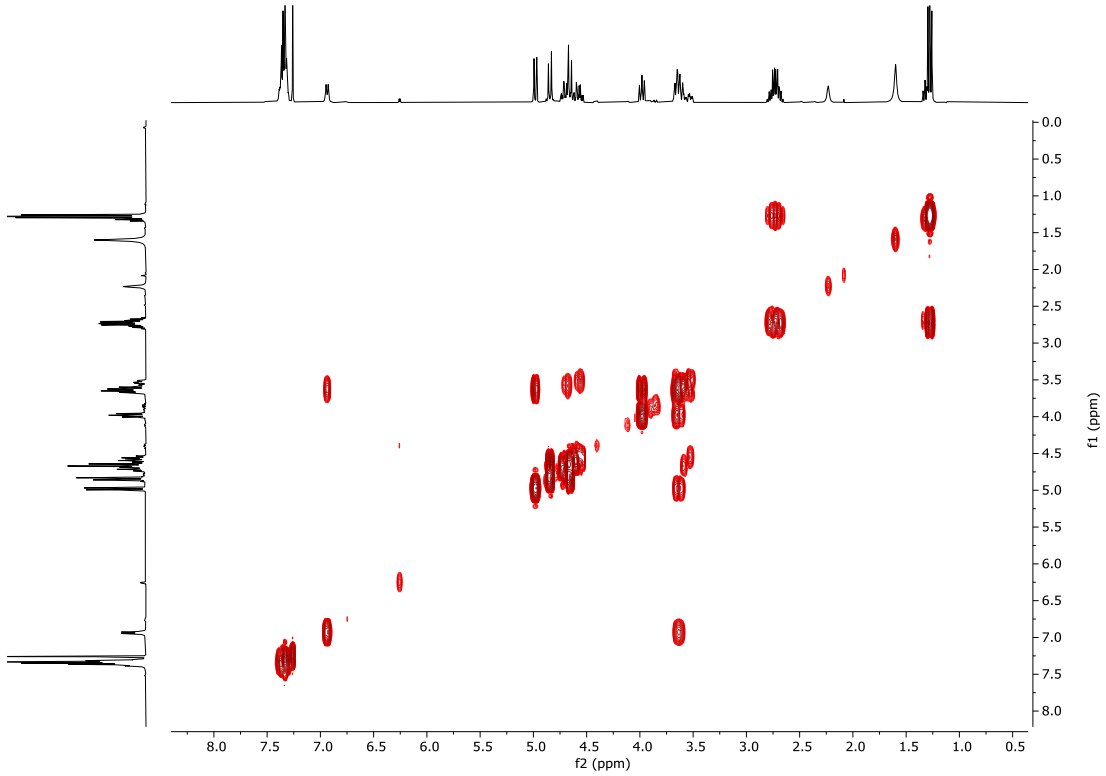

2.1.7 Synthesis of 11

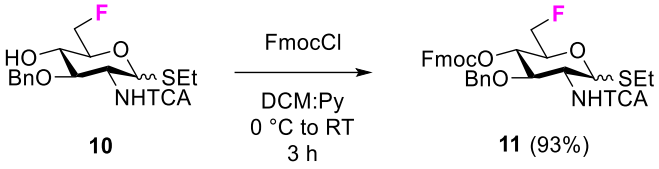

10 (1.42 g, 3.1 mmol) was dissolved in DCM:Py (3:1, 15 mL) and cooled to 0 °C. FmocCl (1.60 g, 6.2 mmol) was dissolved in DCM (0.5 mL) and added to the reaction mixture under Ar atmosphere. The solution was stirred for 20 min at 0 °C then warmed up to RT and stirred for additional 3 h, after which time it was quenched with a 0.5 M solution of citric acid. The crude reaction mixture was diluted with DCM, washed once with 0.5 M citric acid and once with brine. The crude compound was purified by silica gel flash column chromatography (Hexane : Acetone = 3:1→2:1→1:1) and recrystallized from DCM : Hexane to give **11** as an inseparable mixture of anomers (1.84 g, 87%, α:β ratio 3:97).

Analytical data for the β anomer: ^{1}H NMR (400 MHz, Chloroform-*d*) δ 7.76 (dd, J = 7.6, 3.1 Hz, 2H), 7.61 – 7.51 (m, 2H), 7.40 (tt, J = 7.6, 1.7 Hz, 2H), 7.31 – 7.16 (m, 7H), 6.98 (d, J = 8.0 Hz, 1H, N*H*), 5.09 (d, J = 10.2 Hz, 1H, H-1), 4.88 (t, J = 9.5 Hz, 1H, H-4), 4.63 (s, 2H, C*H*$_2$ Fmoc), 4.56 – 4.48 (m, 2H, C*H*$_2$ Bn (1), H-6), 4.45 – 4.36 (m, 2H, C*H*$_2$ Bn (1), H-6'), 4.28 (t, J = 9.4 Hz, 1H, H-3), 4.19 (t, J = 6.9 Hz, 1H, CH Fmoc), 3.76 (dddd, J = 20.5, 10.0, 4.6, 2.9 Hz, 1H, H-5), 3.68 – 3.53 (m, 1H, H-2), 2.83 – 2.65 (m, 2H, C*H*$_2$ SEt), 1.28 (t, J = 7.4 Hz, 3H, C*H*$_3$ SEt). ^{13}C NMR (101 MHz, Chloroform-*d*) δ 161.88, 154.31, 143.13 (d, J = 1.5 Hz), 141.45, 137.25, 128.58, 128.12, 127.96, 127.34, 125.15, 124.99, 120.28, 120.25, 82.44 (C-1), 81.57 (d, J = 175.4 Hz, C-6), 78.50 (C-3), 76.66 (d, J z= 19.6 Hz, C-5), 74.99, 74.70 (d, J = 6.1 Hz, C-4), 70.35, 57.73 (C-2), 46.84, 24.88, 15.24. ^{19}F NMR (376 MHz, Chloroform-*d*) δ -231.05 (td, J = 47.0, 20.5 Hz, F-6 β), -232.92 (td, J = 47.3, 23.9 Hz, F-6 α). $[\alpha]_D^{20}$ +14.06 (c 1.0 g/100 mL, $CHCl_3$). IR ν = 3321, 1754, 1692, 1530, 1257, 758, 742 cm^{-1}. (ESI-HRMS) m/z 704.0836 $[M+Na]^+$ ($C_{32}H_{31}Cl_3FNO_6SNa$ requires 704.0814).

^{1}H NMR of 11 (400 MHz, $CDCl_3$)

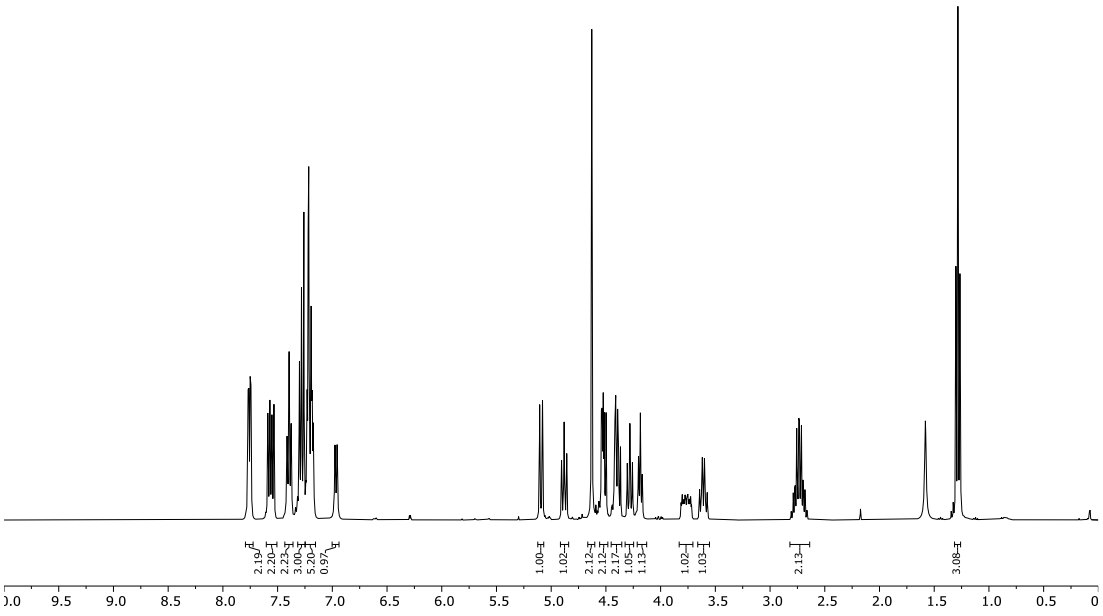

^{13}C NMR of 11 (101 MHz, $CDCl_3$)

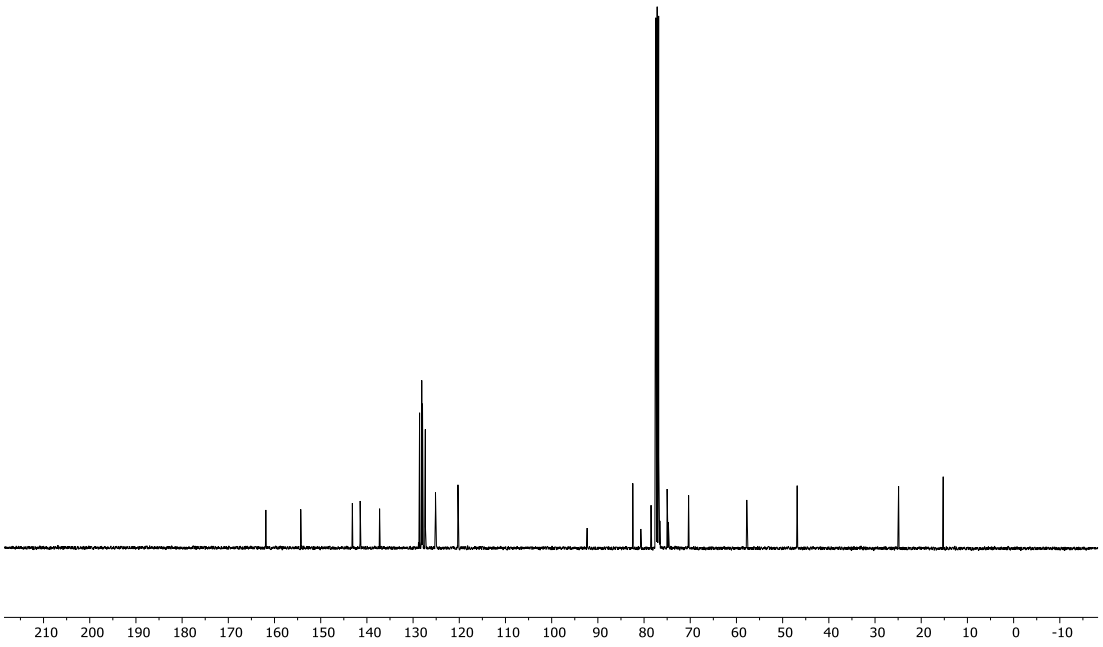

^{19}F NMR of 11 (101 MHz, $CDCl_3$)

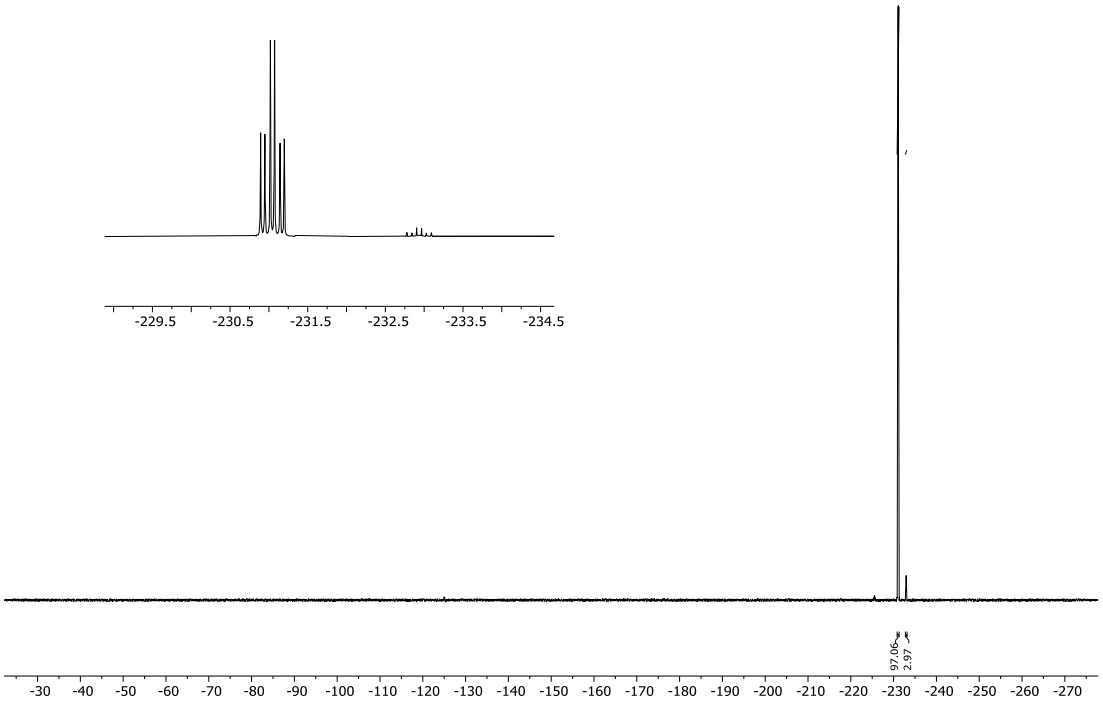

HSQC NMR of 11 ($CDCl_3$)

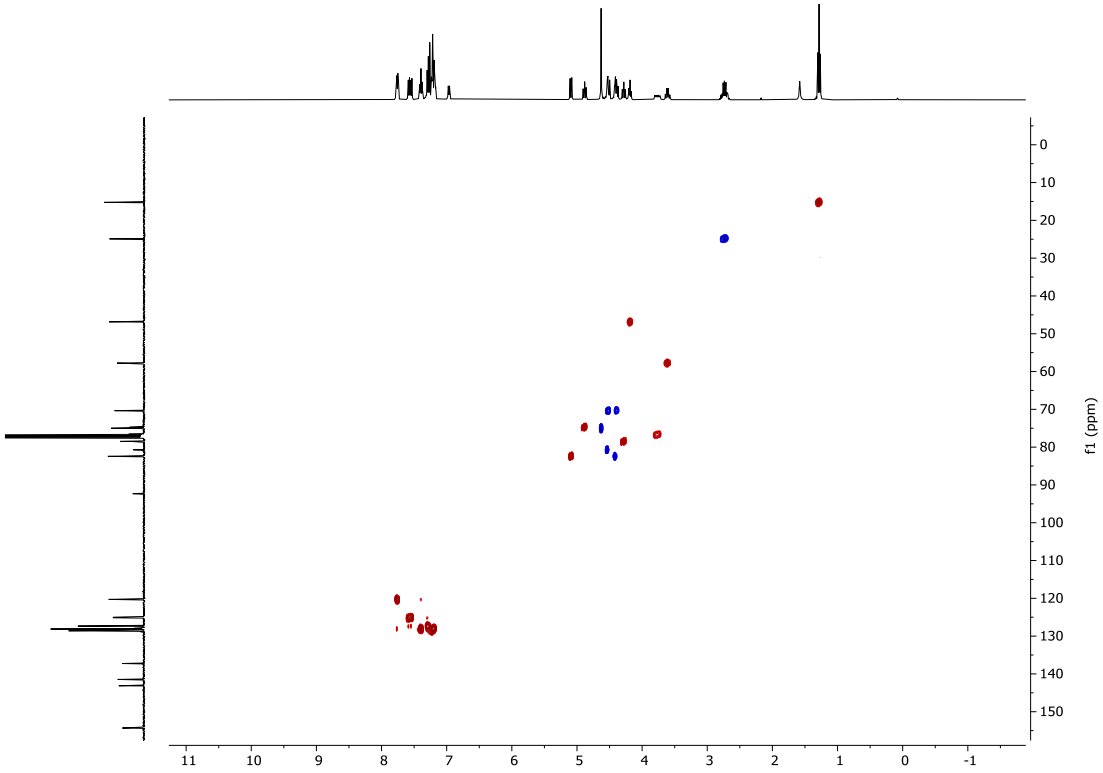

COSY NMR of 11 ($CDCl_3$)

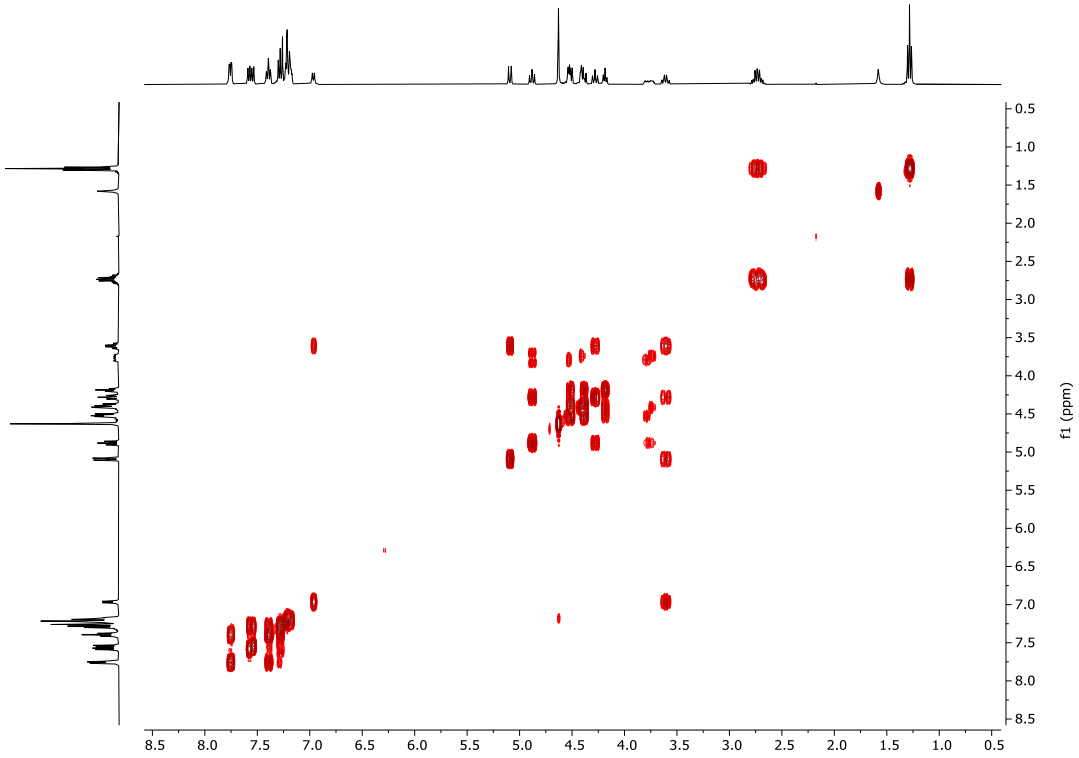

2.1.8 Synthesis of BB5

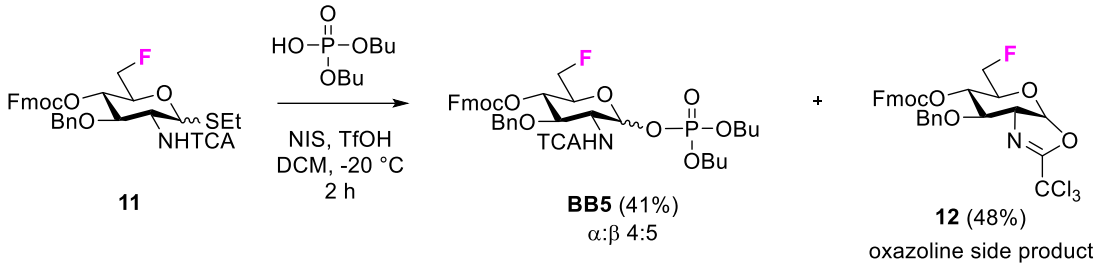

11 (1.90 g, 2.78 mmol) was co-evaporated with toluene three times and dissolved in anhydrous DCM (35 mL). Activated molecular sieves (4 Å) were added to the mixture and the suspension was stirred at RT for 1 h. A solution of dibutyl phosphate (15 mL of a 7%$_v$ solution in DCM stirred in presence of activated 4 Å molecular sieves for 1 h, 5.30 mmol) was added to the solution of **11** and cooled down to -20 °C. NIS (751 mg, 3.34 mmol) and TfOH (17.5 µL, 0.20 mmol) were added and the reaction was slowly allowed to RT. After 2 h, the reaction was quenched with $NaHCO_3$ saturated aqueous solution, filtered, diluted with DCM and washed once with 10% aqueous $Na_2S_2O_3$. The organic layer was dried over Na_2SO_4, concentrated under vacuum and purified by silica gel column chromatography (Hexane : Acetone 5:1→4:1→3:1→2:1) to obtain **BB5** as a sticky colorless solid (952 mg, 41% mixture of anomers, α:β ratio 4:5). The oxazoline side product **12** formed during the reaction and was isolated as a sticky colorless solid (827 mg, 48%).

Analytical data for **BB5**:

^{1}H NMR (400 MHz, $CDCl_3$) δ 8.00 (d, *J* = 6.3 Hz, 0.5H, NH α), 7.81 – 7.72 (m, 2H), 7.62 – 7.49 (m, 2H), 7.40 (td, *J* = 7.4, 4.2 Hz, 2H), 7.32 – 7.27 (m, 2H), 7.25 – 7.17 (m, 5H), 6.88 (d, *J* = 8.6 Hz, 0.5H, NH β), 5.74 (dd, *J* = 6.0, 3.3 Hz, 0.5H, H-1 β), 5.60 – 5.54 (m, 0.5H, H-1α), 4.99 (dd, *J* = 10.4, 9.1 Hz, 0.5H, H-4 β), 4.93 – 4.82 (m, 0.5H, H-3 α), 4.70 – 4.56 (m, 2H, C*H*$_2$ Fmoc), 4.56 – 4.37 (m, 4H, C*H*$_2$ Bn, H-6, H-6'), 4.31 (ddt, *J* = 11.7, 8.8, 3.1 Hz, 0.5H, H-2 β), 4.27 – 3.94 (m, 7H, C*H* Fmoc, H-2 α, -O-C*H*$_2$- Bu x2, H-5 β, H-3 β, H-5 α), 3.80 (ddt, *J* = 18.6, 8.8, 3.8 Hz, 0.5H, H-4 β), 1.76 – 1.55 (m, 4H, -C*H*$_2$- Bu x2), 1.40 (dq, *J* = 14.9, 7.4 Hz, 4H, -C*H*$_2$- Bu x2), 1.00 – 0.87 (m, 6H, C*H*$_3$ Bu x2). ^{13}C NMR (101 MHz, $CDCl_3$) δ 162.37, 162.07, 154.33, 154.15, 143.20, 143.12, 143.06, 143.03, 141.49, 141.46, 137.33, 137.05, 128.69, 128.50, 128.18, 128.15, 128.03, 128.01, 127.36, 127.34, 125.11, 125.09, 124.97, 96.32 (C-1 α), 95.35 (d, *J* = 6.5 Hz, C-1 β), 81.39 (d, *J* = 175.4 Hz, C-6 α or β), 81.00 (d, *J* = 176.3 Hz, C-6 α or β), 78.10 (C-5 α), 75.95 (C-3 β), 74.41 (d, *J* = 13.7 Hz), 73.57 (C-3 α, C-4 β), 73.37 (C-4 α) , 70.73 (d, *J* = 19.4 Hz, C-5 β), 70.38, 70.36, 68.88, 68.81, 68.65, 68.58, 68.55, 68.52, 68.50, 56.90 (d, *J* = 8.9 Hz, C-2 β), 54.33 (d, *J* = 7.8 Hz, C-2 α), 46.90, 46.87, 32.37, 32.35, 32.31, 32.29, 32.21, 32.12, 32.04, 18.73, 18.70, 13.73, 13.70, 13.68. ^{31}P NMR (162 MHz, $CDCl_3$) δ -2.75, -3.58. ^{19}F NMR (376 MHz, $CDCl_3$) δ -230.70 (td, *J* = 46.9, 18.9 Hz), -231.98 (td, *J* = 47.0, 22.4 Hz). IR *ν* = 3252, 2963, 1756, 1719, 1259, 1029, 968 cm^{-1}. (ESI-HRMS) m/z 852.1664 $[M+Na]^+$ ($C_{38}H_{44}Cl_3FNO_{10}PNa$ requires 852.1644).

Analytical data for **12**:

^{1}H NMR (400 MHz, $CDCl_3$) δ 7.82 – 7.76 (m, 2H), 7.65 – 7.59 (m, 2H), 7.44 (t, *J* = 7.5 Hz, 2H), 7.40 – 7.27 (m, 7H), 6.39 (d, *J* = 7.4 Hz, 1H, H-1), 4.98 (dt, *J* = 8.0, 1.6 Hz, 1H, H-4), 4.86 (d, *J* = 12.2 Hz, 1H, C*H*$_2$ Bn (1)), 4.71 (d, *J* = 12.2 Hz, 1H, C*H*$_2$ Bn (1)), 4.65 (dd, *J* = 7.7, 3.6 Hz, 1H, H-6), 4.53 (dd, *J* = 7.4, 3.6 Hz, 1H, H-6'), 4.50 – 4.40 (m, 3H, C*H*$_2$ Fmoc, H-2), 4.27 (t, *J* = 7.5 Hz, 1H, C*H* Fmoc), 4.19 (s, 1H, H-3), 3.88 (dddd, *J* = 22.5, 7.4, 4.4, 2.7 Hz, 1H, H-5). ^{13}C NMR (101 MHz, $CDCl_3$) δ 163.02, 154.16, 143.16, 143.10, 141.43, 141.41, 137.13, 128.69, 128.28, 128.17, 128.12, 127.37, 127.31, 125.34, 125.29, 103.73 (H-1), 82.24 (d, *J* = 176.8 Hz, C-6), 73.48 (C-3), 71.95, 70.47, 69.89 (d, *J* = 6.7 Hz, C-4), 69.40 (d, *J* = 19.1 Hz, C-5), 65.52 (C-2), 46.72. ^{19}F NMR (376 MHz, $CDCl_3$) δ -230.89 (td, *J* = 47.1, 22.5 Hz). IR *ν* = 2956, 1751, 1259, 981, 742 cm^{-1}. (ESI-HRMS) m/z 620.1012 $[M+Na]^+$ ($C_{30}H_{26}Cl_3FNO_6$ requires 620.0804).

^{1}H NMR of BB5 (400 MHz, $CDCl_3$)

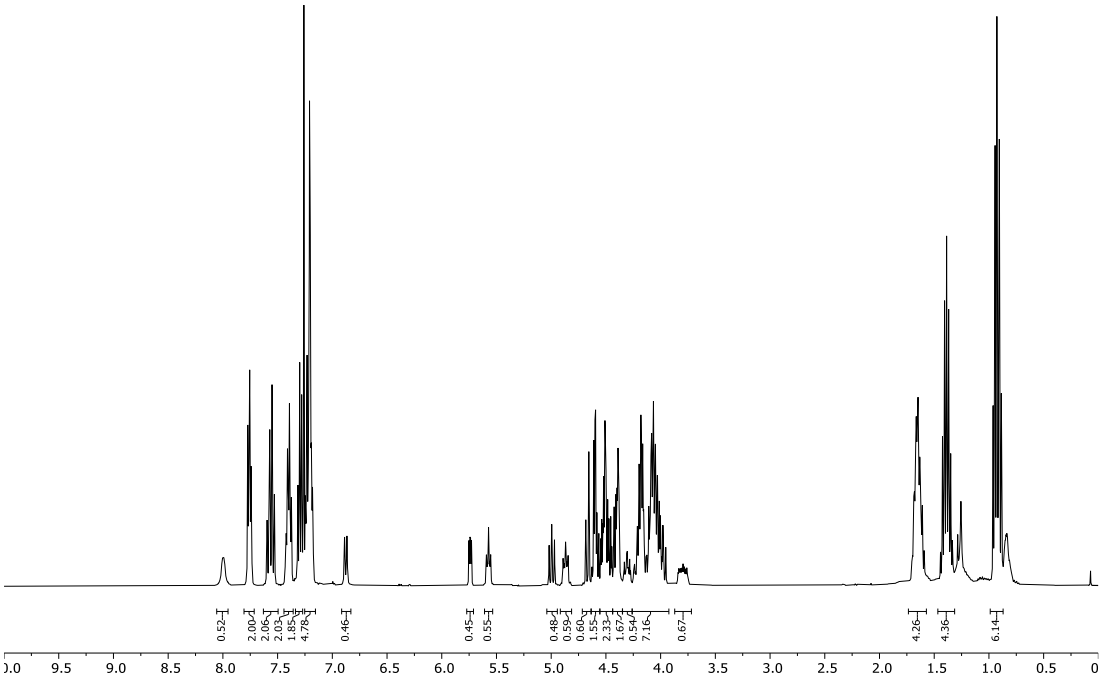

^{13}C NMR of BB5 (101 MHz, $CDCl_3$)

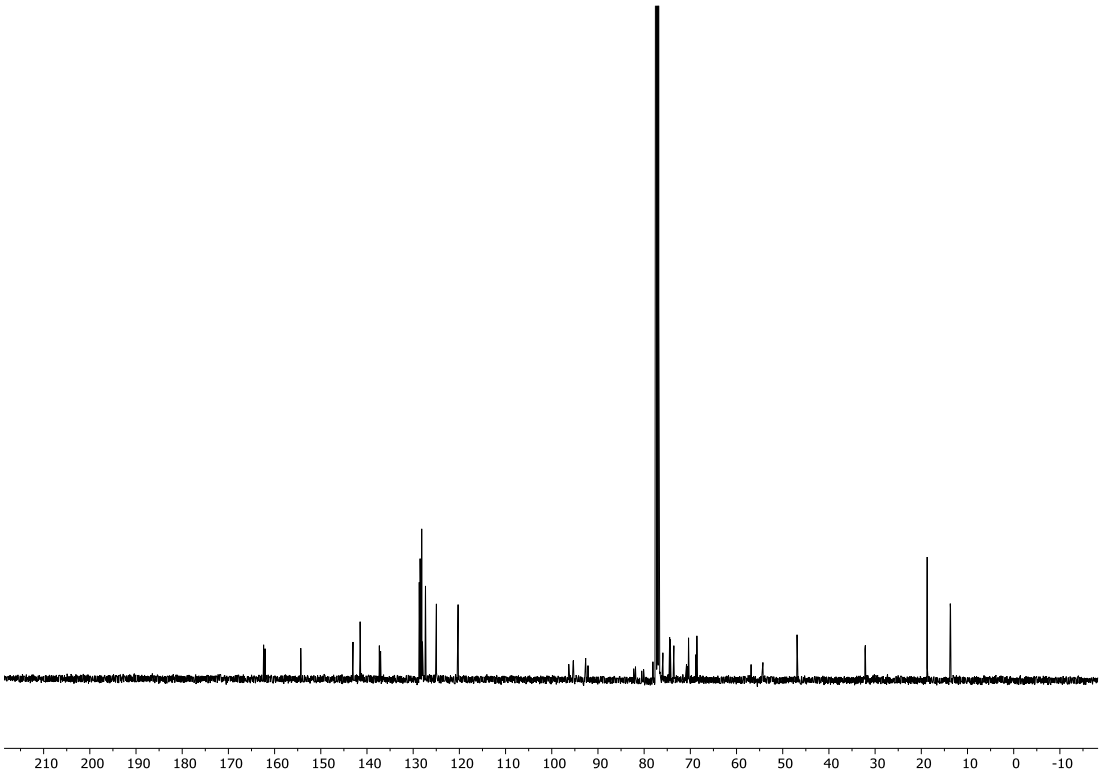

^{31}P NMR of BB5 (162 MHz, $CDCl_3$)

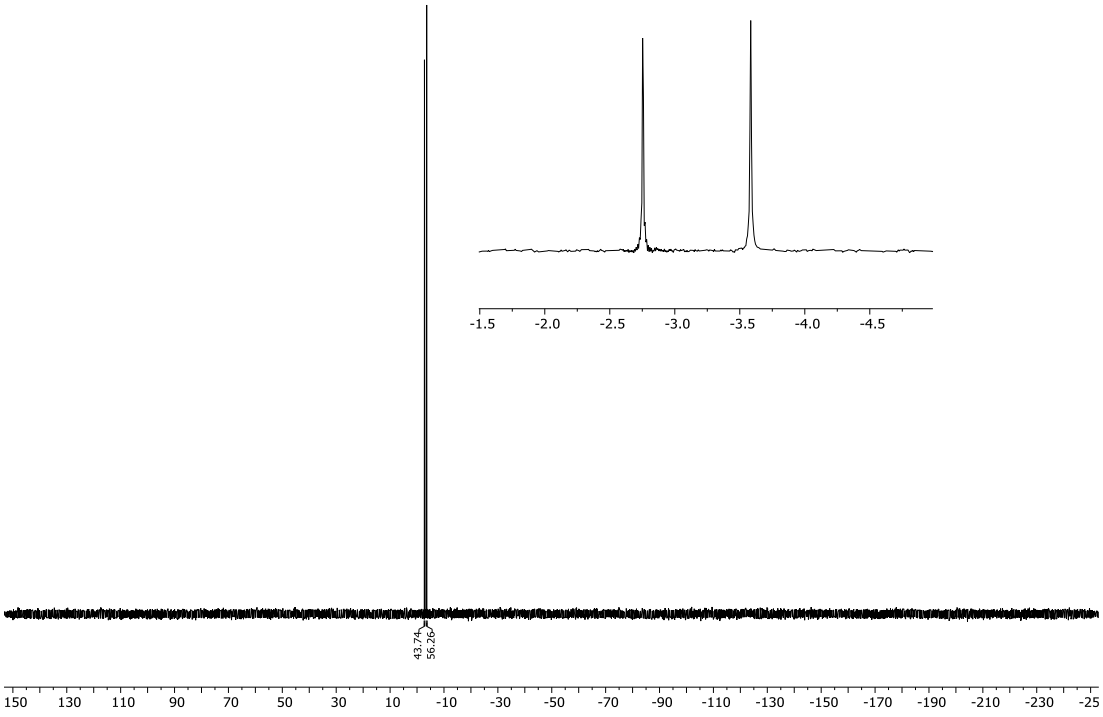

^{19}F NMR of BB5 (101 MHz, $CDCl_3$)

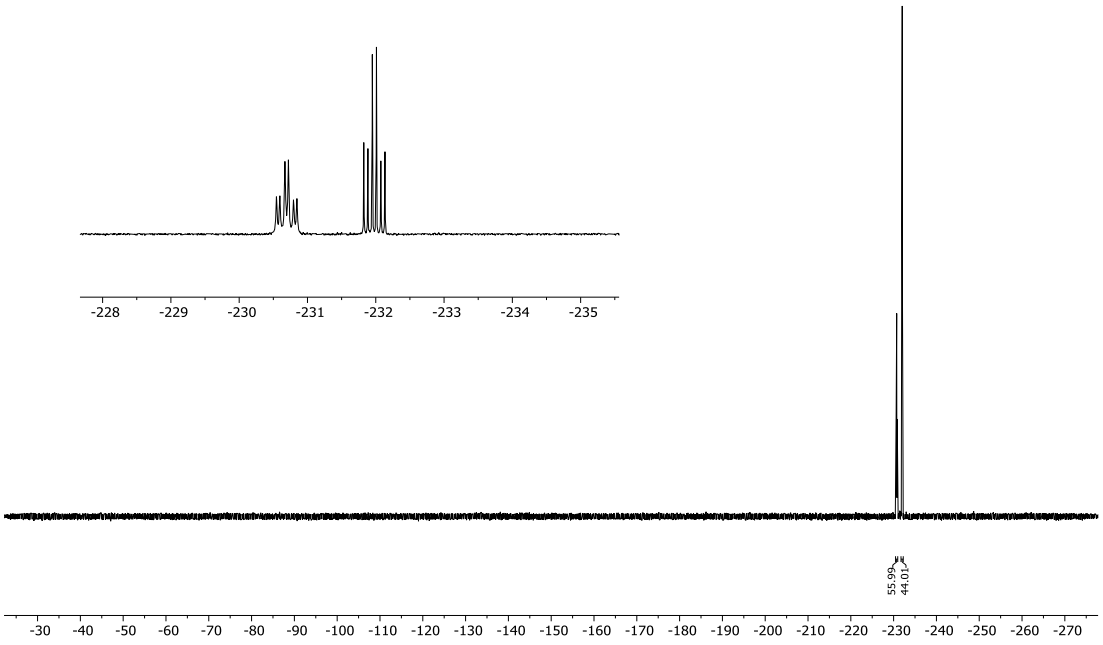

HSQC NMR of BB5 ($CDCl_3$)

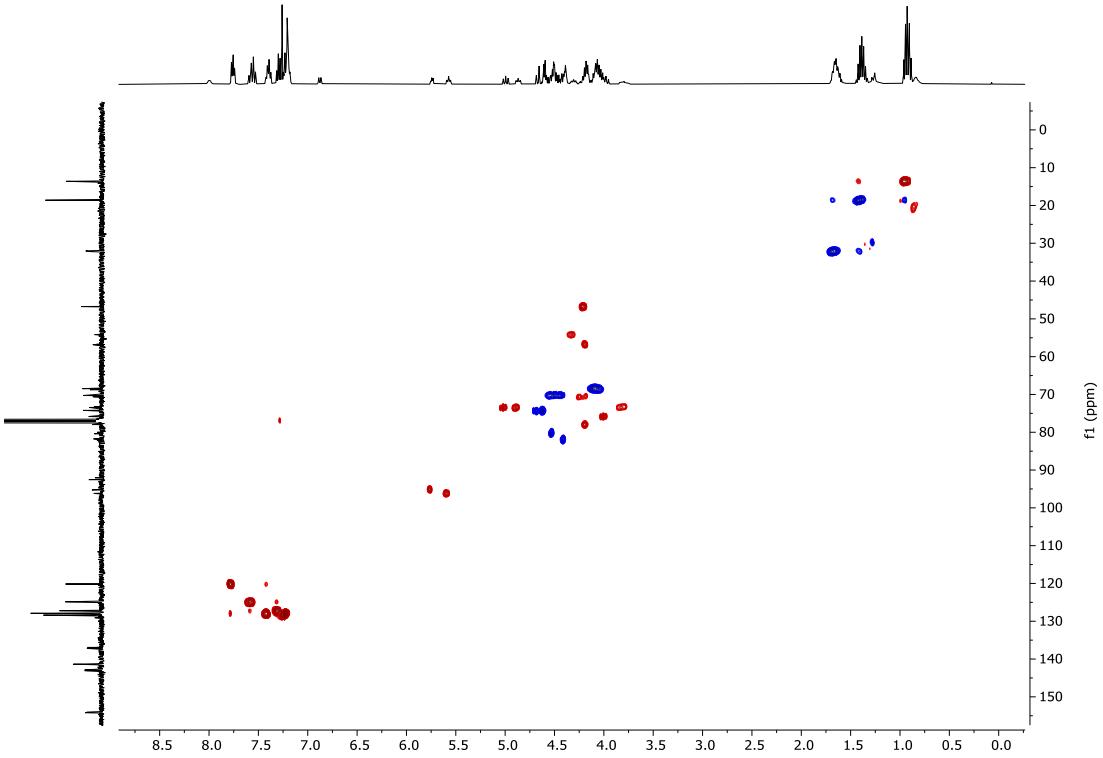

Coupled HSQC NMR of BB5 ($CDCl_3$)

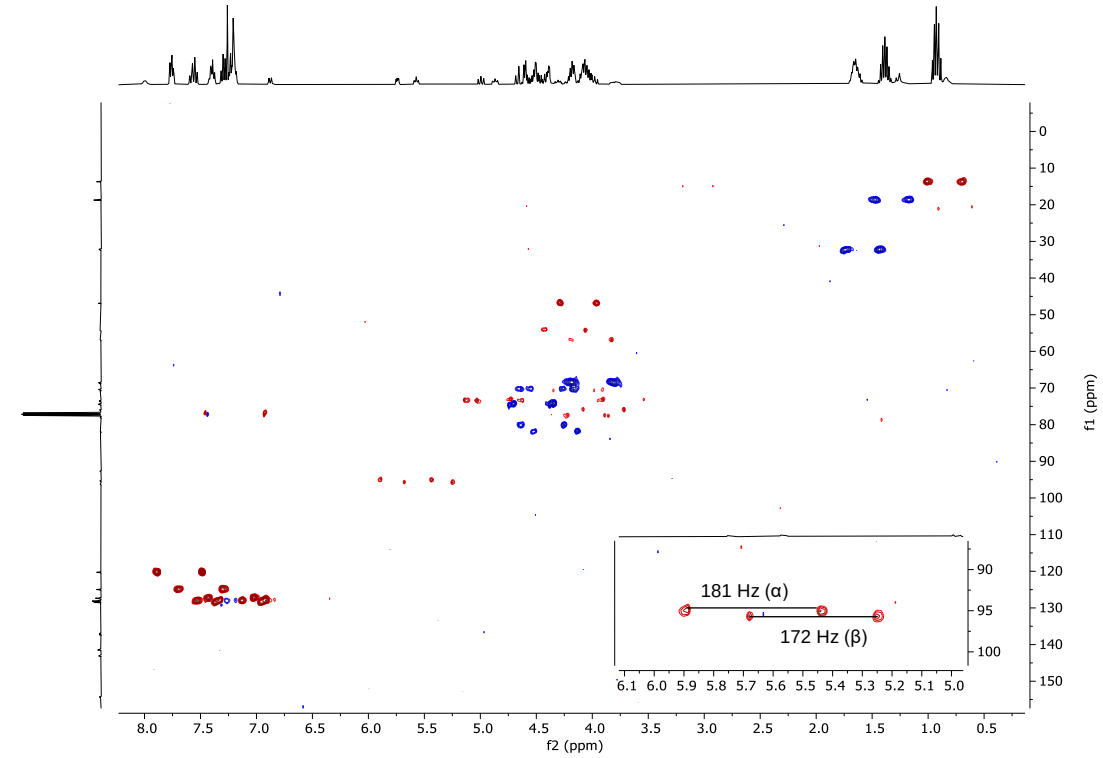

COSY NMR of BB5 ($CDCl_3$)

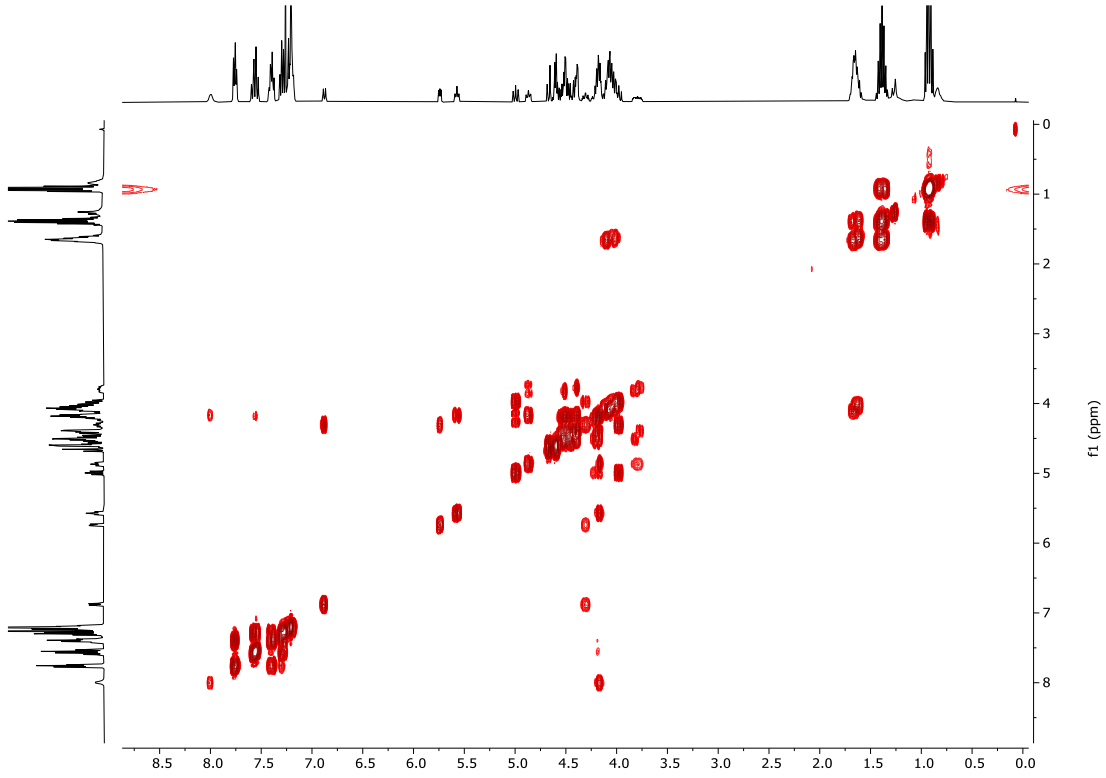

^{1}H NMR of 12 (400 MHz, $CDCl_3$)

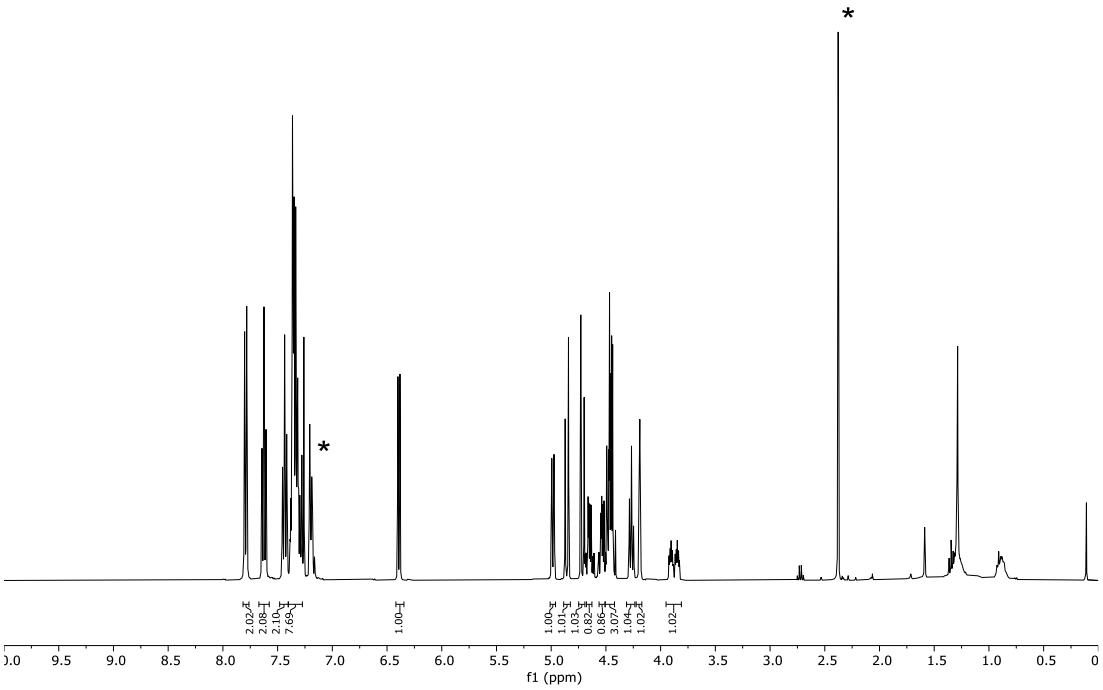

*Peaks belonging to residual Toluene.

^{13}C NMR of 12 (101 MHz, $CDCl_3$)

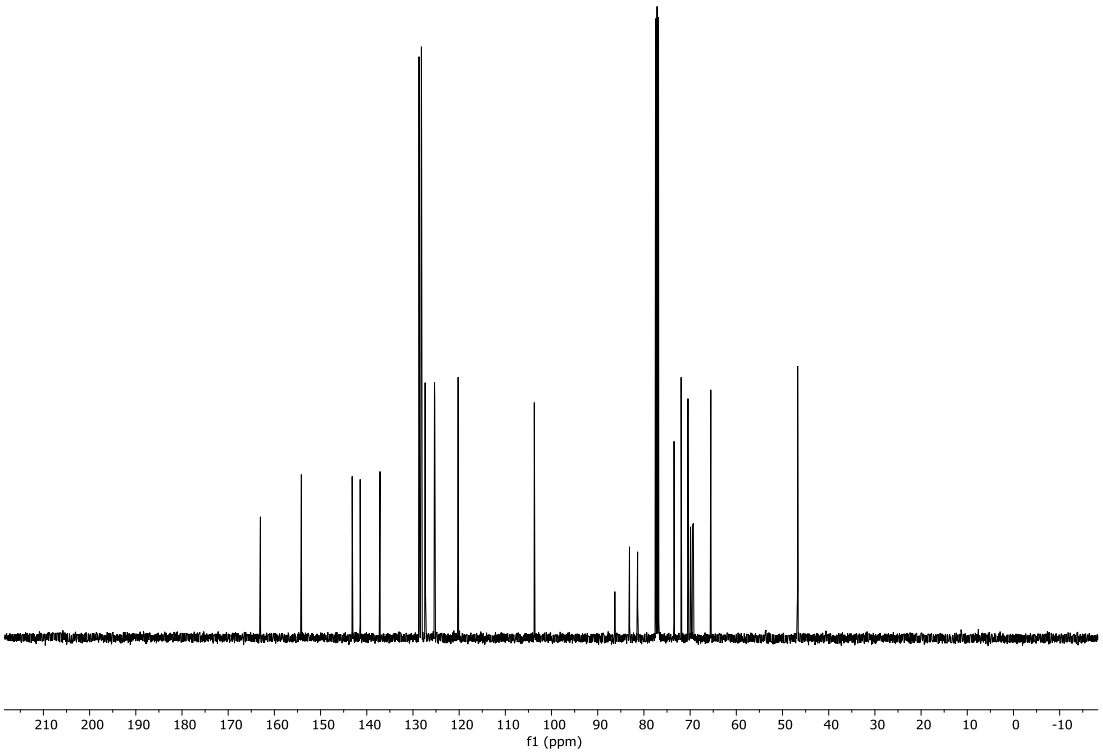

^{19}F NMR of 12 (101 MHz, $CDCl_3$)

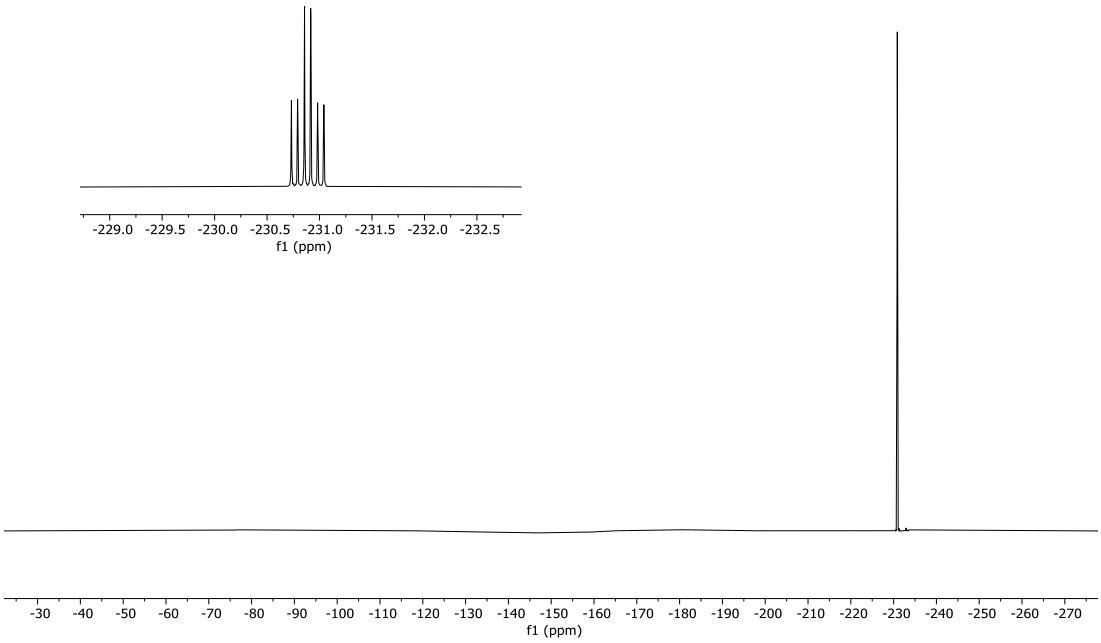

HSQC NMR of 12 ($CDCl_3$)

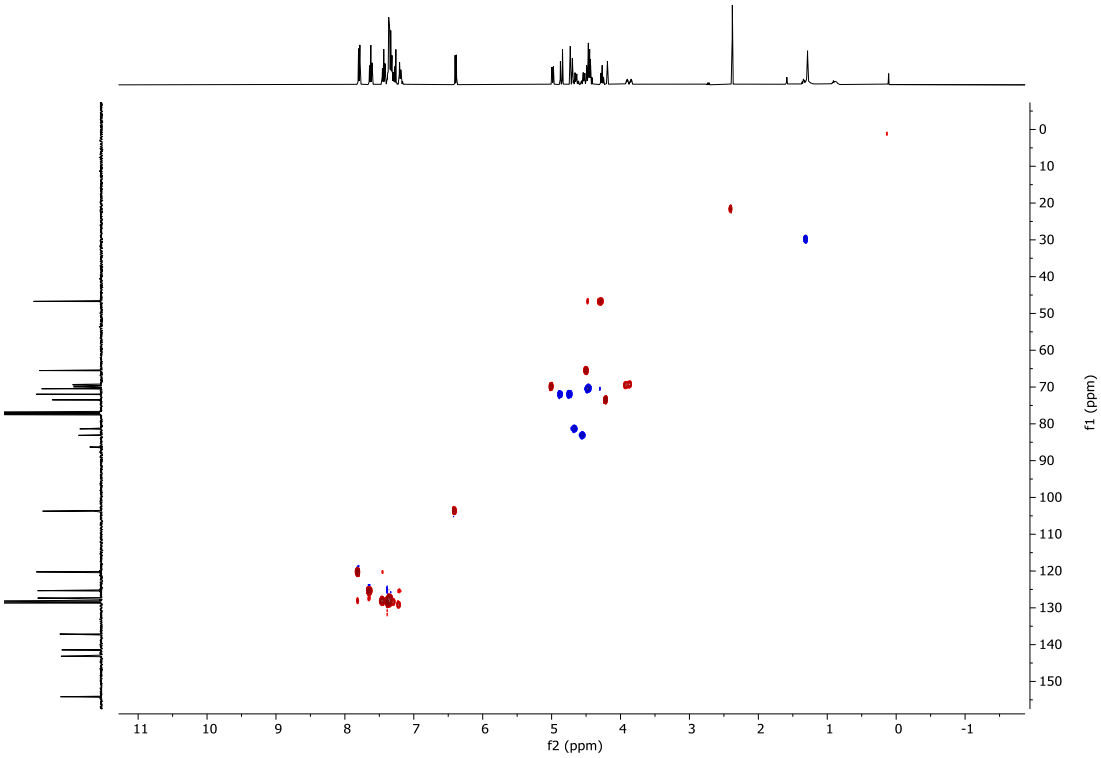

COSY NMR of 12 ($CDCl_3$)

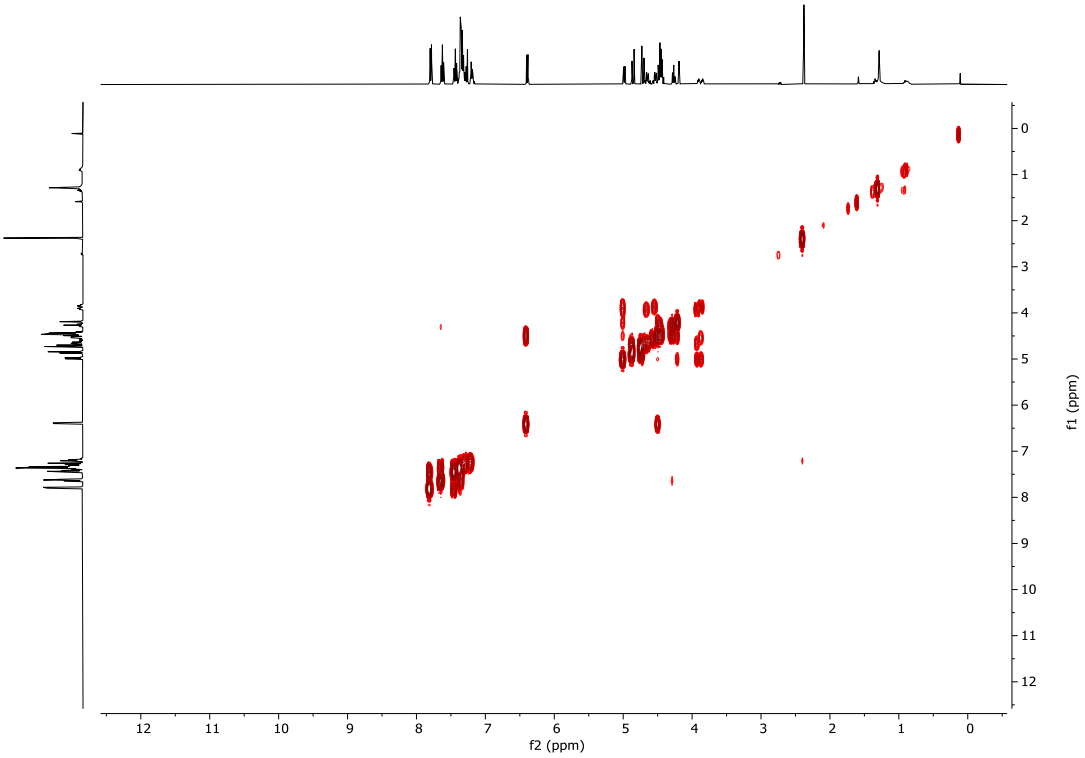

2.1.9 Recovery of the oxazoline side product 12

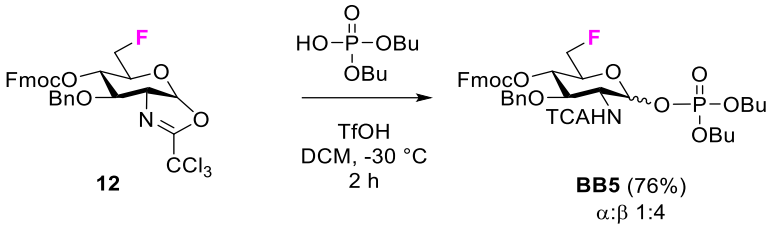

12 (781 mg, 1.26 mmol) was co-evaporated with toluene three times and dissolved in anhydrous DCM (15 mL). Activated molecular sieves (4 Å) were added to the mixture and the suspension was stirred at RT for 1 h. A solution of dibutyl phosphate (10 mL of a 7.5%$_v$ solution in DCM stirred in presence of activated 4 Å molecular sieves for 1 h, 3.78 mmol) was added to the mixture and cooled down to -30 °C. TfOH (50 µL, 0.57 mmol) was added dropwise and the reaction stirred at -30 °C for 2 h, after which time it was quenched with NEt_3 (90 µL). The reaction was diluted with EtOAc, passed through a short plug of silica, and concentrated under vacuum. The crude was purified by silica gel flash column chromatography (Toluene 100%→10% EtOAc : Toluene) to yield **BB5** as a sticky colorless solid (843 mg, 76%, α:β ratio 1:4).

3 Automated Glycan Assembly

3.1 General materials and methods

The automated syntheses were performed on a home-built synthesizer developed at the Max Planck Institute of Colloids and Interfaces. All solvents used were HPLC-grade. The solvents used for the building blocks, activator, TMSOTf and capping solutions were taken from an anhydrous solvent system (J.C. Meyer). The building blocks were co-evaporated three times with toluene and dried for 1 h on high vacuum before use. Oven-heated, argon-flushed flasks were used to prepare all moisture-sensitive solutions. Activator, capping, deprotection, acidic wash and building block solutions were freshly prepared and kept under argon during the automation run. All yields of products obtained by AGA were calculated on the basis of resin loading. Resin loading was determined following previously established procedures.[4]

3.2 Preparation of stock solutions

- **Building block solution**: between 0.06 and 0.10 mmol of building block (depending on the BB, see Module C1 and C2) was dissolved in DCM (1 mL).
- **NIS/TfOH activator solution**: 1.35 g (6.0 mmol) of recrystallized NIS was dissolved in 40 mL of a 2:1 v/v mixture of anhydrous DCM and anhydrous dioxane. Then triflic acid (55 µL, 0.6 mmol) was added. The solution is kept at 0 °C (ice bath) for the duration of the automation run.
- **Fmoc deprotection solution**: a solution of 20%$_{v/v}$ piperidine in DMF was prepared.
- **Lev deprotection solution**: hydrazine acetate (550 mg, 5.97 mmol) was dissolved in pyridine/AcOH/H_2O (40mL, v/v, 32:8:2) and sonicated for 10 min.
- **TMSOTf solution**: TMSOTf (0.45 mL, 2.49 mmol) was added to DCM (40 mL).
- **Capping solution**: a solution of 10%$_{v/v}$ acetic anhydride and 2%$_{v/v}$ methanesulfunic acid in DCM was prepared.

3.3 Modules for automated synthesis

Module A: Resin preparation

All automated syntheses were performed on 0.0125 mmol scale. Resin (**L1** or **L2**) is placed in the reaction vessel and swollen in DCM for 20 min at RT prior to the synthesis. During this time, all reagent lines needed for the synthesis are washed and primed. After the swelling, the resin is washed with DMF, THF, and DCM (three times each with 2 mL for 25 s).

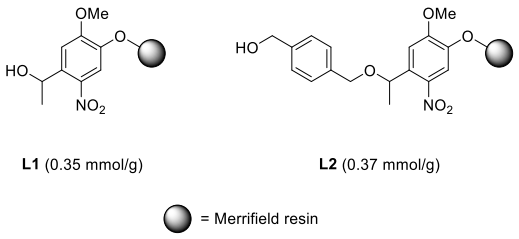

Module B: Acidic wash with TMSOTf solution (20 min)

The resin is swollen in 2 mL DCM and the temperature of the reaction vessel adjusted to -20 °C. Upon reaching the low temperature, TMSOTf solution (1 mL) is added dropwise to the reaction vessel. After bubbling for 3 min, the acidic solution is drained and the resin washed with 2 mL DCM for 25 s.

Action	Cycles	Solution	Amount	T (°C)	Incubation time
Cooling	-	-	-	-20	(15 min)*

Deliver	1	DCM	2 mL	-20	-
Deliver	1	TMSOTf solution	1 mL	-20	3 min
Wash	1	DCM	2 mL	-20	25 sec

*Time required to reach the desired temperature.

Module C1: Thioglycoside glycosylation (35 min-55 min)

The building block solution (0.10 mmol of BB in 1 mL of DCM per glycosylation) is delivered to the reaction vessel. After the set temperature is reached, the reaction is started by dropwise addition of the NIS/TfOH activator solution (1.0 mL, excess). The glycosylation conditions (T_1, T_2, t_1, and t_2) are building block dependent and are reported in for each synthesis. After completion of the reaction, the solution is drained and the resin is washed with DCM, DCM:dioxane (1:2, 3 mL for 20 s) and DCM (two times, each with 2 mL for 25 s). The temperature of the reaction vessel is increased to 25 °C for the next module. In case of a double cycle (C1*, *Double cycle), module C1 is repeated twice.

Action	Cycles	Solution	Amount	T (°C)	Incubation time
Cooling	-	-	-	T_1	-
Deliver	1	BB solution	1 mL	T_1	-
Deliver	1	NIS/TfOH activator solution	1 mL	T_1	-
Reaction time (BB dependent)	1	-	-	T_1 to T_2	t_1 t_2
Wash	1	DCM	2 mL	T_2	5 sec
Wash	1	DCM : Dioxane (1:2)	2 mL	T_2	20 sec
Heating	-	-	-	25	-
Wash	2	DCM	2 mL	> 0	25 sec

Module C2: Glycosyl phosphate glycosylation (45 min)

The building block solution (0.06 mmol of BB in 1 mL of DCM per glycosylation) is delivered to the reaction vessel. After the set temperature is reached, the reaction is started by dropwise addition of the TMSOTf solution (1.0 mL, stoichiometric). After completion of the reaction, the solution is drained and the resin washed with DCM (six times, each with 2 mL for 25 s). The temperature of the reaction vessel is increased to 25 °C for the next module. In case of a double cycle (C2*, *Double cycle), module C2 is repeated twice.

Action	Cycles	Solution	Amount	T (°C)	Incubation time
Cooling	-	-	-	-30	-
Deliver	1	BB solution	1 mL	-30	-
Deliver	1	TMSOTf solution	1 mL	-30	-
Reaction time	1	-	-	-30	5 min

(BB dependent)				to -10	40 min
Wash	1	DCM	2 mL	-10	5 sec
Heating	-	-	-	25	-
Wash	6	DCM	2 mL	> 0	25 sec

Module D: Capping (30 min)

The resin is washed with DMF (two times with 2 mL for 25 s) and the temperature of the reaction vessel adjusted to 25 °C. A pyridine solution (2 mL, 10%$_{v/v}$ in DMF) is delivered into the reaction vessel. After 1 min, the reaction solution is drained and the resin washed with DCM (three times with 3 mL for 25 s). Capping solution (4 mL) is delivered into the reaction vessel. After 20 min, the reaction solution is drained and the resin washed with DCM (three times with 3 mL for 25 s).

Action	Cycles	Solution	Amount	T (°C)	Incubation time
Heating	-	-	-	25	(5 min)*
Wash	2	DMF	2 mL	25	25 sec
Deliver	1	10% Pyridine in DMF	2 mL	25	1 min
Wash	3	DCM	2 mL	25	25 sec
Deliver	1	Capping Solution	4 mL	25	20 min
Wash	3	DCM	2 mL	25	25 sec

*Time required to reach the desired temperature.

Module E1: Fmoc deprotection (9 min)

The resin is washed with DMF (three times with 2 mL for 25 s) and the temperature of the reaction vessel adjusted to 25 °C. Fmoc deprotection solution (2mL) is delivered to the reaction vessel and kept under Ar bubbling. After 5 min, the reaction solution is drained and the resin washed with DMF (three times with 3 mL for 25 s) and DCM (five times each with 2 mL for 25 s). The temperature of the reaction vessel is decreased to -20 °C for the next module.

Action	Cycles	Solution	Amount	T (°C)	Incubation time
Wash	3	DMF	2 mL	25	25 sec
Deliver	1	Fmoc depr. solution	2 mL	25	5 min
Wash	1	DMF	2 mL		
Cooling	-	-	-	-20	-
Wash	3	DMF	2 mL	< 25	25 sec
Wash	5	DCM	2 mL	< 25	25 sec

3.4 Post-AGA manipulations

Module F: On-resin methanolysis
The resin is suspended in THF (4 mL). MeONa in MeOH (0.5 M, 0.4 mL) is added and the suspension is gently shaken at room temperature. After micro-cleavage (see *Module G2*) indicates the complete removal of benzoyl groups, the resin is repeatedly washed with MeOH (3 x 2 mL) and DCM (3 x 2 mL).

Module G1: Cleavage from solid support
The oligosaccharides are cleaved from the solid support using a continuous-flow photoreactor as described previously.[5]

Module G2: Micro-cleavage from solid support
Trace amount of resin (around 20 beads) is dispersed in DCM (0.1 mL) and irradiated with a UV lamp (6 W, 356 nm) for 10 minutes. ACN (10 µL) is then added to the resin and the resulting solution analyzed by MALDI.

Module H1: Hydrogenolysis
The crude compound obtained from *Module G1* is dissolved in 2 mL of EtOAc:*t*BuOH:H_2O (2:1:1). 100% by weight Pd/C (10%$_w$) or $Pd(OH)_2$/C (10-20%$_w$, moistened with water) is added and the reaction stirred in a pressurized reactor under H_2 pressure (4 bar). The reaction progress is monitored to avoid undesired side products formation (*i.e.* degradation of reducing end).[6] Upon completion, the reaction is filtered (PTFE 0.45 µm 25 mm syringe filter, Fisher scientific) and washed with EtOAc, H_2O, and ACN (4 mL each). The filtrates are concentrated *in vacuo*.

Module H2: Hydrogenolysis at ambient pressure
The crude compound obtained from *Module G1* is dissolved in 2 mL of EtOAc:*t*BuOH:H_2O (2:1:1). 100% by weight Pd/C (10%$_w$) is added to the stirred flask, the reaction purged for 5 min with a N_2 balloon, and equipped with a H_2 balloon. The reaction progress is monitored to avoid undesired side products formation (*i.e.* degradation of reducing end).[6] Upon completion, the reaction is filtered (PTFE 0.45 µm 25 mm syringe filter, Fisher scientific) and washed with EtOAc, H_2O, and ACN (4 mL each). The filtrates are concentrated *in vacuo*.

Module I: Purification
The final compounds are analyzed using analytical normal or reverse phase HPLC (Agilent 1200 Series, Methods A1, B1, and C1). The purification of the crudes is conducted using normal or reverse phase HPLC (Agilent 1200 Series, Method A2, B2, and C2).

- **Method A1**: (Hypercarb column, ThermoFisher scientific, 150 x 4.6 mm, 3 µm) flow rate of 0.7 mL/min with H_2O (0.1% formic acid) and ACN as eluents [isocratic (5 min), linear gradient to 40% ACN (30 min), linear gradient to 100% ACN (5 min), isocratic 100% ACN (5 min)].

- **Method A2 (Prep)**: (Hypercarb column, ThermoFisher scientific, 150 x 10 mm, 5 µm), flow rate of 3 mL /min with H_2O (0.1% formic acid) and ACN as eluents [isocratic (5 min), linear gradient to 40% ACN (30 min), linear gradient to 100% ACN (5 min), isocratic 100% ACN (5 min)].

- **Method B1**: (Synergi Hydro RP18 column, Phenomenex, 250 x 4.6 mm), flow rate of 1.0 mL/min with H_2O (0.1% formic acid) and ACN as eluents [isocratic (5 min), linear gradient to 30% ACN (30 min), linear gradient to 100% ACN (5 min), isocratic 100% ACN (5 min)].

- **Method B2 (Prep)**: (Synergi Hydro RP18 column, Phenomenex, 250 x 10 mm) flow rate of 4.0 mL/min with H_2O (0.1% formic acid) and ACN as eluents [isocratic (5 min), linear gradient to 30% ACN (30 min), linear gradient to 100% ACN (5 min), isocratic 100% ACN (5 min)].

- **Method C (Prep)**: (Manual reverse phase C_{18} silica gel column chromatography, 80 x 15 mm): H_2O (0.1% formic acid, 10 mL), 3% MeOH (10 mL), 6% MeOH (10 mL), 9% MeOH (10 mL), 12% MeOH (10 mL), 15% MeOH (10 mL).

- **Method D1**: (Synergi Hydro RP18 column, Phenomenex, 250 x 4.6 mm), flow rate of 1.0 mL/min with H_2O (0.1% formic acid) and ACN as eluents [isocratic (5 min), linear gradient to 15% ACN (45 min), linear gradient to 100% ACN (5 min), isocratic 100% ACN (5 min)].

- **Method D2 (Prep)**: (Synergi Hydro RP18 column, Phenomenex, 250 x 10 mm) flow rate of 4.0 mL/min with H_2O (0.1% formic acid) and ACN as eluents [isocratic (5 min), linear gradient to 15% ACN (45 min), linear gradient to 100% ACN (5 min), isocratic 100% ACN (5 min)].

- **Method E1**: (YMC-Diol-300 column, 150 x 4.6 mm), flow rate of 1.0 mL/min with Hexane and EtOAc as eluents [isocratic 20% EtOAc (5 min), linear gradient to 50% EtOAc (35 min), linear gradient to 100% EtOAc (5 min)].

- **Method E2 (Prep)**: (YMC-Diol-300 column, 150 x 20 mm), flow rate of 15 mL/min with Hexane and EtOAc as eluents [isocratic 20% EtOAc (5 min), linear gradient to 50% EtOAc (35 min), linear gradient to 100% EtOAc (5 min)].

Following final purification, all deprotected products are lyophilized on a Christ Alpha 2-4 LD plus freeze dryer prior to characterization.

3.5 Oligosaccharide synthesis

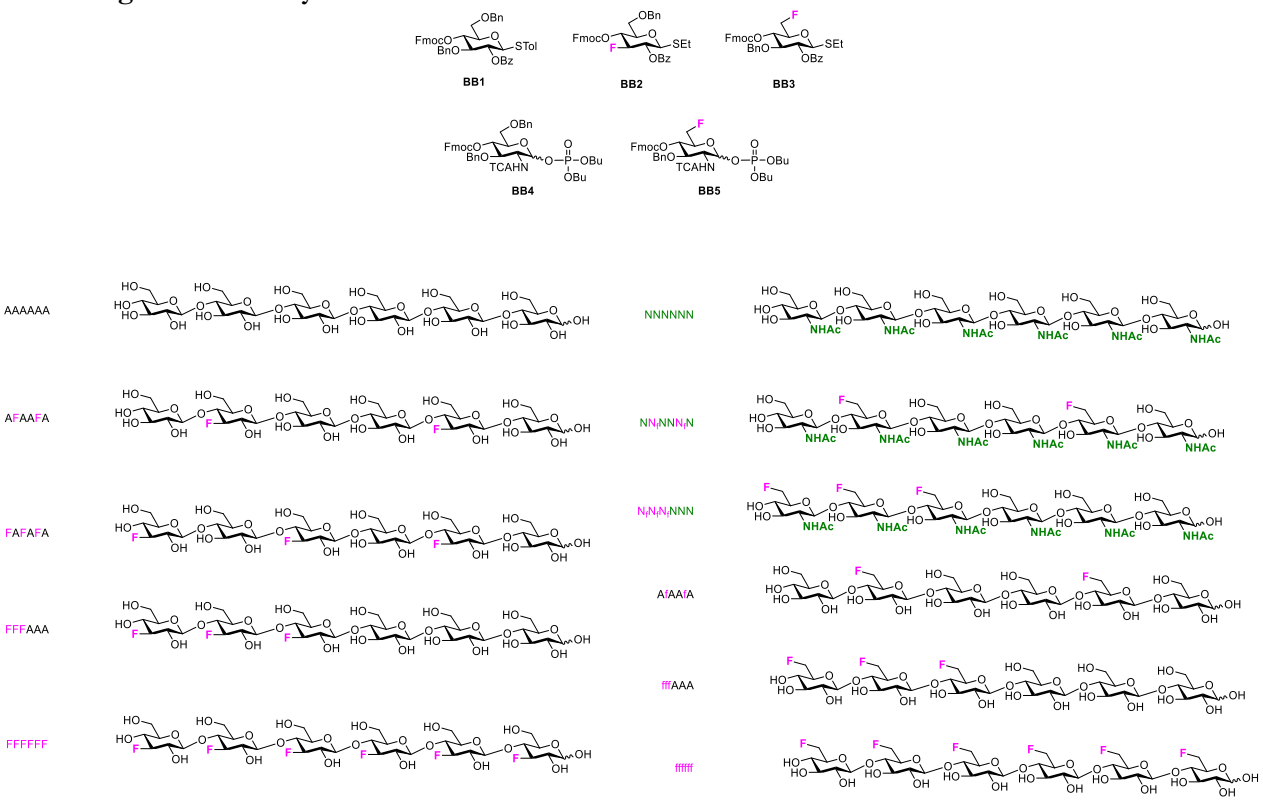

Figure S1 BBs used for the AGA and fluorinated cellulose and chitin analogs.

Compounds $\mathbf{A_6}$, $\mathbf{(FA)_3}$, $\mathbf{(AFA)_2}$, and $\mathbf{N_6}$ were synthesized according to previously reported protocols.[7–9] **BB4** and **BB2** were synthesized according to previously reported protocols.[7,8] **BB1** was purchased from GlycoUniverse (Germany). The synthesis of **BB3** and **BB5** is reported herein.

3.5.1 Synthesis of F_3A_3

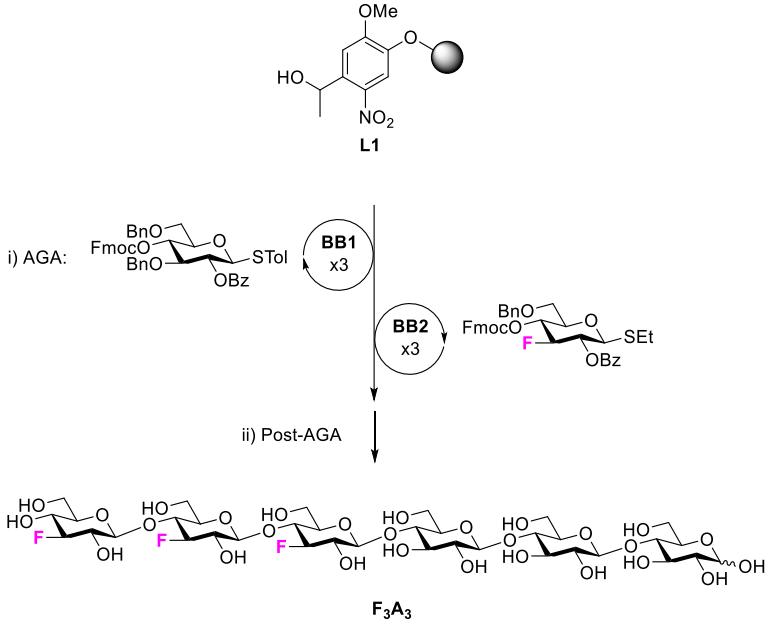

Step	BB	Modules	Notes
	-	**A**	**L1** swelling
AGA	(**BB1**)x3	(**B**, **C1**, **D**, **E**)x3	**C1**: (**BB1**, -20 °C for 5 min, 0°C for 20 min)
	(**BB2**)x3	(**B**, **C1**, **D**, **E**)x3	**C1**: (**BB2**, -20 °C for 5 min, 0°C for 20 min)
			F: (30 h)
Post-AGA	-	**F**, **G1**, **H2**, **I**	**H2**: (4 h)
			I: (Method C)

Automated synthesis, global deprotection, and purification afforded **F_3A_3** as a white solid (3.5 mg, 25% overall yield).

^{1}H NMR (600 MHz, D_2O) δ 5.09 (d, *J* = 3.8 Hz, 0.4H, H-1 α), 4.55 – 4.38 (m, 7.6H, H-1 β, H-1x5, C*H*Fx2), 4.31 (dt, *J* = 52.8, 8.9 Hz, 1H, C*H*F), 3.94 – 3.75 (m, 8H), 3.70 (dddt, *J* = 20.1, 11.4, 7.8, 4.3 Hz, 6.4H), 3.64 – 3.41 (m, 15H), 3.34 (dd, *J* = 10.0, 5.3 Hz, 1H), 3.22 (td, *J* = 8.3, 5.1 Hz, 2H), 3.18 – 3.12 (m, 0.6H). ^{13}C NMR (151 MHz, D_2O) δ 102.29, 102.28, 101.54, 101.46, 101.38, 101.32, 96.77, 95.69, 95.57, 94.99, 94.89, 93.77, 93.67, 91.75, 78.56, 78.41, 78.18, 78.08, 75.59, 75.54, 75.48, 75.42, 74.75, 74.73, 74.72, 74.65, 74.59, 74.18, 73.94, 73.86, 73.82, 73.80, 73.75, 73.69, 73.64, 72.88, 71.90, 71.82, 71.81, 71.69, 71.23, 71.16, 70.05, 67.84, 67.72, 60.14, 60.13, 59.94, 59.78, 59.71, 59.50. ^{19}F NMR (564 MHz, D_2O) δ -192.33 (dt, *J* = 52.2, 14.0 Hz), -192.53 (dt, *J* = 52.2, 13.9 Hz), -195.00 (dt, *J* = 52.8, 13.9 Hz). (ESI-HRMS) m/z 1019.310 $[M+Na]^+$ ($C_{36}H_{59}F_3O_{28}Na$ requires 1019.304).

RP HPLC of F_3A_3 (ELSD trace, Method B1, t_R = 17.2 min)

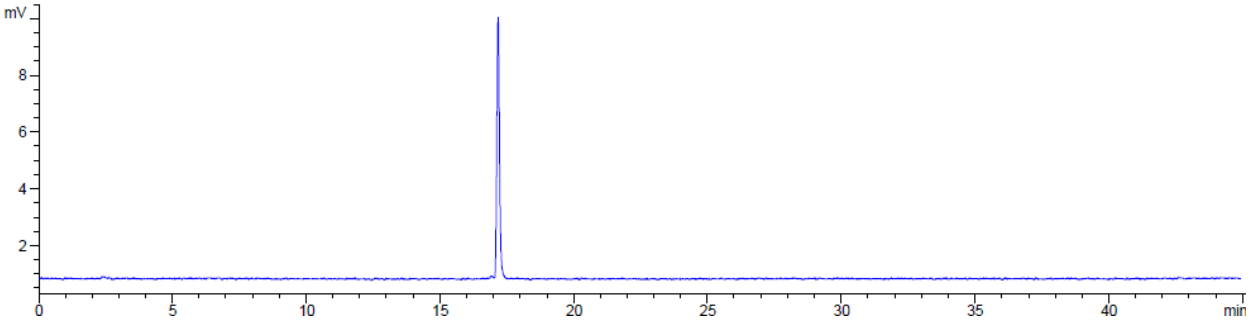

^{1}H NMR of F_3A_3 (600 MHz, Deuterium Oxide)

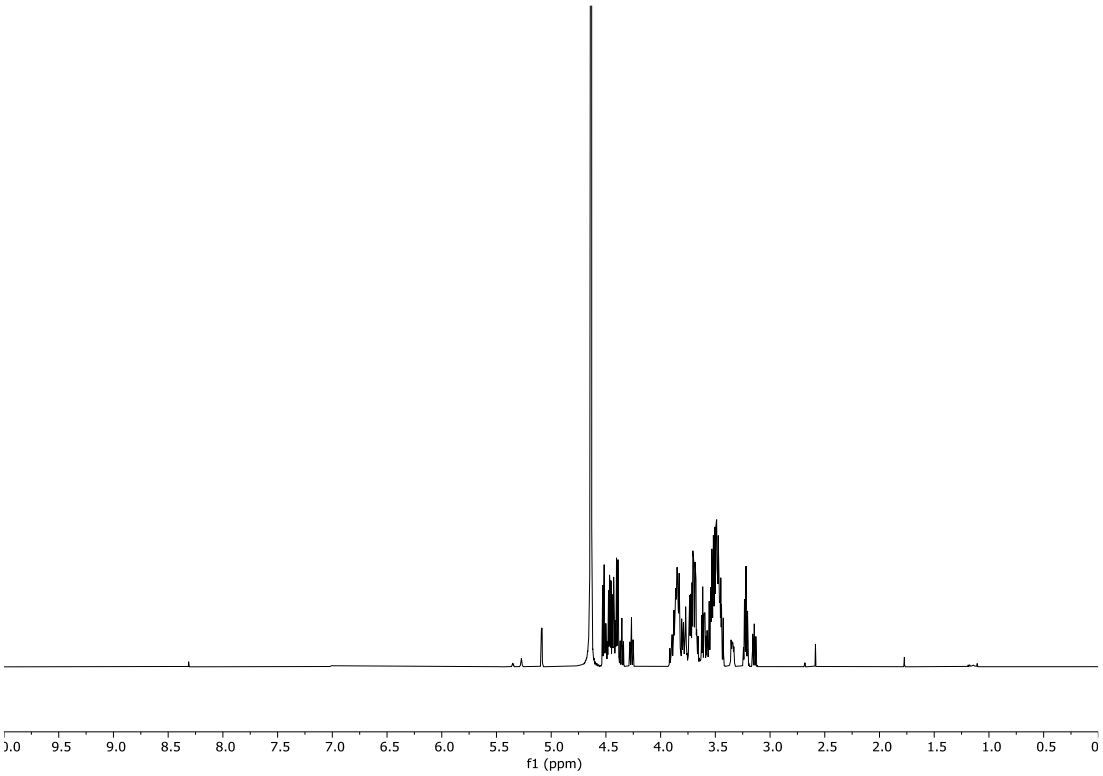

^{13}C NMR of F_3A_3 (151 MHz, Deuterium Oxide)

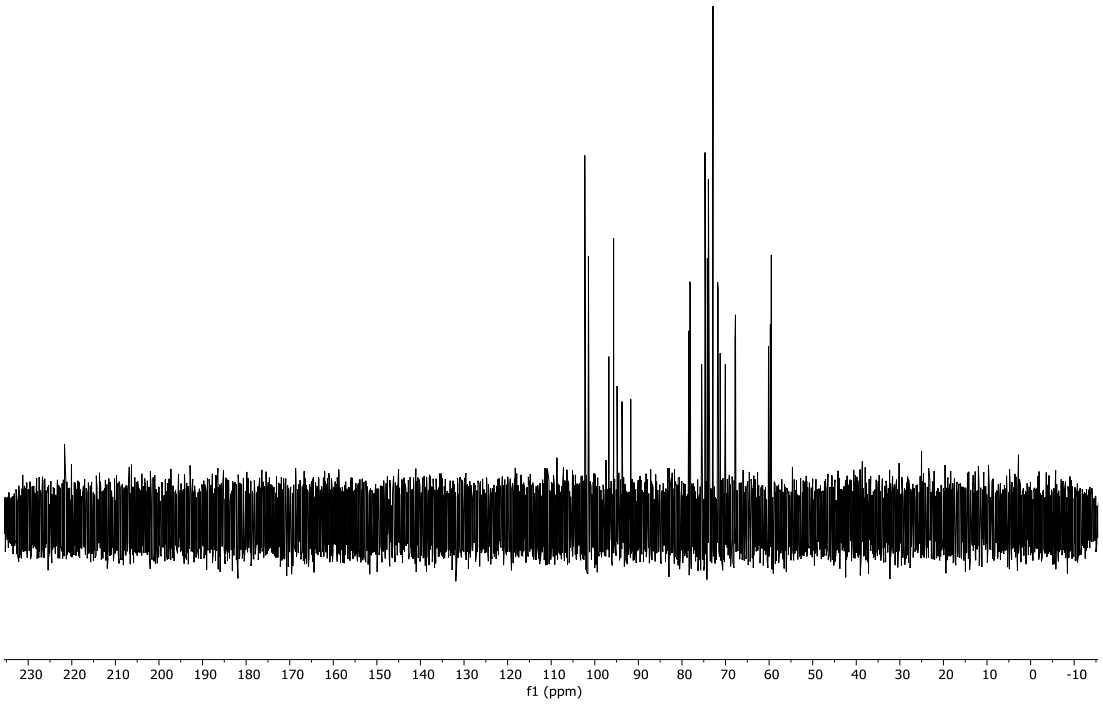

^{19}F NMR of F_3A_3 (564 MHz, Deuterium Oxide)

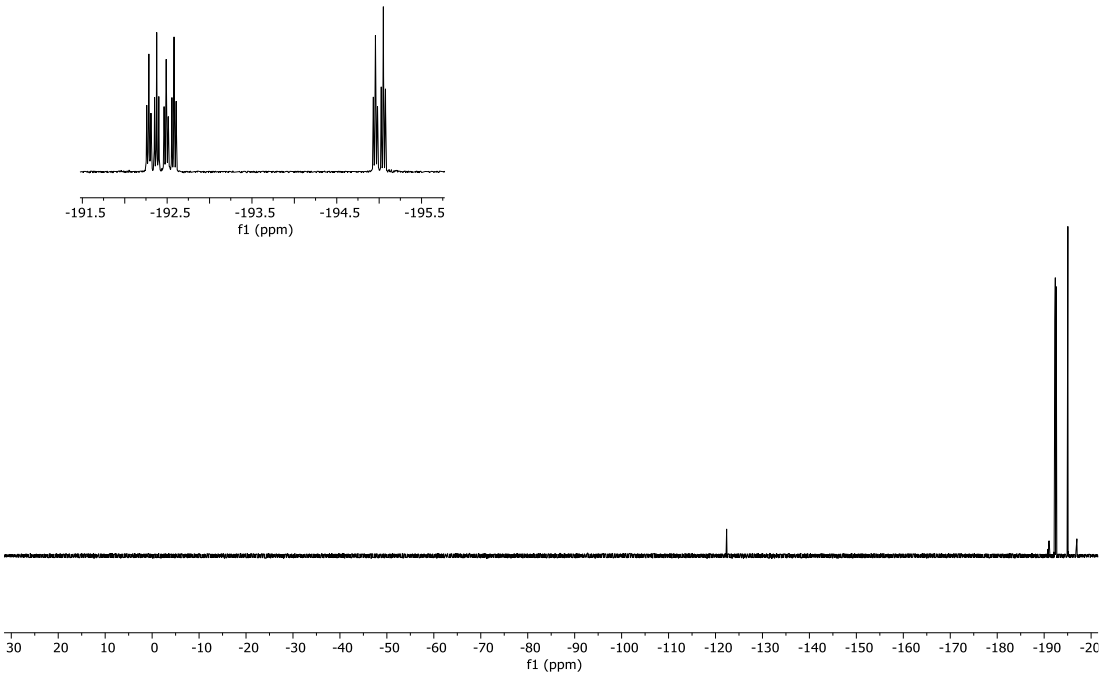

HSQC NMR of F_3A_3 (Deuterium Oxide)

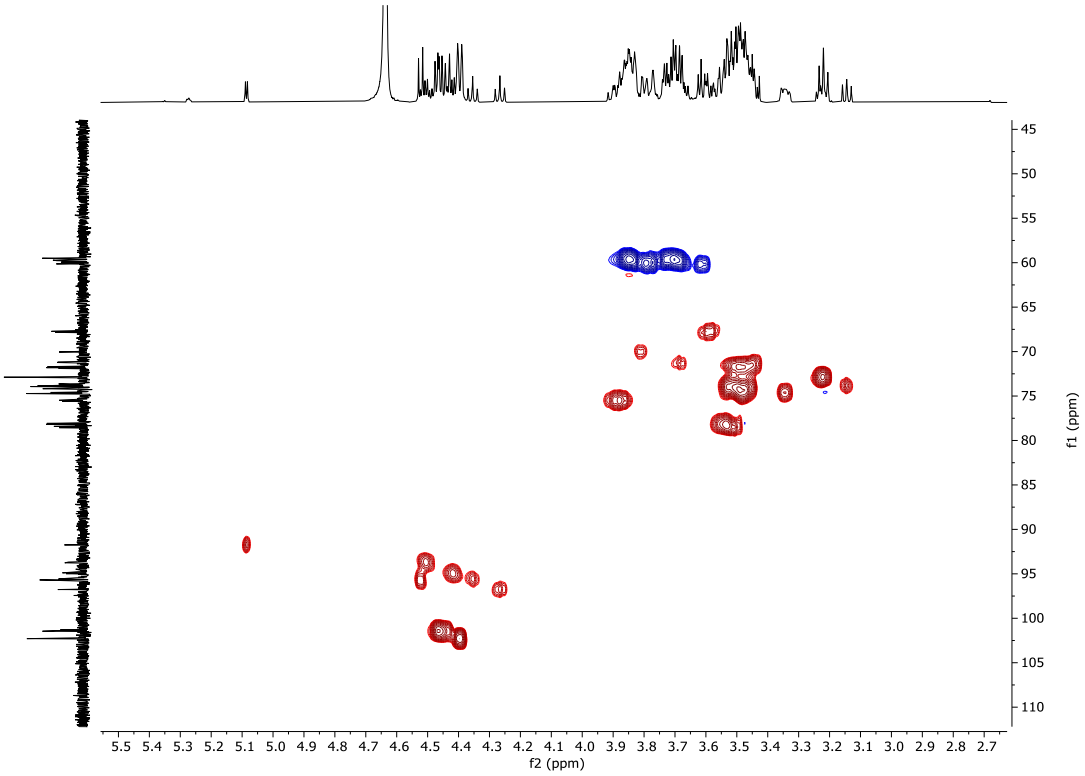

3.5.2 Synthesis of F_6

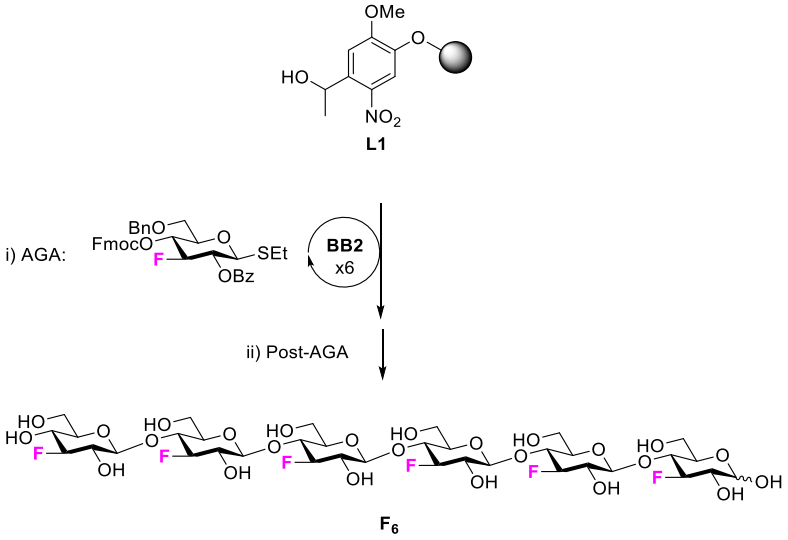

Step	BB	Modules	Notes
AGA	-	**A**	**L1** swelling
	(**BB2**)x6	(**B**, **C1**, **D**, **E**)x6	**C1**: (**BB2**, -20 °C for 5 min, 0 °C for 20 min)
Post-AGA	-	**F**, **G1**, **H2**, **I**	**F**: (16 h) **H2**: (5 h) **I**: (Method C)

Automated synthesis, global deprotection, and purification afforded **F_6** as a white solid (0.4 mg, 3% overall yield).

^{1}H NMR (700 MHz, D_2O) δ 5.19 (t, *J* = 3.6 Hz, 0.5H, H-1 α), 4.62 (d, *J* = 8.0 Hz, 1H, H-1), 4.58 – 4.45 (m, 9.5H, H-1 β, H-1x4, C*H*Fx5), 4.37 (dt, *J* = 52.8, 8.9 Hz, 1H, C*H*F), 3.92 (dd, *J* = 17.5, 8.2 Hz, 10H), 3.85 – 3.79 (m, 3H), 3.76 (dd, *J* = 12.7, 4.7 Hz, 5H), 3.71 – 3.61 (m, 2H), 3.59 – 3.45 (m, 9H), 3.40 (s, 1H). ^{19}F NMR (564 MHz, D_2O) δ -192.14 – -192.48 (m), -194.93 – -195.09 (m). (ESI-HRMS) m/z 1025.295 $[M+Na]^+$ ($C_{36}H_{56}F_6O_{25}Na$ requires 1025.291).

^{13}C NMR was not recorded due to limited amount of sample.

RP HPLC of F_6 (ELSD trace, Method B1, t_R = 19.5 min)

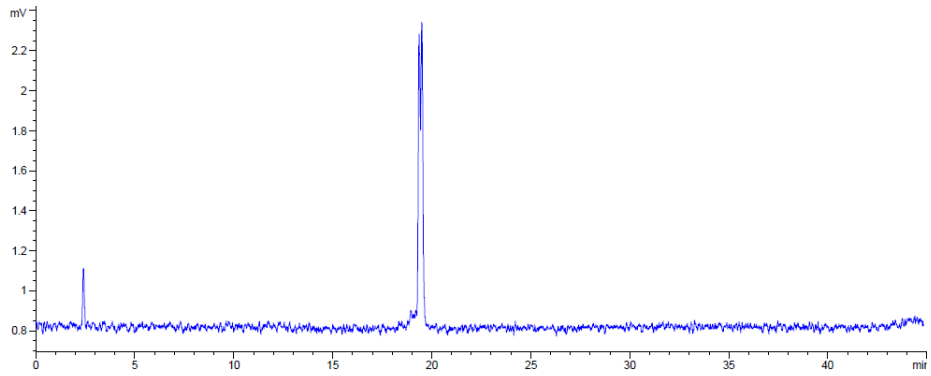

^{1}H NMR of F_6 (600 MHz, Deuterium Oxide)

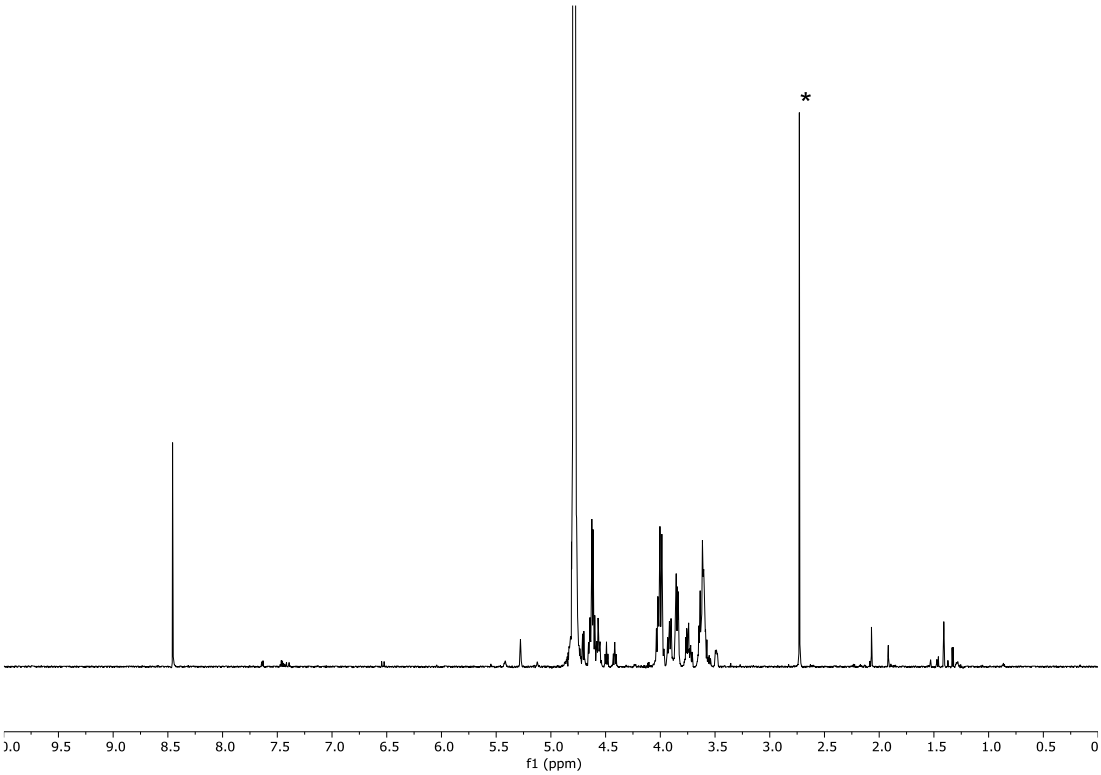

*Unidentified impurity

^{19}F NMR of F_6 (376 MHz, Deuterium Oxide)

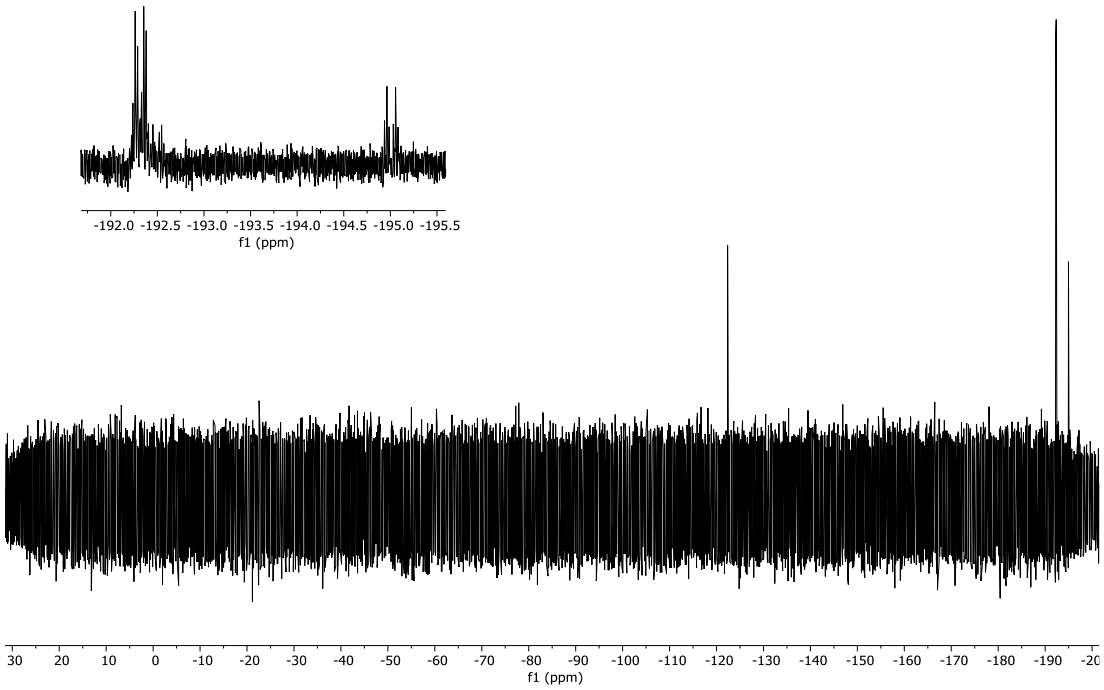

HSQC NMR of F_6 (Deuterium Oxide)

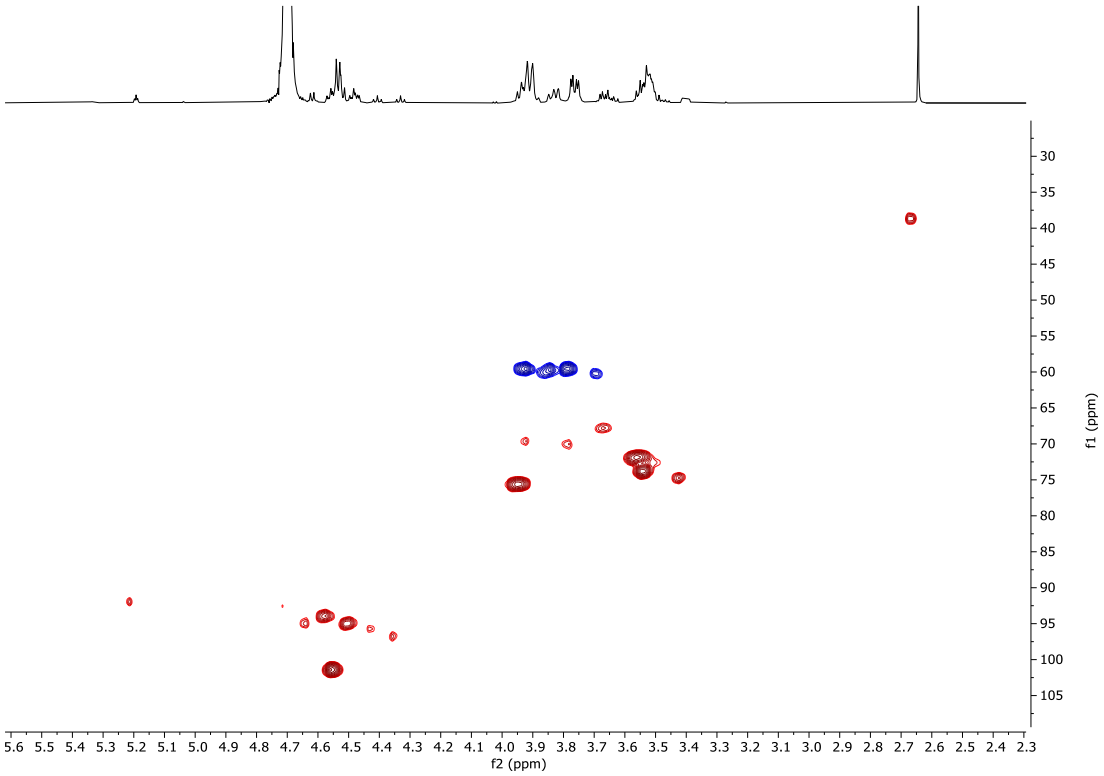

3.5.3 Synthesis of $(AfA)_2$

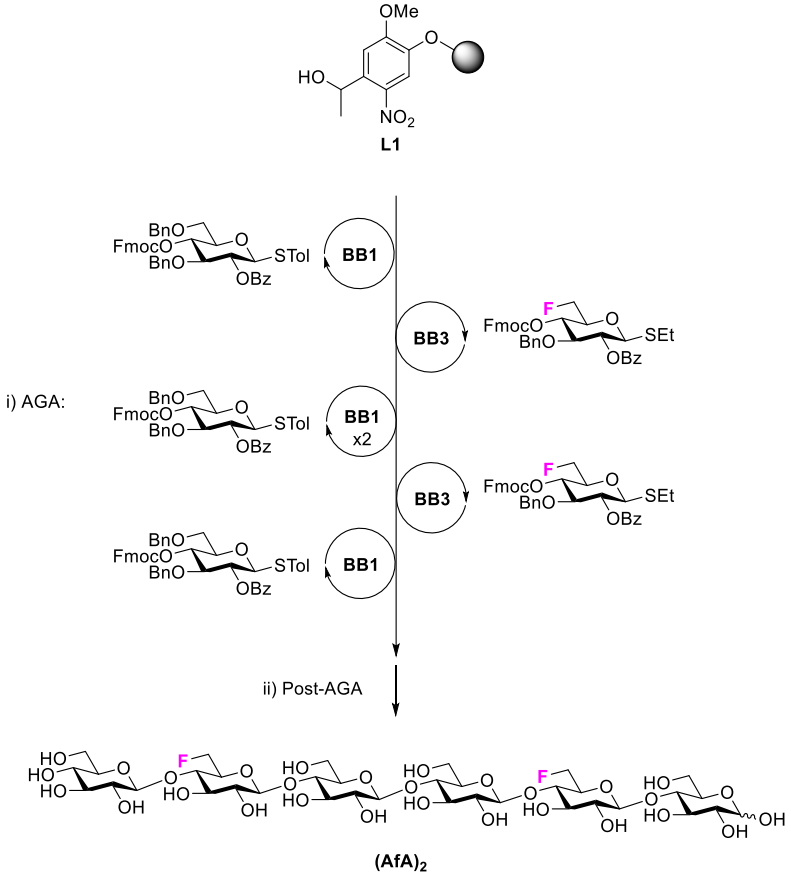

Step	BB	Modules	Notes
AGA	-	**A**	**L1** swelling
	BB1	**B**, **C1**, **D**, **E**	**C1**: (**BB1**, -20 °C for 5 min, 0 °C for 20 min)
	BB3	**B**, **C1**, **D**, **E**	**C1**: (**BB3**, -20 °C for 5 min, 0 °C for 20 min)
	(**BB1**)x2	(**B**, **C1**, **D**, **E**)x2	**C1**: (**BB1**, -20 °C for 5 min, 0 °C for 20 min)
	BB3	**B**, **C1**, **D**, **E**	**C1**: (**BB3**, -20 °C for 5 min, 0 °C for 20 min)
	BB1	**B**, **C1**, **D**, **E**	**C1**: (**BB1**, -20 °C for 5 min, 0 °C for 20 min)
Post-AGA	-	**F**, **G1**, **H2**, **I**	**F**: (16 h) **H2**: (6 h) **I**: (Method D2, t_R = 23.4 min)

Automated synthesis, global deprotection, and purification afforded **$(AfA)_2$** as a white solid (1.7 mg, 14% overall yield).

^{1}H NMR (600 MHz, D_2O) δ 5.22 (d, *J* = 3.7 Hz, 0.3H, H-1 α), 4.89 – 4.82 (m, 2H, C*H*$_2$F), 4.74 (d, *J* = 10.6 Hz, 2H, C*H*$_2$F), 4.65 (d, *J* = 7.9 Hz, 0.7H, H-1 β), 4.58 – 4.47 (m, 5H, H-1x5), 4.01 – 3.93 (m, 3H), 3.93 – 3.86 (m, 2H), 3.86 – 3.71 (m, 8H), 3.71 – 3.55 (m, 10H), 3.53 – 3.46 (m, 2H), 3.44 – 3.40 (m, 1H), 3.40 – 3.29 (m, 5H), 3.27 (t, *J* = 8.2 Hz, 1H). ^{13}C NMR (101 MHz, D_2O) δ 102.54, 102.46, 102.33, 102.24, 95.64, 91.72, 81.40 (d, *J* = 167.4 Hz), 78.76, 78.59, 78.38, 78.05, 77.32, 77.24, 75.86, 75.33, 74.68, 74.09, 73.84,

73.73, 73.26, 73.08, 73.01, 72.88, 71.15, 69.97, 69.28, 60.42, 59.68. ^{19}F NMR (376 MHz, D_2O) δ -233.42 – -234.14 (m). (ESI-HRMS) m/z 1017.310 $[M+Na]^+$ ($C_{36}H_{60}F_2O_{29}Na$ requires 1017.308).

RP HPLC of $(AfA)_2$ (ELSD trace, Method D1, t_R = 23.4 min)

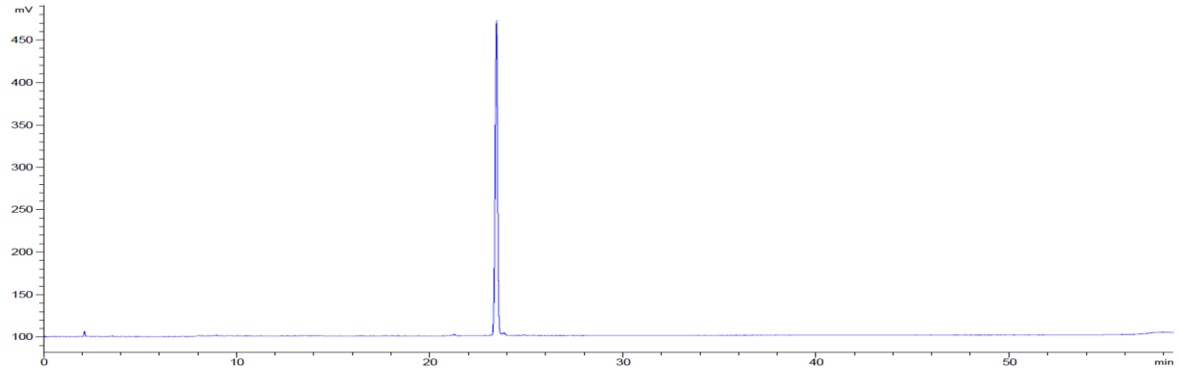

^{1}H NMR of $(AfA)_2$ (600 MHz, Deuterium Oxide)

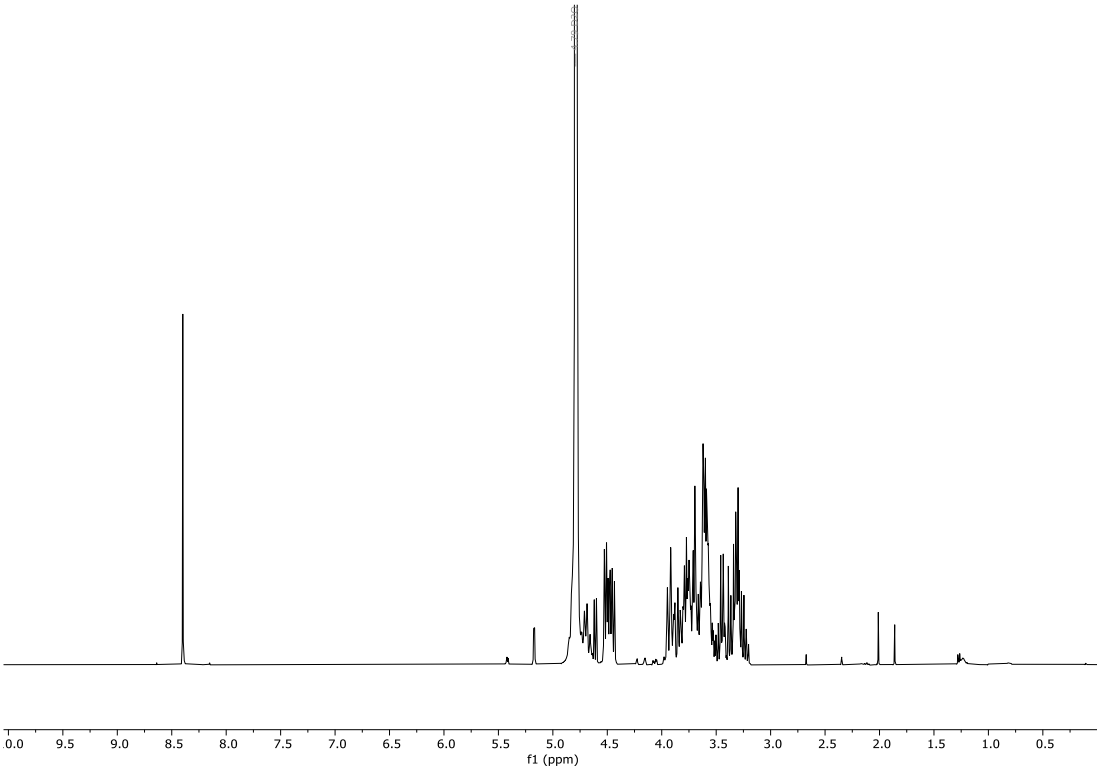

^{13}C NMR of $(AfA)_2$ (151 MHz, Deuterium Oxide)

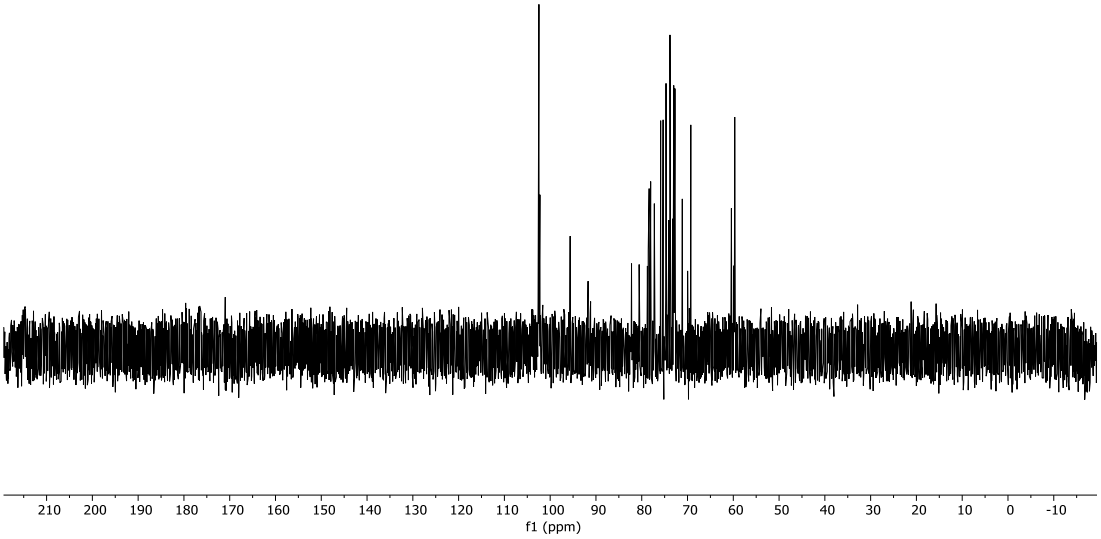

^{19}F NMR of $(AfA)_2$ (564 MHz, Deuterium Oxide)

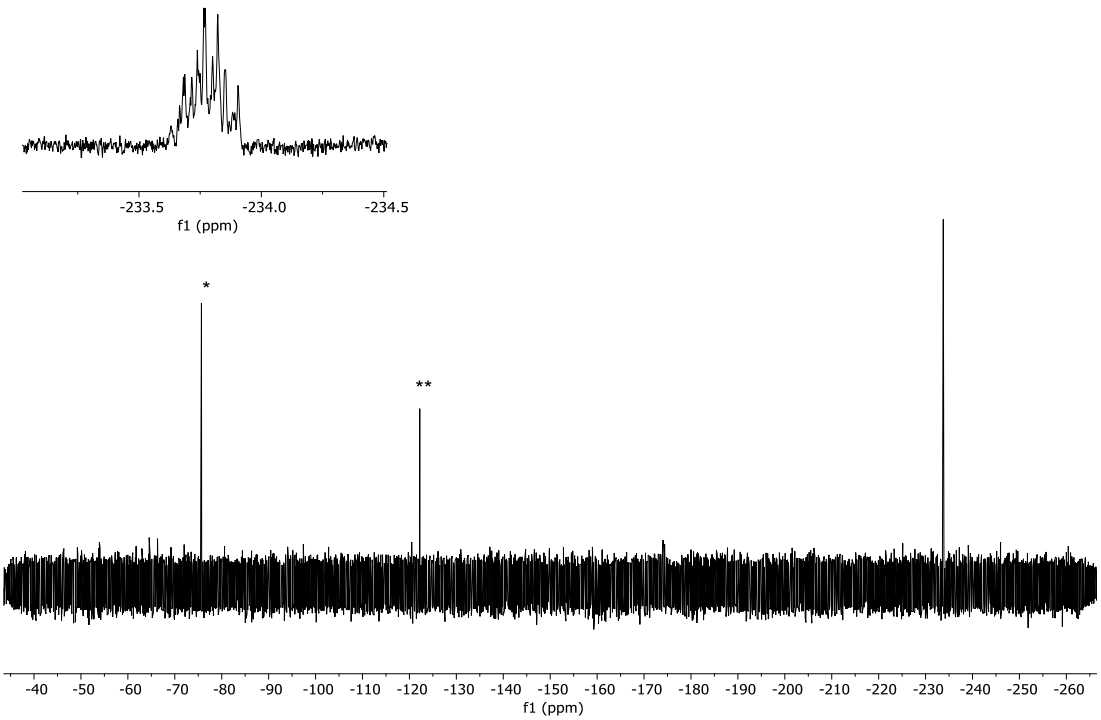

* The peak at -75.7 ppm is a TFA impurity

**The peak at -122.2 ppm is a fluoride impurity

HSQC NMR of $(AfA)_2$ (Deuterium Oxide)

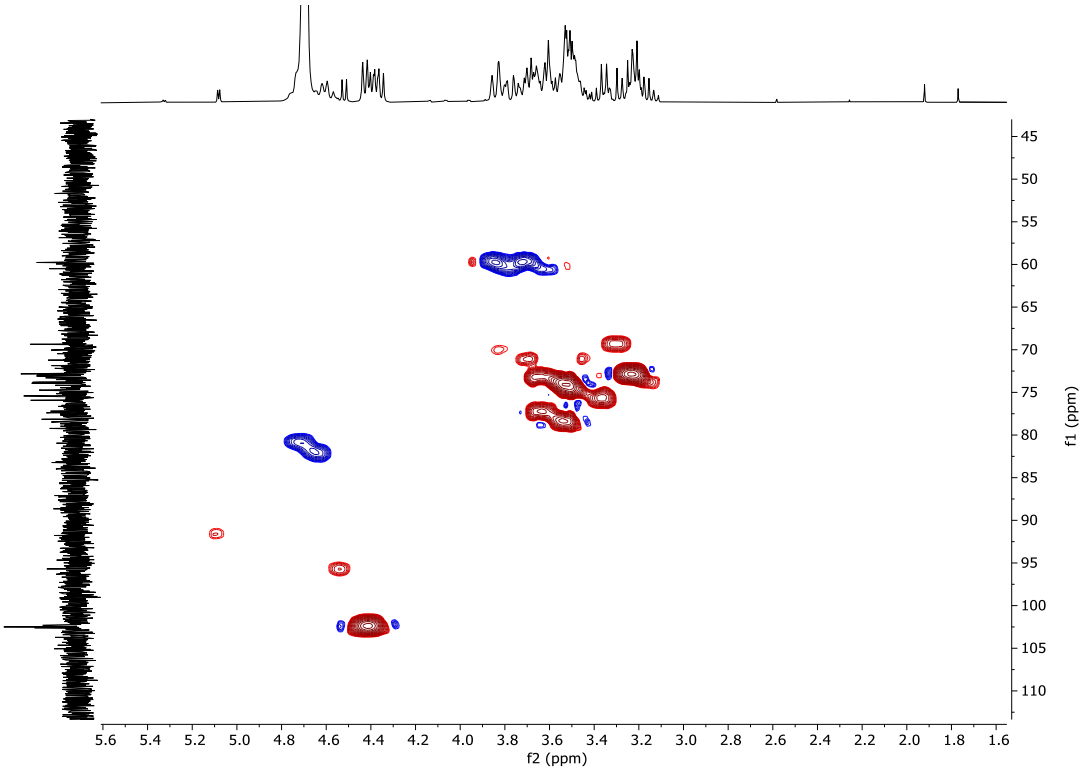

3.5.4 Synthesis of f_3A_3

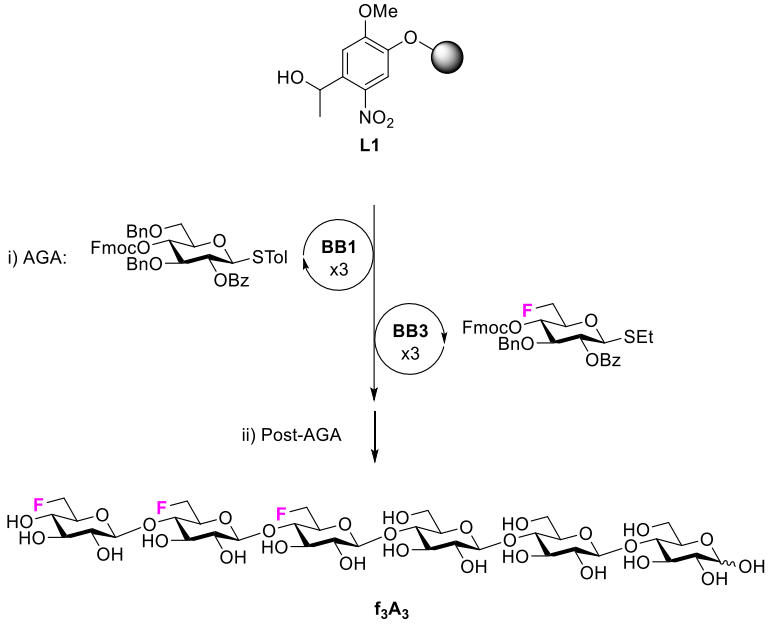

Step	BB	Modules	Notes
AGA	-	**A**	**L1** swelling
	(**BB1**)x3	(**B**, **C1**, **D**, **E**)x3	**C1**: (**BB1**, -20 °C for 5 min, 0 °C for 20 min)
	(**BB3**)x3	(**B**, **C1**, **D**, **E**)x3	**C1**: (**BB3**, -20 °C for 5 min, 0 °C for 20 min)
Post-AGA	-	**F**, **G1**, **H2**, **I**	**F**: (16 h) **H2**: (3 h) **I**: (Method C)

Automated synthesis, global deprotection, and purification afforded **f_3A_3** as a white solid (4.6 mg, 35% overall yield).

^{1}H NMR (600 MHz, D_2O) δ 5.24 (d, *J* = 3.8 Hz, 0.4H, H-1 α), 4.92 – 4.66 (m, 6H, C*H*$_2$Fx3), 4.68 (d, *J* = 7.9 Hz, 0.6H, H-1 β), 4.62 – 4.50 (m, 5H, H-1x5), 4.03 – 3.94 (m, 3H), 3.93 – 3.80 (m, 5H), 3.80 – 3.74 (m, 3H), 3.73 – 3.51 (m, 14H), 3.42 – 3.27 (m, 5H). ^{13}C NMR (151 MHz, D_2O) δ 102.72, 102.51, 102.45, 102.27, 95.68, 91.75, 82.07 (d, *J* = 167.6 Hz), 81.49 (d, *J* = 167.6 Hz), 78.56, 78.46, 78.41, 78.20, 77.72, 77.69, 77.59, 77.55, 75.20, 74.75, 74.73, 74.71, 74.35, 74.24, 74.18, 73.94, 73.89, 73.82, 73.77, 73.73, 73.24, 73.20, 73.12, 73.08, 72.95, 72.92, 72.89, 72.88, 72.85, 72.78, 71.23, 71.16, 70.05, 68.29, 68.24, 59.94, 59.76. ^{19}F NMR (564 MHz, D_2O) δ -233.89 (qd, *J* = 47.7, 27.2 Hz), -234.89 (td, *J* = 47.1, 25.8 Hz). (ESI-HRMS) m/z 1019.321 $[M+Na]^+$ ($C_{36}H_{59}F_3O_{28}Na$ requires 1019.304).

RP HPLC of f_3A_3 (ELSD trace, Method B1, t_R = 16.5 min)

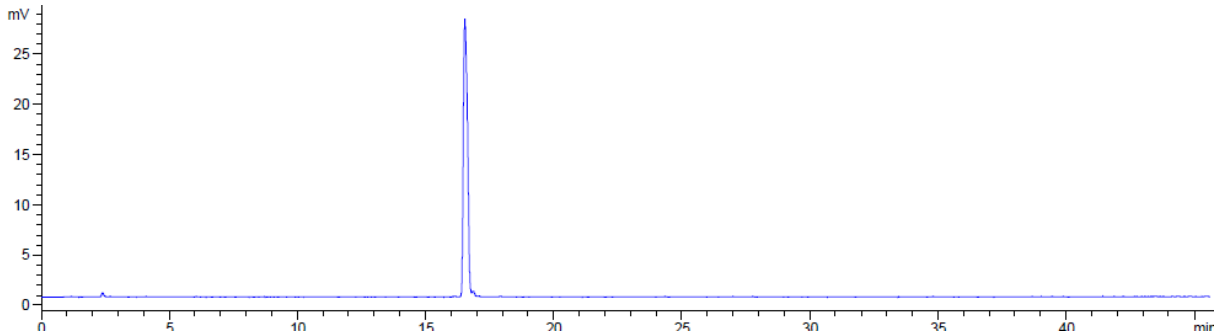

^{1}H NMR of f_3A_3 (600 MHz, Deuterium Oxide)

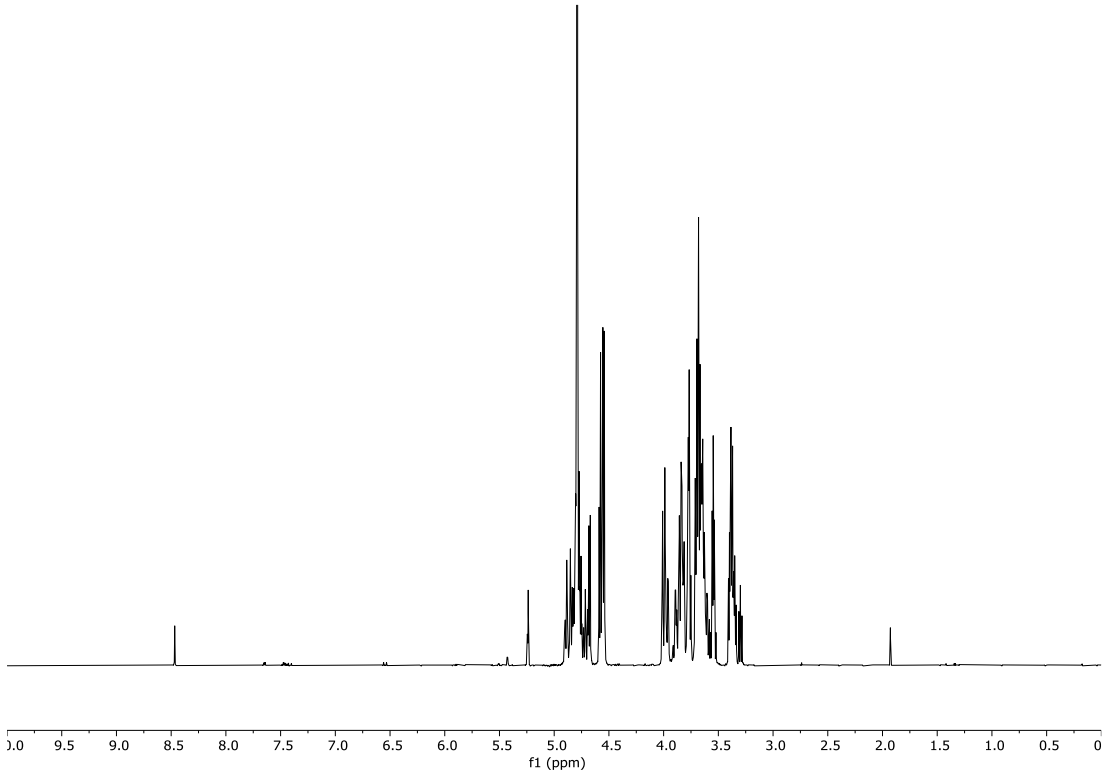

^{13}C NMR of f_3A_3 (151 MHz, Deuterium Oxide)

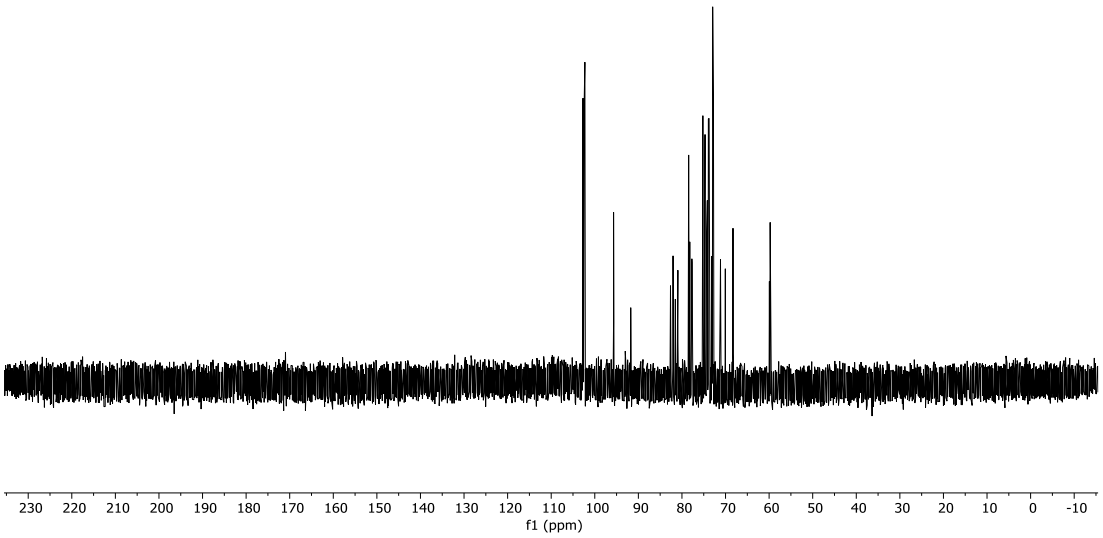

^{19}F NMR of f_3A_3 (564 MHz, Deuterium Oxide)

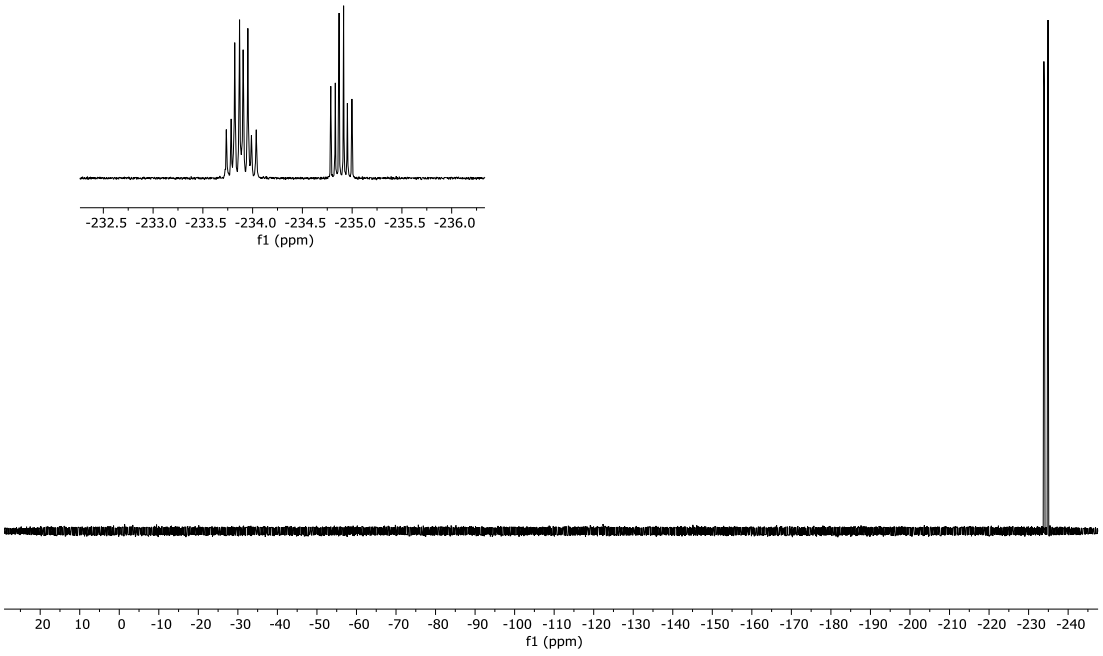

HSQC NMR of f_3A_3 (Deuterium Oxide)

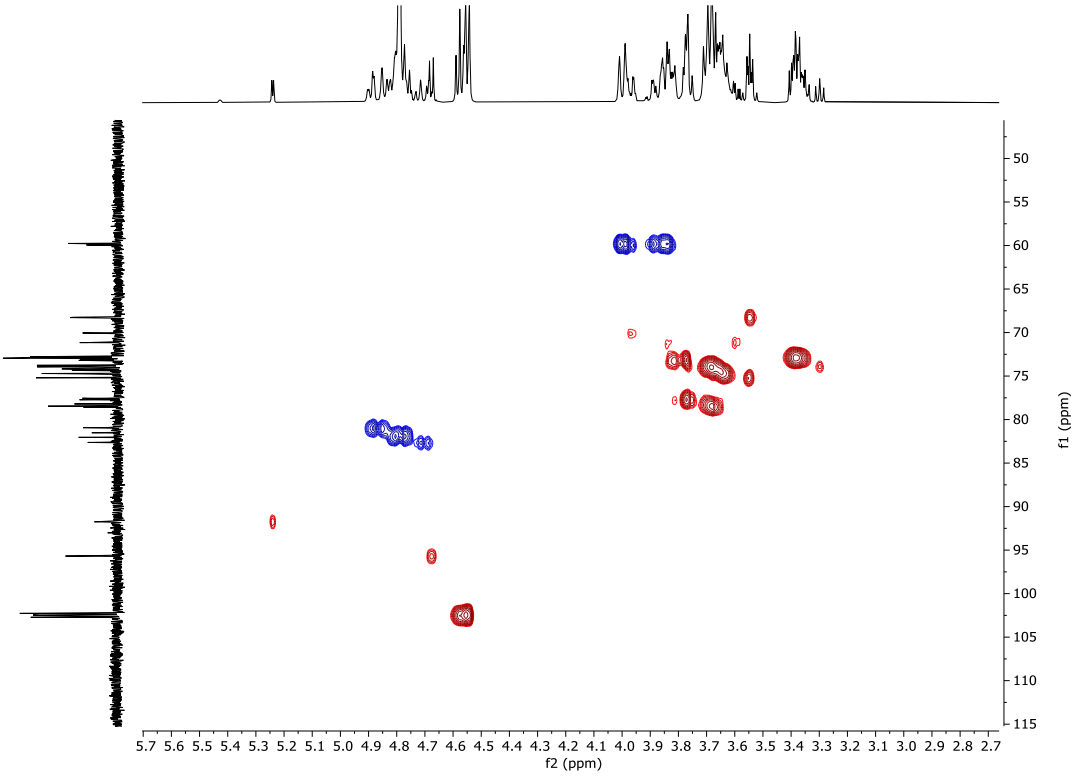

3.5.5 Synthesis of f_6

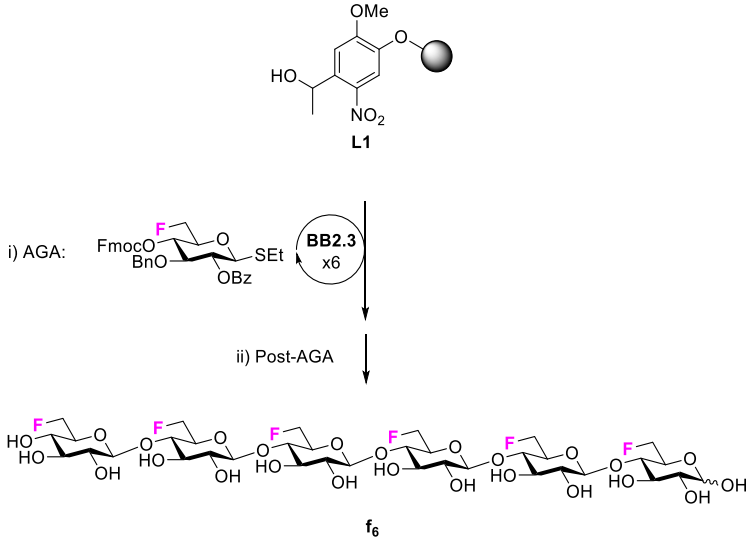

Step	BB	Modules	Notes
AGA	-	**A**	**L1** swelling
	(**BB3**)x6	**B**, **C1**, **D**, **E**	**C1**: (**BB3**, -20 °C for 5 min, 0 °C for 20 min)
Post-AGA	-	**F**, **G1**, **H2**, **I**	**F**: (16 h) **H2**: (3 h) **I**: (Method C)

Automated synthesis, global deprotection, and purification afforded **f_6** as a white solid (3.7 mg, 30% overall yield).

^{1}H NMR (600 MHz, D_2O) δ 5.27 (d, *J* = 3.7 Hz, 0.4H, H-1 α), 4.79 (s, 12.6H, H-1 β, C*H*$_2$Fx6), 4.56 (dd, *J* = 13.5, 8.0 Hz, 5H, H-1x5), 4.10 (dd, *J* = 31.1, 10.1 Hz, 0.6H), 3.91 – 3.63 (m, 16H), 3.60 (dd, *J* = 9.8, 3.8 Hz, 0.4H), 3.58 – 3.50 (m, 2H), 3.44 – 3.29 (m, 5H). ^{13}C NMR (151 MHz, D_2O) δ 102.71, 102.52, 95.83, 82.07 (d, *J* = 168.3 Hz), 81.47 (d, *J* = 167.8 Hz), 77.68, 77.56, 77.52, 75.19, 74.35, 74.23, 73.96, 73.73, 73.23, 73.11, 72.95, 72.82, 72.78, 71.09, 68.28. ^{19}F NMR (564 MHz, D_2O) δ -233.70 – -234.10 (m), -234.47 (td, *J* = 47.5, 31.2 Hz), -234.89 (td, *J* = 47.2, 25.7 Hz). (ESI-HRMS) m/z 1025.311 $[M+Na]^+$ ($C_{36}H_{56}F_6O_{25}Na$ requires 1025.291).

RP HPLC of f_6 (ELSD trace, Method B1, t_R = 20.5, 21.5 min)

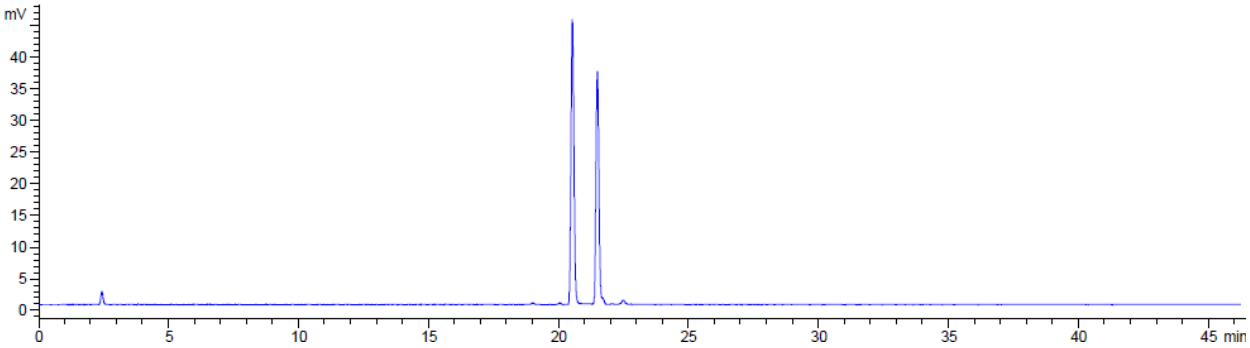

^{1}H NMR of f_6 (600 MHz, Deuterium Oxide)

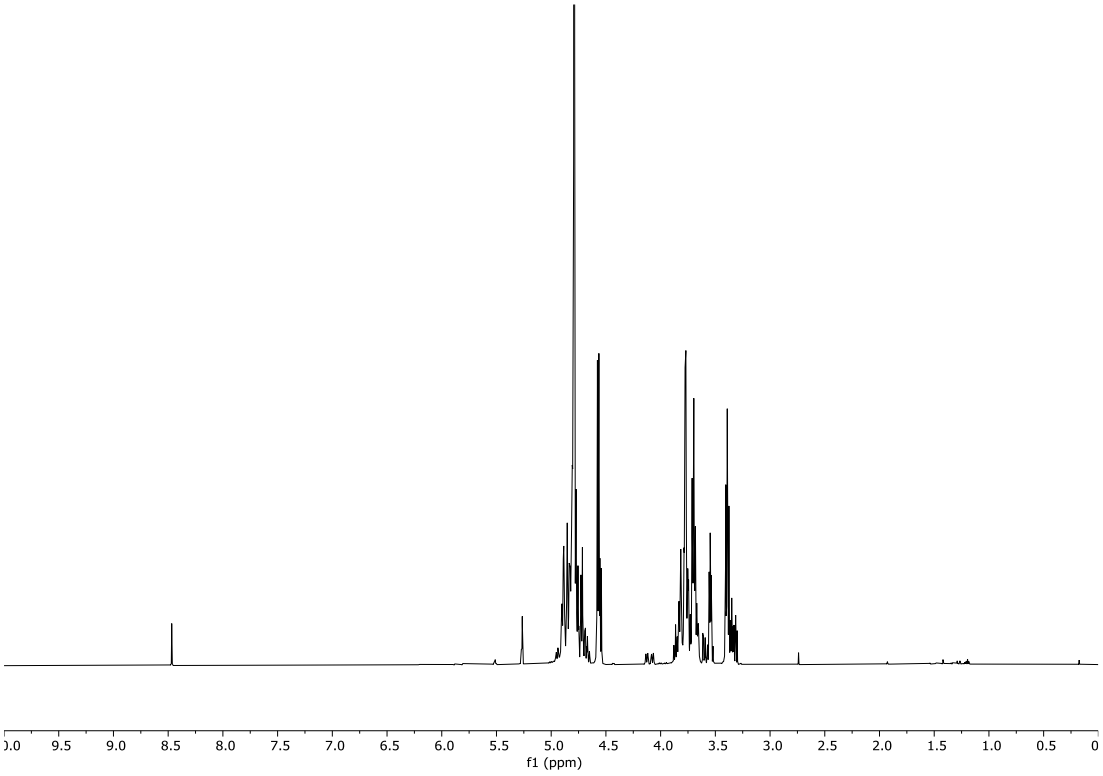

^{13}C NMR of f_6 (151 MHz, Deuterium Oxide)

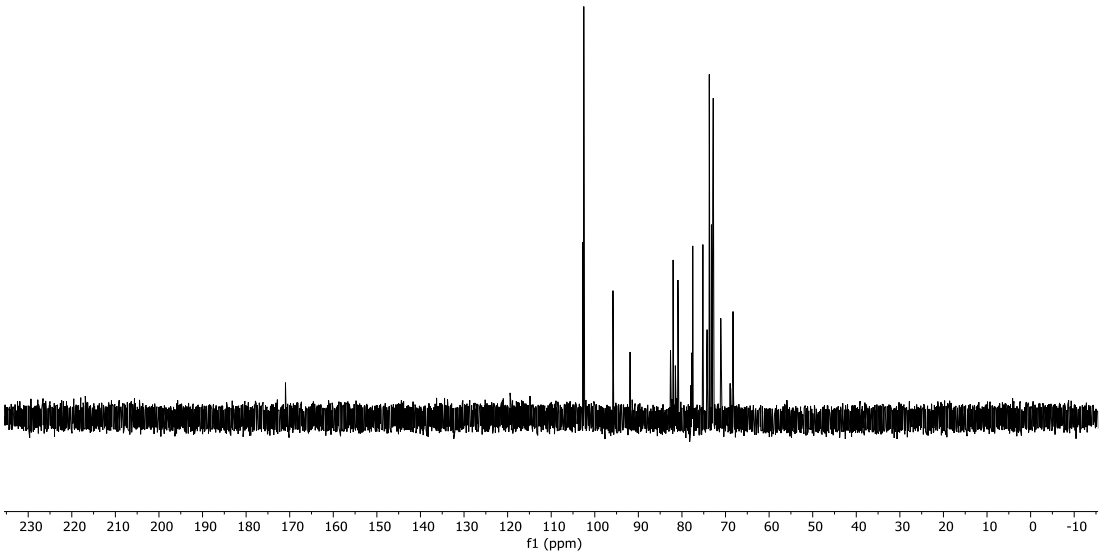

^{19}F NMR of f_6 (564 MHz, Deuterium Oxide)

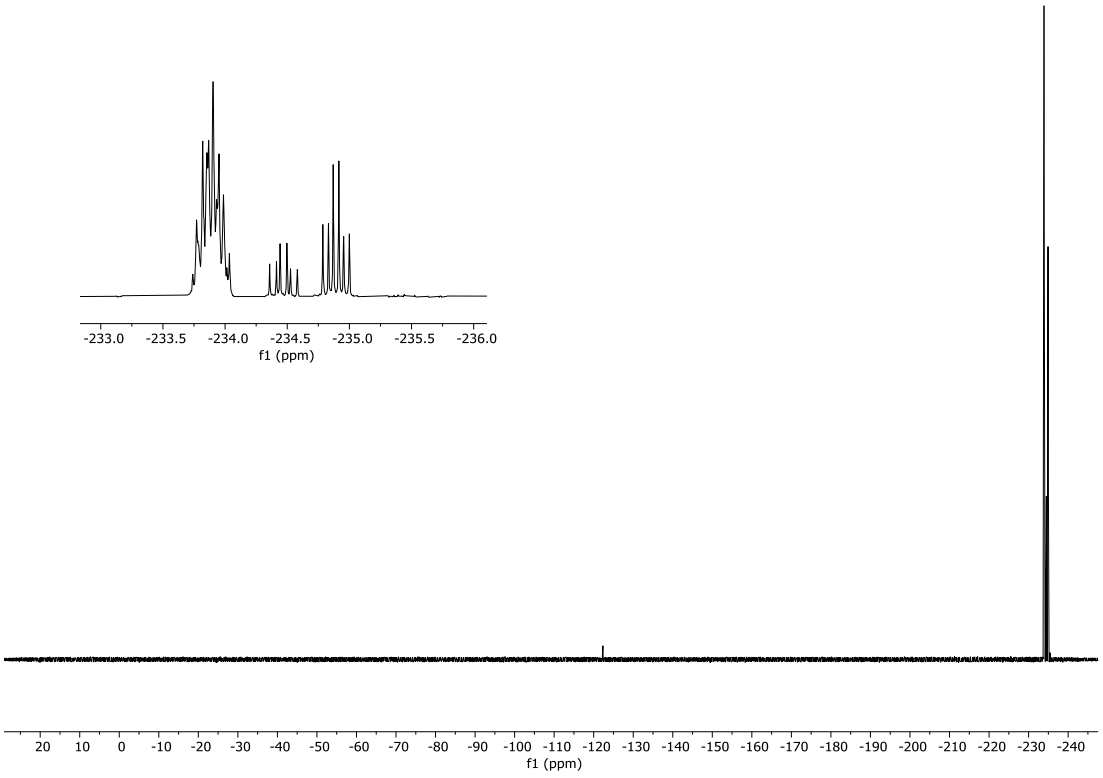

HSQC NMR of f_6 (Deuterium Oxide)

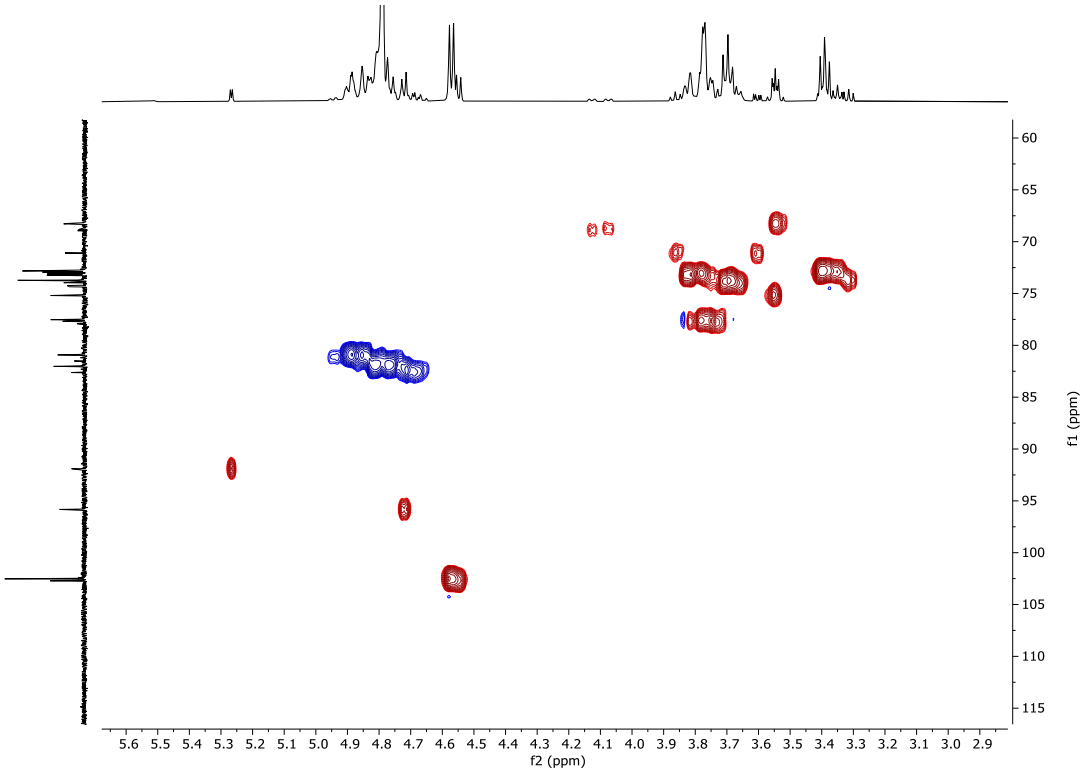

3.5.6 Synthesis of $(NN^fN)_2$

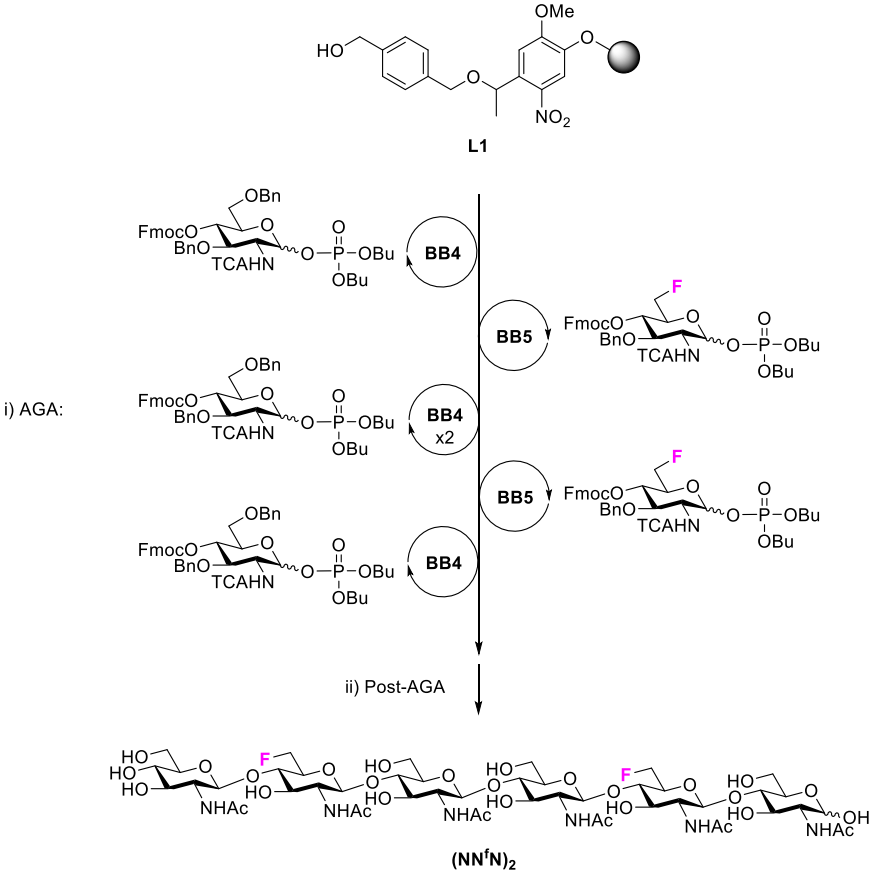

Step	BB	Modules	Notes
AGA	-	A	**L2** swelling
	BB4	B, C2, D, E	**C2**: (**BB4**, -30 °C for 5 min, -10 °C for 40 min)
	BB5	B, C2, D, E	**C2**: (**BB5**, -30 °C for 5 min, -10 °C for 40 min)
	BB4	B, C2*, D, E	**C2***: (**BB4**, -30 °C for 5 min, -10 °C for 40 min). *Double cycle
	BB4	B, C2, D, E	**C2**: (**BB4**, -30 °C for 5 min, -10 °C for 40 min)
	BB5	B, C2, D, E	**C2**: (**BB5**, -30 °C for 5 min, -10 °C for 40 min)
	BB4	B, C2*, D, E	**C2***: (**BB4**, -30 °C for 5 min, -10 °C for 40 min). *Double cycle
Post-AGA	-	G1, I*, H1, I**	**I***: (Method E2, t_R = 40.7 min) **H1**: (9 h) **I****: (Method A2, t_R = 23.3, 25.1 min)

Automated synthesis, global deprotection, and purification afforded **$(NN^fN)_2$** as a white solid (1.3 mg, 9% overall yield).

^{1}H NMR (700 MHz, Deuterium Oxide) δ 5.18 (bs, 0.7H, H-1 α), 4.73 – 4.54 (m, 9.3H, C*H*$_2$Fx2, H-1 β, H-1x5), 4.12 – 3.43 (m, 32H), 2.06 (s, 15H, *CH*$_3$CO), 2.04 (s, 3H, *CH*$_3$CO). ^{13}C NMR (176 MHz, Deuterium Oxide) δ 174.6, 101.4, 101.2, 79.0, 75.9, 74.5, 73.5, 72.0, 69.6, 62.4, 60.5, 59.9, 55.6, 55.1, 53.7, 22.0. ^{19}F NMR (564 MHz, Deuterium oxide) δ -233 – -234 (m, 2F). (ESI-HRMS) m/z 1241.486 $[M+H]^+$ ($C_{48}H_{79}F_2N_6O_{29}$ requires 1241.485).

RP HPLC of $(NN^{f}N)_2$ (ELSD trace, Method A1, t_R = 24.6, 26.1 min)

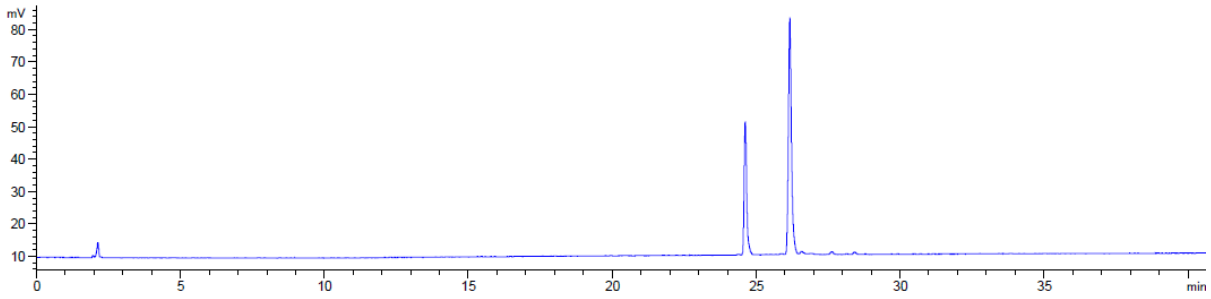

^{1}H NMR of $(NN^{f}N)_2$ (700 MHz, Deuterium Oxide)

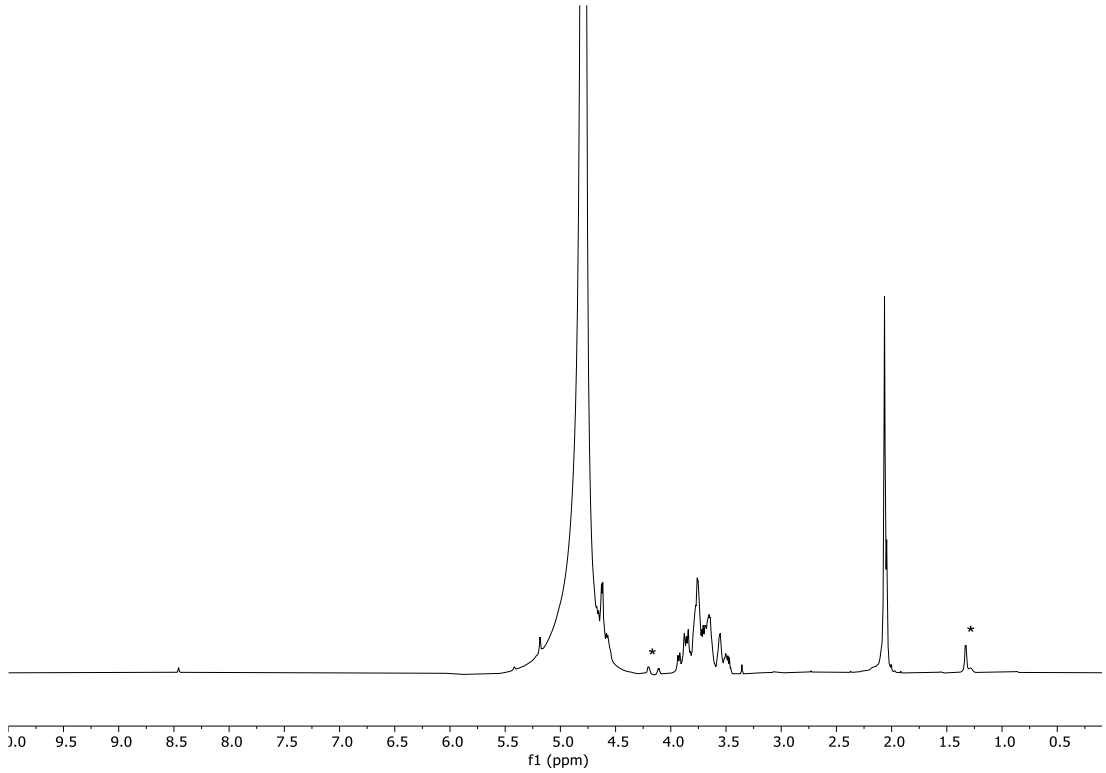

*Unidentified impurities

^{13}C NMR of $(NN^{f}N)_2$ (176 MHz, Deuterium Oxide)

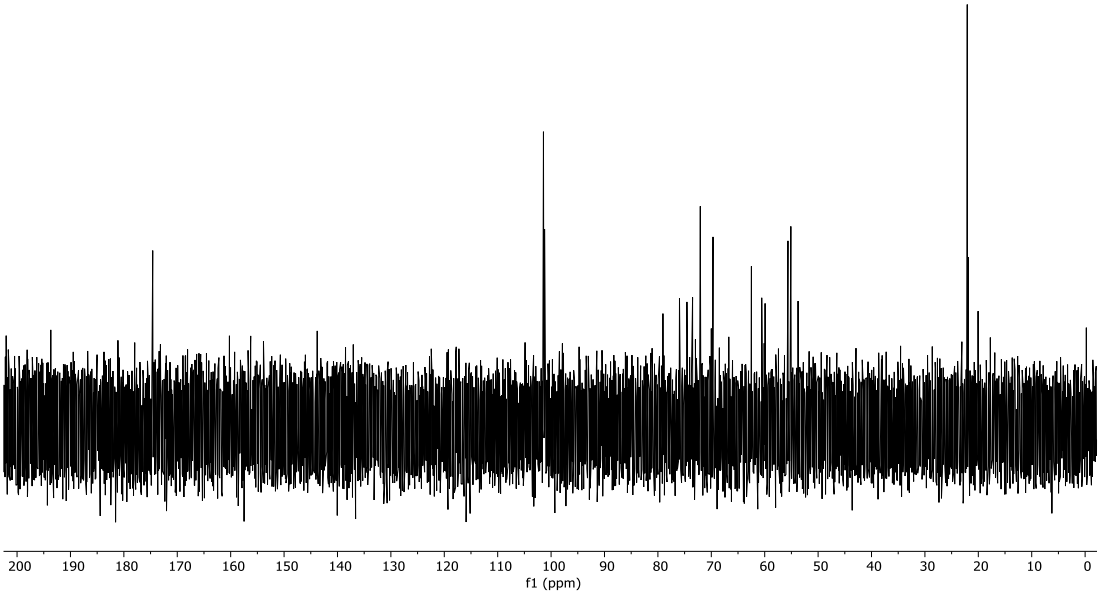

^{19}F NMR of $(NN^{f}N)_2$ (564 MHz, Deuterium Oxide)

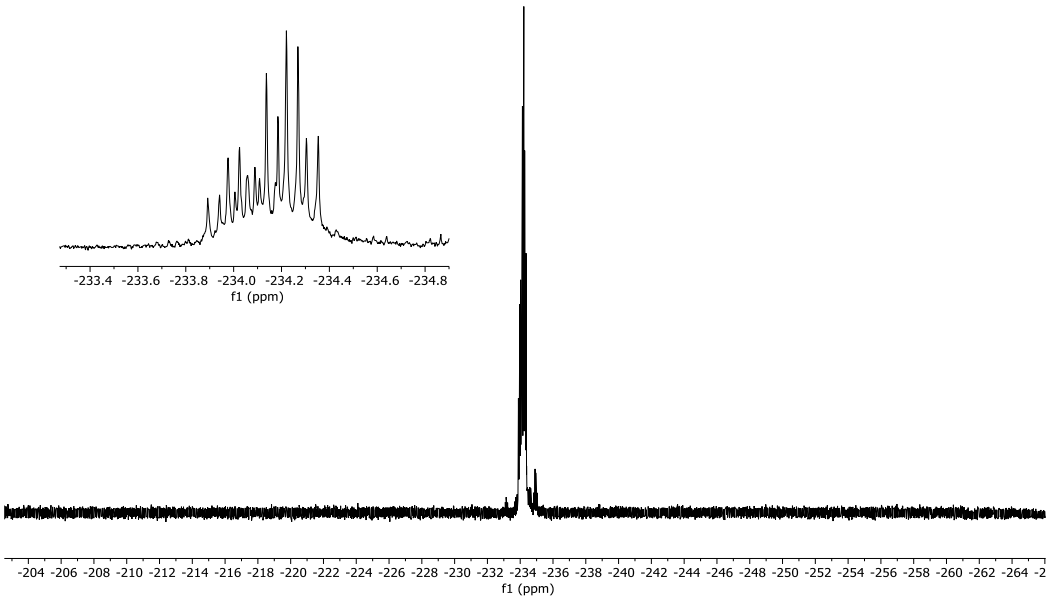

HSQC NMR of $(NN^{f}N)_2$ (Deuterium Oxide)

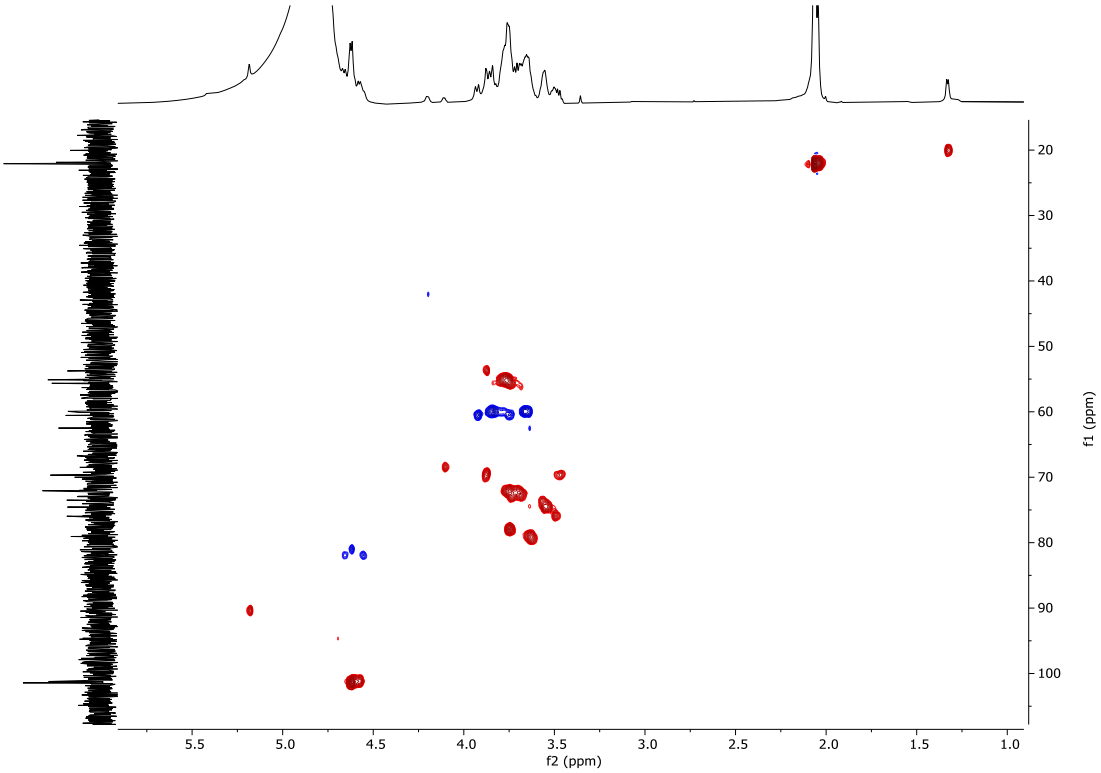

3.5.7 Synthesis of $N^f_3N_3$

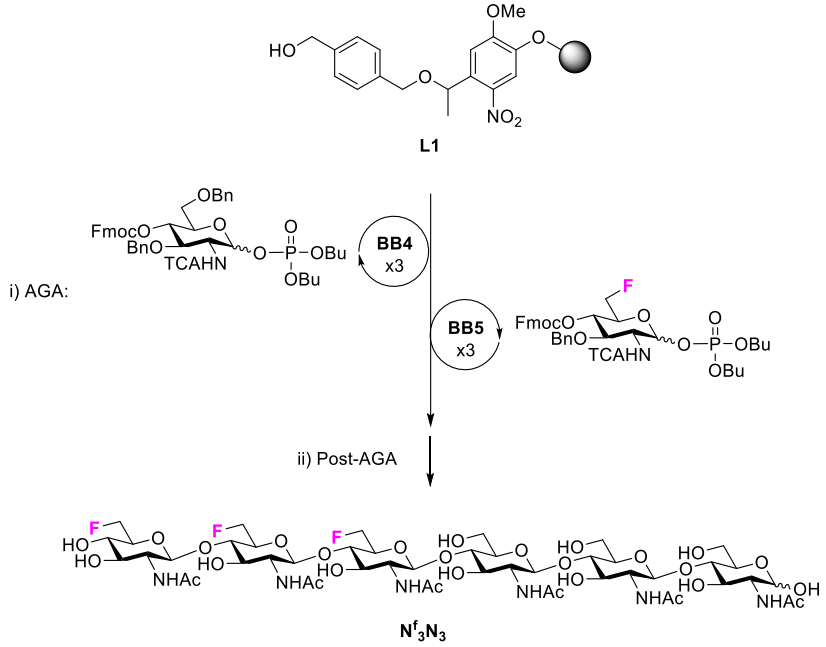

Step	BB	Modules	Notes
AGA	-	**A**	**L2** swelling
	(**BB4**)x3	(**B**, **C2**, **D**, **E**)x3	**C2**: (**BB4**, -30 °C for 5 min, -10 °C for 40 min)
	BB5	**B**, **C2**, **D**, **E**	**C2**: (**BB5**, -30 °C for 5 min, -10 °C for 40 min)
	(**BB5**)x2	(**B**, **C2***, **D**, **E**)x2	**C2***: (**BB5**, -30 °C for 5 min, -10 °C for 40 min). *Double cycle
Post-AGA	-	**G1**, **I***, **H1**, **I****	**I***: (Method E2, t_R = 41 min) **H1**: (6 h) **I****: (Method A2, t_R = 24.0, 25.2 min)

Automated synthesis, global deprotection, and purification afforded $\mathbf{N^f_3N_3}$ as a white solid (1.2 mg, 8% overall yield).

^{1}H NMR (700 MHz, Deuterium Oxide) δ 5.19 (d, *J* = 2.3 Hz, 0.7H, H-1 **α**), 4.80 – 4.52 (m, 11.3H, C*H*$_2$Fx3, H-1 β, H-1x5), 3.88 – 3.51 (m, 32H), 2.06 (s, 15H, *CH*$_3$-CO), 2.04 (s, 3H, *CH*$_3$-CO). ^{13}C NMR (176 MHz, Deuterium Oxide) δ 174.7, 171.0, 101.3, 94.8, 74.5, 73.3, 72.0, 68.5, 59.9, 55.6, 55.2, 22.1. ^{19}F NMR (564 MHz, Deuterium oxide) δ -234.3 (td, *J* = 47.5, 28.0 Hz, 1F, CH$_2$-*F*), -234.5 (td, *J* = 47.2, 27.9 Hz, 1F, CH$_2$-*F*), -235.0 (td, *J* = 47.1, 25.0 Hz, 1F, CH$_2$-*F*). (ESI-HRMS) m/z 1243.487 $[M+H]^+$ ($C_{48}H_{78}F_3N_6O_{28}$ requires 1243.481).

RP HPLC of $N^f_3N_3$ (ELSD trace, Method A1, t_R = 25.4, 26.4 min)

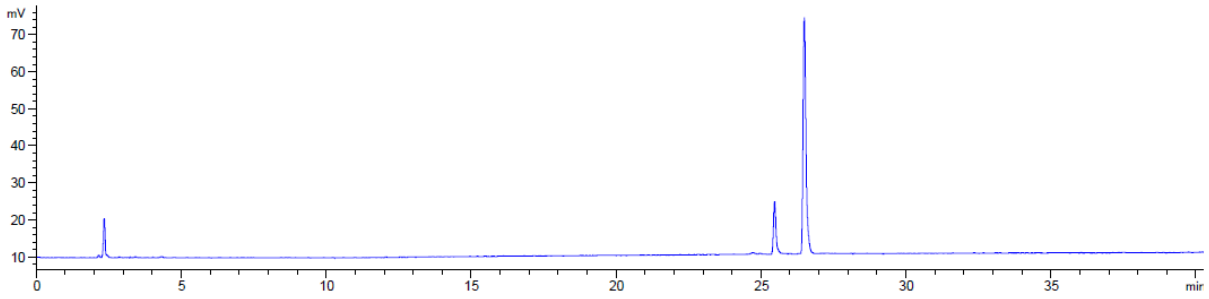

^{1}H NMR of $N^f_3N_3$ (700 MHz, Deuterium Oxide)

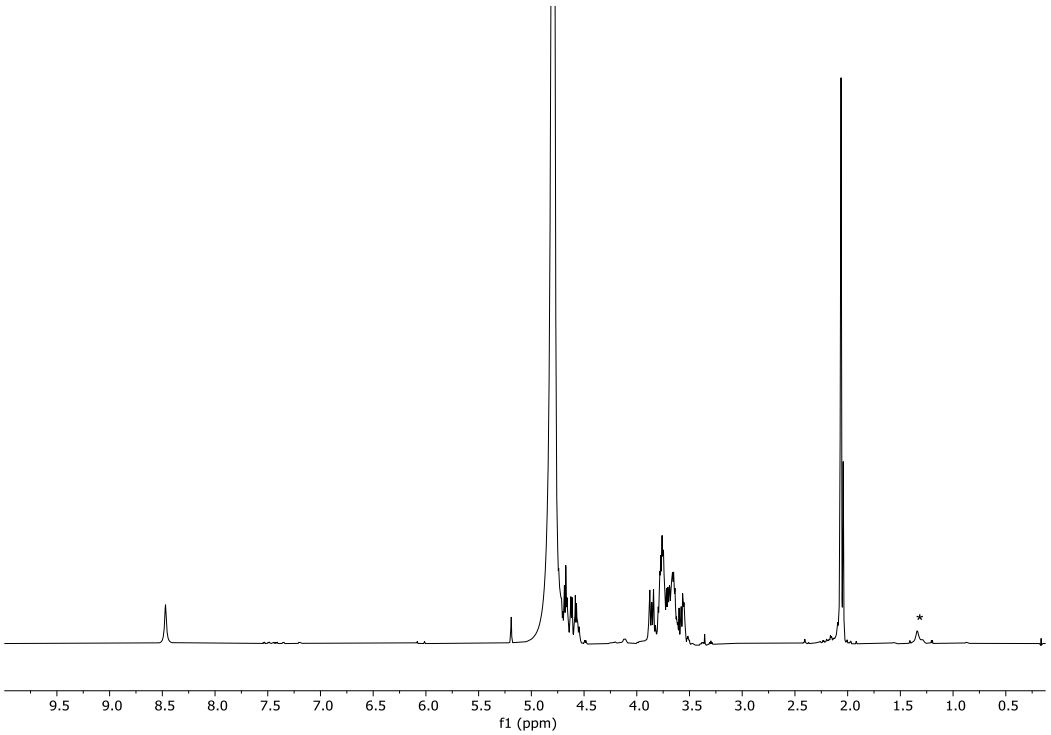

*Unidentified impurity

^{13}C NMR of $N^f_3N_3$ (176 MHz, Deuterium Oxide)

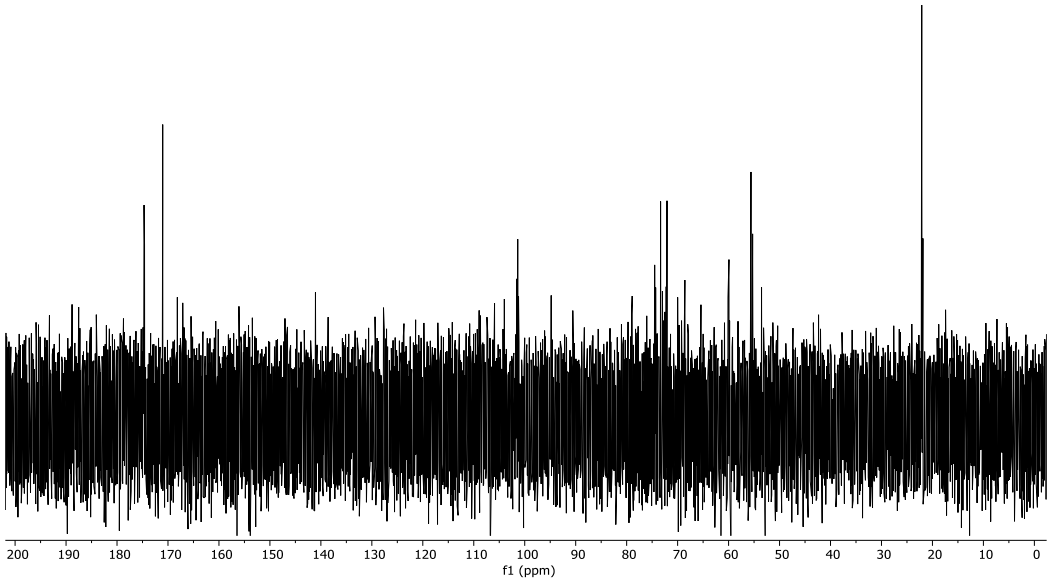

^{19}F NMR of $N^f_3N_3$ (564 MHz, Deuterium Oxide)

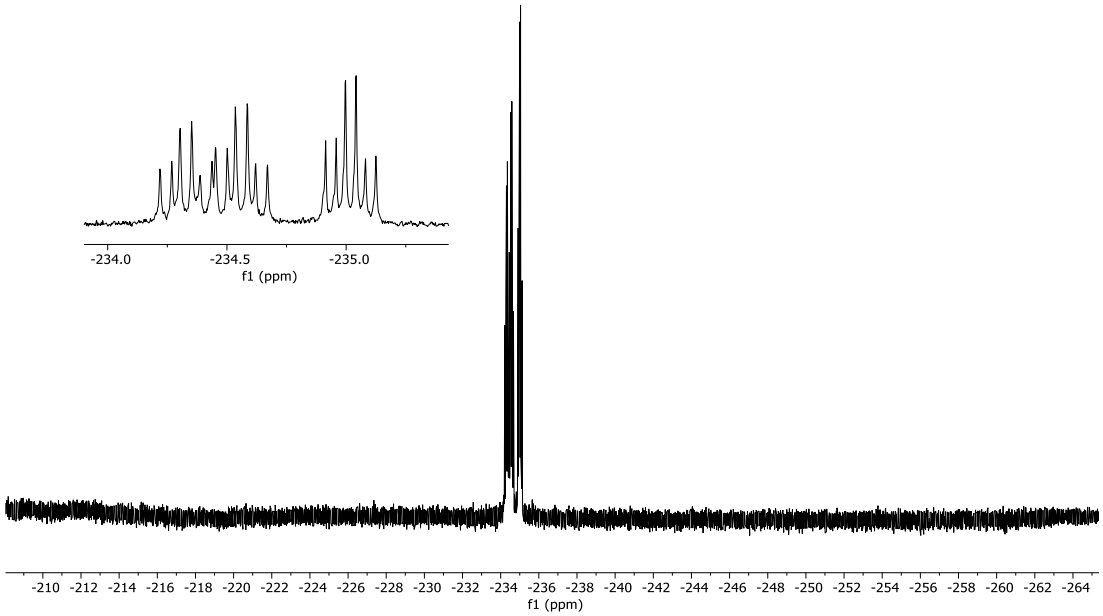

HSQC NMR of $N^{f}_{3}N_{3}$ (Deuterium Oxide)

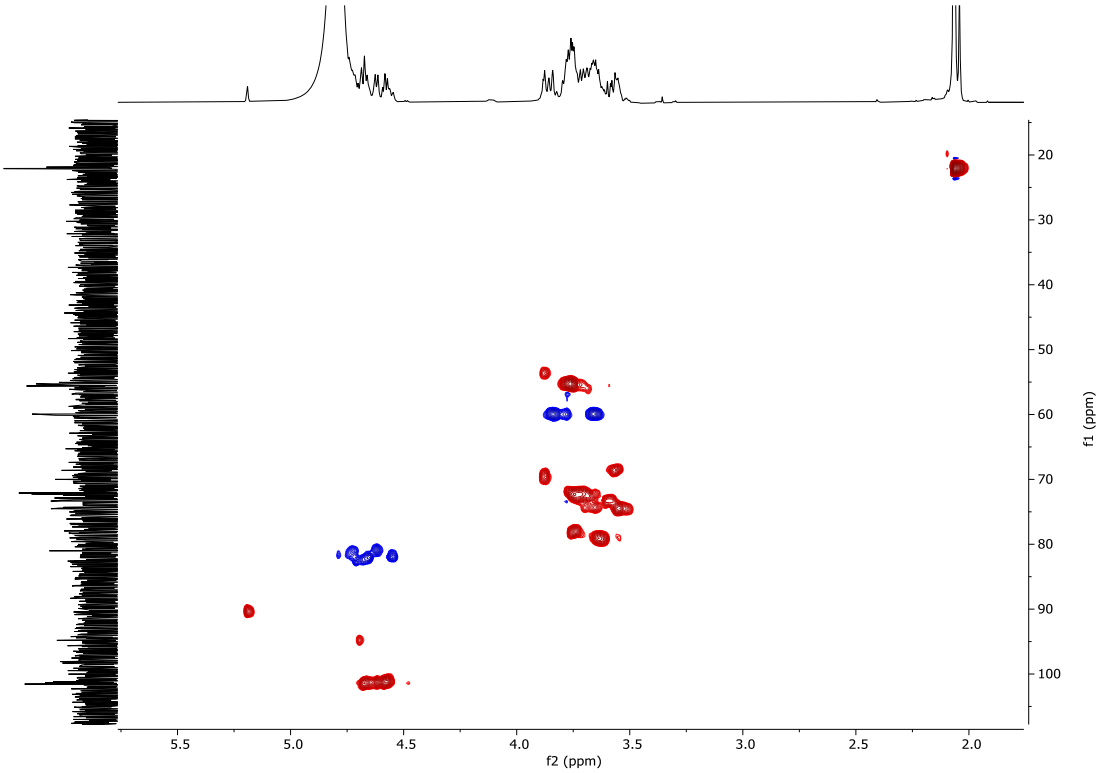

3.5.8 Side product containing α-glycosidic linkages observed during the synthesis of AfAAfA

While employing **BB3** for the synthesis of 6F-cellulose analogues, we observed a small amount of α glycosidic linkages in the synthesis of certain 6F-cellulose analogs despite the C-2 participating protecting group. Possible causes of the reduced β-stereoselectivity of the glycosylation reaction could be 1) the low nucleophilicity of the 6F-Glc acceptors bound to the solid support and 2) the presence of dioxane in the glycosylation solution (see Module C1).[10] The side-products containing α-glycosidic bonds could be partially separated by preparative RP-HPLC (see Module I, Method D2).

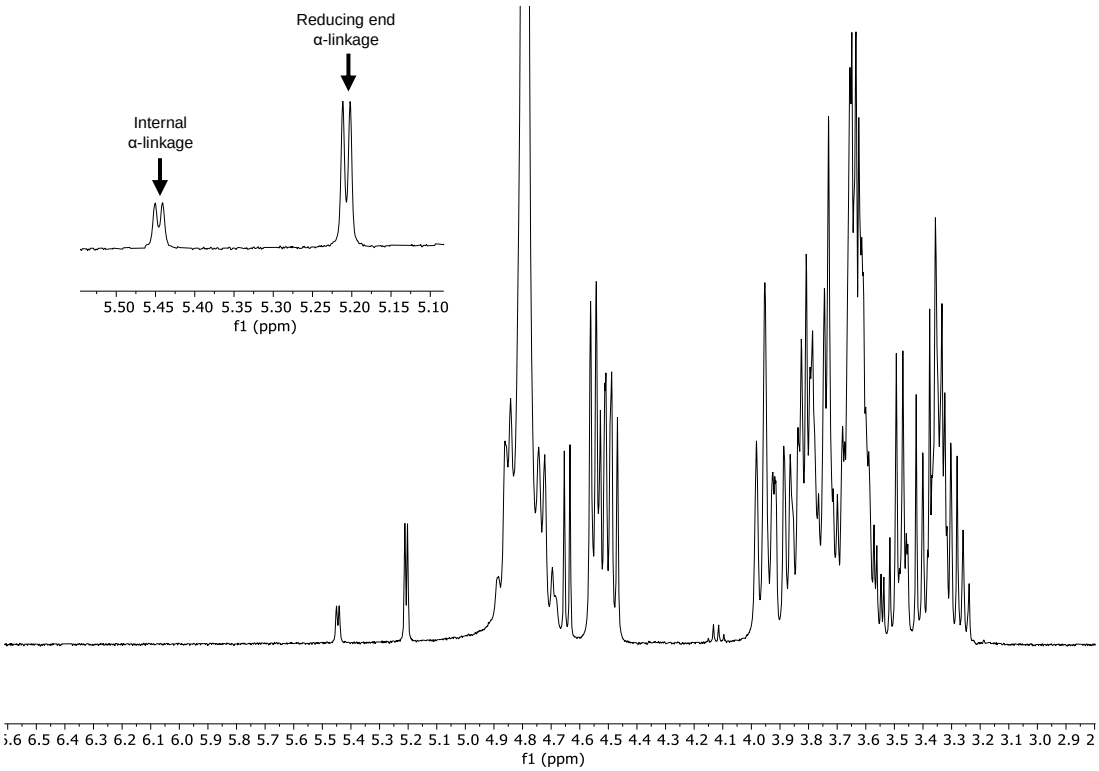

Figure S2 ^{1}H NMR (400 MHz, D_2O) of the crude product AfAAfA after hydrogenolysis (Module H1 or H2). The doublet at δ 5.45 (d, J = 3.8 Hz) corresponds to α-glycosidic linkages (previously reported at δ 5.45 – 5.37 ppm[11]).

4 Molecular Dynamics Simulations

4.1 General materials and methods

For all simulations, the modified version GLYCAM06$_{OSMO,r14}$ force field was used.[12,13] Partial charges for non-standard monomers were derived using the R.E.D. tools scripts[14] following the GLYCAM06 protocol. Structure optimization for the charge derivation was performed using Gaussian (Gaussian, Inc., Wallingford CT, 2004) at the HF/6-31G* and the HF/6-31++G** level of theory. Initial conformations for single hexamer simulations were constructed with the Glycam Carbohydrate builder and tleap (https://glycam.org/). The topology was subsequently converted using the python script acpype. All simulations were performed in water as solvent using TIP5P as water model.[16] The simulation time for the single molecule experiments was 500 ns, while concentrated experiments run for 1 µs. Bonds involving hydrogens were constrained using the LINCS to allow a 2 fs time steps. Non-bonded interactions were cut-off at 1.4 nm, long range electrostatics were calculated using the particle mesh Ewald method.[17] A concentrated experiment for a hexamer contains 25 molecules in a simulation box of 6 nm x 6 nm x 6 nm size. After energy minimization (steepest descent algorithm) and before the production run, the systems were equilibrated at 300 K for 50 ns in a canonical (NVT) ensemble (constant number of particles, volume and temperature) and subsequently at 300 K and 1 bar for 50 ns in an isothermal-isobaric (NPT) ensemble. All molecular dynamics simulations were performed using Gromacs 5.1.2.[18] A Nosé-Hoover thermostat[19] kept the constant temperature of 303 K constant while a Parrinello-Rahman barostat[20] ensured a constant pressure of 1 bar. The analysis was visualized using OriginPro 2021b. Puckering analysis of all simulated structures confirmed the $^1C_4$ chair as major conformation (>90%).

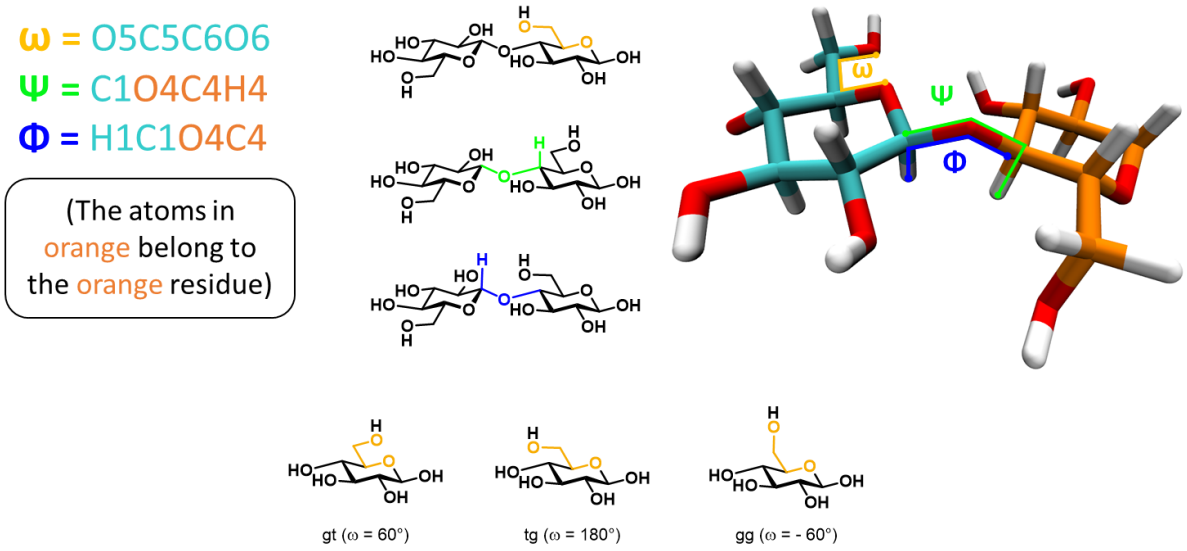

Figure S3 Definition of dihedrals in a disaccharide.

4.2 End-to-end distance plots

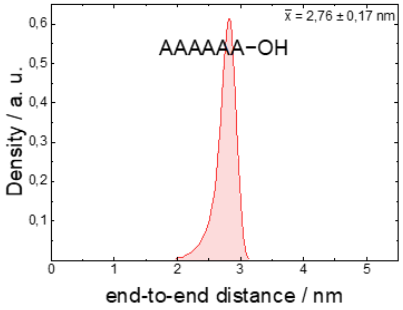

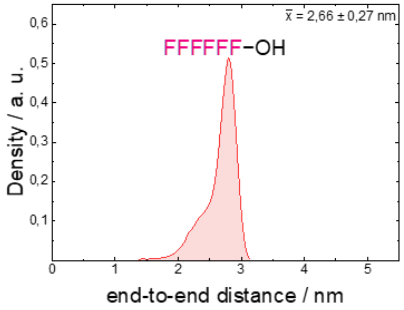

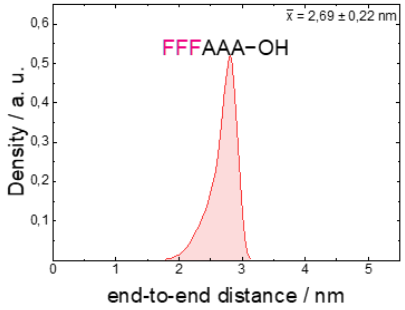

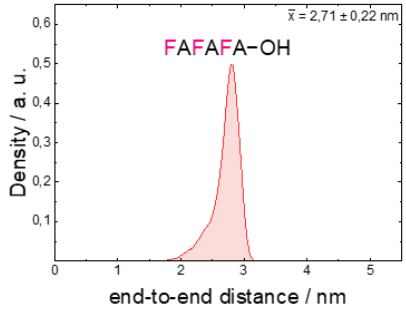

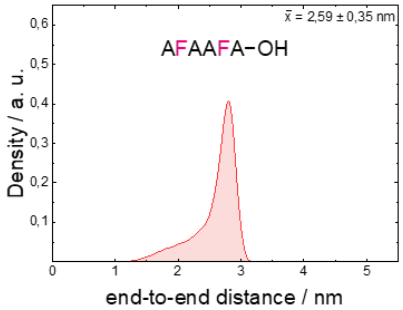

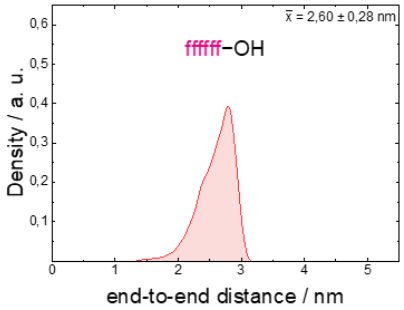

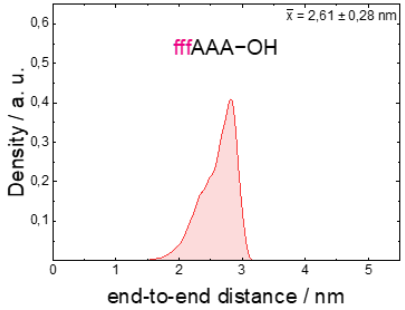

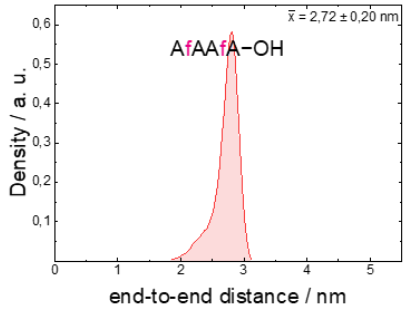

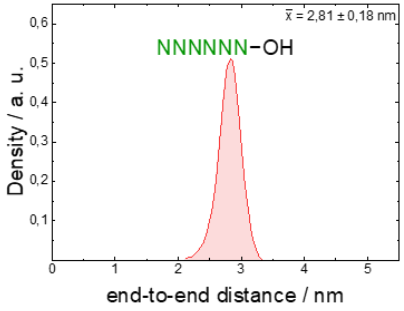

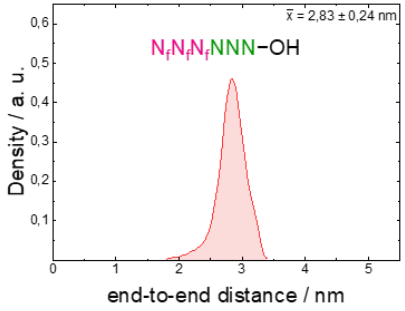

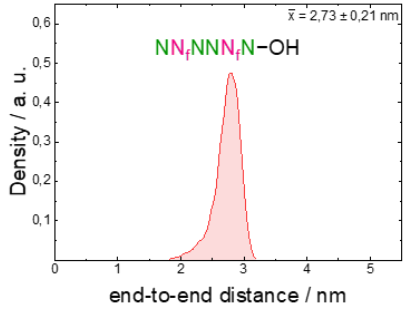

4.3 Radius of gyration plots

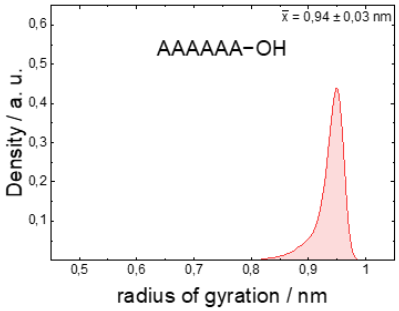

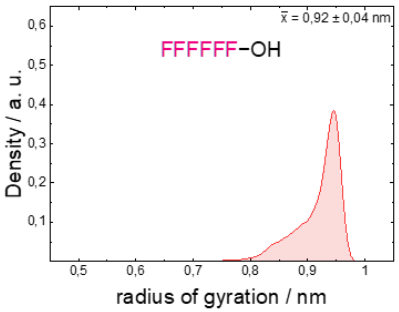

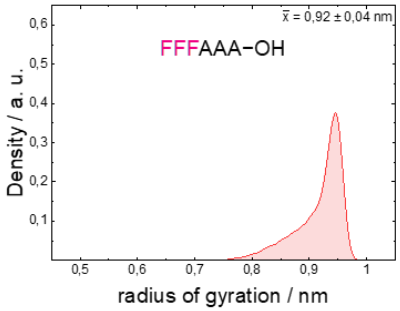

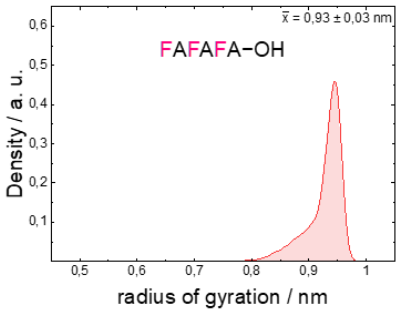

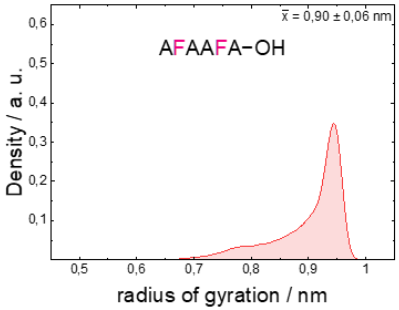

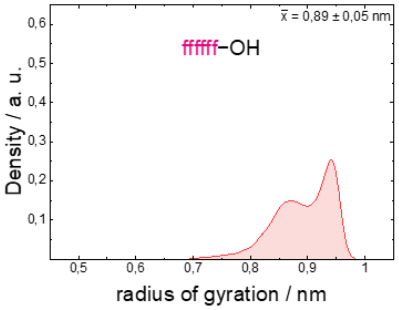

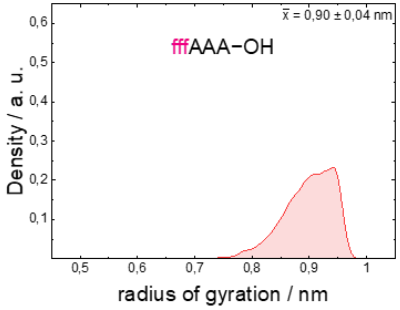

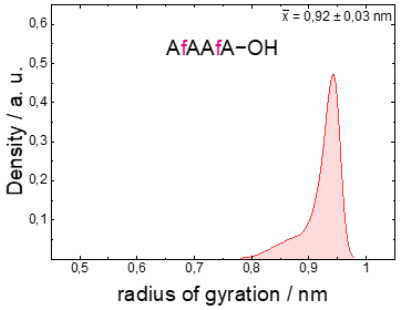

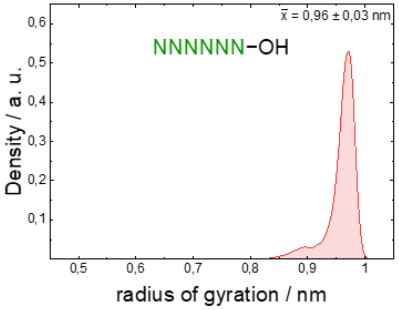

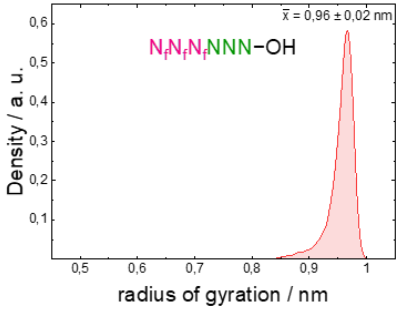

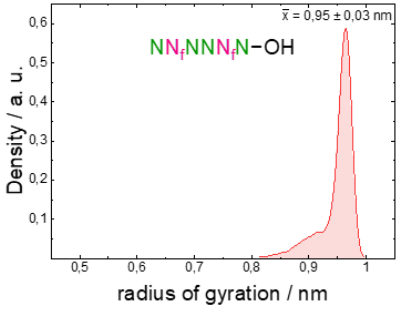

4.4 Ring puckering analysis

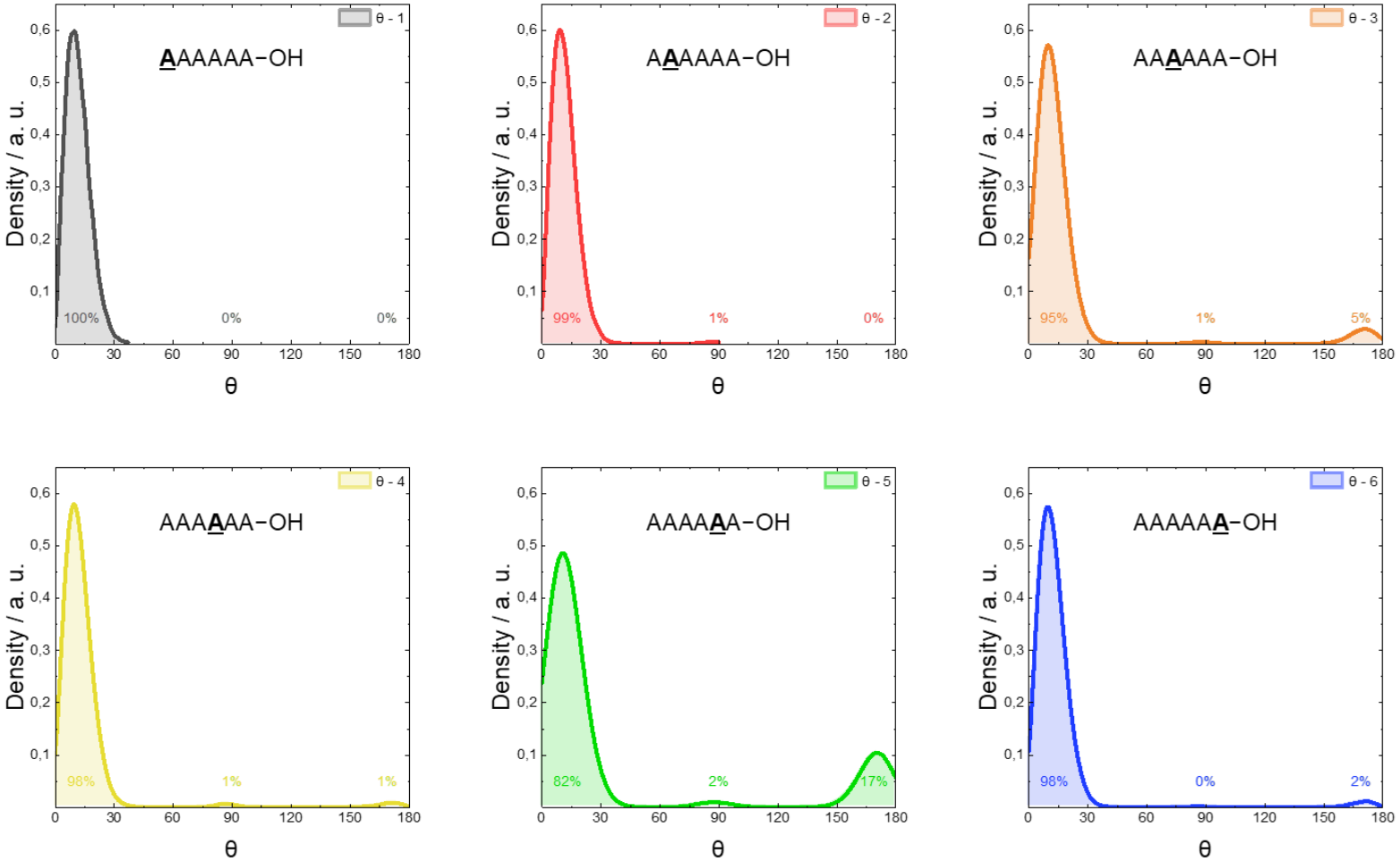

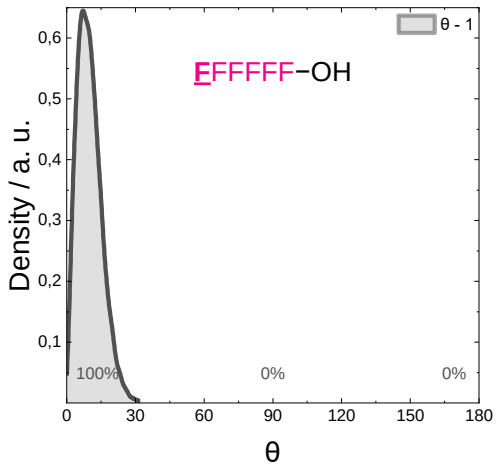
θ - 1
FFFFFF−OH
Density / a. u.
θ
100%
0%
0%

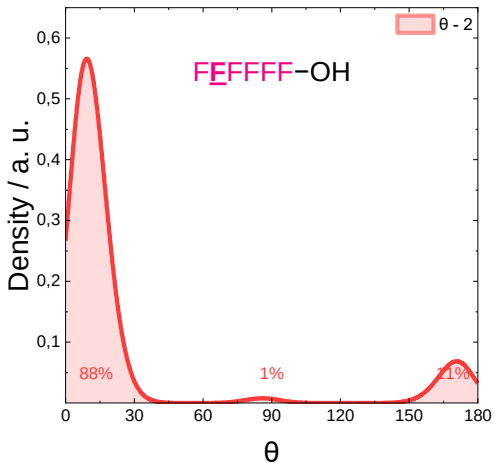
θ - 2
FFFFFF−OH
Density / a. u.
θ
88%
1%
11%

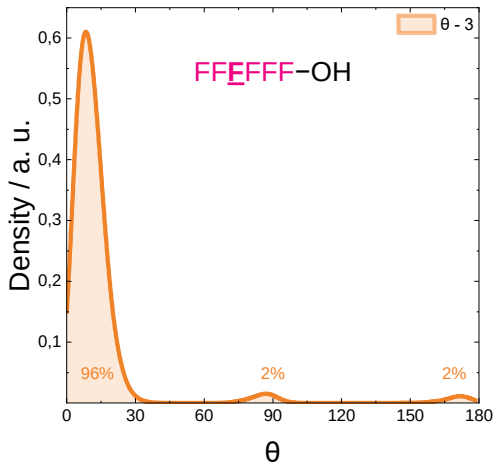
θ - 3
FFFFFF−OH
Density / a. u.
θ
96%
2%
2%

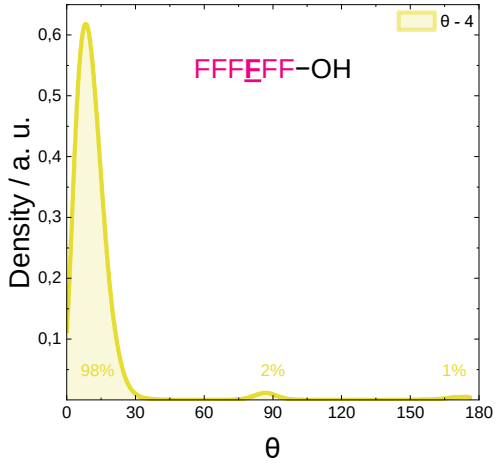
θ - 4
FFFFFF−OH
Density / a. u.
θ
98%
2%
1%

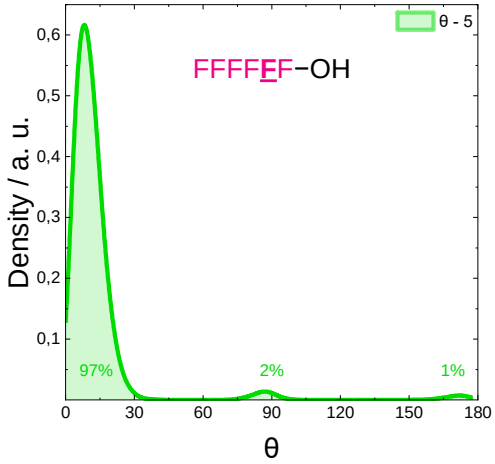
θ - 5
FFFFFF−OH
Density / a. u.
θ
97%
2%
1%

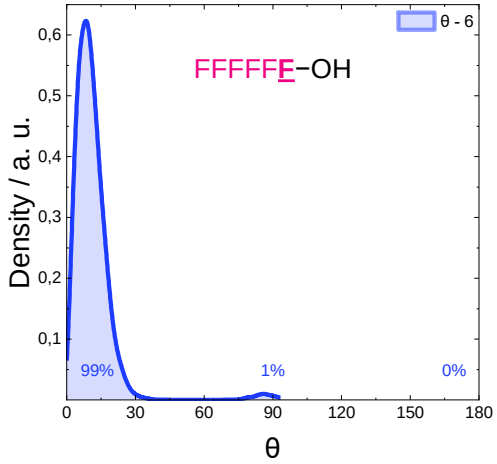
θ - 6
FFFFFF−OH
Density / a. u.
θ
99%
1%
0%

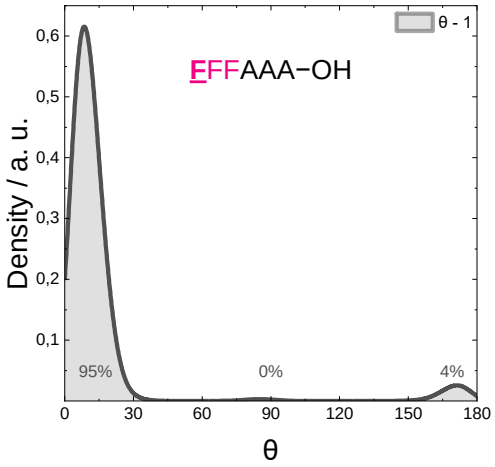
θ - 1
FFFAAA−OH
Density / a. u.
θ
95%
0%
4%

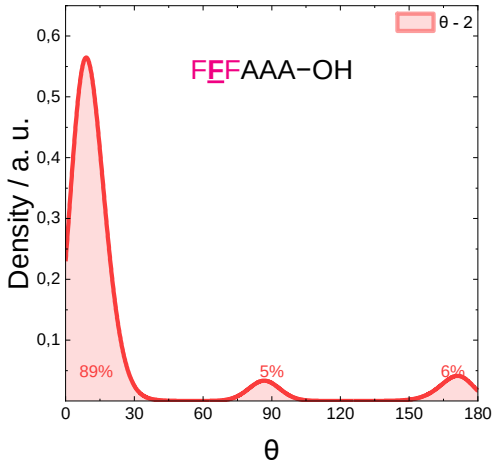
θ - 2
FFFAAA−OH
Density / a. u.
θ
89%
5%
6%

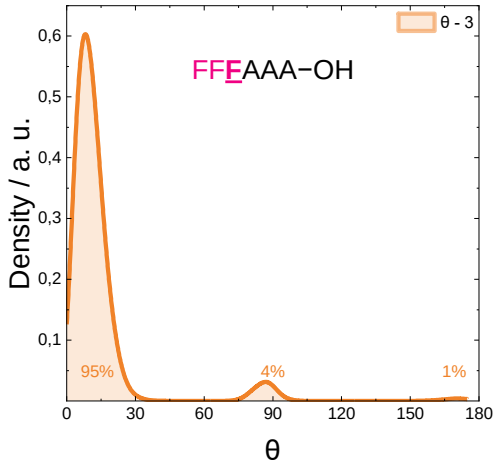
θ - 3
FFFAAA−OH
Density / a. u.
θ
95%
4%
1%

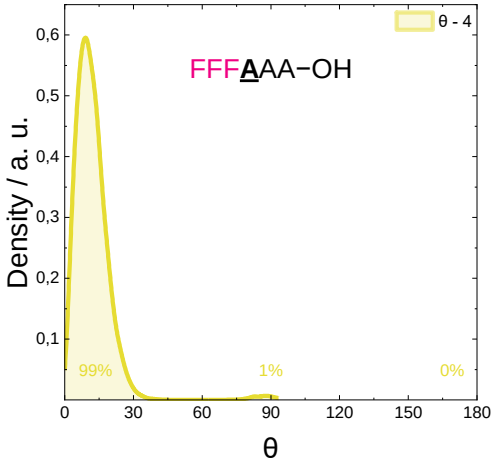
θ - 4
FFFAAA−OH
Density / a. u.
θ
99%
1%
0%

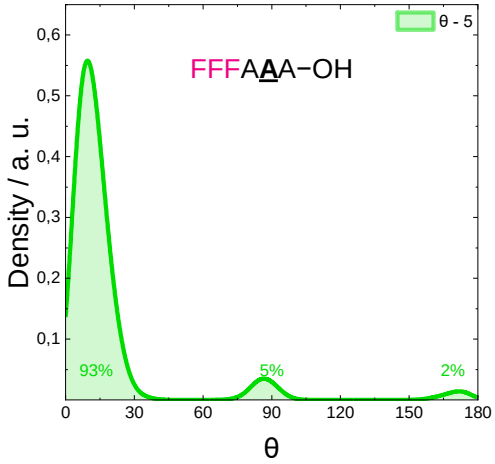
θ - 5
FFFAAA−OH
Density / a. u.
θ
93%
5%
2%

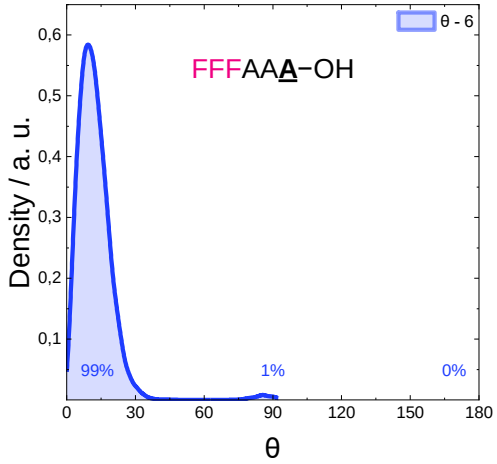
θ - 6
FFFAAA−OH
Density / a. u.
θ
99%
1%
0%

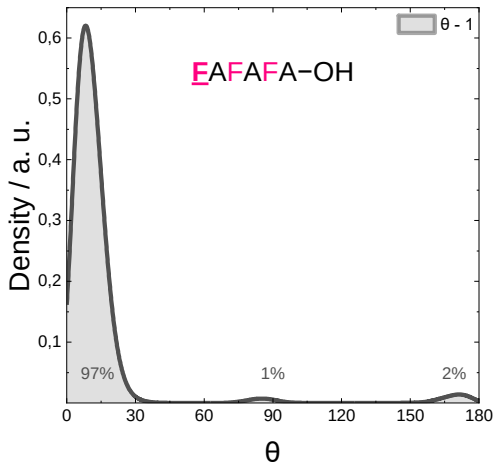
θ - 1
FAFAFA−OH
Density / a. u.
θ
97%
1%
2%

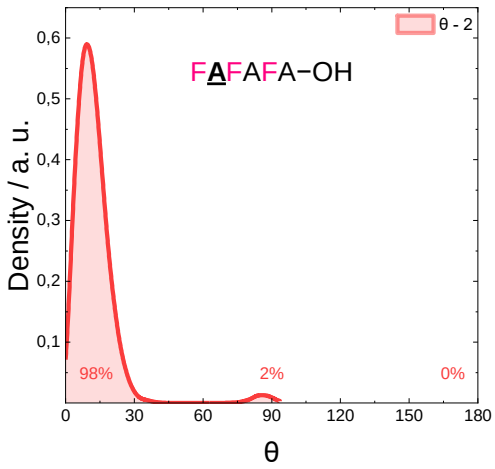
θ - 2
FAFAFA−OH
Density / a. u.
θ
98%
2%
0%

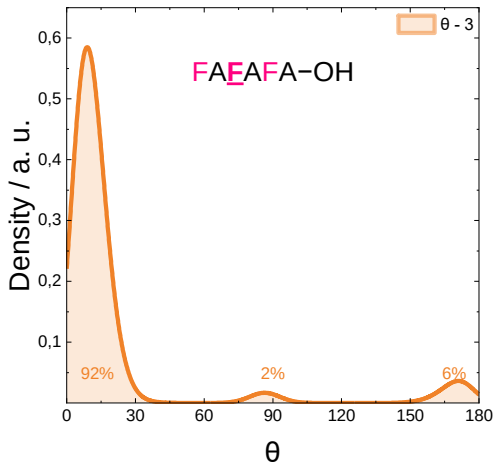
θ - 3
FAFAFA−OH
Density / a. u.
θ
92%
2%
6%

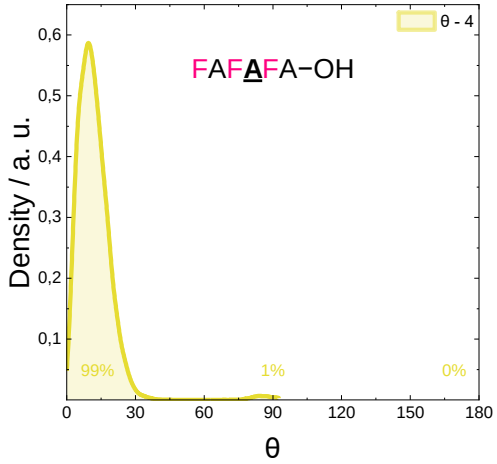
θ - 4
FAFAFA−OH
Density / a. u.
θ
99%
1%
0%

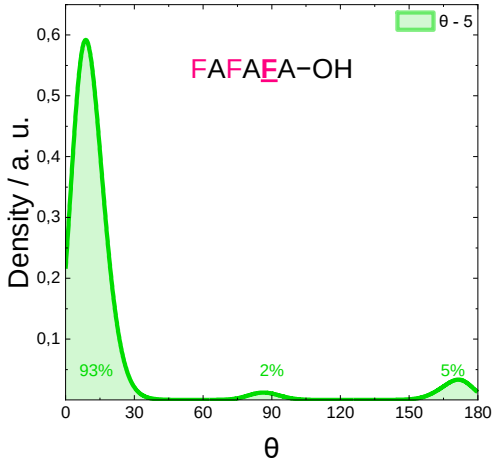
θ - 5
FAFAFA−OH
Density / a. u.
θ
93%
2%
5%

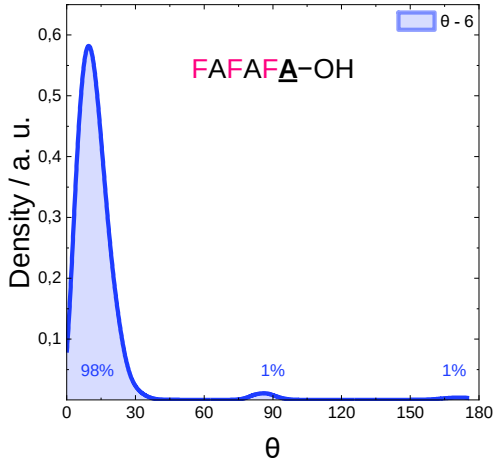
θ - 6
FAFAFA−OH
Density / a. u.
θ
98%
1%
1%

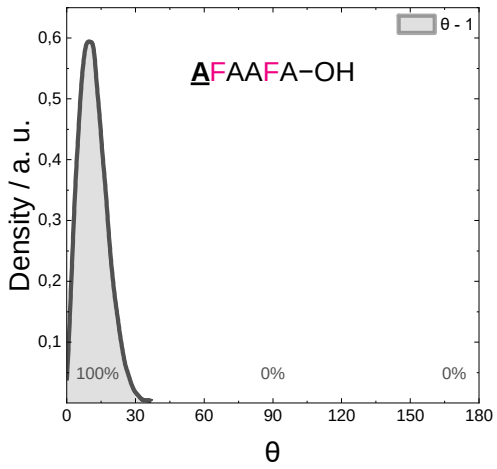
θ - 1
AFAAFA−OH
Density / a. u.
θ
100%
0%
0%

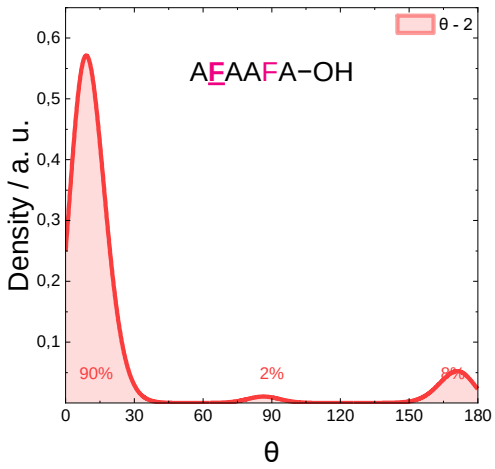
θ - 2
AFAAFA−OH
Density / a. u.
θ
90%
2%
8%

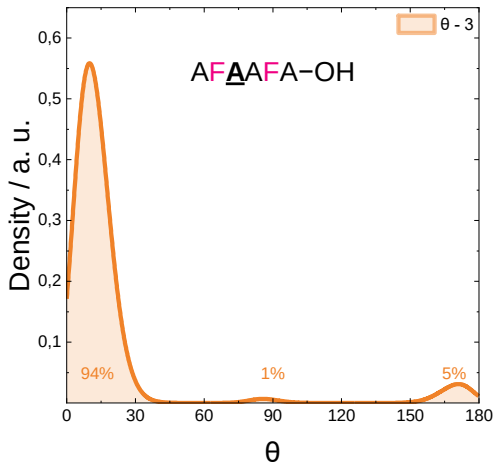
θ - 3
AFAAFA−OH
Density / a. u.
θ
94%
1%
5%

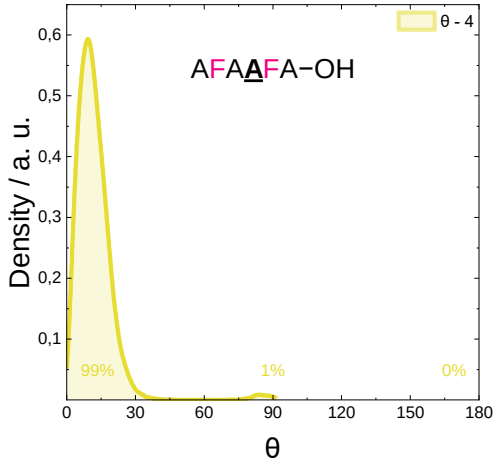
θ - 4
AFAAFA−OH
Density / a. u.
θ
99%
1%
0%

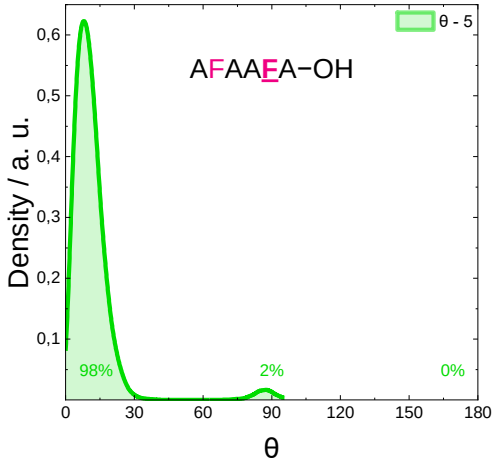
θ - 5
AFAAFA−OH
Density / a. u.
θ
98%
2%
0%

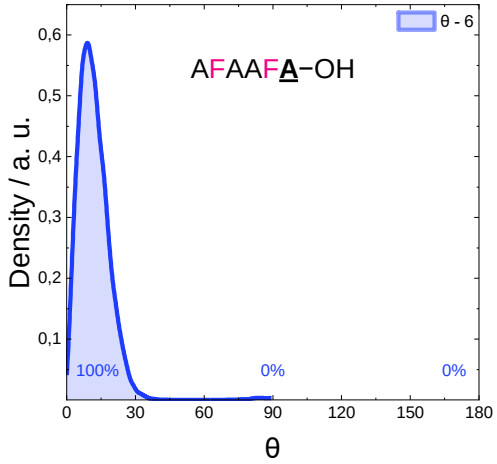
θ - 6
AFAAFA−OH
Density / a. u.
θ
100%
0%
0%

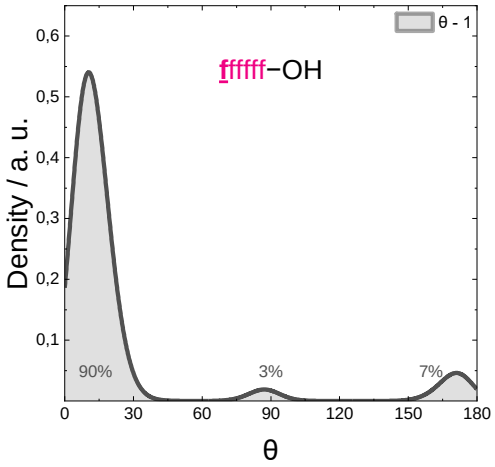
θ - 1
fffff−OH
Density / a. u.
θ
90%
3%
7%

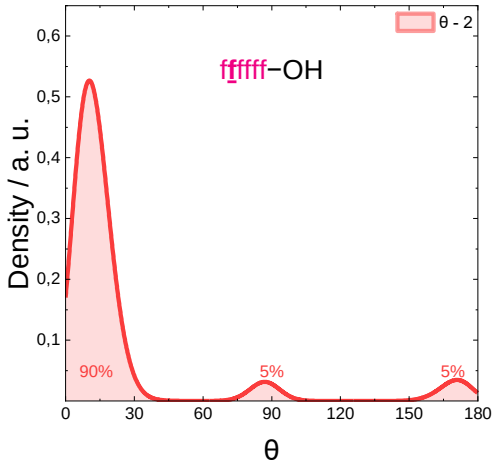
θ - 2
ffffff−OH
Density / a. u.
θ
90%
5%
5%

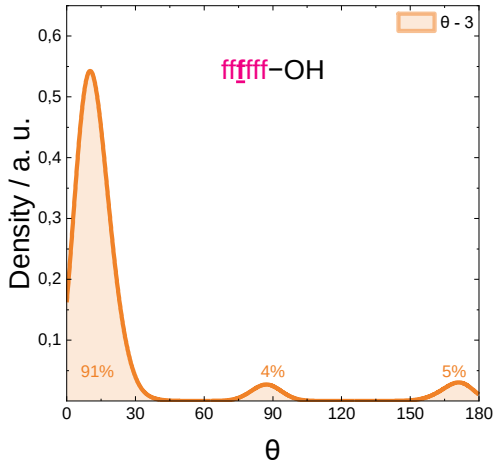
θ - 3
fffffff−OH
Density / a. u.
θ
91%
4%
5%

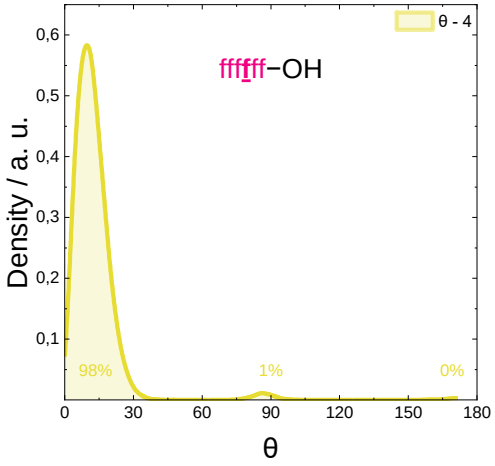
θ - 4
ffffff−OH
Density / a. u.
θ
98%
1%
0%

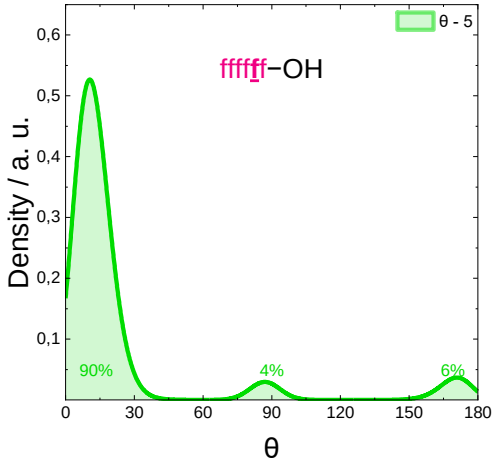
θ - 5
fffffff−OH
Density / a. u.
θ
90%
4%
6%

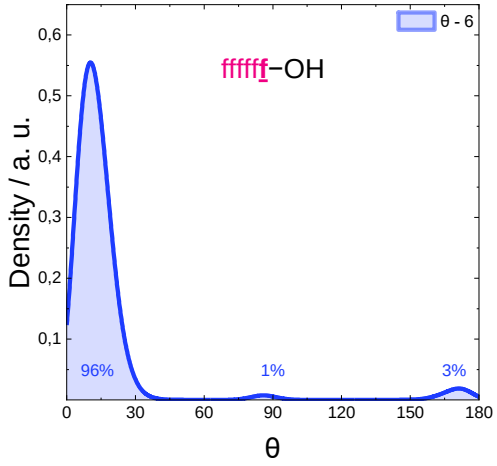
θ - 6
ffffff−OH
Density / a. u.
θ
96%
1%
3%

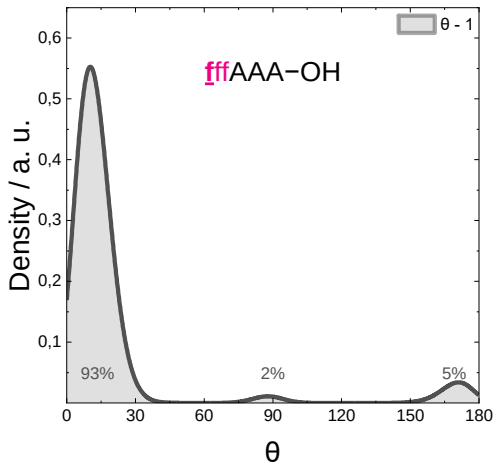
θ - 1
fffAAA−OH
Density / a. u.
θ
93%
2%
5%

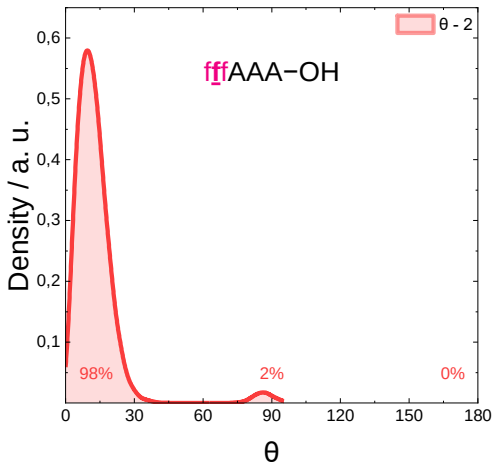
θ - 2
fffAAA−OH
Density / a. u.
θ
98%
2%
0%

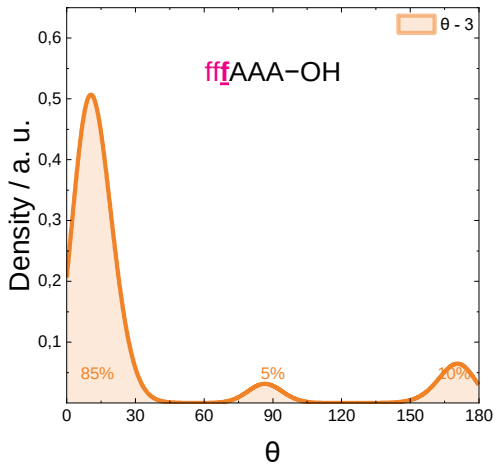
θ - 3
fffAAA−OH
Density / a. u.
θ
85%
5%
10%

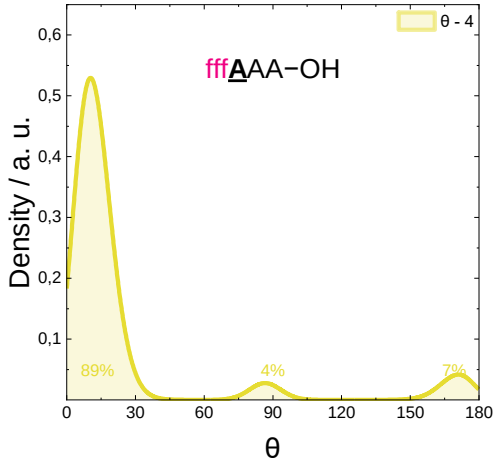
θ - 4
fffAAA−OH
Density / a. u.
θ
89%
4%
7%

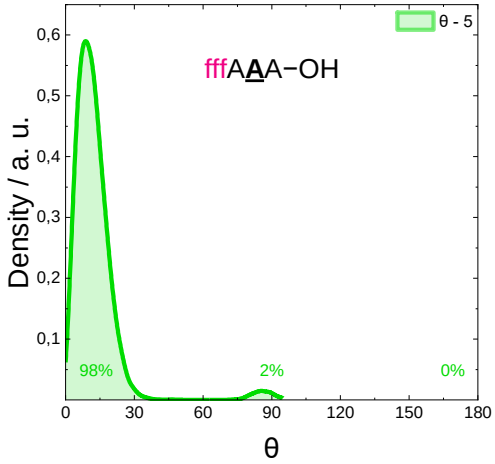
θ - 5
fffAAA−OH
Density / a. u.
θ
98%
2%
0%

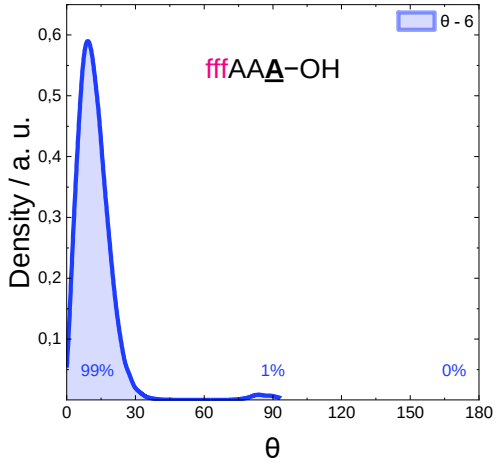
θ - 6
fffAAA−OH
Density / a. u.
θ
99%
1%
0%

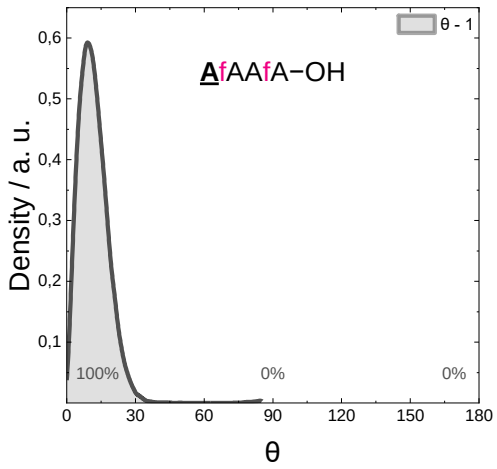
θ - 1
AfAAfA−OH
Density / a. u.
θ
100%
0%
0%

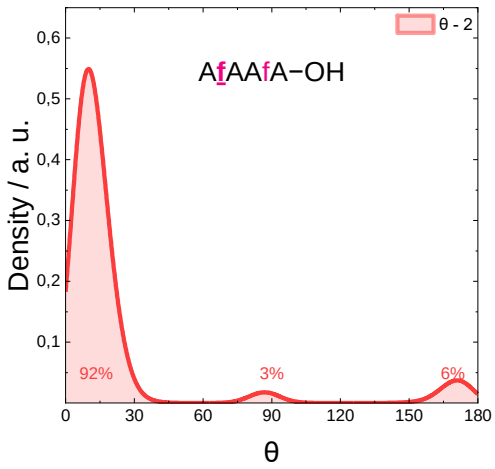
θ - 2
AfAAfA−OH
Density / a. u.
θ
92%
3%
6%

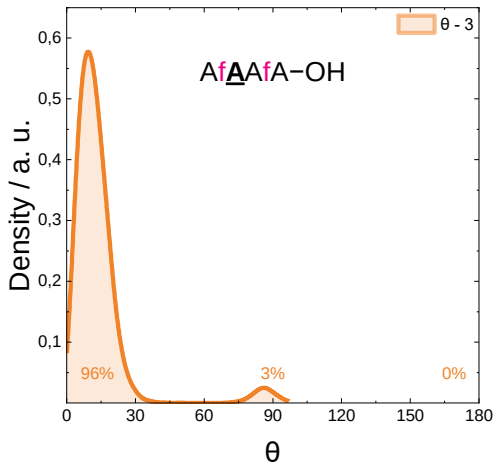
θ - 3
AfAAfA−OH
Density / a. u.
θ
96%
3%
0%

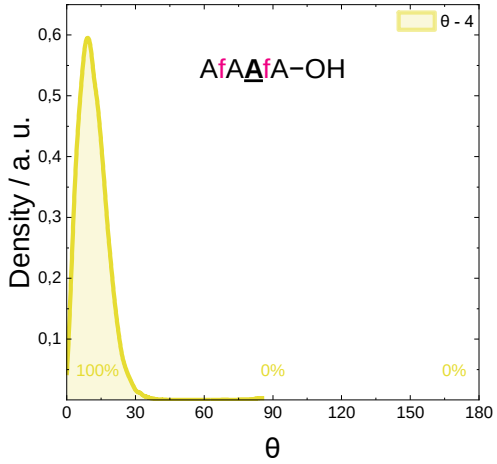
θ - 4
AfAAfA−OH
Density / a. u.
θ
100%
0%
0%

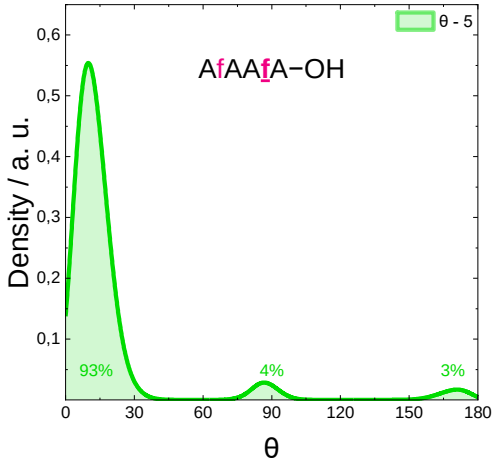
θ - 5
AfAAfA−OH
Density / a. u.
θ
93%
4%
3%

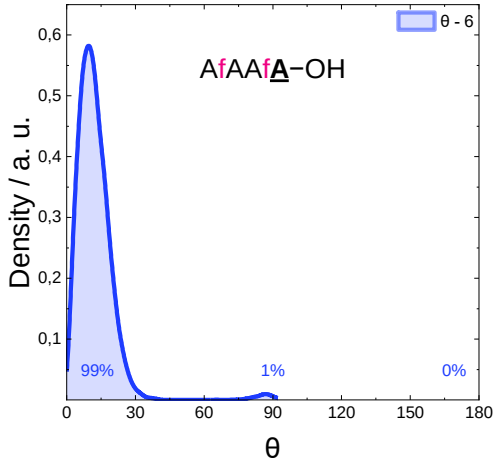
θ - 6
AfAAfA−OH
Density / a. u.
θ
99%
1%
0%

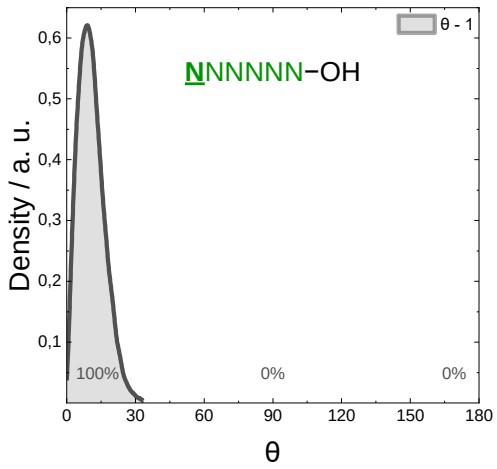
θ - 1
NNNNNN−OH
Density / a. u.
θ
100%
0%
0%

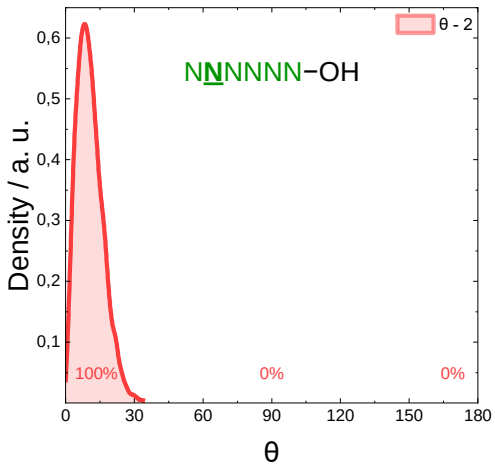
θ - 2
NNNNNN−OH
Density / a. u.
θ
100%
0%
0%

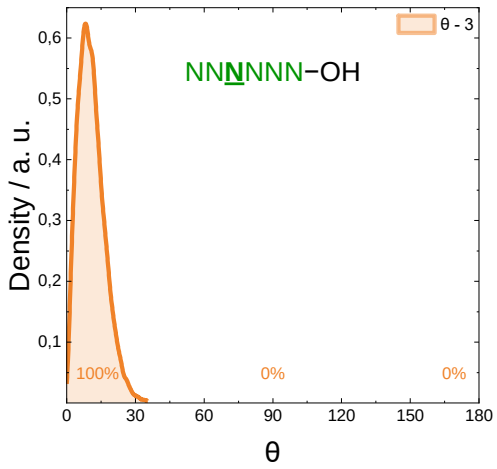
θ - 3
NNNNNN−OH
Density / a. u.
θ
100%
0%
0%

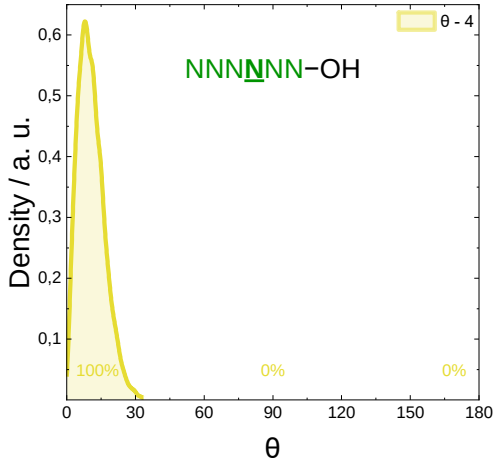
θ - 4
NNNNNN−OH
Density / a. u.
θ
100%
0%
0%

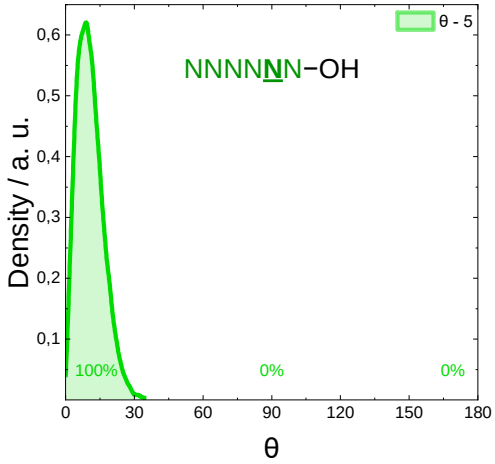
θ - 5
NNNNNN−OH
Density / a. u.
θ
100%
0%
0%

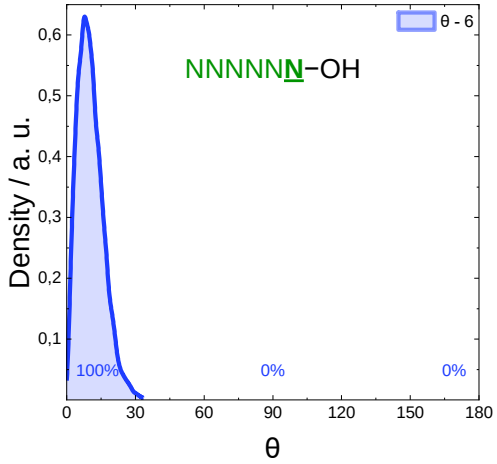
θ - 6
NNNNNN−OH
Density / a. u.
θ
100%
0%
0%

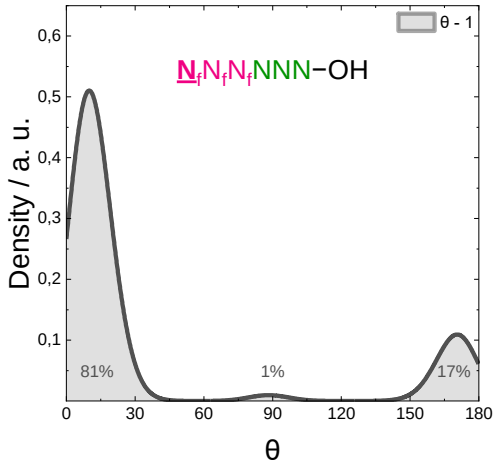
θ - 1
NfNfNfNNN−OH
Density / a. u.
θ
81%
1%
17%

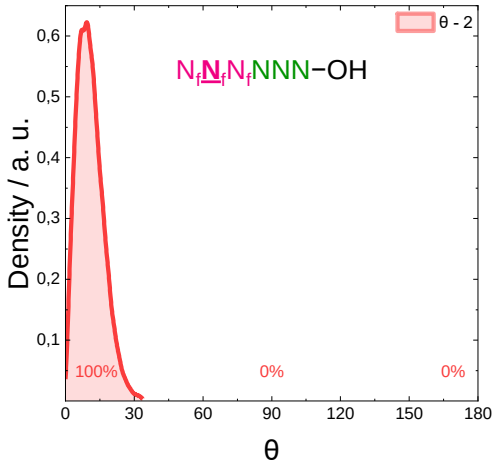
θ - 2
NfNfNfNNN−OH
Density / a. u.
θ
100%
0%
0%

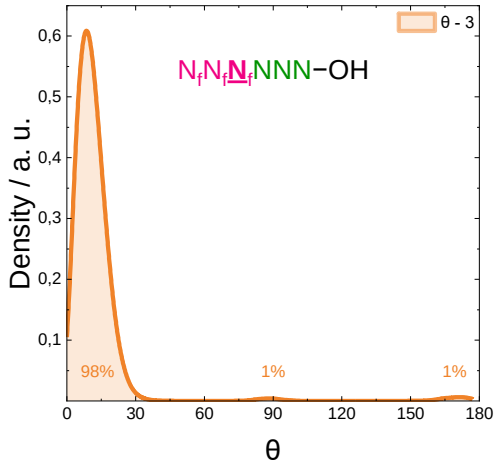
θ - 3
NfNfNfNNN−OH
Density / a. u.
θ
98%
1%
1%

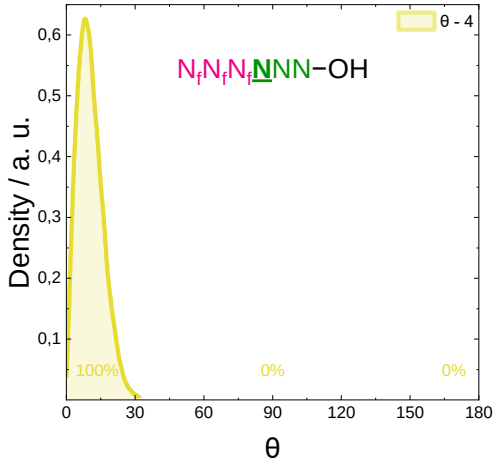
θ - 4
NfNfNfNNN−OH
Density / a. u.
θ
100%
0%
0%

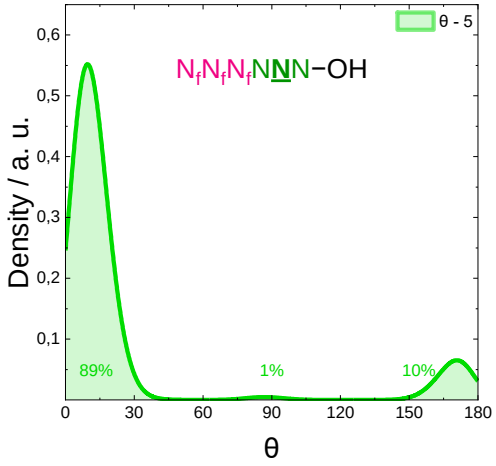
θ - 5
NfNfNfNNN−OH
Density / a. u.
θ
89%
1%
10%

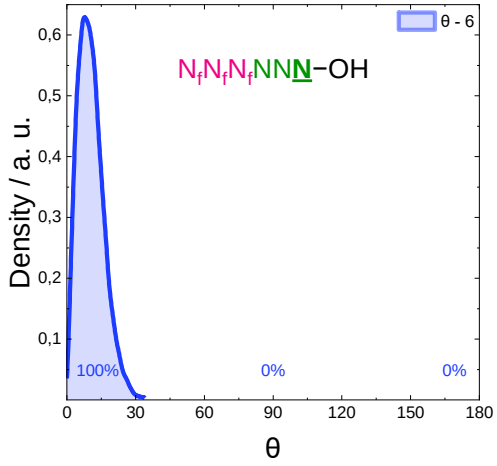
θ - 6
NfNfNfNNN−OH
Density / a. u.
θ
100%
0%
0%

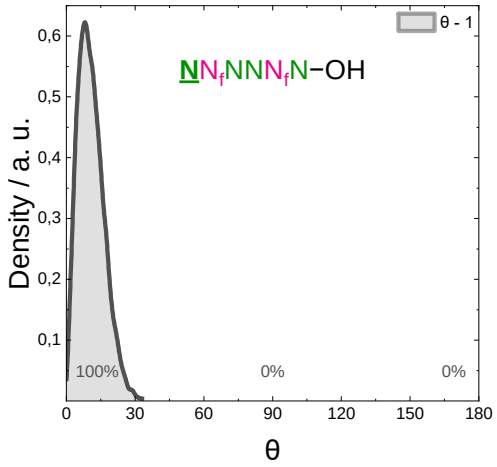
θ - 1
NNfNNNfN−OH
Density / a. u.
θ
100%
0%
0%

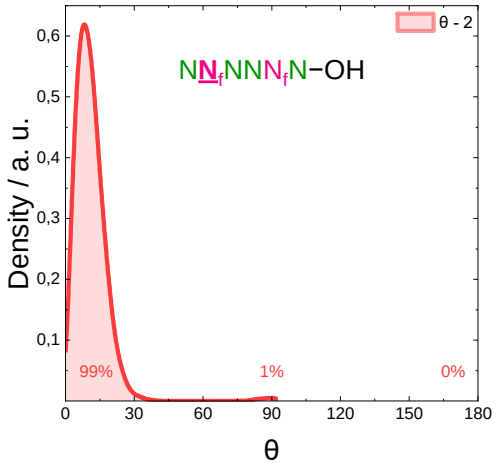
θ - 2
NNfNNNfN−OH
Density / a. u.
θ
99%
1%
0%

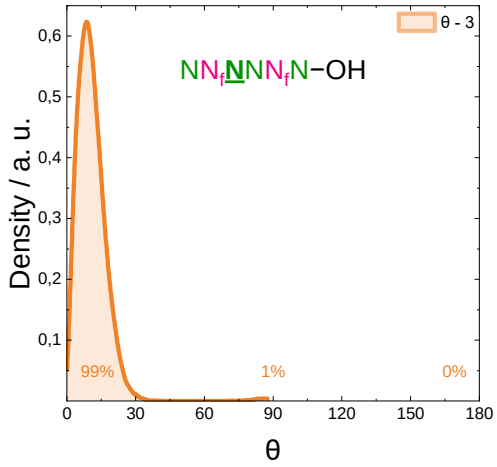
θ - 3
NNfNNNfN−OH
Density / a. u.
θ
99%
1%
0%

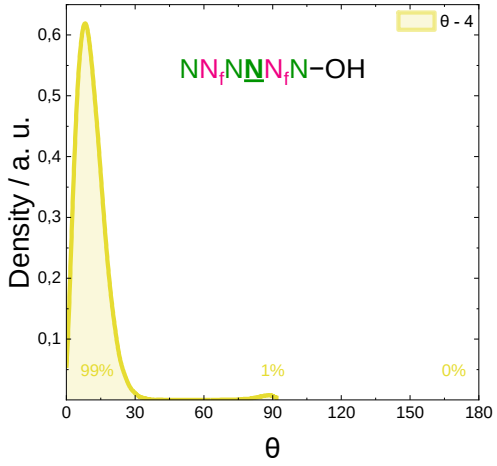
θ - 4
NNfNNNfN−OH
Density / a. u.
θ
99%
1%
0%

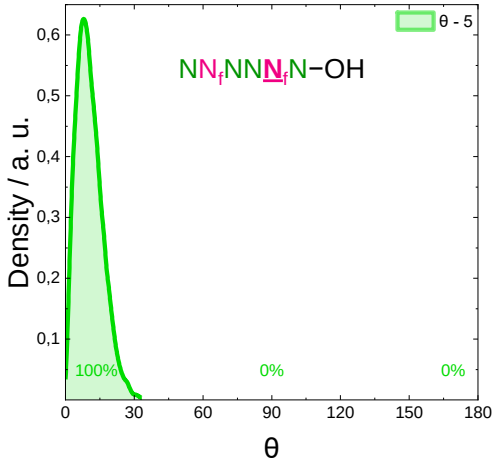
θ - 5
NNfNNNfN−OH
Density / a. u.
θ
100%
0%
0%

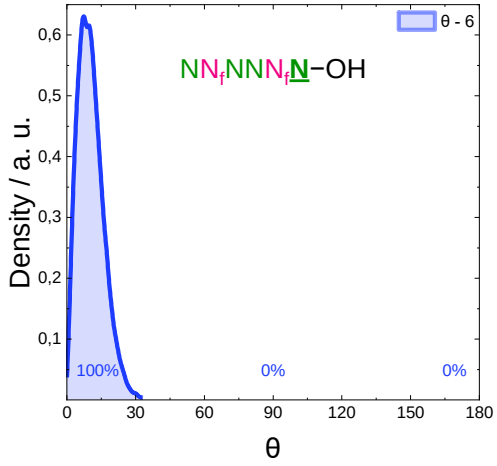
θ - 6
NNfNNNfN−OH
Density / a. u.
θ
100%
0%
0%

4.5 Ramachandran plots

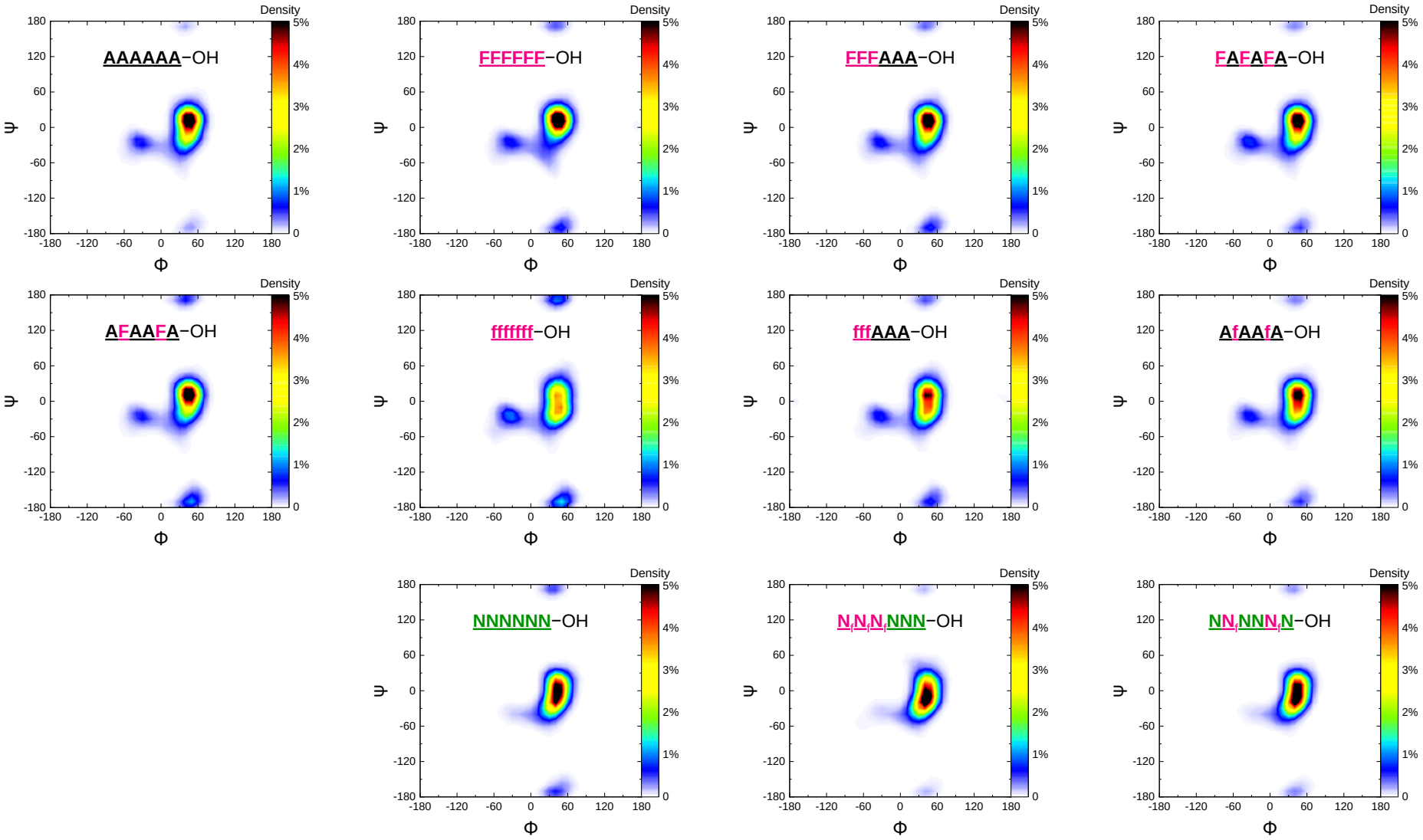

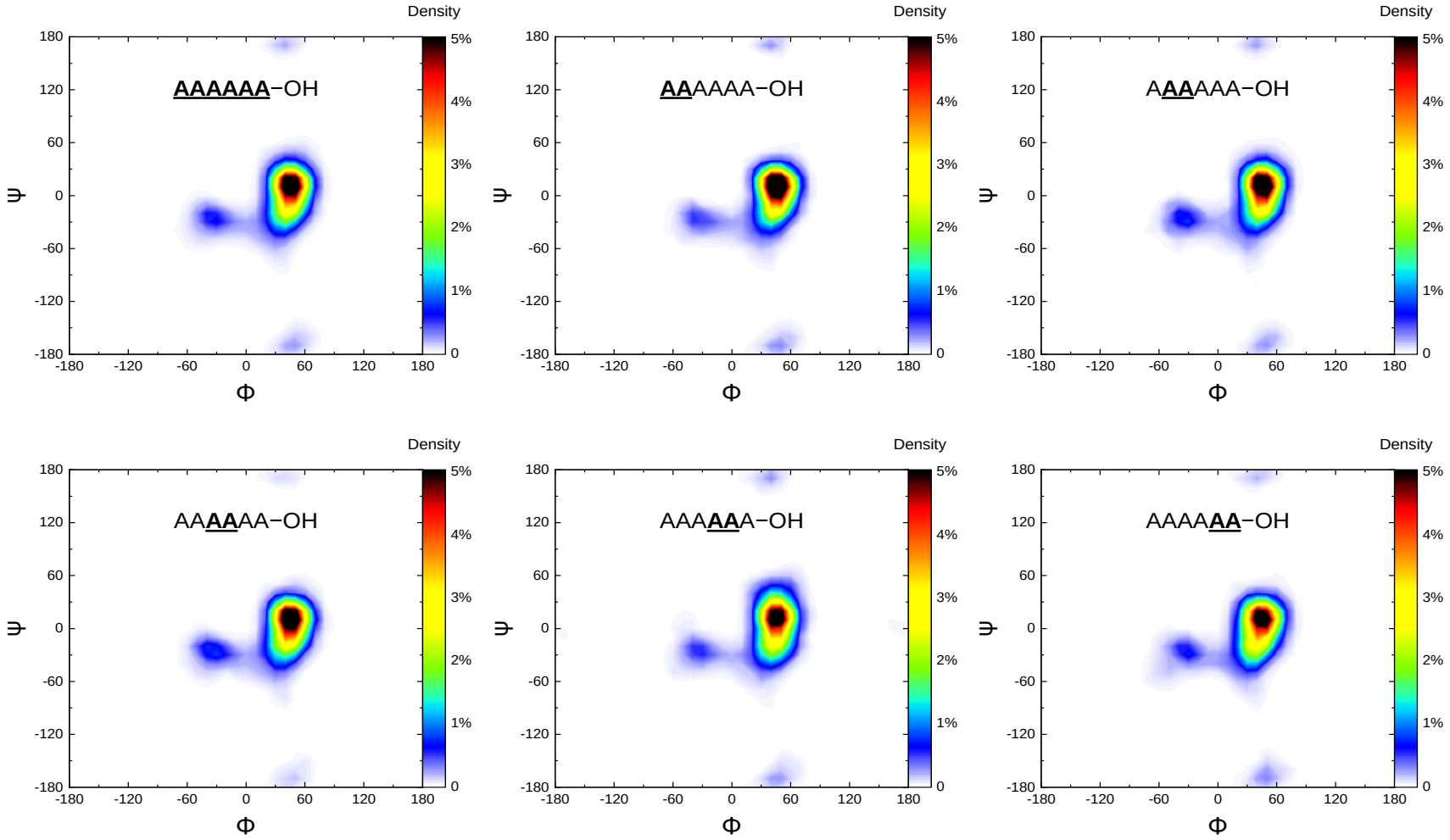
Density
AAAAAA−OH
AAAAAA−OH
AAAAAA−OH
AAAAAA−OH
AAAAAA−OH
AAAAAA−OH
Ψ
Φ
180
120
60
0
-60
-120
-180
-180 -120 -60 0 60 120 180
5%
4%
3%
2%
1%
0

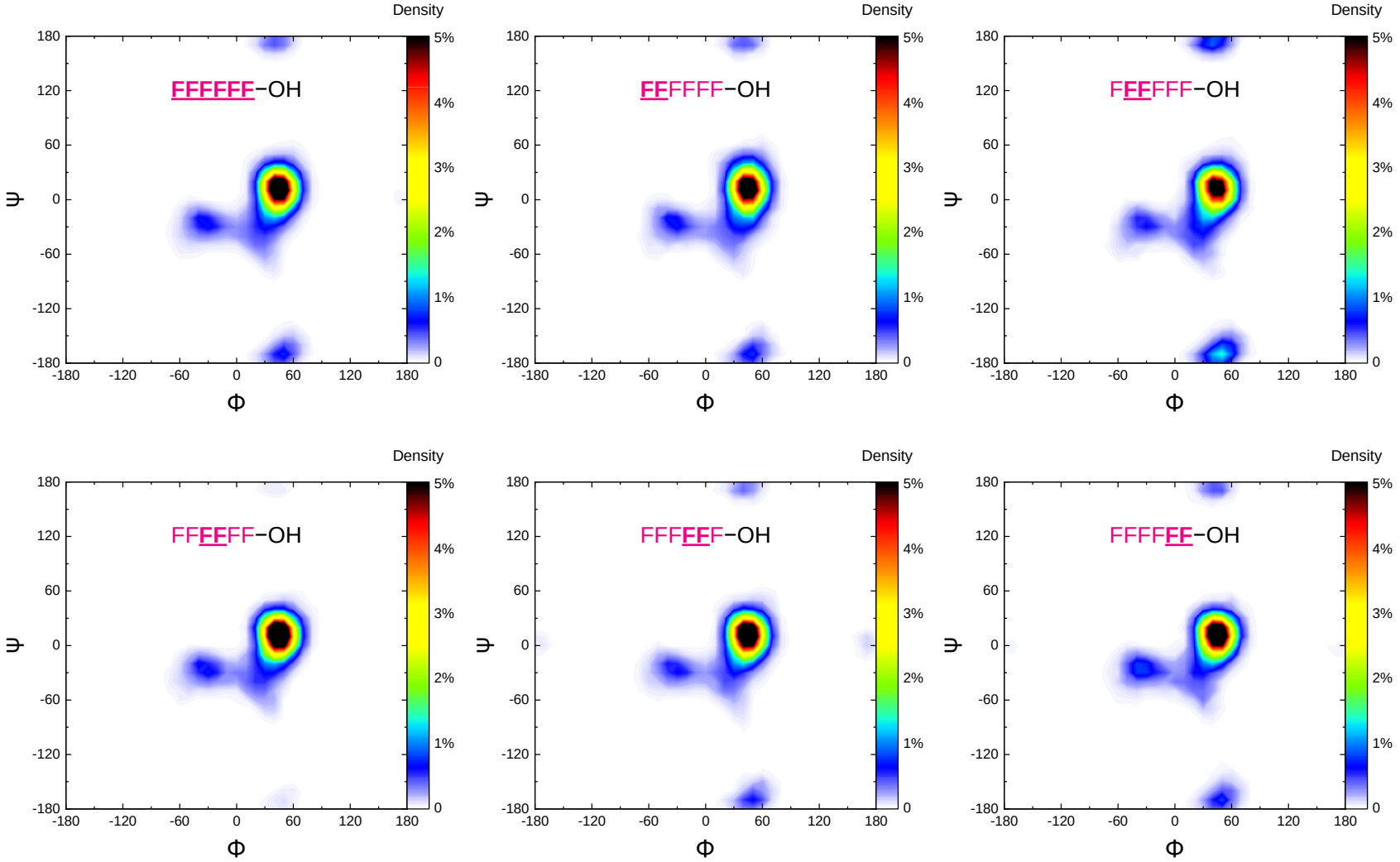
Density
FFFFFF−OH
FFFFFF−OH
FFFFFF−OH
FFFFFF−OH
FFFFFF−OH
FFFFFF−OH
Ψ
Φ
180
120
60
0
-60
-120
-180
5%
4%
3%
2%
1%
0

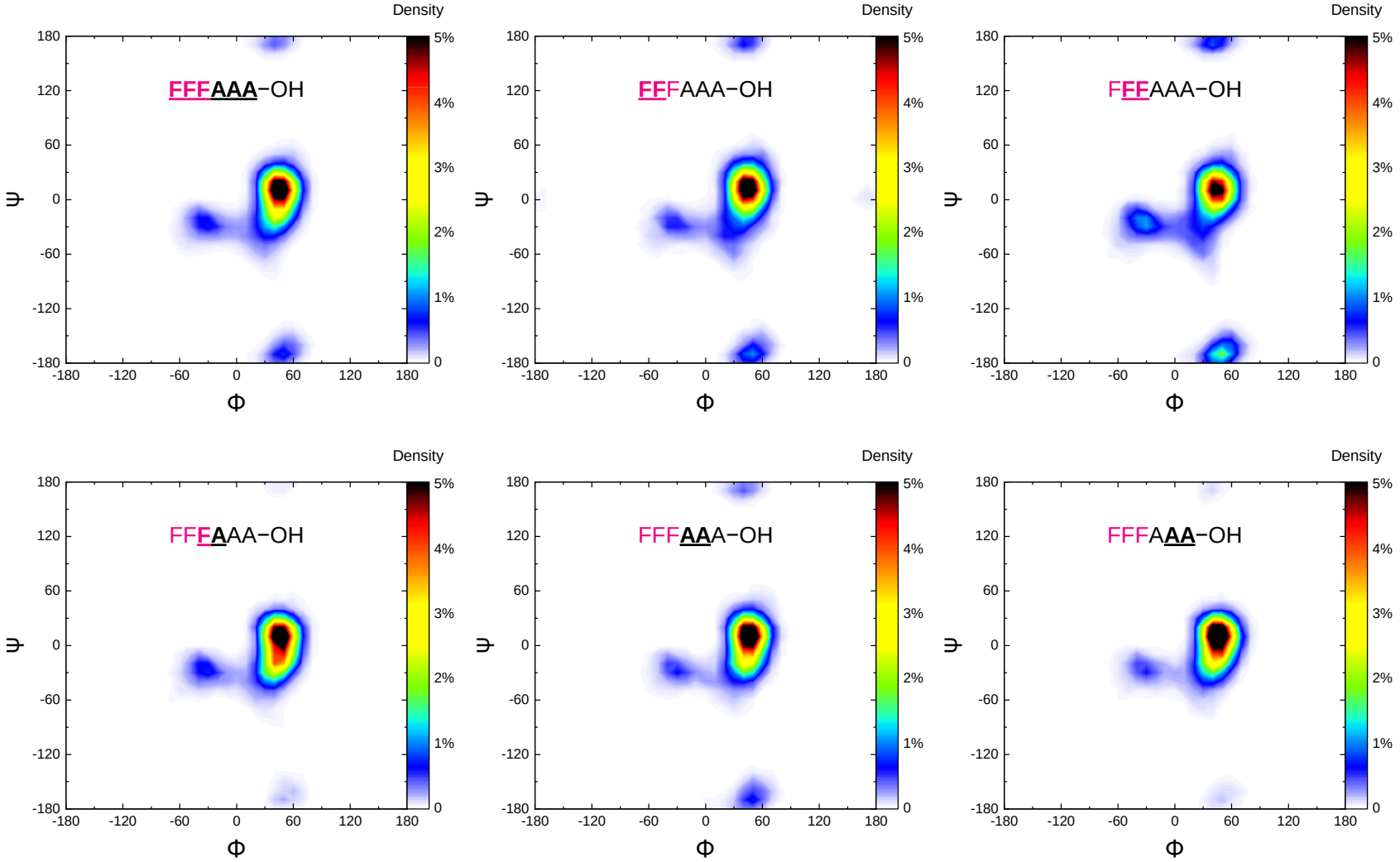
Density
FFFAAA−OH
FFFAAA−OH
FFFAAA−OH
FFFAAA−OH
FFFAAA−OH
FFFAAA−OH
Ψ
Φ
180
120
60
0
-60
-120
-180
5%
4%
3%
2%
1%
0

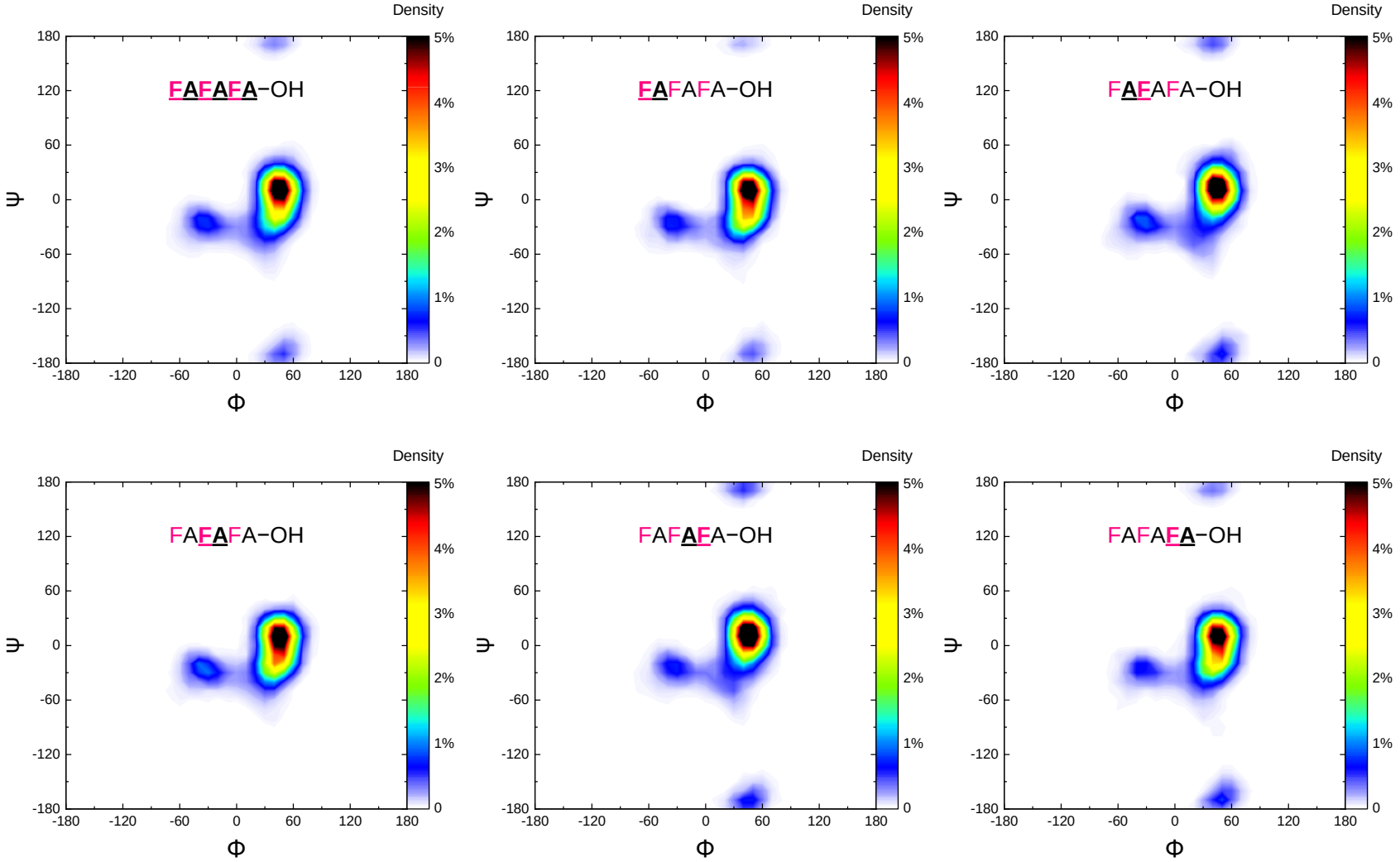
Density
FAFAFA−OH
FAFAFA−OH
FAFAFA−OH
FAFAFA−OH
FAFAFA−OH
FAFAFA−OH
Ψ
Φ
180
120
60
0
-60
-120
-180
5%
4%
3%
2%
1%
0

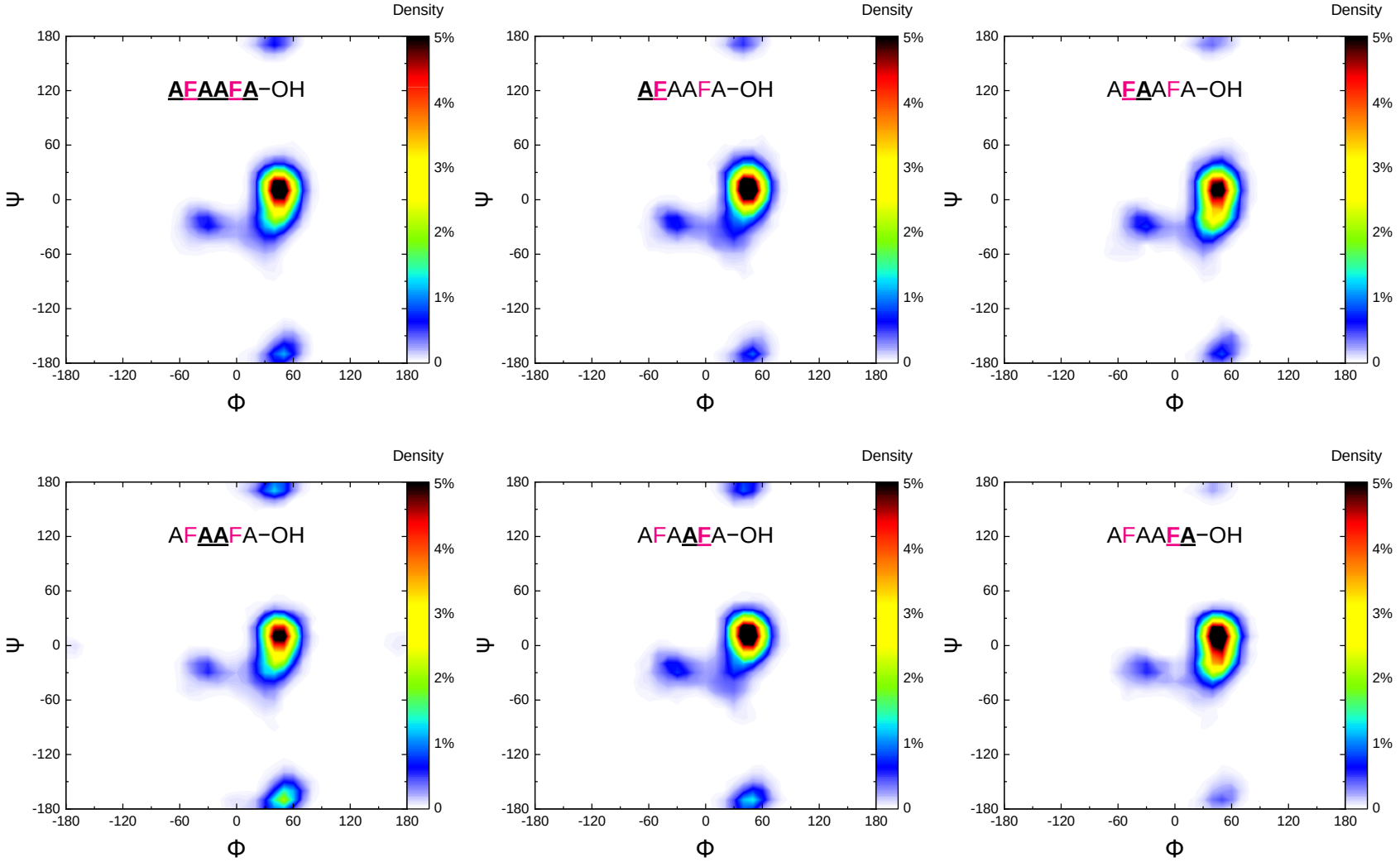
Density
AFAAFA−OH
AFAAFA−OH
AFAAFA−OH
AFAAFA−OH
AFAAFA−OH
AFAAFA−OH
Ψ
Φ
180
120
60
0
-60
-120
-180
5%
4%
3%
2%
1%
0

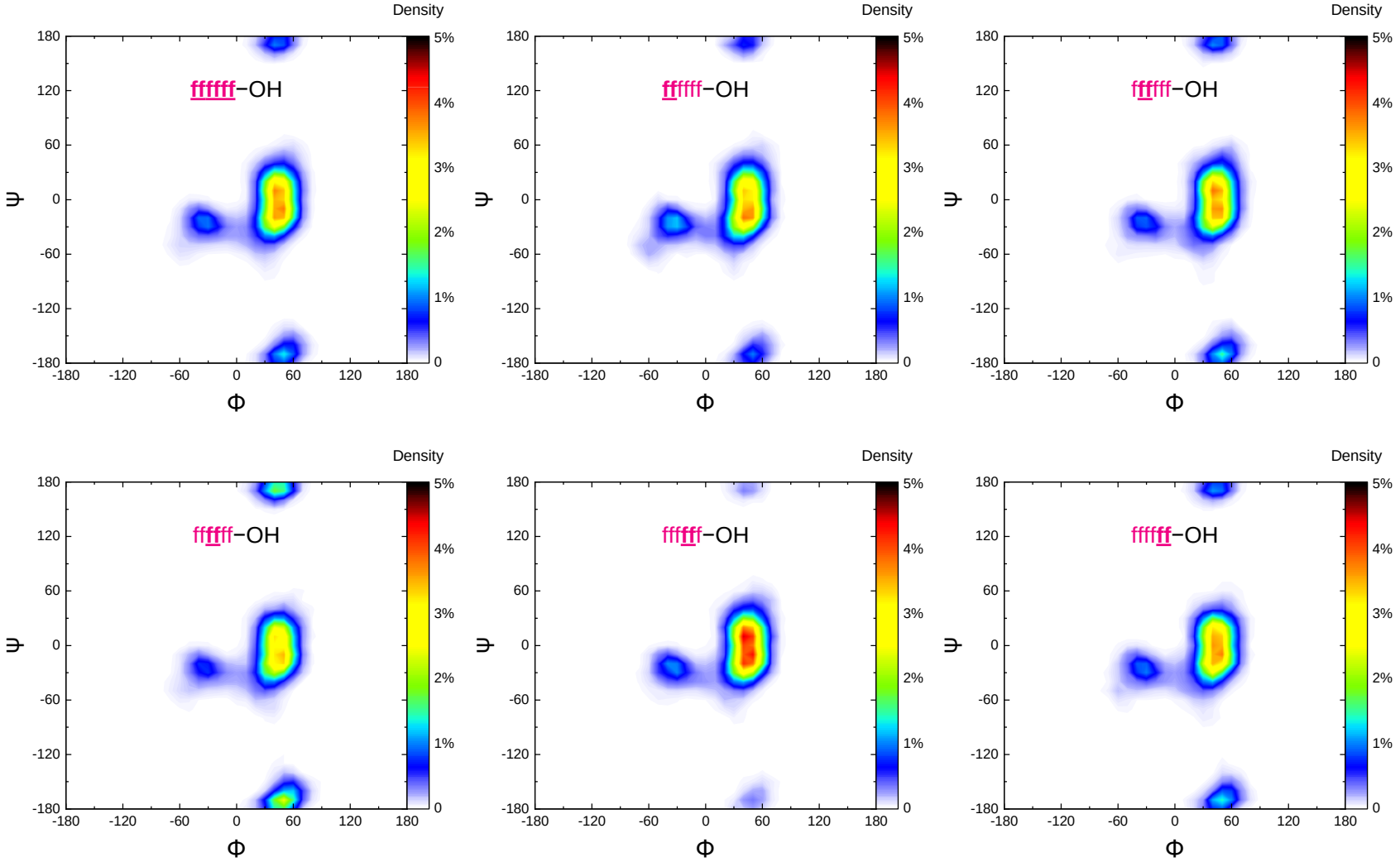
Density
fffffff−OH
ffffff−OH
fffffff−OH
ffffff−OH
fffffff−OH
ffffffff−OH
Ψ
Φ
180
120
60
0
-60
-120
-180
5%
4%
3%
2%
1%
0

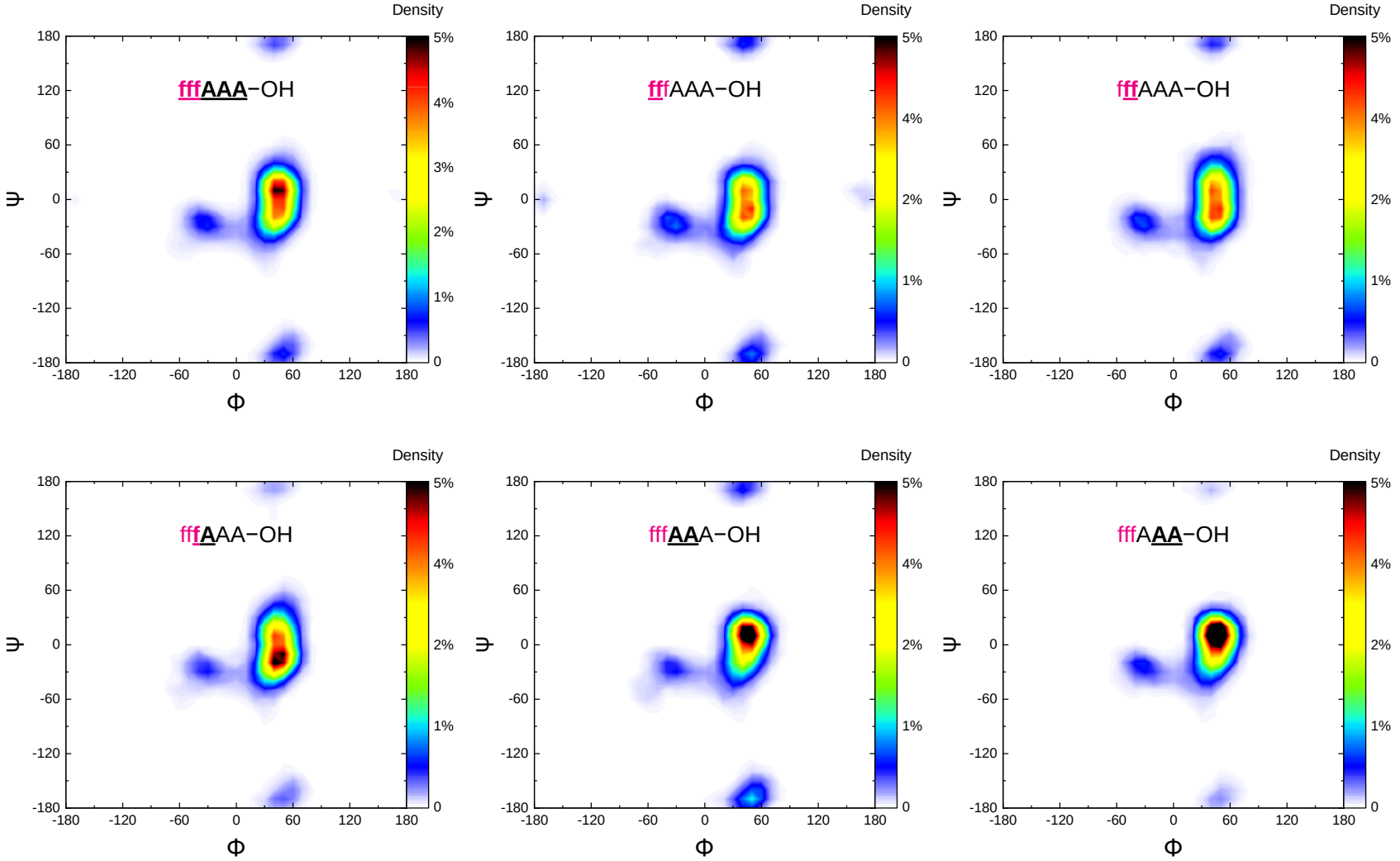
Density
fffAAA−OH
fffAAA−OH
fffAAA−OH
fffAAA−OH
fffAAA−OH
fffAAA−OH
Ψ
Φ
180
120
60
0
-60
-120
-180
5%
4%
3%
2%
1%
0

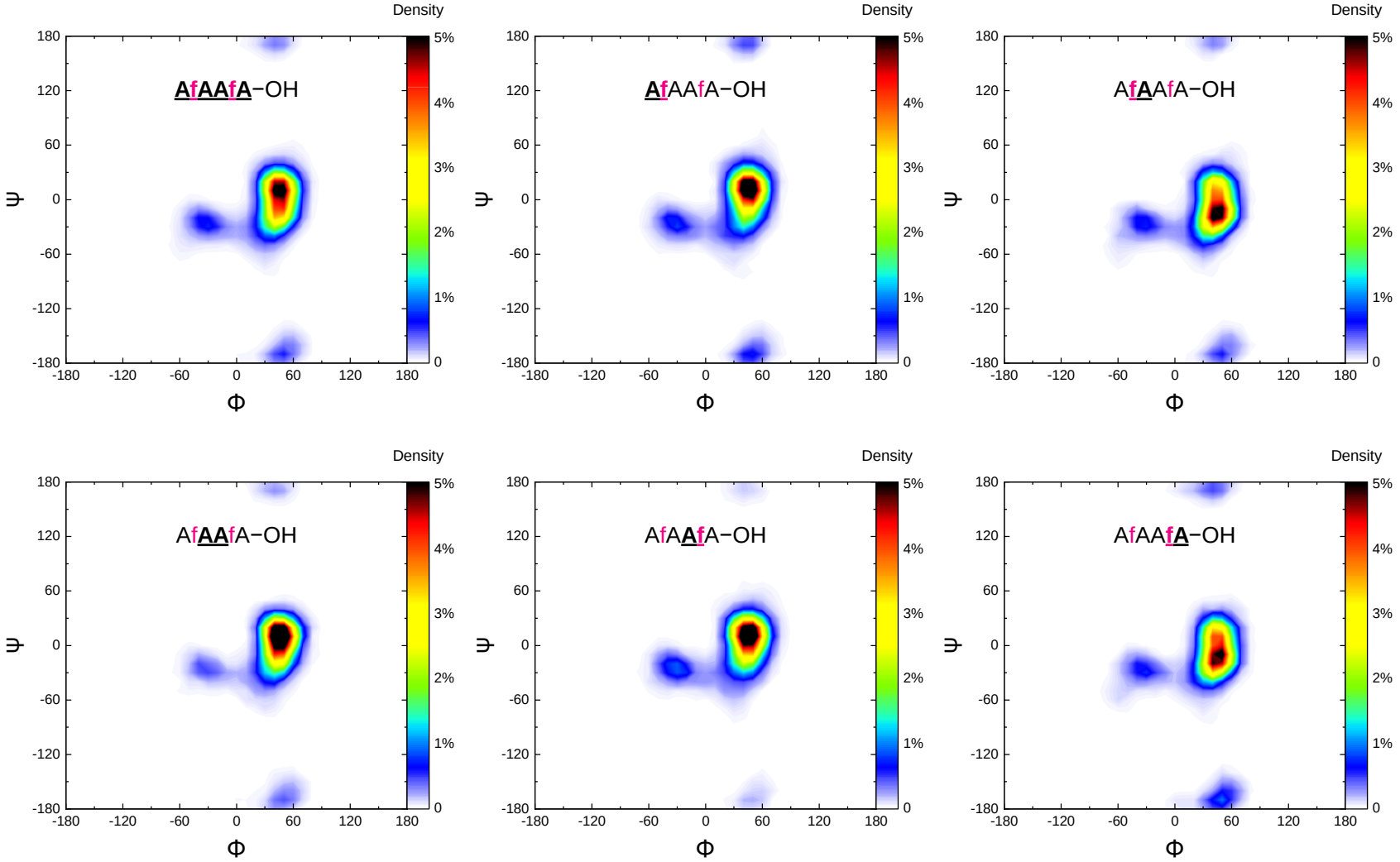
Density
AfAAfA−OH
AfAAfA−OH
AfAAfA−OH
AfAAfA−OH
AfAAfA−OH
AfAAfA−OH
Ψ
Φ
180
120
60
0
-60
-120
-180
5%
4%
3%
2%
1%
0

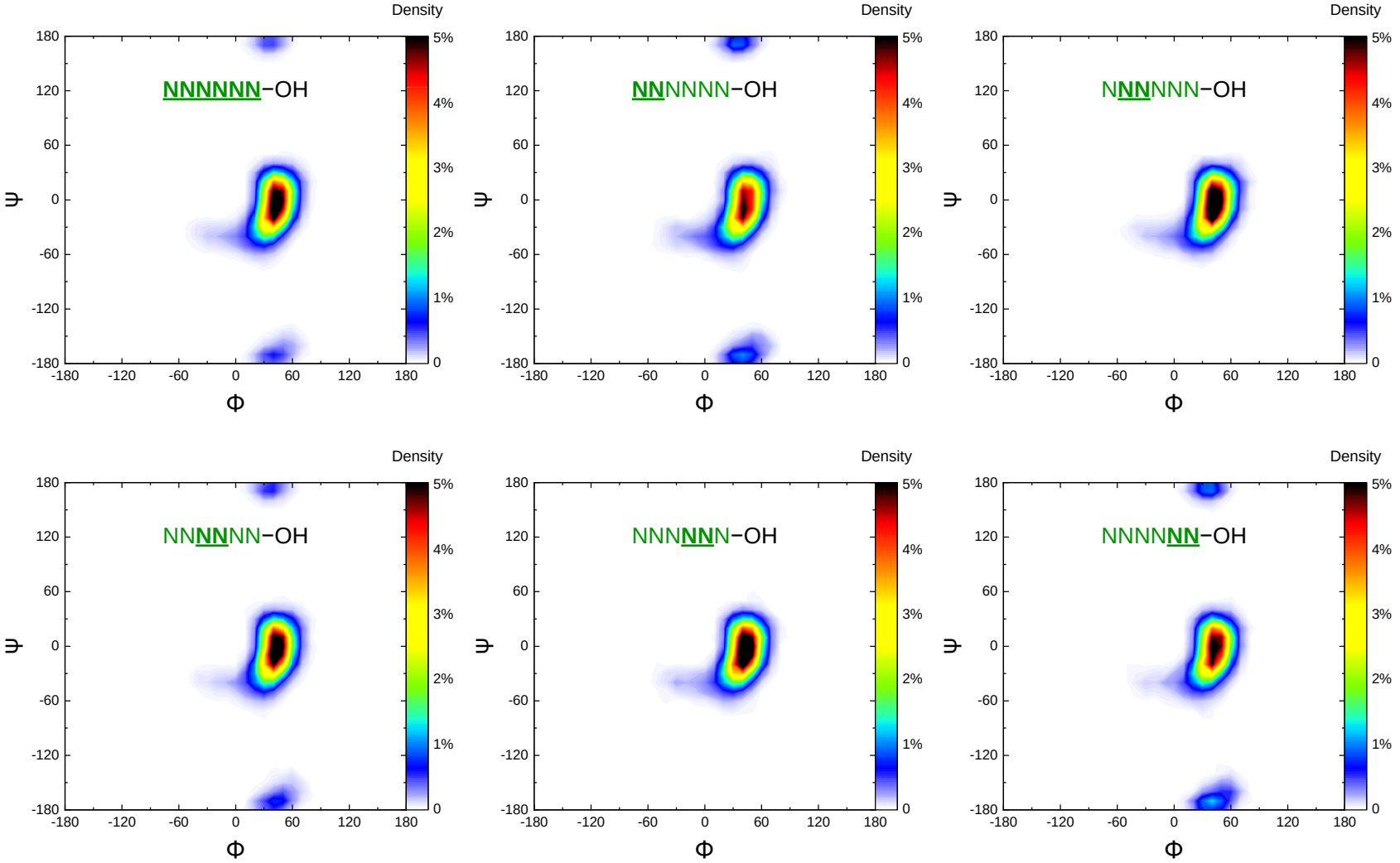
Density
NNNNNN−OH
NNNNNN−OH
NNNNNN−OH
NNNNNN−OH
NNNNNN−OH
NNNNNN−OH
Ψ
Φ
180
120
60
0
-60
-120
-180
5%
4%
3%
2%
1%
0

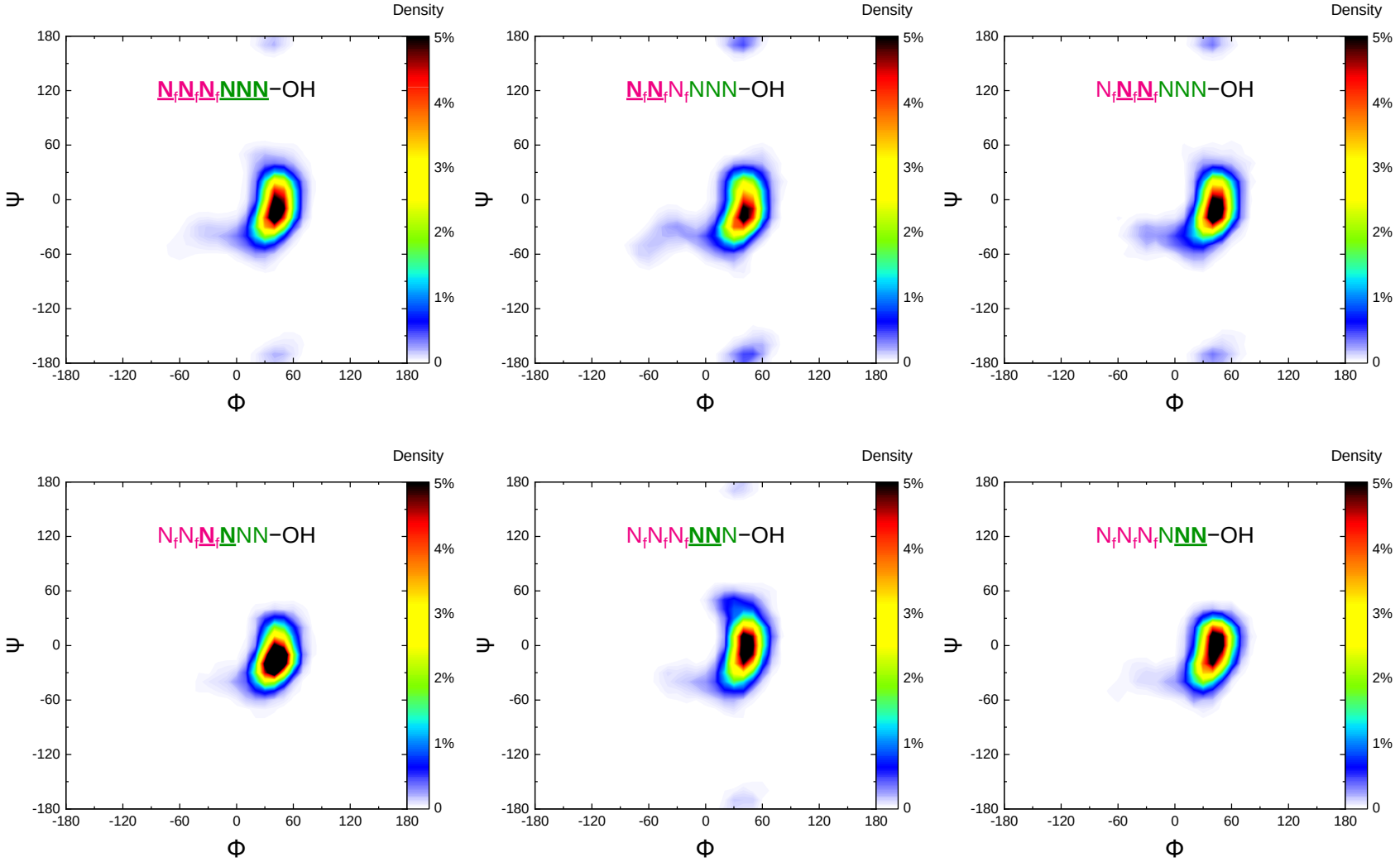
Density
5%
4%
3%
2%
1%
0
180
120
60
0
-60
-120
-180
Ψ
-180
-120
-60
0
60
120
180
Φ
NfNfNfNNN−OH
NfNfNfNNN−OH
NfNfNfNNN−OH
NfNfNfNNN−OH
NfNfNfNNN−OH
NfNfNfNNN−OH

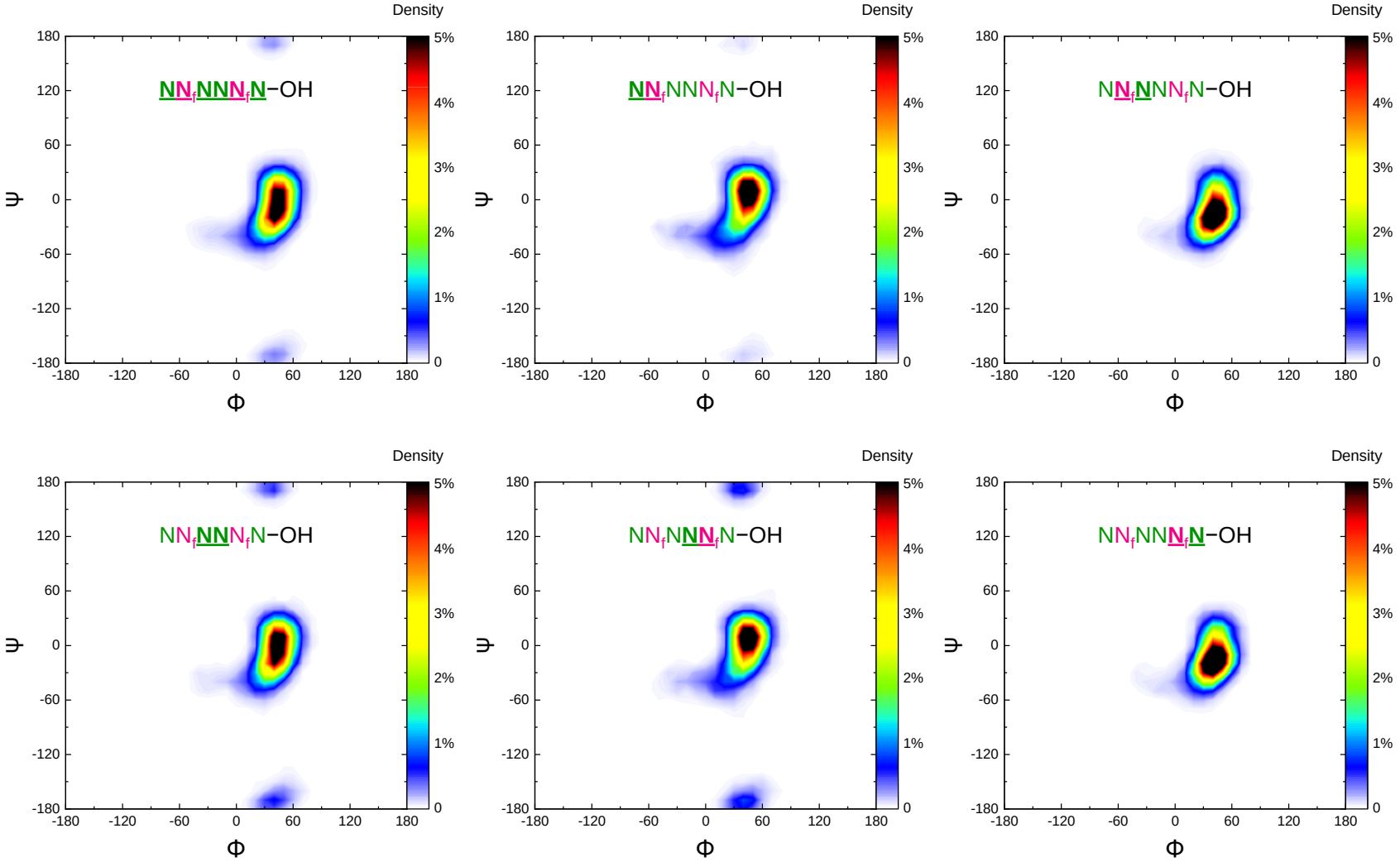
Density
NNfNNNfN−OH
NNfNNNfN−OH
NNfNNNfN−OH
NNfNNNfN−OH
NNfNNNfN−OH
NNfNNNfN−OH
Ψ
Φ
180
120
60
0
-60
-120
-180
5%
4%
3%
2%
1%
0

4.6 ω dihedral angle analysis

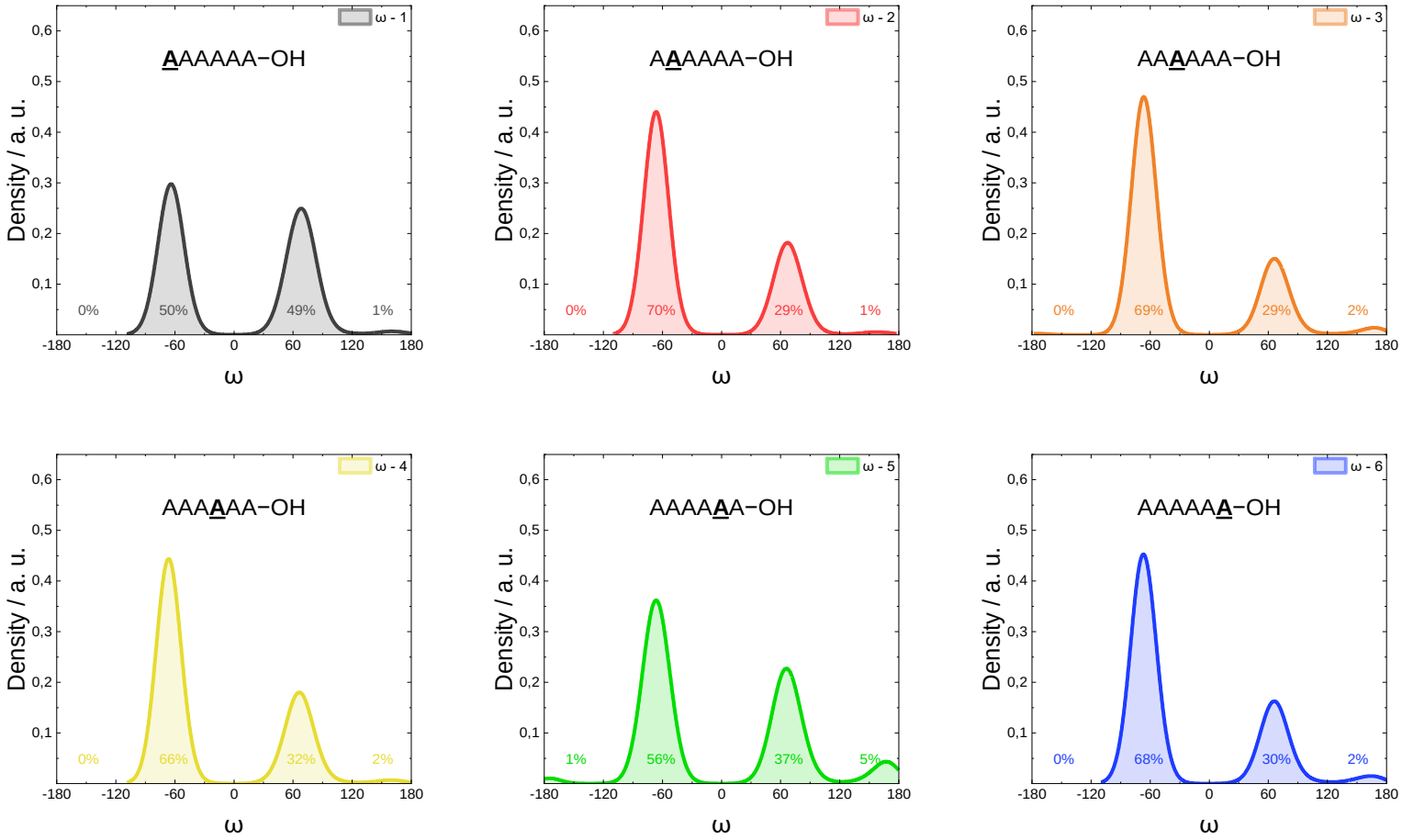

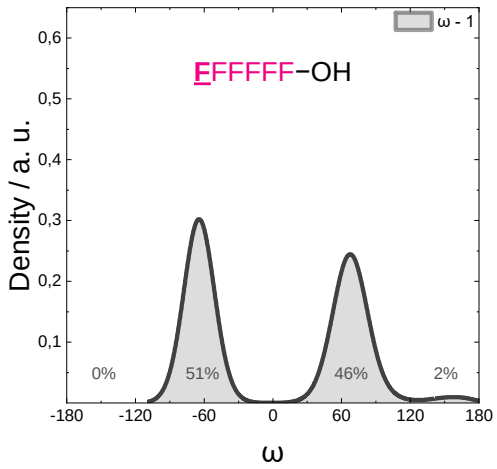
ω - 1
FFFFFF−OH
Density / a. u.
0,6
0,5
0,4
0,3
0,2
0,1
0%
51%
46%
2%
-180
-120
-60
0
60
120
180
ω

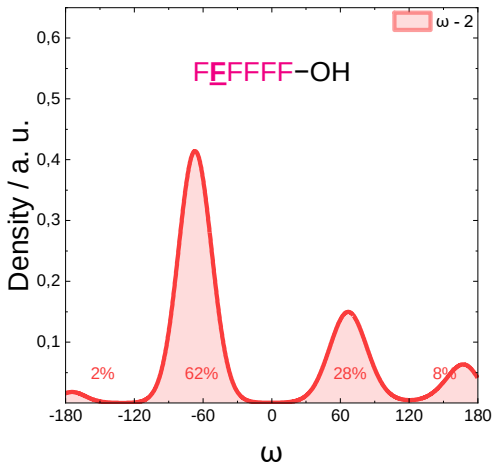
ω - 2
FFFFFF−OH
Density / a. u.
0,6
0,5
0,4
0,3
0,2
0,1
2%
62%
28%
8%
-180
-120
-60
0
60
120
180
ω

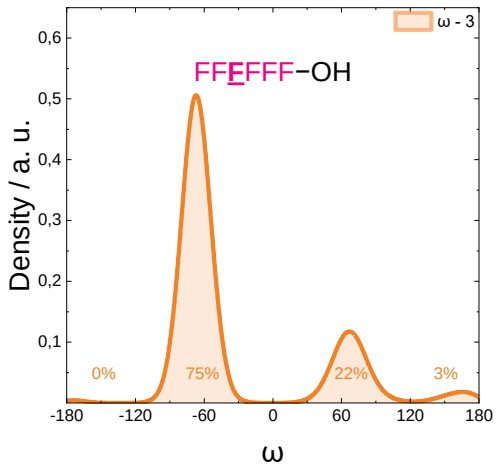
ω - 3
FFFFFF−OH
Density / a. u.
0,6
0,5
0,4
0,3
0,2
0,1
0%
75%
22%
3%
-180
-120
-60
0
60
120
180
ω

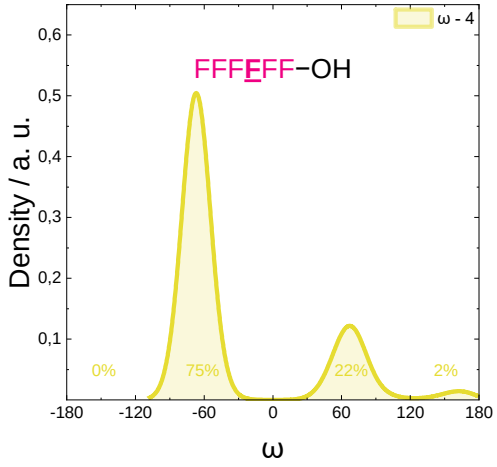
ω - 4
FFFFFF−OH
Density / a. u.
0,6
0,5
0,4
0,3
0,2
0,1
0%
75%
22%
2%
-180
-120
-60
0
60
120
180
ω

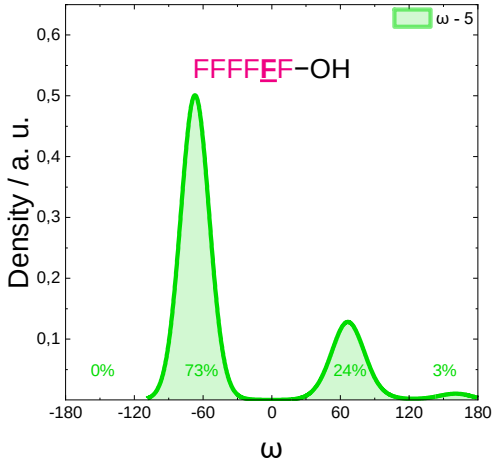
ω - 5
FFFFFF−OH
Density / a. u.
0,6
0,5
0,4
0,3
0,2
0,1
0%
73%
24%
3%
-180
-120
-60
0
60
120
180
ω

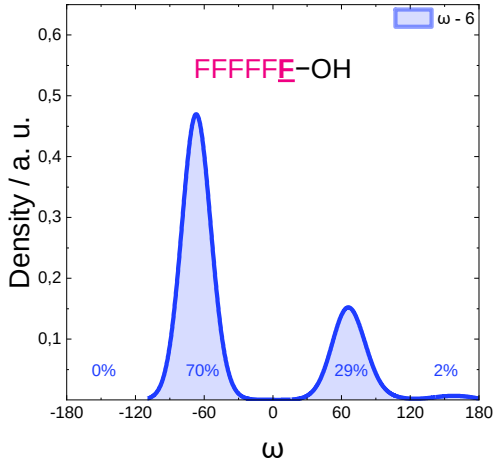
ω - 6
FFFFFF−OH
Density / a. u.
0,6
0,5
0,4
0,3
0,2
0,1
0%
70%
29%
2%
-180
-120
-60
0
60
120
180
ω

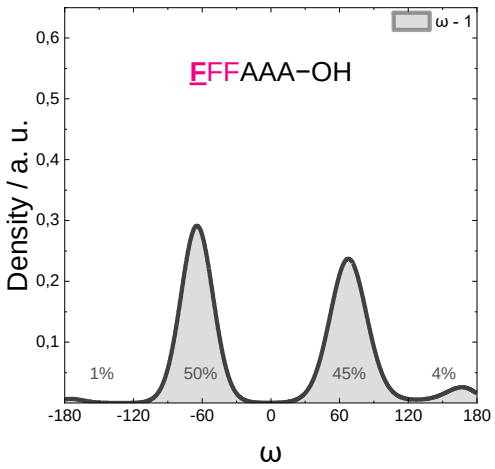
ω - 1
FFFAAA−OH
Density / a. u.
0,6
0,5
0,4
0,3
0,2
0,1
1%
50%
45%
4%
-180
-120
-60
0
60
120
180
ω

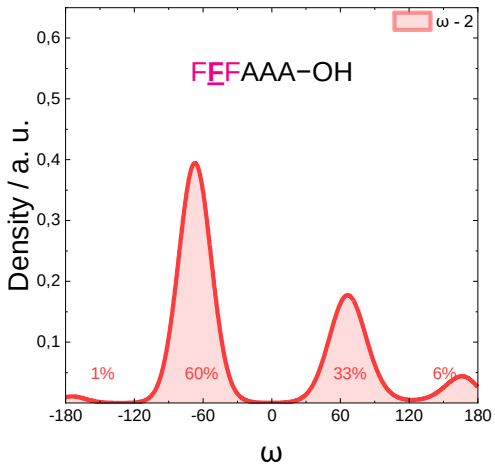
ω - 2
FFFAAA−OH
Density / a. u.
0,6
0,5
0,4
0,3
0,2
0,1
1%
60%
33%
6%
-180
-120
-60
0
60
120
180
ω

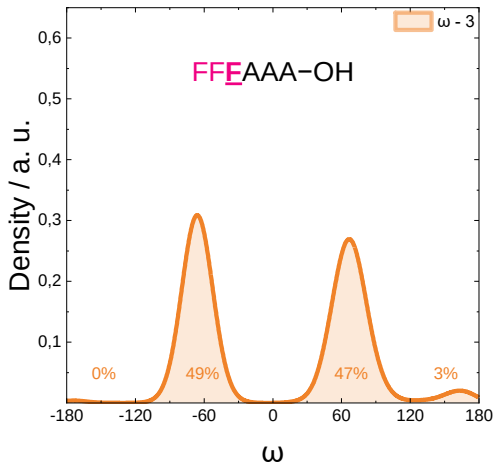
ω - 3
FFFAAA−OH
Density / a. u.
0,6
0,5
0,4
0,3
0,2
0,1
0%
49%
47%
3%
-180
-120
-60
0
60
120
180
ω

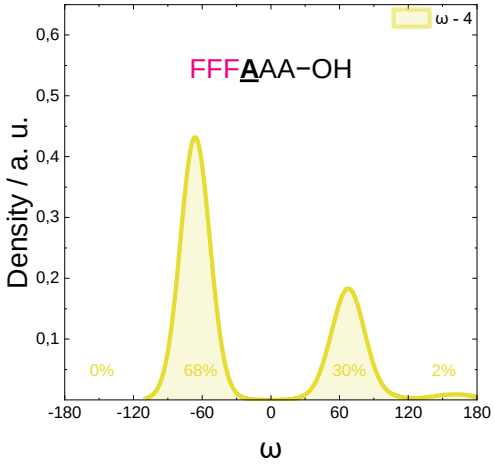
ω - 4
FFFAAA−OH
Density / a. u.
0,6
0,5
0,4
0,3
0,2
0,1
0%
68%
30%
2%
-180
-120
-60
0
60
120
180
ω

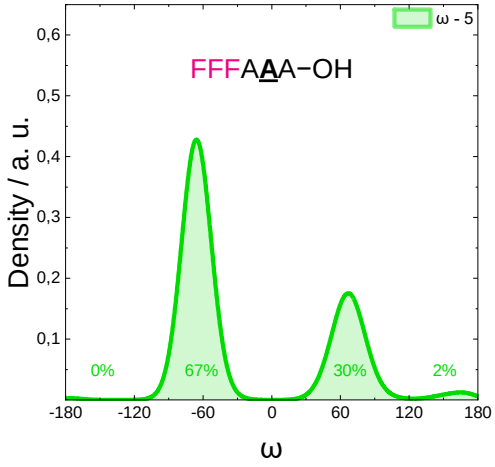
ω - 5
FFFAAA−OH
Density / a. u.
0,6
0,5
0,4
0,3
0,2
0,1
0%
67%
30%
2%
-180
-120
-60
0
60
120
180
ω

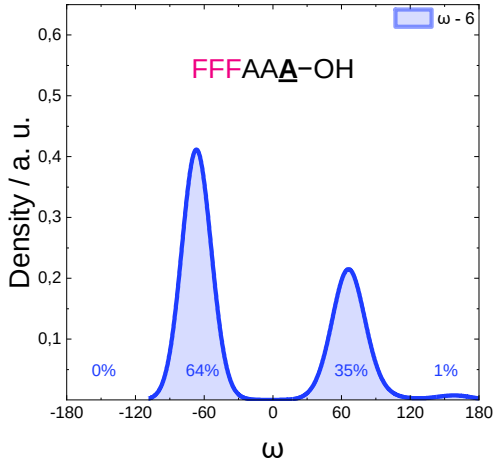
ω - 6
FFFAAA−OH
Density / a. u.
0,6
0,5
0,4
0,3
0,2
0,1
0%
64%
35%
1%
-180
-120
-60
0
60
120
180
ω

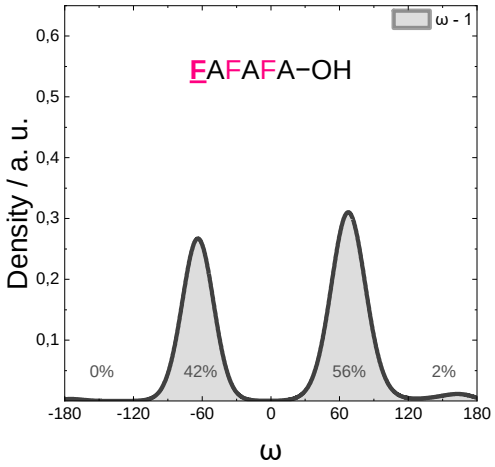
ω - 1
FAFAFA−OH
Density / a. u.
0,6
0,5
0,4
0,3
0,2
0,1
0%
42%
56%
2%
-180
-120
-60
0
60
120
180
ω

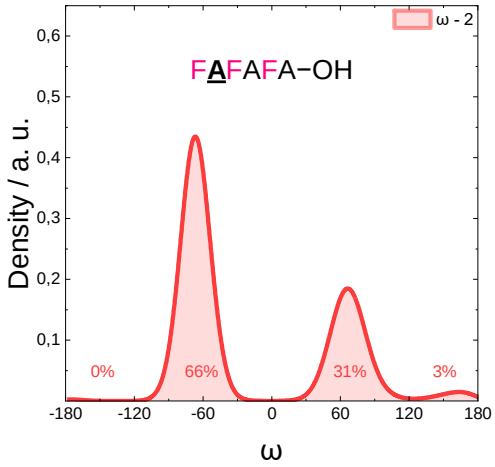
ω - 2
FAFAFA−OH
Density / a. u.
0,6
0,5
0,4
0,3
0,2
0,1
0%
66%
31%
3%
-180
-120
-60
0
60
120
180
ω

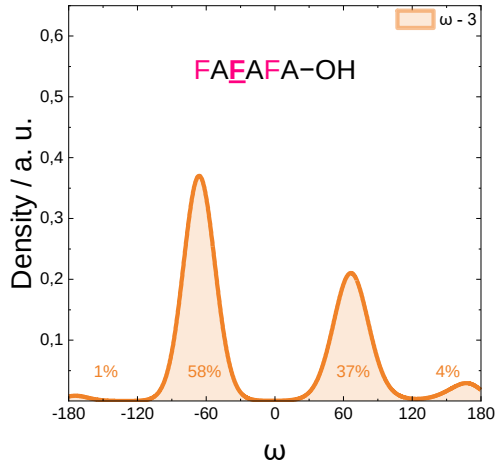
ω - 3
FAFAFA−OH
Density / a. u.
0,6
0,5
0,4
0,3
0,2
0,1
1%
58%
37%
4%
-180
-120
-60
0
60
120
180
ω

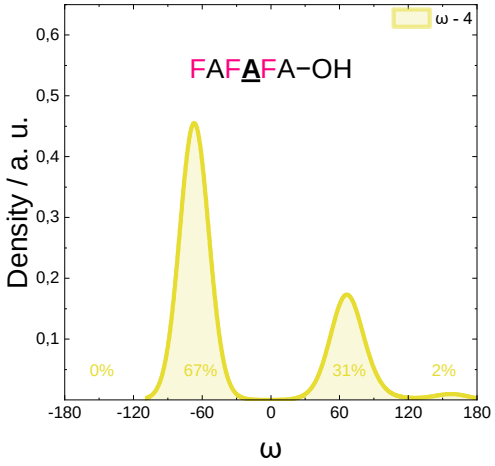
ω - 4
FAFAFA−OH
Density / a. u.
0,6
0,5
0,4
0,3
0,2
0,1
0%
67%
31%
2%
-180
-120
-60
0
60
120
180
ω

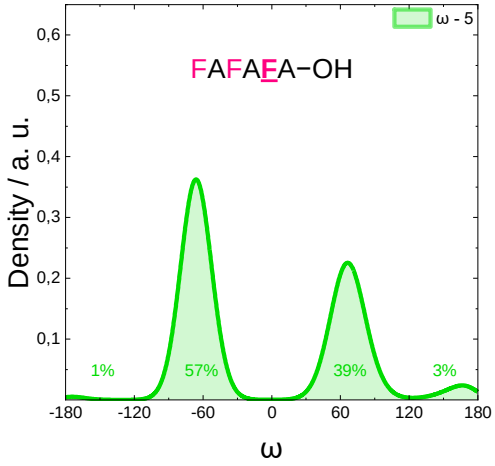
ω - 5
FAFAFA−OH
Density / a. u.
0,6
0,5
0,4
0,3
0,2
0,1
1%
57%
39%
3%
-180
-120
-60
0
60
120
180
ω

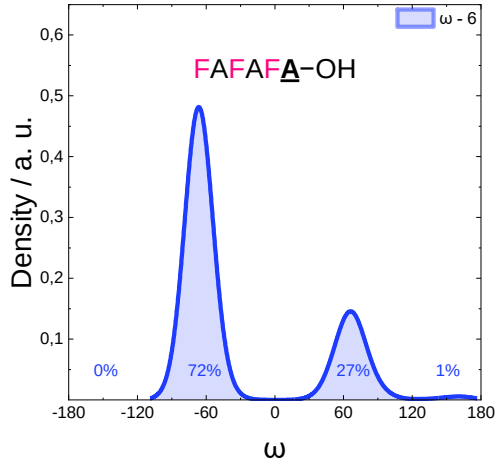
ω - 6
FAFAFA−OH
Density / a. u.
0,6
0,5
0,4
0,3
0,2
0,1
0%
72%
27%
1%
-180
-120
-60
0
60
120
180
ω

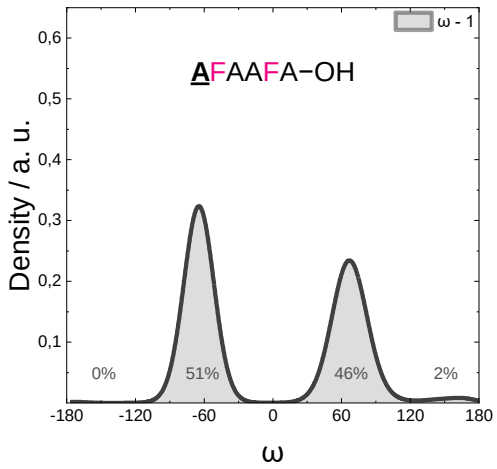
ω - 1
AFAAFA−OH
Density / a. u.
0,6
0,5
0,4
0,3
0,2
0,1
0%
51%
46%
2%
-180
-120
-60
0
60
120
180
ω

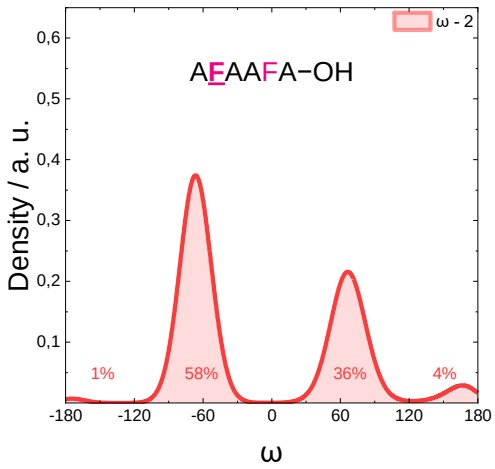
ω - 2
AFAAFA−OH
Density / a. u.
0,6
0,5
0,4
0,3
0,2
0,1
1%
58%
36%
4%
-180
-120
-60
0
60
120
180
ω

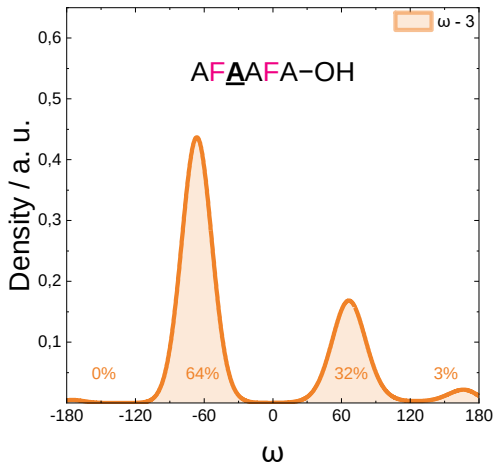
ω - 3
AFAAFA−OH
Density / a. u.
0,6
0,5
0,4
0,3
0,2
0,1
0%
64%
32%
3%
-180
-120
-60
0
60
120
180
ω

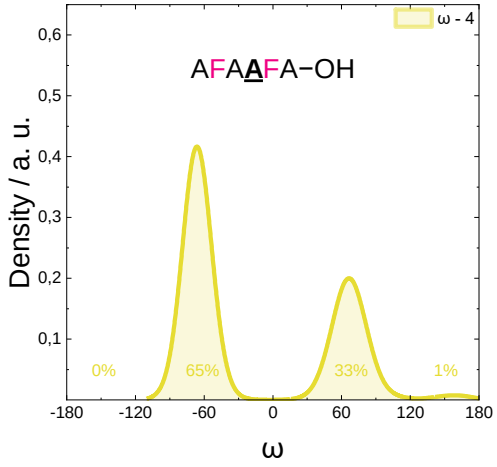
ω - 4
AFAAFA−OH
Density / a. u.
0,6
0,5
0,4
0,3
0,2
0,1
0%
65%
33%
1%
-180
-120
-60
0
60
120
180
ω

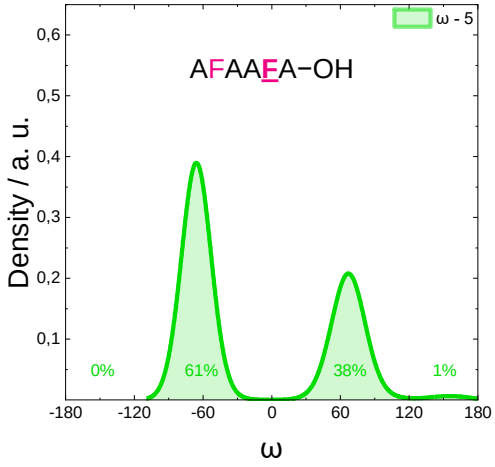
ω - 5
AFAAFA−OH
Density / a. u.
0,6
0,5
0,4
0,3
0,2
0,1
0%
61%
38%
1%
-180
-120
-60
0
60
120
180
ω

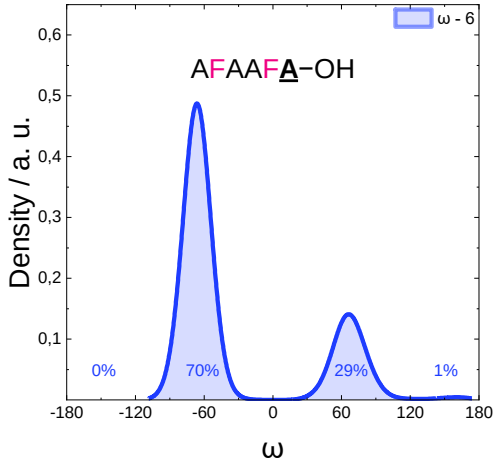
ω - 6
AFAAFA−OH
Density / a. u.
0,6
0,5
0,4
0,3
0,2
0,1
0%
70%
29%
1%
-180
-120
-60
0
60
120
180
ω

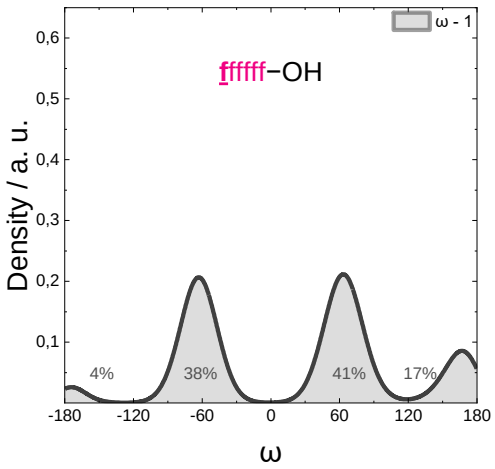
ω - 1
fffff−OH
Density / a. u.
0,6
0,5
0,4
0,3
0,2
0,1
4%
38%
41%
17%
-180
-120
-60
0
60
120
180
ω

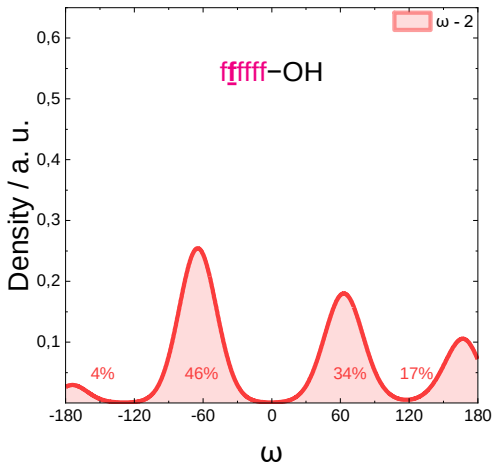
ω - 2
ffffff−OH
Density / a. u.
0,6
0,5
0,4
0,3
0,2
0,1
4%
46%
34%
17%
-180
-120
-60
0
60
120
180
ω

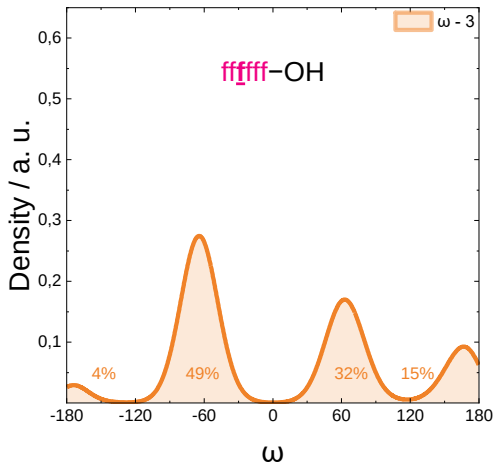
ω - 3
fffffff−OH
Density / a. u.
0,6
0,5
0,4
0,3
0,2
0,1
4%
49%
32%
15%
-180
-120
-60
0
60
120
180
ω

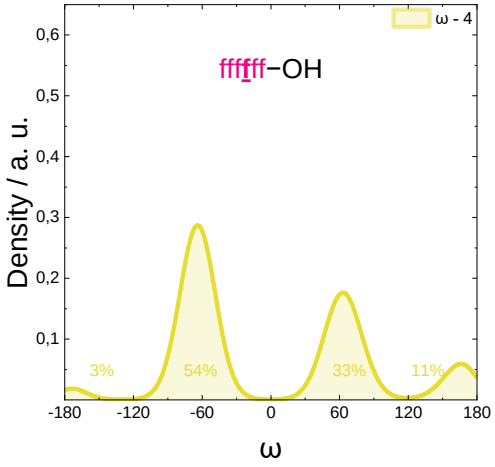
ω - 4
ffffff−OH
Density / a. u.
0,6
0,5
0,4
0,3
0,2
0,1
3%
54%
33%
11%
-180
-120
-60
0
60
120
180
ω

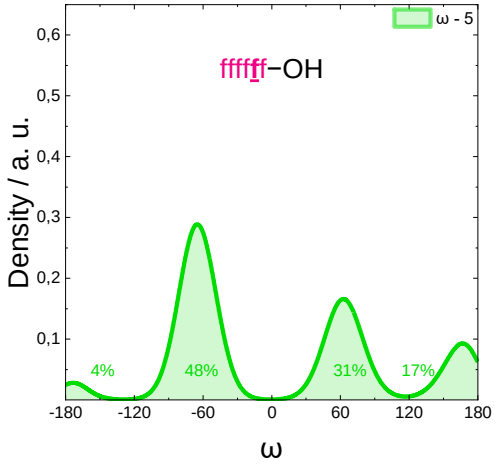
ω - 5
fffffff−OH
Density / a. u.
0,6
0,5
0,4
0,3
0,2
0,1
4%
48%
31%
17%
-180
-120
-60
0
60
120
180
ω

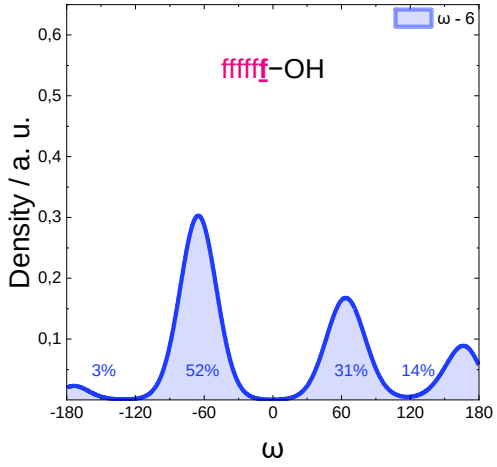
ω - 6
ffffff−OH
Density / a. u.
0,6
0,5
0,4
0,3
0,2
0,1
3%
52%
31%
14%
-180
-120
-60
0
60
120
180
ω

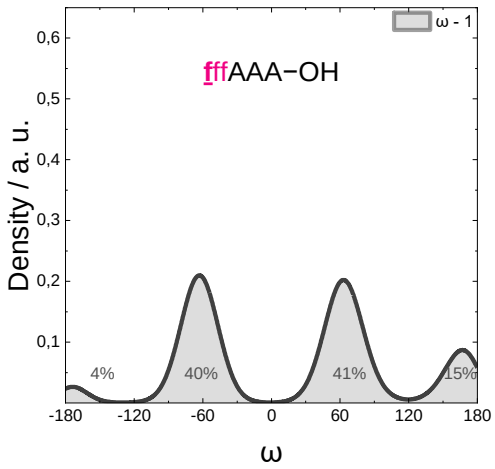
ω - 1
fffAAA−OH
Density / a. u.
0,6
0,5
0,4
0,3
0,2
0,1
4%
40%
41%
15%
-180
-120
-60
0
60
120
180
ω

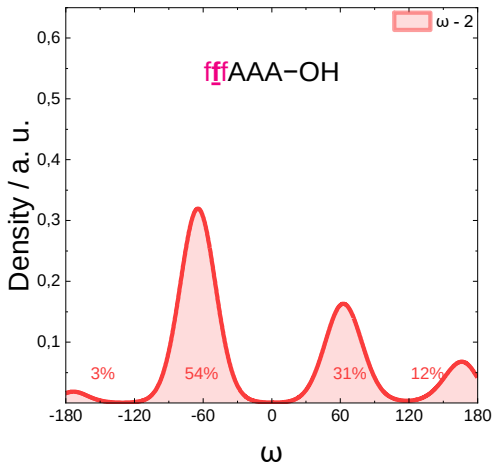
ω - 2
fffAAA−OH
Density / a. u.
0,6
0,5
0,4
0,3
0,2
0,1
3%
54%
31%
12%
-180
-120
-60
0
60
120
180
ω

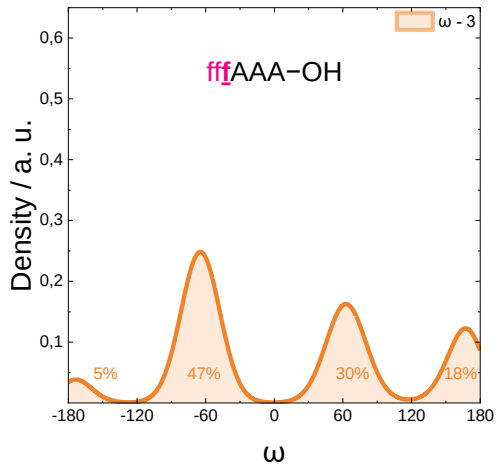
ω - 3
fffAAA−OH
Density / a. u.
0,6
0,5
0,4
0,3
0,2
0,1
5%
47%
30%
18%
-180
-120
-60
0
60
120
180
ω

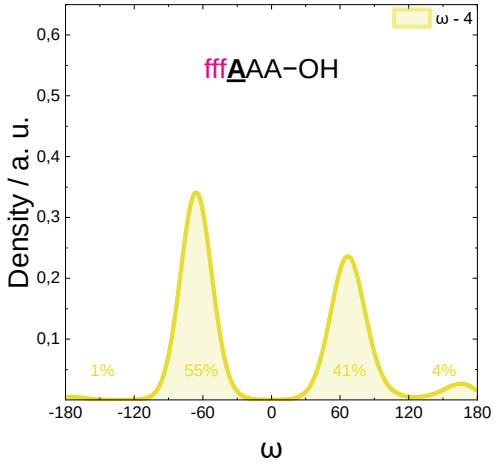
ω - 4
fffAAA−OH
Density / a. u.
0,6
0,5
0,4
0,3
0,2
0,1
1%
55%
41%
4%
-180
-120
-60
0
60
120
180
ω

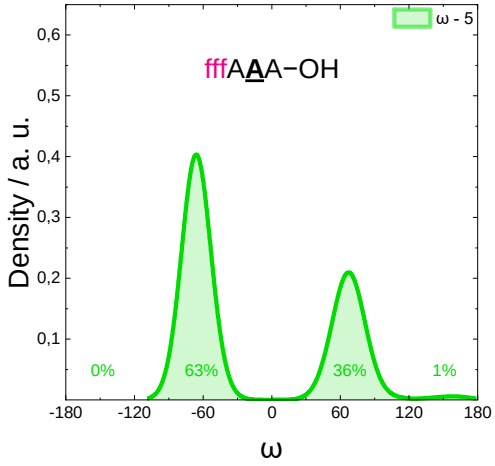
ω - 5
fffAAA−OH
Density / a. u.
0,6
0,5
0,4
0,3
0,2
0,1
0%
63%
36%
1%
-180
-120
-60
0
60
120
180
ω

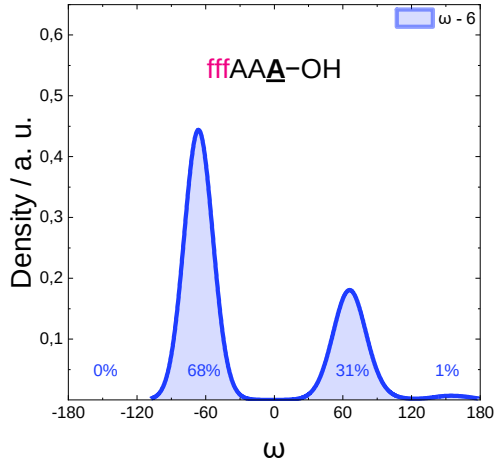
ω - 6
fffAAA−OH
Density / a. u.
0,6
0,5
0,4
0,3
0,2
0,1
0%
68%
31%
1%
-180
-120
-60
0
60
120
180
ω

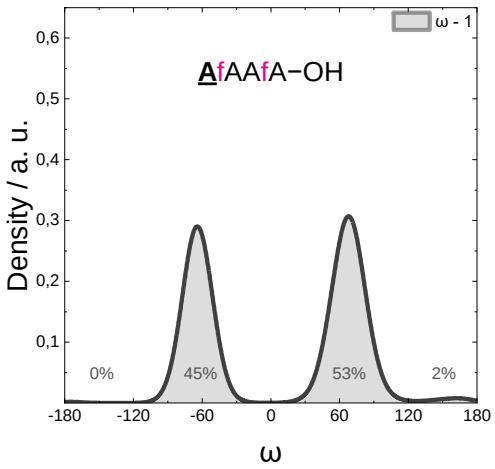
ω - 1
AfAAfA−OH
Density / a. u.
ω
0%
45%
53%
2%

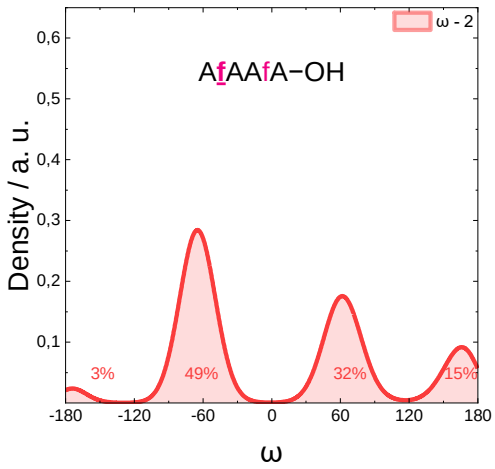
ω - 2
AfAAfA−OH
Density / a. u.
ω
3%
49%
32%
15%

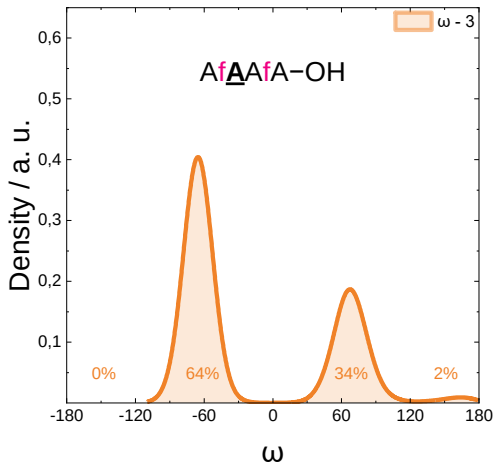
ω - 3
AfAAfA−OH
Density / a. u.
ω
0%
64%
34%
2%

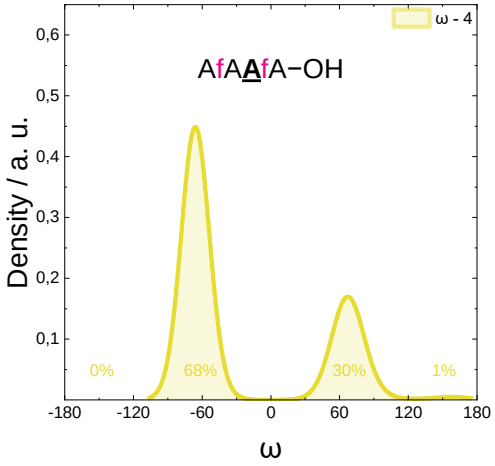
ω - 4
AfAAfA−OH
Density / a. u.
ω
0%
68%
30%
1%

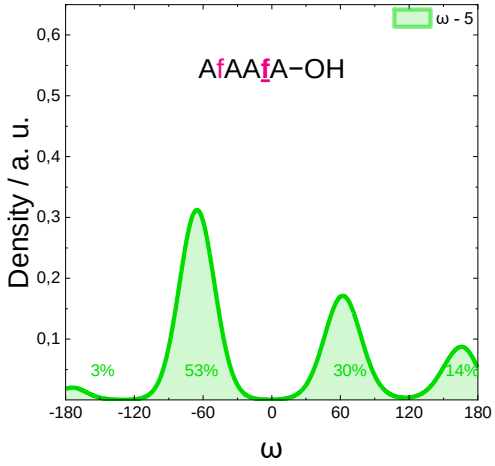
ω - 5
AfAAfA−OH
Density / a. u.
ω
3%
53%
30%
14%

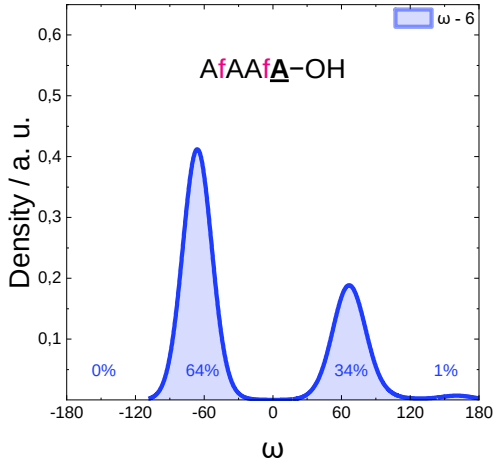
ω - 6
AfAAfA−OH
Density / a. u.
ω
0%
64%
34%
1%

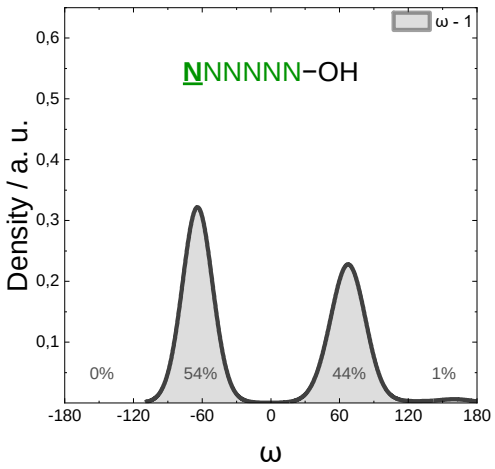
ω - 1
NNNNNN−OH
Density / a. u.
0,6
0,5
0,4
0,3
0,2
0,1
0%
54%
44%
1%
-180
-120
-60
0
60
120
180
ω

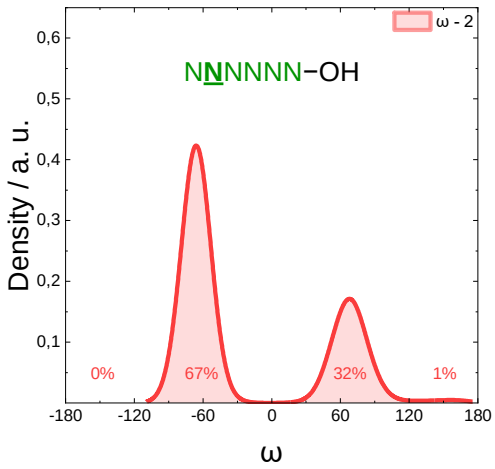
ω - 2
NNNNNN−OH
Density / a. u.
0,6
0,5
0,4
0,3
0,2
0,1
0%
67%
32%
1%
-180
-120
-60
0
60
120
180
ω

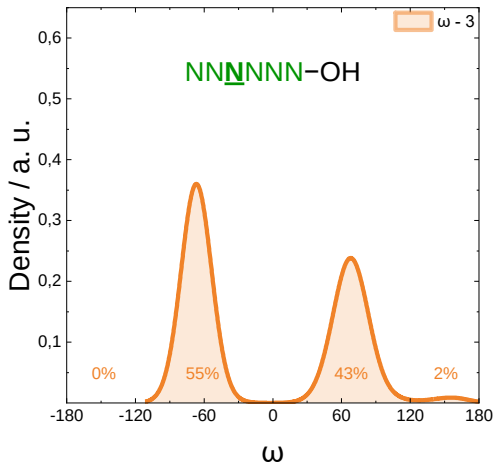
ω - 3
NNNNNN−OH
Density / a. u.
0,6
0,5
0,4
0,3
0,2
0,1
0%
55%
43%
2%
-180
-120
-60
0
60
120
180
ω

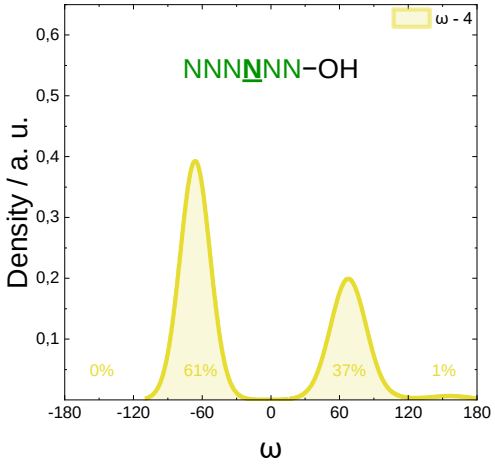
ω - 4
NNNNNN−OH
Density / a. u.
0,6
0,5
0,4
0,3
0,2
0,1
0%
61%
37%
1%
-180
-120
-60
0
60
120
180
ω

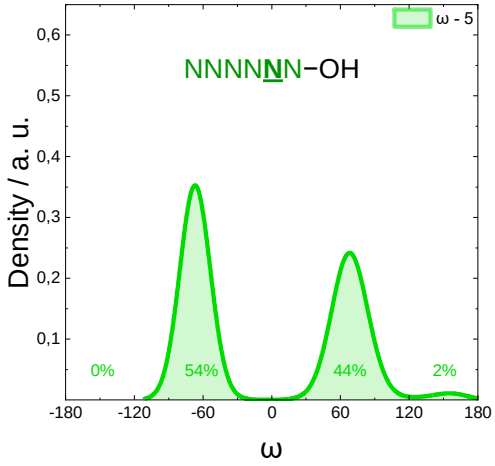
ω - 5
NNNNNN−OH
Density / a. u.
0,6
0,5
0,4
0,3
0,2
0,1
0%
54%
44%
2%
-180
-120
-60
0
60
120
180
ω

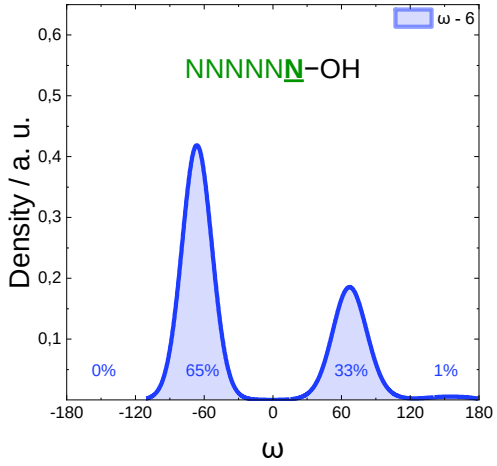
ω - 6
NNNNNN−OH
Density / a. u.
0,6
0,5
0,4
0,3
0,2
0,1
0%
65%
33%
1%
-180
-120
-60
0
60
120
180
ω

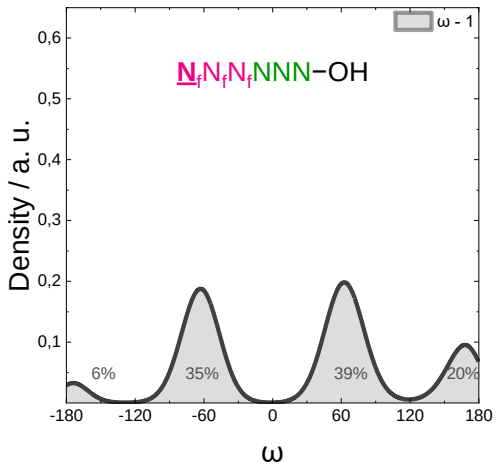
ω - 1
NfNfNfNNN−OH
Density / a. u.
ω
6%
35%
39%
20%

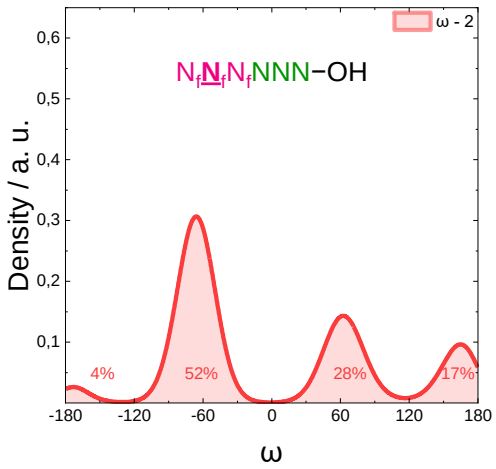
ω - 2
NfNfNfNNN−OH
Density / a. u.
ω
4%
52%
28%
17%

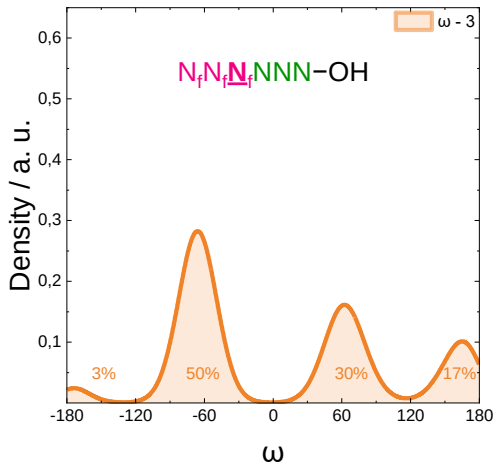
ω - 3
NfNfNfNNN−OH
Density / a. u.
ω
3%
50%
30%
17%

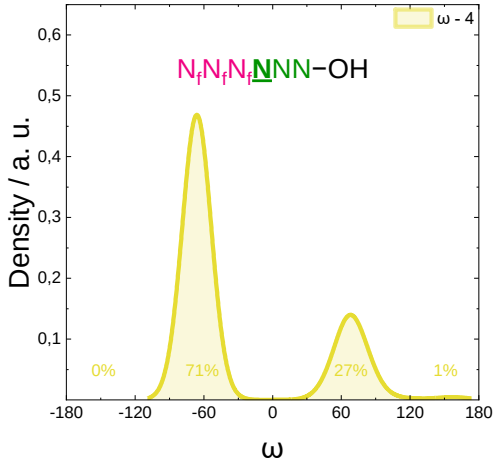
ω - 4
NfNfNfNNN−OH
Density / a. u.
ω
0%
71%
27%
1%

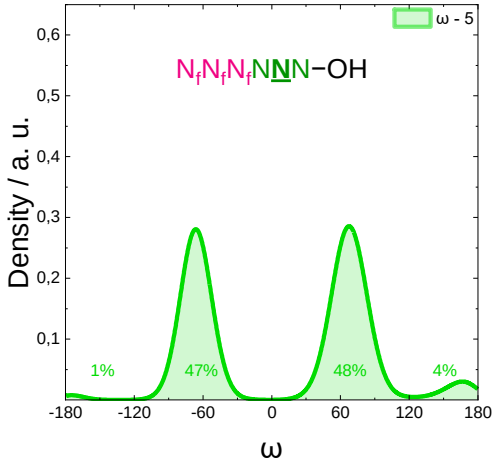
ω - 5
NfNfNfNNN−OH
Density / a. u.
ω
1%
47%
48%
4%

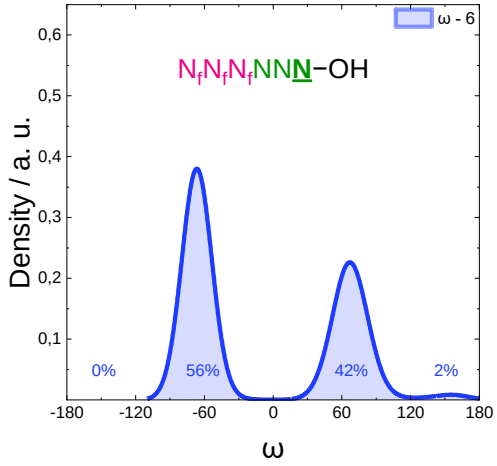
ω - 6
NfNfNfNNN−OH
Density / a. u.
ω
0%
56%
42%
2%

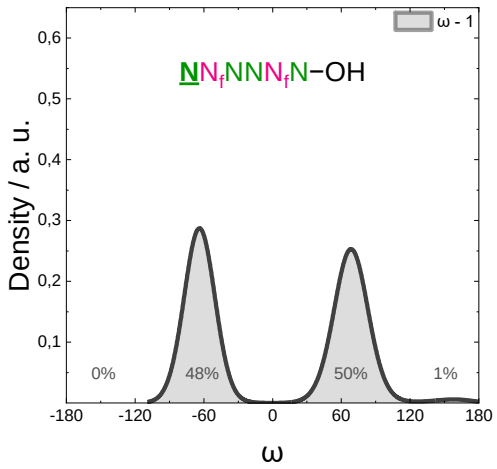
ω - 1
NNfNNNfN−OH
Density / a. u.
ω
0%
48%
50%
1%

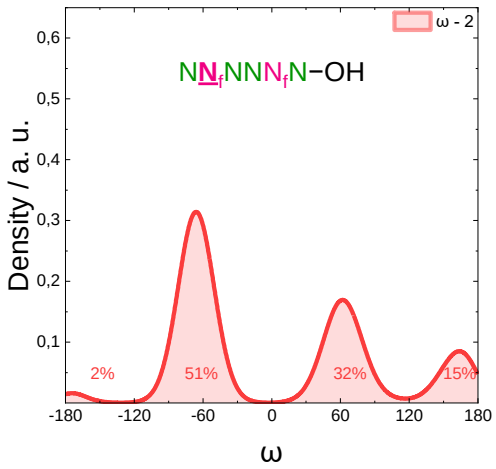
ω - 2
NNfNNNfN−OH
Density / a. u.
ω
2%
51%
32%
15%

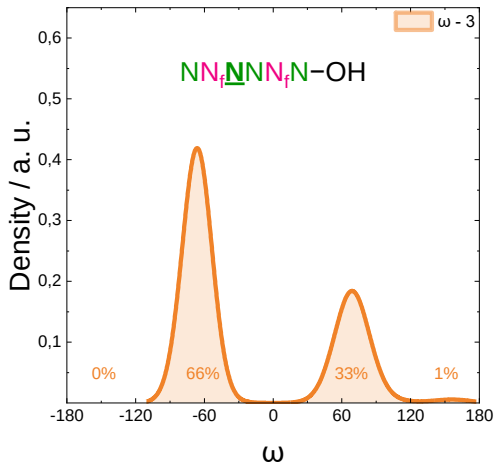
ω - 3
NNfNNNfN−OH
Density / a. u.
ω
0%
66%
33%
1%

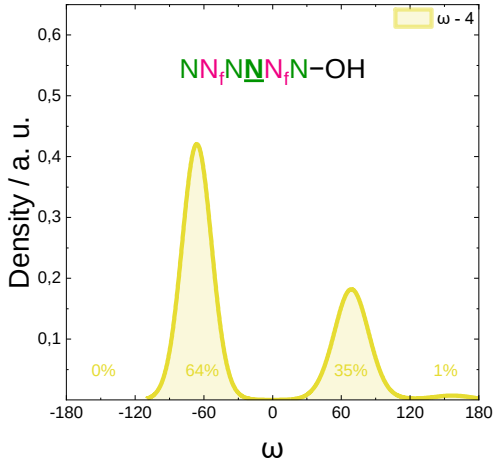
ω - 4
NNfNNNfN−OH
Density / a. u.
ω
0%
64%
35%
1%

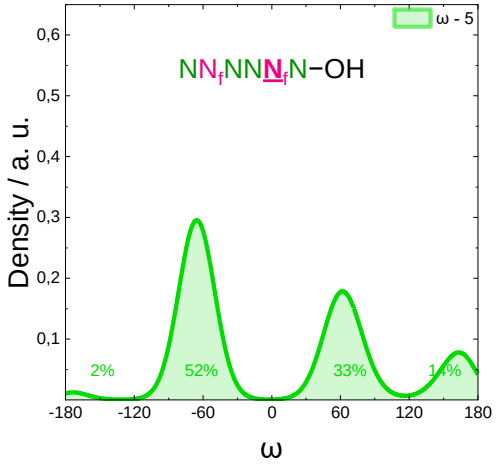
ω - 5
NNfNNNfN−OH
Density / a. u.
ω
2%
52%
33%
1%

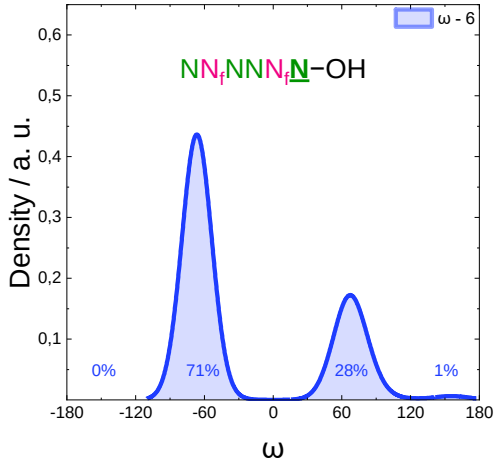
ω - 6
NNfNNNfN−OH
Density / a. u.
ω
0%
71%
28%
1%

4.7 Hydrogen bond analysis

To investigate the impact of fluorine substitution to the surrounding hydration shell, hydrogen bonds were analyzed. Hydrogen bonds are determined based on cutoffs for the angle Hydrogen - Donor - Acceptor (zero is extended) and the distance Donor - Acceptor. Dummy hydrogen atoms are assumed to be connected to the first preceding non-hydrogen atom. For the analysis two groups have to be specified, which must be either identical or non-overlapping. All hydrogen bonds between the two groups were analyzed. In this case group 1 is the underlined sugar unit while group 2 is bulk water. To focus the analysis around position 6, a shell with a diameter of 5 Å around the heteroatom was introduced. In **fffAAA**, the average number of hydrogen bonds around the fluorine residues is significantly lower compared to the one around the OH-6 found in **AAAAAA**. The loss of hydrogen bond donation ability that comes with the introduction of fluorine seems to affect the structure of the hydration shell, endowing the 6F rotamers with higher conformational freedom, that is expressed in a boarder distribution of ω.

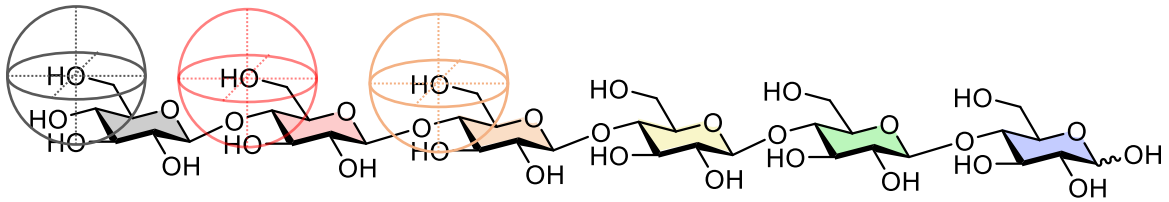

Figure S4 Introduced shells for local hydrogen bond analysis for the hexasaccharide $\mathbf{A_6}$.

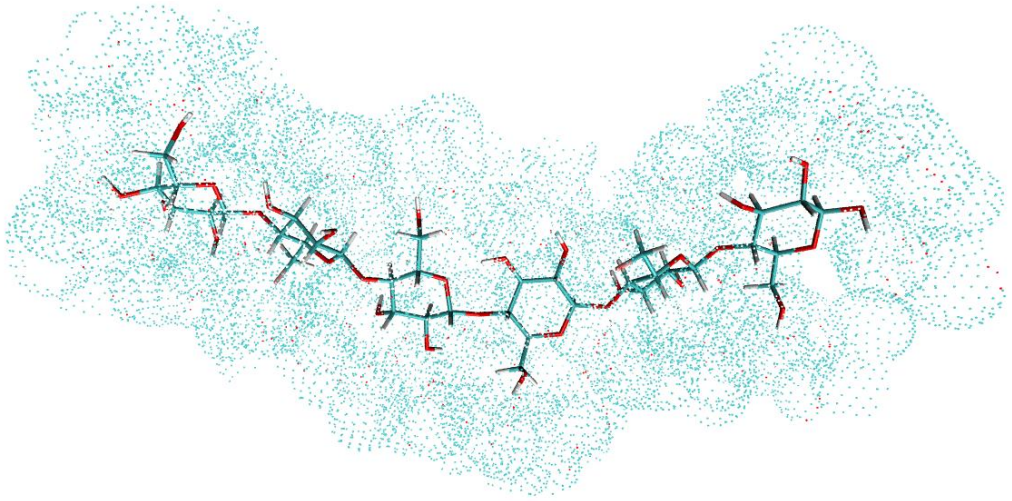

Figure S5 Representative hydration shell of **AfAAfA** hexamer.

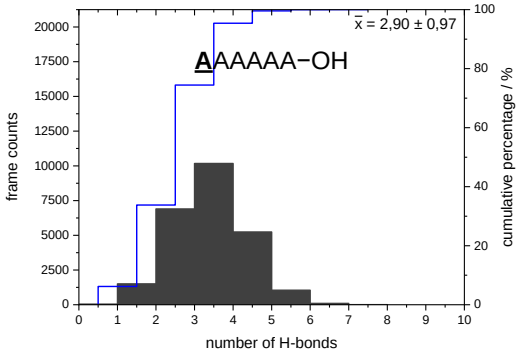
x̄ = 2,90 ± 0,97
AAAAAA−OH
frame counts
cumulative percentage / %
number of H-bonds

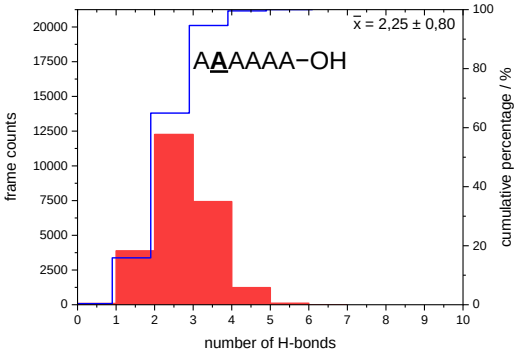
x̄ = 2,25 ± 0,80
AAAAAA−OH
frame counts
cumulative percentage / %
number of H-bonds

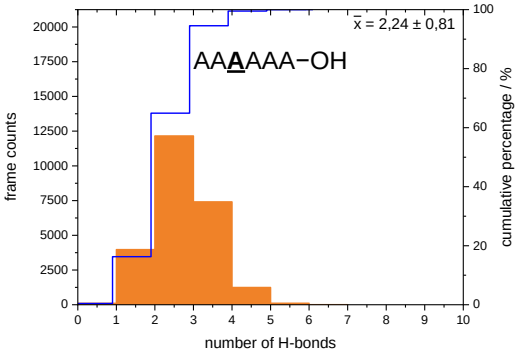
x̄ = 2,24 ± 0,81
AAAAAA−OH
frame counts
cumulative percentage / %
number of H-bonds

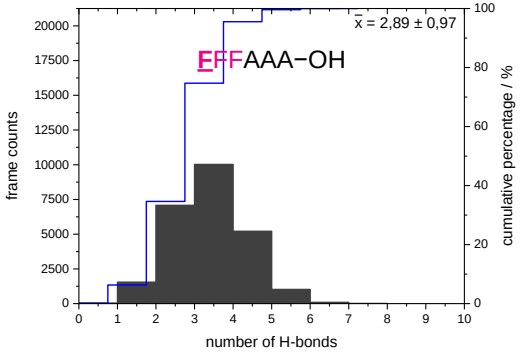
x̄ = 2,89 ± 0,97
FFFAAA−OH
frame counts
cumulative percentage / %
number of H-bonds

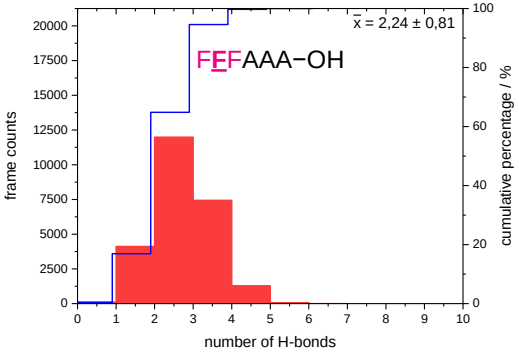
x̄ = 2,24 ± 0,81
FFFAAA−OH
frame counts
cumulative percentage / %
number of H-bonds

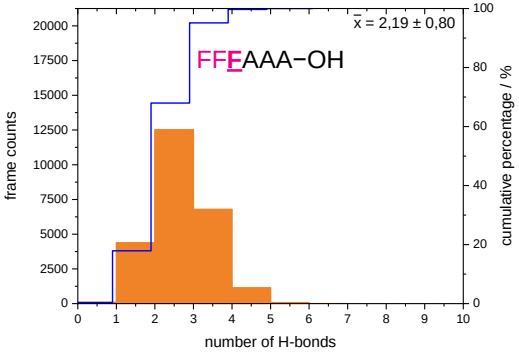
x̄ = 2,19 ± 0,80
FFFAAA−OH
frame counts
cumulative percentage / %
number of H-bonds

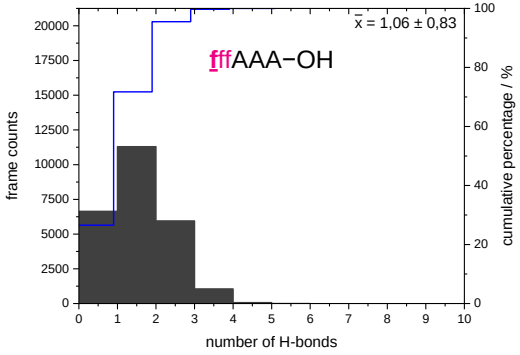
x̄ = 1,06 ± 0,83
fffAAA−OH
frame counts
cumulative percentage / %
number of H-bonds

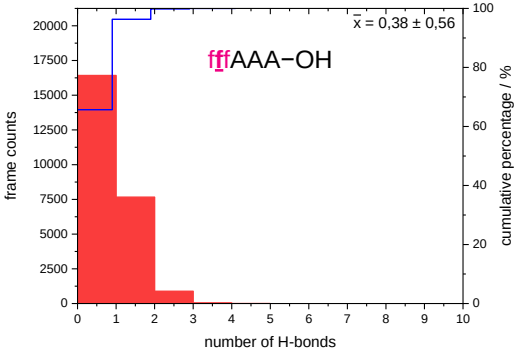
x̄ = 0,38 ± 0,56
fffAAA−OH
frame counts
cumulative percentage / %
number of H-bonds

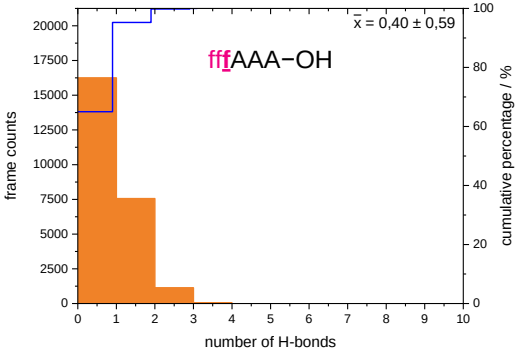
x̄ = 0,40 ± 0,59
fffAAA−OH
frame counts
cumulative percentage / %
number of H-bonds

4.8 Concentrated environment simulations

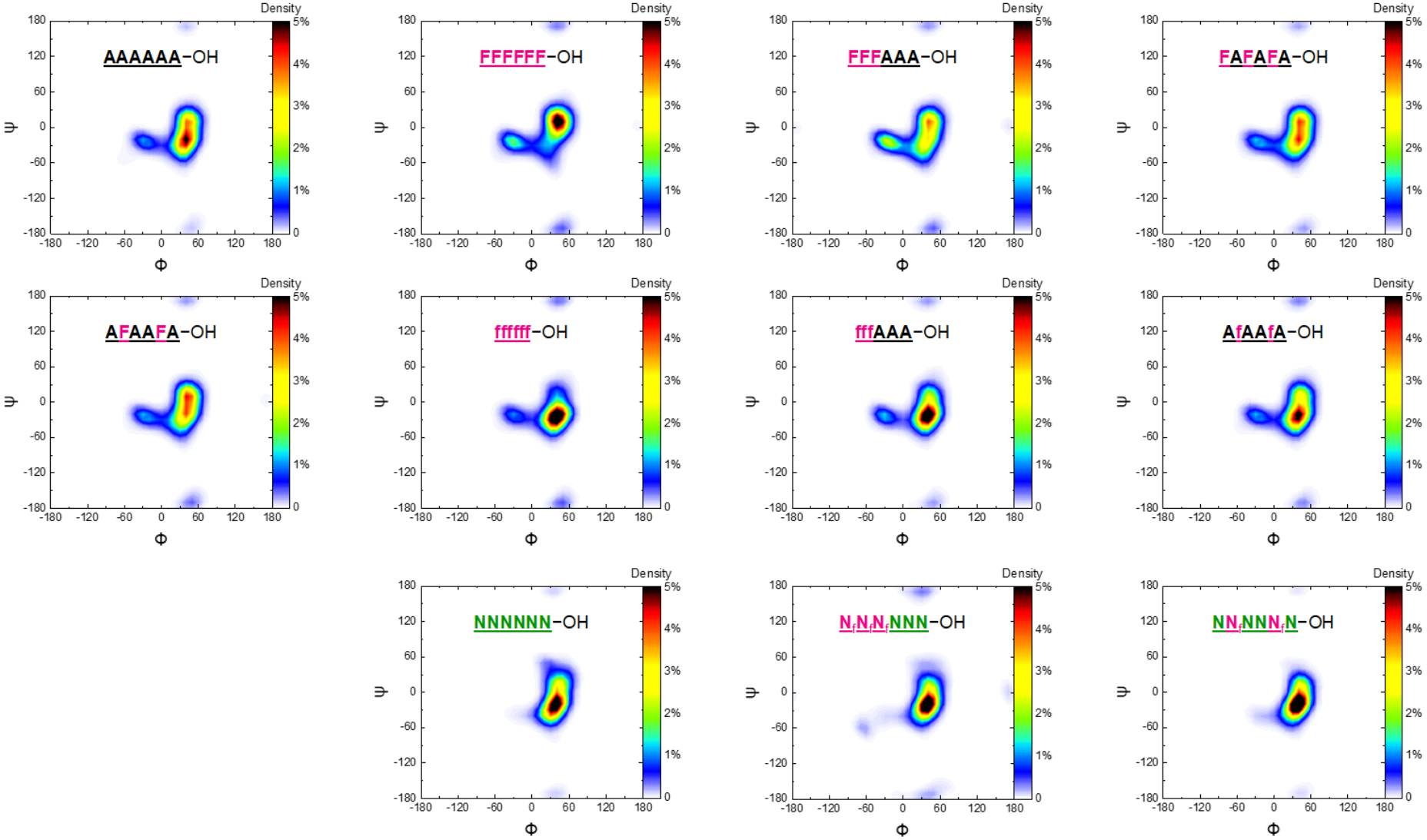

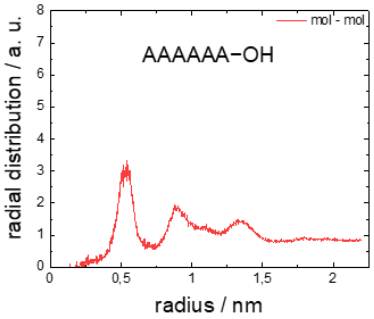
mol - mol
AAAAAA-OH
radial distribution / a. u.
radius / nm

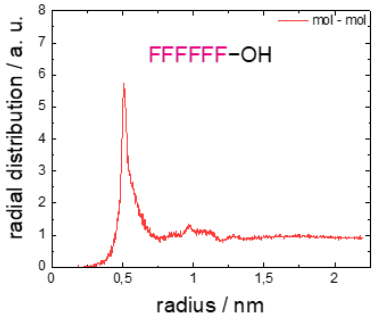
mol - mol
FFFFFF-OH
radial distribution / a. u.
radius / nm

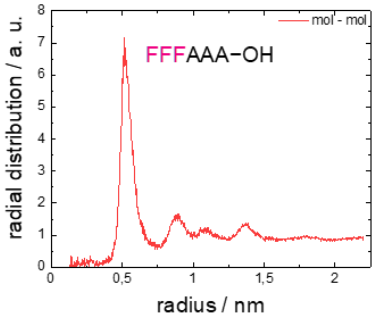
mol - mol
FFFAAA-OH
radial distribution / a. u.
radius / nm

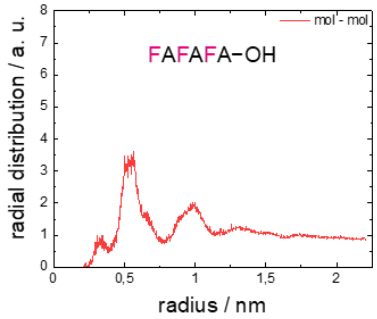
mol - mol
FAFAFA-OH
radial distribution / a. u.
radius / nm

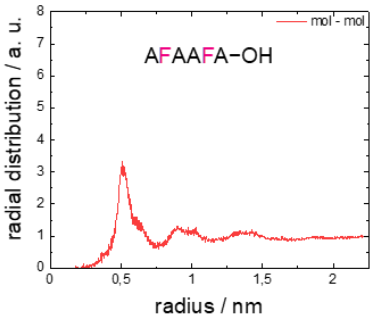
mol - mol
AFAAFA-OH
radial distribution / a. u.
radius / nm

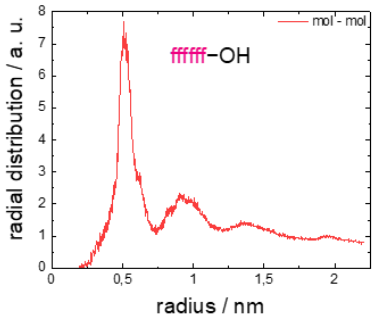
mol - mol
ffffff-OH
radial distribution / a. u.
radius / nm

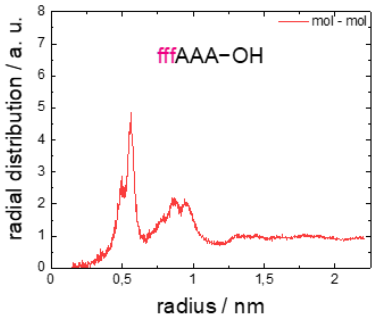
mol - mol
fffAAA-OH
radial distribution / a. u.
radius / nm

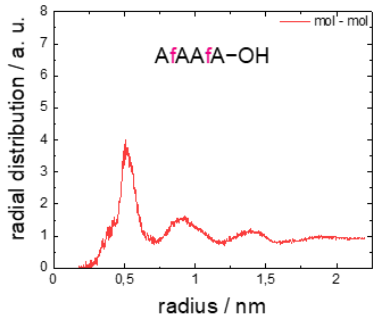
mol - mol
AfAAfA-OH
radial distribution / a. u.
radius / nm

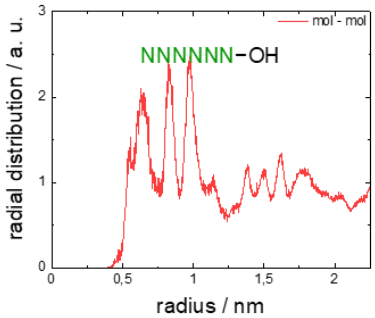
mol - mol
NNNNNN-OH
radial distribution / a. u.
radius / nm

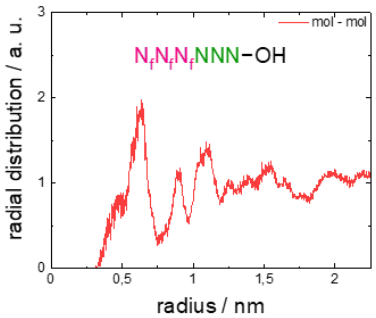
mol - mol
NfNfNfNNN-OH
radial distribution / a. u.
radius / nm

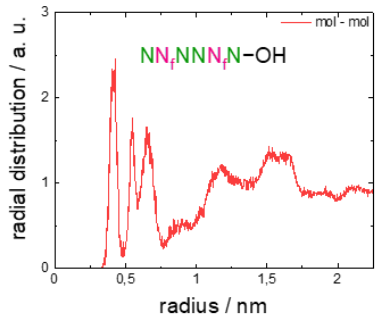
mol - mol
NNfNNNfN-OH
radial distribution / a. u.
radius / nm

5 NMR studies on 6F-chitin

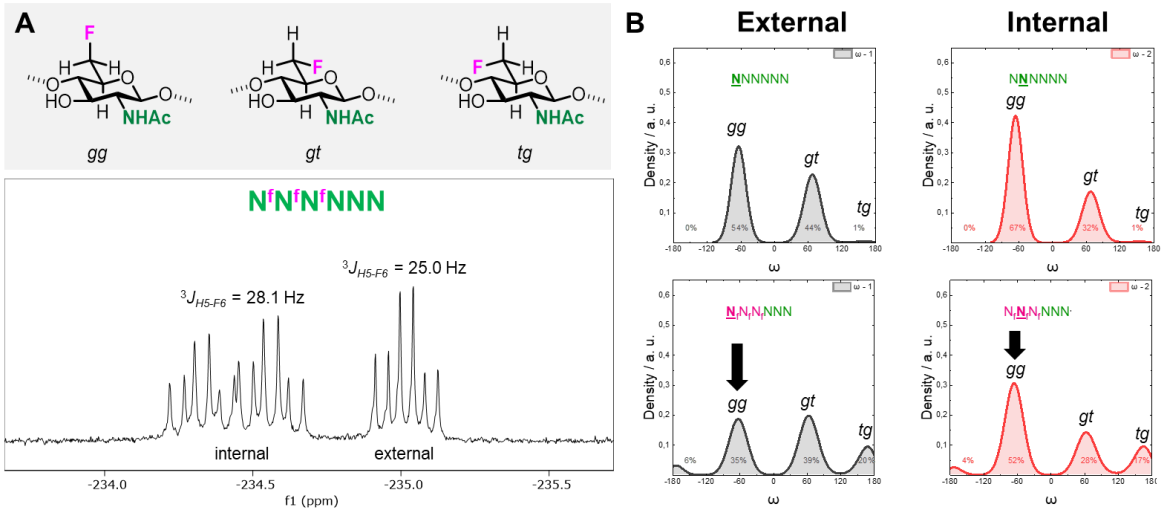

Figure S6 A) Definition of *gg*, *gt*, and *tg* rotamers of the ω dihedral angle for GlcNAc (*top*). Excerpt of the ^{19}F NMR of **N^{f}N^{f}N^{f}AAA** and respective $^{3}J_{H5\text{-}F6}$ values (*bottom*). B) Predicted populations of the rotamers for the ω dihedral angles for external (*left*) and internal (*right*) residues of two analogs.

6 References

(1) Eller, S.; Collot, M.; Yin, J.; Hahm, H. S.; Seeberger, P. H. Automated Solid-Phase Synthesis of Chondroitin Sulfate Glycosaminoglycans. *Angew. Chem., Int. Ed.* **2013**, *52* (22), 5858–5861. https://doi.org/10.1002/anie.201210132.

(2) Zegelaar-Jaarsveld, K.; Smits, S. A. W.; Van Der Marel, G. A.; Van Boom, J. H. Synthesis of a Pentasaccharide Corresponding to the Repeating Unit of the Exopolysaccharide from Cryptococcus Neoformans Serovar D. *Bioorganic Med. Chem.* **1996**, *4* (11), 1819–1832. https://doi.org/10.1016/S0968-0896(96)00164-2.

(3) Joseph, A. A.; Verma, V. P.; Liu, X. Y.; Wu, C. H.; Dhurandhare, V. M.; Wang, C. C. TMSOTf-Catalyzed Silylation: Streamlined Regioselective One-Pot Protection and Acetylation of Carbohydrates. *Eur. J. Org. Chem.* **2012**, No. 4, 744–753. https://doi.org/10.1002/ejoc.201101267.

(4) Gude, M.; Ryf, J.; White, P. D. An Accurate Method for the Quantitation of Fmoc-Derivatized Solid Phase Supports. *Lett. Pept. Sci.* **2002**, *9* (4), 203–206. https://doi.org/doi.org/10.1023/A:1024148619149.

(5) Hurevich, M.; Kandasamy, J.; Ponnappa, B. M.; Collot, M.; Kopetzki, D.; McQuade, D. T.; Seeberger, P. H. Continuous Photochemical Cleavage of Linkers for Solid-Phase Synthesis. *Org. Lett.* **2014**, *16* (6), 1794–1797. https://doi.org/10.1021/ol500530q.

(6) Ohara, K.; Lin, C.-C.; Yang, P.-J.; Hung, W.-T.; Yang, W.-B.; Cheng, T.-J. R.; Fang, J.-M.; Wong, C.-H. Synthesis and Bioactivity of β-(1→4)-Linked Oligomannoses and Partially Acetylated Derivatives. *J. Org. Chem.* **2013**, *78* (13), 6390–6411. https://doi.org/10.1021/jo4005266.

(7) Yu, Y.; Tyrikos-Ergas, T.; Zhu, Y.; Fittolani, G.; Bordoni, V.; Singhal, A.; Fair, R. J.; Grafmüller, A.; Seeberger, P. H.; Delbianco, M. Systematic Hydrogen-Bond Manipulations To Establish Polysaccharide Structure-Property Correlations. *Angew. Chem., Int. Ed.* **2019**, *58* (37), 13127–13132. https://doi.org/10.1002/anie.201906577.

(8) Tyrikos- Ergas, T.; Bordoni, V.; Fittolani, G.; Chaube, M. A.; Grafmüller, A.; Seeberger, P. H.; Delbianco, M. Systematic Structural Characterization of Chitooligosaccharides Enabled by Automated Glycan Assembly. *Chem. – A Eur. J.* **2021**, *27* (7), 2321–2325. https://doi.org/10.1002/chem.202005228.

(9) Fittolani, G.; Vargová, D.; Seeberger, P. H.; Ogawa, Y.; Delbianco, M. Bottom-Up Approach to Understand Chirality Transfer across Scales in Cellulose Assemblies. *J. Am. Chem. Soc.* **2022**, *144* (27), 12469–12475. https://doi.org/10.1021/jacs.2c04522.

(10) Schumann, B.; Parameswarappa, S. G.; Lisboa, M. P.; Kottari, N.; Guidetti, F.; Pereira, C. L.; Seeberger, P. H. Nucleophile-Directed Stereocontrol Over Glycosylations Using Geminal-Difluorinated Nucleophiles. *Angew. Chem., Int. Ed.* **2016**, *55* (46), 14431–14434. https://doi.org/10.1002/anie.201606774.

(11) Zhu, Y.; Delbianco, M.; Seeberger, P. H. Automated Assembly of Starch and Glycogen Polysaccharides. *J. Am. Chem. Soc.* **2021**, *143* (26), 9758–9768. https://doi.org/10.1021/jacs.1c02188.

(12) Kirschner, K. N.; Yongye, A. B.; Tschampel, S. M.; González-Outeiriño, J.; Daniels, C. R.; Foley, B. L.; Woods, R. J. GLYCAM06: A Generalizable Biomolecular Force Field. Carbohydrates. *J. Comput. Chem.* **2008**, *29* (4), 622–655. https://doi.org/10.1002/jcc.20820.

(13) Sauter, J.; Grafmüller, A. Predicting the Chemical Potential and Osmotic Pressure of Polysaccharide Solutions by Molecular Simulations. *J. Chem. Theory Comput.* **2016**, *12* (9), 4375–4384. https://doi.org/10.1021/acs.jctc.6b00295.

(14) Dupradeau, F.-Y.; Pigache, A.; Zaffran, T.; Savineau, C.; Lelong, R.; Grivel, N.; Lelong, D.; Rosanski, W.; Cieplak, P. The R.E.D. Tools: Advances in RESP and ESP Charge Derivation and Force Field Library Building. *Phys. Chem. Chem. Phys.* **2010**, *12* (28), 7821.

https://doi.org/10.1039/c0cp00111b.

(15) Trucks, G.; Schlegel, H.; Scuseria, G.; Robb, M.; Cheeseman, J.; Montgomery Jr, J.; Vreven, T.; Kudin, K.; Burant, J.; Millam, J. No Title. *Gaussian* **2004**.

(16) Mahoney, M. W.; Jorgensen, W. L. A Five-Site Model for Liquid Water and the Reproduction of the Density Anomaly by Rigid, Nonpolarizable Potential Functions. *J. Chem. Phys.* **2000**, *112* (20), 8910–8922. https://doi.org/10.1063/1.481505.

(17) Darden, T.; York, D.; Pedersen, L. Particle Mesh Ewald: An N · log(N) Method for Ewald Sums in Large Systems. *J. Chem. Phys.* **1993**, *98* (12), 10089–10092. https://doi.org/10.1063/1.464397.

(18) Van Der Spoel, D.; Lindahl, E.; Hess, B.; Groenhof, G.; Mark, A. E.; Berendsen, H. J. C. GROMACS: Fast, Flexible, and Free. *J. Comput. Chem.* **2005**, *26* (16), 1701–1718. https://doi.org/10.1002/jcc.20291.

(19) Evans, D. J.; Holian, B. L. The Nose–Hoover Thermostat. *J. Chem. Phys.* **1985**, *83* (8), 4069–4074. https://doi.org/10.1063/1.449071.

(20) Parrinello, M.; Rahman, A. Polymorphic Transitions in Single Crystals: A New Molecular Dynamics Method. *J. Appl. Phys.* **1981**, *52* (12), 7182–7190. https://doi.org/10.1063/1.328693.